Cetacean distribution and habitat use in the central and north-eastern North Atlantic

Nadya Carolina Ramirez Martinez

A thesis submitted for the degree of PhD
at the
University of St Andrews

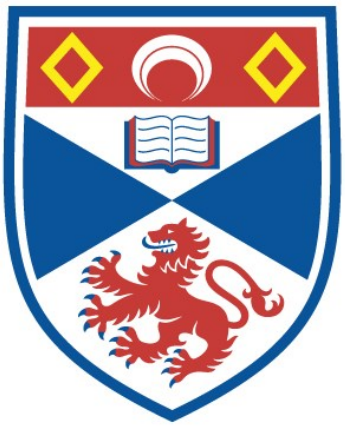

2021

Intentionally left blank

Candidate's declaration

I, Nadya Carolina Ramírez Martínez, do hereby certify that this thesis, submitted for the degree of PhD, which is approximately 70,000 words in length, has been written by me, and that it is the record of work carried out by me, or principally by myself in collaboration with others as acknowledged, and that it has not been submitted in any previous application for any degree.

I was admitted as a research student at the University of St Andrews in April 2015.

I received funding from an organisation or institution and have acknowledged the funder(s) in the full text of my thesis.

Date Signature of candidate

Supervisors' declaration

I hereby certify that the candidate has fulfilled the conditions of the Resolution and Regulations appropriate for the degree of PhD in the University of St Andrews and that the candidate is qualified to submit this thesis in application for that degree.

Date Signature of supervisor

Permission for publication

In submitting this thesis to the University of St Andrews we understand that we are giving permission for it to be made available for use in accordance with the regulations of the University Library for the time being in force, subject to any copyright vested in the work not being affected thereby. We also understand, unless exempt by an award of an embargo as requested below, that the title and the abstract will be published, and that a copy of the work may be made and supplied to any bona fide library or research worker, that this thesis will be electronically accessible for personal or research use and that the library has the right to migrate this thesis into new electronic forms as required to ensure continued access to the thesis.

I, Nadya Carolina Ramírez Martínez, confirm that my thesis does not contain third-party material that requires copyright clearance.

The following is an agreed request by candidate and supervisor regarding the publication of this thesis:

Printed copy

No embargo on print copy.

Electronic copy

No embargo on electronic copy.

Date Signature of candidate

Date Signature of supervisor

Underpinning Research Data or Digital Outputs

Candidate's declaration

I, Nadya Carolina Ramírez Martínez, hereby certify that no requirements to deposit original research data or digital outputs apply to this thesis and that, where appropriate, secondary data used have been referenced in the full text of my thesis.

Date Signature of candidate

ACKNOWLEDGEMENTS

"If I have seen further, it is by standing in the shoulder of giants." This is something that is credited to Newton by has been said by many others throughout history as well. While this phrase refers to the advancement in knowledge, it I not only the giants in our fields that provide us shoulders to stand on. There are big academic and personal support giants that have given me a way to step higher.

Thanks to my supervisor, Phil Hammond who has continuously supported me throughout my master and my PhD, as a teacher, a thoughtful researcher, and an exemplary person. Thank you not only for supporting my wild ideas (including coming with us to Chile), but also for guiding me and helping me focus, and for all the patience, especially in regard to my writing. Thank you!

To our data collaborators for their efforts keeping monitoring programs through decades and allow us to use their datasets, in addition to answering my many questions: Bjarni Mikkelsen, Gísli Víkingsson, Thorvaldur Gunnlaugsson, and Nils Øien. Specially to Gísli Víkingsson and Daniel Pike for inviting me to join them in Iceland during TWO field work seasons, next time we'll find some *Mola mola* for you Dan!

To my very patient honorary teachers Clint Blight, Dave Miller, and Raul Martínez, for their help in mapping, stats, coding. Many thanks for all their help and being so generous with their time.

To the Bute-tifuls for all the cake: Gui and his wonderful family (gave me so many happy days), Joyce (our office mom), Marie (made me fat!), Claire, Janneke, Emily, Anna, Luis, Tilen, Crystel, Iosu, Alex C., Chloe, Jaime, Eilidh, Filipa, Paul, Saana, Ben, Mathilde, Miguel, Sara, Takashi, and Kathryn, for everything including the nice academic and no-academic discussions.

Also SMRU, CREEM, CBD, and physics crew: Theo (also made me fat), Alina & Gustav (all the lovely post-surgical care), Teresa, Jo, Rene, Aubrie, Jo O., Lucia, Popi, Esme, Maria Joao, Kaithlin, Sophie S., Monica, Andrew, Chris M., Sara, Braulio, Thomas, Tania, Nick, Izzy, Katheryn, Steve B., Holly, Ana R., Sonia, Heather, Debbie, Carl, Theoni, Catriona, Monique, Valentin, Petros, Alex, and Alfredo for the extracurricular activities, public engagement, hockey, and academic activities off course.

To my new colleagues in Germany for being so supportive in transition Abbo, Tobias, Britta, Caro, Jeff, Maria, Susanne, Simon, Luca, Jana, Franzy, Patrick, Robabe, Marcus, Steph, Jan,

Miriam, Conny, Cristina, Christine, and Ursula. Especially to the formatting gurus, Elena and Johannes; to the best officemate Joy; and to our little team supporting my multitasking year Anita, Dominik, and Bianca, thank you.

Thanks to my friends that read parts of my thesis Braulio, Luz Ma, Joy, Marie L. and my sister Alexandra R.

Thanks to the friends that I have gained while working with cetaceans. They have been a great network of friendship and support Judy Allen, Daniel Palacios, Rikke Guldborg, Sölvi Vignisson, Peter Stevick, Rosie Seton, Mindy Viechnicki, Dan DenDanto, Sean Todd and Toby Stephenson.

Thanks to my lifetime friends Tati, LuzMa, Sergio, Calu, Adriana, Astrid, Lina, Isra, Damian, Cata, Raquel, Jairo, Marta, Chris, and Jackie for the inspiration, strength, laughter when is needed and care to my family when I am far.

More than thank you to my family, my parents, for being my Giants, for their unmeasurable love, and exemplary work ethics, so happy you are healthy again as I write this. To my favorite sister Alex, always grateful of your love and support.

Thanks to the rest of the big family we have my grandmas, uncles, aunts, cousins, and baby cousins, to the ones are not with us anymore for teaching us so much, for all the big family happiness and chaos, life is much better with all of you. And to my cousin Esperanza and her family, I am so glad you are only a few hours away, Philipp and Patrick are such a joy and good teaching German.

Environmental data supplied by NERC Earth Observation Data Acquisition and Analysis Service (NEODAAS), I would like to thank Peter Miller for preparing all the frontal data and Nick Selmes for helping re-processing the data with quality issues.

This project was supported by Colciencias (Departamento Administrativo de Ciencia, Tecnología e Innovación, Colombia) [Convocatoria No. 646 de 2014]; the University of St Andrews (School of Biology); the University of St Andrews (St Leonard's 7th Century Scholarship Postgraduate); and NAMMCO (North Atlantic Marine Mammal Commission).

TABLE OF CONTENTS

LIST OF FIGURES

LIST OF TABLES

ABSTRACT

Major changes in the distribution of some cetaceans have been observed coincident with changing oceanography of the North Atlantic over the last 30 years. This study aimed to improve understanding of the underlying ecological drivers and their mechanisms on the changes in cetacean distribution. Data from two series of summer surveys were used to model density of sperm, long-finned pilot, northern bottlenose (deep diver guild), fin, humpback, minke (baleen whale guild) and killer whales, and white-beaked dolphins (delphinid guild) as a function of static (relief), physical and biological oceanographic covariates using GAMs. The best models were used to predict distribution. The study was divided into two periods, 1987-1989 and 1998-2015, based on environmental changes in the area and data availability. The common covariates that best explained these species' distributions in both periods were depth and sea surface temperature, indicating these are useful indirect proxies for prey. Relationships between cetacean density and depth were generally maintained over time, except for the year-round species pilot whale, killer whale, and white-beaked dolphin. The relationships between cetacean density and dynamic oceanographic variables were found in summer for baleen whales (lower trophic feeders), in spring for sperm and pilot whales (higher trophic feeders) and unclear for northern bottlenose whale and the two delphinid species. Changes in distribution between the two periods varied among species and guilds. Overall, there was an expansion to a broader distribution, especially in new areas close to the limits with Arctic waters, and increased usage of some areas, for example the Barents Sea for baleen whales. This new knowledge will help improve understanding of how these species may respond over this wide area to a changing environment and inform their conservation and management to reduce the negative effects of climate change and the increasing anthropogenic impacts.

Intentionally left blank

1 INTRODUCTION

Ecology studies how organisms interact with their ecosystem. Both physical and biological features of ecosystems can influence or limit the range of species in time and space. Equally, interactions within and between trophic levels can influence distribution and abundance. Higher predators in ecosystems, such as marine mammals, can have top-down influences on community structure through their impact on lower trophic levels. However, species at or near the top of food webs are also influenced by bottom-up effects on distribution and abundance. An important goal in ecology is thus to understand the underlying processes driving animal distribution and how this influences the way in which they use their habitat; this knowledge also provides scientific advice for management and conservation (Redfern et al., 2006). In the marine environment, providing scientific advice for management and conservation continues to grow in importance because of increasing overlap between anthropogenic activities and the ranges of marine species, linked with the technological advances and the high demand for resources of the increasing human population (Avila et al., 2018; Halpern et al., 2015, 2008). Physical changes during the last decades in the North Atlantic (*e.g.* warmer temperatures) have been linked to biological changes, which have been detected in fish species such as capelin (*Mallotus villosus*), herring (*Clupea harengus*), mackerel (*Scomber scombrus*), and blue whiting (*Micromesistius poutassou*) (Astthorsson et al., 2012; Hátún et al., 2009; Huse et al., 2015; Trenkel et al., 2014; Valdimarsson et al., 2012). The mechanisms of how physical and biological changes are linked and the effects through multiple trophic levels are not well understood. Environmental variability and prey availability are assumed to be responsible for the non-random distribution of cetaceans (Forney, 2000; Redfern et al., 2006).

In the North Atlantic, decadal-scale changes in the abundance and distribution of cetaceans during the summer months have been shown in Icelandic, Faroese and Norwegian waters (e.g. Hátún et al., 2009; Nøttestad et al., 2015; Øien and Bøthun, 2009; Pike et al., 2009a, 2009b;

Víkingsson et al., 2015). To understand the underlying physical and ecological processes occurring in this region, which could be linked to cetacean distribution, this introduction is divided in four main sections: ecological links with climate, oceanography and oscillations of the North Atlantic, variation in the marine ecosystem in the North Atlantic, and marine mammals in the North Atlantic. This structure goes from general considerations, to more specific topics regarding factors that could drive cetacean distribution to conclude with some generalities about the animals in the region. Species-specific introductions are included in each corresponding chapter.

1.1 Ecological links with climate

It is repeatedly highlighted in the ecology literature, natural resource management, and endangered species conservation that there is a need for a better understanding of relationships and responses of species to climate variability and climate change. Studies about the climate and its effects on populations are fundamental to understand ecosystem dynamics (Lima and Estay, 2013; Stenseth et al., 2002; Walther et al., 2002; Williams et al., 2013). The climatic conditions that influence ecological processes are assessed by either studying a) local weather parameters or b) large-scale patterns that have effects inter-annually and/or at longer time scales (Stenseth et al., 2002). Since assessing only local parameters will miss the broad scale of atmospheric events; studies have increasingly focused more on evaluating the larger climatic scales driving the ecological systems (Lima and Estay, 2013; Stenseth et al., 2002).

Even though there have only been a few decades of research on global warming (anthropogenic caused warming), the ecological responses are noticeable for many species over a wide range of areas; more than 30 years of warmer temperatures indicate effects in the phenology of organisms, the range and distribution of species, and the composition and dynamics of communities (Walther et al., 2002). Although ecological datasets are typically shorter-term and smaller-scale than climatological datasets; the comparisons and links between population-community dynamics (extrapolated from individual studies) and atmospheric and oceanic processes from global-scale studies remain challenging (Walther et al., 2002). So far, research explaining ecological effects through climatic variations has shown the occurrence of clear patterns and responses. But there is also uncertainty explaining the mechanisms behind the ecological patterns caused by climate variability, partly due to the differences in scale.

The effects of climate variability on individuals could be direct or indirect, the former through physiology such as metabolic or reproductive processes and the latter though ecosystem processes such as food-web interactions (Stenseth et al., 2002). To understand and predict systematic species shifts, several studies evaluating climate variation impacts have focused on changes in abundance and distribution. Walther et al. (2002) suggest that changes in distribution are often related with physiological species-specific tolerance limits. But the relationships between species distribution and the factors that affect it are complex; in fact, simple correlations as described above are not always found. A further aspect to consider is that the range of responses among and within species shifts greatly depending on their dispersal capacities. For example, many cetacean species are highly mobile and range over large areas; variation in distribution patterns can therefore be the expected response to changes in their environment (Forney, 2000). Changes in the distribution patterns of cetaceans are expected to be mediated by variation in the availability and distribution of their prey; in other words, the result of food-web interactions (Hastie et al., 2004; Laran and Drouot-Dulau, 2007; Moore, 2008; Moore and Huntington, 2008).

As mentioned above, to link climate variability and ecological processes appropriately, the longer and the larger scale of the ecological data available the better because oceanographic and atmospheric events occur at these scales. One area where a large amount of research has been done is the North Atlantic (Kaschner et al., 2012); as a result, some of the most extensive ecological datasets are available from this region (such as those used in this thesis). The North Atlantic also has high human concentrations that have a large anthropogenic impact on the ecosystem; poorly managed impacts on ecosystems could push them to their limits and climate change can strengthen these negative effects (Walther et al., 2002).

1.2 The oceanography and oscillations of the North Atlantic Ocean

The North Atlantic is a large, complex and dynamic ocean that encompasses different oceanographic processes and is important in the transfer of heat to higher latitudes. The mid-Atlantic ridge dominates the topography, dividing the Atlantic Ocean in two. Smaller basins are formed by transverse ridges that have given rise to the Azores, Iceland, the Faroe Islands,

and Jan Mayen; depths can reach 5000 m. The European continental shelf rises east of the mid-Atlantic ridge. The North and Barents Seas are the two shelf seas of the region with average depth of 95 m and 230 m, respectively (Figure 1.1).

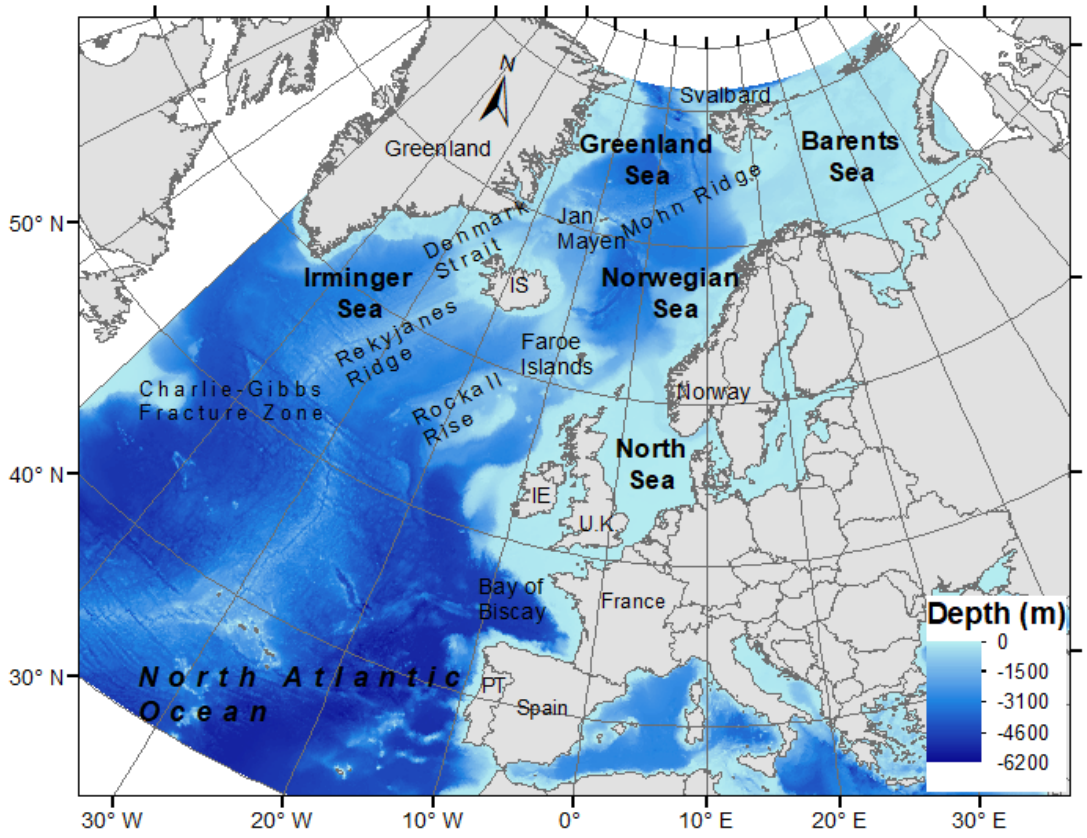

Figure 1.1 Physiographical map of the central and eastern North Atlantic, including major sea floor features. Background bathymetry is from ETOPO2. Projection is Albers.

Important drivers of surface currents in the North Atlantic are the North Atlantic Gyre (Subtropical Gyre) and further north the Subpolar Gyre (Figure 1.2). The North Atlantic Gyre circulation is anti-cyclonic; it is influenced by northeast trade winds between 10° and 30°N and by westerlies between 40° and 60°N. The North Atlantic Subpolar Gyre is located just beneath a region of low pressure; its circulation is cyclonic between 50° and 65°N (Häkkinen and Rhines, 2004). The climate in Europe is influenced by the warm and salty waters of the Gulf Stream that runs from south to north and west to east. This current starts in the south of Florida, then runs northeast crossing the Atlantic to the Barents Sea (Lynch-Stieglitz et al., 1999; Trenkel et al., 2014). However, before reaching the Barents Sea many sub-currents split off (Sverdrup and Armbrust, 2009). The major surface currents are driven by the northern part of the North

Atlantic Current and the Norwegian Current that carries relatively warm water northward. The southward cold East Greenland Current flows along the east coast of Greenland. And the southward-flowing Labrador Current runs into the Labrador Sea and off the coast of Canada (Trenkel et al., 2014). All these currents propagate a variety of different habitats, productivity and exchange that support a diverse range of marine organisms, including cetaceans.

Deep and intermediate currents (below 1000 m) are also key regulators of the distribution and ecological responses of cetacean populations in the North Atlantic. An increased deep-water formation in the North Atlantic, which can be detected using subpolar gyre indices, is a good indicator of a faster Atlantic Meridional Overturning Circulation (AMOC) (Häkkinen and Rhines, 2004; Yong-Qi and Lei, 2008). An increased AMOC entails a higher exchange between the warm surface waters and the cooler dense water. AMOC plays an important role in climate and global water circulation (Rahmstorf, 2003), hence it is an important process to consider when evaluating decadal-scale changes in North Atlantic marine ecosystems.

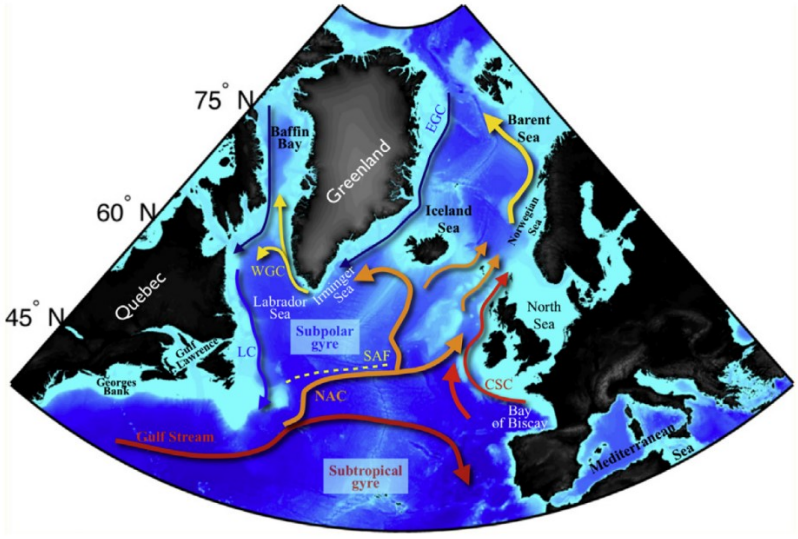

Figure 1.2. Map of physical oceanographic features in North Atlantic, major currents depicted with coloured arrows: Gulf Stream, North Atlantic Current (NAC); Continental Shelf Current (CSC); Eastern Greenland Current (EGC); Labrador Current (LC); Western Greenland Current (WGC); Subarctic Front (SAF) (Trenkel et al., 2014).

As mentioned above, human activities have driven climate changes such as regional and global temperatures and salinity (Levitus et al., 2012). As climate change continues, including ocean

warming, it is likely that effects on ecosystems will persist, for example as changes in species distribution (e.g. Astthorsson et al., 2012; Cheung et al., 2009; Moore et al., 2019; Perry et al., 2005; Walther et al., 2002). However, the question remains as to how climate oscillations also play a role in species shifts in a changing climate (Gulev and Latif, 2015; Roberts, 2019). Natural cyclical changes at different scales are a common feature of the climate of the planet. There are cycles at long scales (tens of thousands of years) linked to changes in the planet's orbit and cycles at annual scales related to seasons. Some oscillations can occur in less regular cycles and may last from a few months to several decades. They may generate changes in a particular area of the planet and have global effects on the weather. Changes could be of an oceanic-atmospheric nature such as change of air pressure, sea temperature and wind direction over the oceans, where ocean and atmosphere interact and influence each other as a system. El Niño-Southern Oscillation (ENSO) is a natural oscillation with the strongest influence affecting global weather patterns over different time and geographic scales. Two important oscillations in the North Atlantic are the Atlantic Multi-decadal Oscillation (AMO) and the North Atlantic Oscillation (NAO).

The Atlantic Multi-decadal Oscillation (AMO) describes varying SST anomalies over the entire North Atlantic (0°–70°N, 80°W–10°E) (Kerr, 2000), and thus describes superficial changes, not those beneath the surface. Several processes can cause changes in SST across the North Atlantic, such as variability in surface heat fluxes, wind driven currents, variability in sea ice, changes in AMOC (e.g. strength) and anthropogenic forcing (e.g. Booth et al., 2012; Chiang and Bitz, 2005; Deser and Blackmon, 1993; Deser et al., 2002; Dickson et al., 1988; Hansen and Bezdek, 1996; Lozier, 2010; Mann and Emanuel, 2006; Saravanan and McWilliams, 1998 In: Alexander et al., 2014). The AMO has warm (positive) and cold (negative) phases, with a period varying between about 55 to 70 years. There can be slight differences in the timing of the phases depending on the data and index calculation, but cold phases have been described during approximately 1900-1925 and 1965-1994, and warm phases during approximately 1875-1899, 1926-1965, and 1995-present (Rayner et al., 2003 In: Alexander et al., 2014).

The NAO is a large-scale atmospheric meridional variation. It relates to the distribution of atmospheric masses between the subtropical high-pressure system close to the Azores and the subpolar low-pressure system close to Iceland. NAO has a period of around 10 years. In

atmospheric circulation at a decadal-scale level, the NAO is one of the main drivers of seasonal variability in the Northern Hemisphere, which is more conspicuous during winter (Hurrell, 1995). Its phase fluctuations produce changes in average wind speed and direction over the Atlantic, air temperature, humidity, precipitation, heat transport between the Atlantic Ocean and the neighbouring continents, and the quantity of storms, their intensity, and trajectories (Drinkwater et al., 2003; Hurrell et al., 2003). These atmospheric changes affect water temperature, salinity, vertical mixing, circulation patterns and ice formation. Some authors suggest that the changes recorded in the weakening of the Subpolar Gyre during the mid-1990s were triggered by a switch in the NAO from positive until 1995 to negative in 1996-97 (Bersch, 2002; Flatau et al., 2003), while others suggest the weakening was driven only by oceanographic processes (Hakkinen and Rhines, 2004). Either way, the oceanographic changes potentially linked to NAO oscillations have been found to impact several components of marine ecosystems, including population dynamics, abundance and spatial distribution (Drinkwater et al., 2003; Ottersen et al., 2001).

The North Atlantic multi-decadal hydrographic variability has large-scale effects on marine ecosystems (Flatau et al., 2003; Häkkinen and Rhines, 2004). In the last 30 years waters around Iceland, Norway and neighbouring areas have shown warming and/or salinification anomalies (Bersch, 2002; Hátún et al., 2005; Havforskningsinstituttet, 2020; Malmberg and Valdimarsson, 2003, 1999; Mork et al., 2019; Mortensen and Valdimarsson, 1999; Valdimarsson et al., 2012) and some of these changes have been linked with changes in the ecosystem. The Atlantic Multi-decadal Oscillation (AMO) and the North Atlantic Oscillation (NAO) are both candidates to help understand the changes occurring in the marine ecosystem in the North Atlantic. However, the mechanistic linkages between the oscillations and species ecology is obscure and may be the result of a combination of interacting processes (e.g. Roberts, 2019). For example, the NAO is based on changes of atmospheric pressure while the oceanographic and ecological responses are lagged (e.g. Drinkwater et al., 2003; Greene and Pershing, 2004, 2000). Although results may suggest relationships with the oscillations, it will be difficult to link any such relationships with the rest of the ecosystem because the underlying mechanisms are not well understood. Here, in this study, neither of these oscillation indexes are used to try to explain the cetacean ecology in the area. However, the AMO is relevant because the data used in this study cover the transition from a cold phase (pre-1995) to a warm phase (see sections 1.4 and 2.2.2.1).

1.3 Variation in the marine ecosystem in the North Atlantic

Changes in the distribution and abundance of a wide range of marine organisms have been reported in the North Atlantic. Changes in marine ecosystems have been liked to oceanographic variations, such as in circulation, water masses, warming, and salinification (Arrigo and van Dijken, 2015; Dalpadado et al., 2020; Häkkinen and Rhines, 2004; Hátún et al., 2009; Mork et al., 2019; Valdimarsson et al., 2012) or to atmospheric variations that have triggered the oceanographic changes (Drinkwater et al., 2003; Ottersen et al., 2001).

At the base of marine tropic webs are phytoplankton, the biomass of which can be estimated indirectly through its pigment - chlorophyll *a* - *in situ* (fluorescence) or by satellite. In addition, net primary production (NPP) can be estimated using algorithms applied to chlorophyll *a*, sea surface temperature (SST), and ice cover data. In the Barents Sea, Dalpadado et al. (2020) observed trends in phytoplankton phenology associated with changes in the ice cover, driven by an increase in SST. Positive relationships were found between ice-free conditions and NPP during 1998-2017. Similar results were found during 1998-2012 by Arrigo and van Dijken (2015) in the Arctic Ocean, including the Barents Sea. However, a significant decline in NPP was found in the Greenland Sea (outflow shelf) indicating that nutrients had been consumed farther upstream. Further south, Hátún et al. (2009) found a relationship between phytoplankton colour data from the Continuous Plankton Recorder (CPR) surveys and the sub-polar gyre both spatially and temporally (1960-2005). Besides this, the strongest phytoplankton signal (highest chlorophyll *a* concentration) is most apparent south of Iceland, where it is related to the physical variables SST and Sea Surface Height (SSH) (Hátún et al., 2009). As water masses change, the species abundance and composition also change; the effect on the ecosystem as a whole is one of bottom-up control (e.g. Dalpadado et al., 2020; Hátún et al., 2009).

With bottom-up control, it is expected that changes in phytoplankton will generate a cascade effect in zooplankton. Across the North Atlantic, one of the most common species of zooplankton in terms of numbers and biomass is the copepod *Calanus finmarchicus* (Kann and Wishner, 1995); it is one of the keystone species between phytoplankton and fish (Fransz et al., 1991). Changes in *C. finmarchicus* distribution and abundance corresponding to oceanographic

and atmospheric variations have been reported all over the North Atlantic (Drinkwater et al., 2003; Greene and Pershing, 2000; Hátún et al., 2009; Ottersen et al., 2001). Water mass variations, including subpolar gyre weakening, have been linked to changes in *C. finmarchicus* occurrence in the central Atlantic Ocean (an increase until the mid-1990s followed by a sudden decline) (Hátún et al., 2009), who suggested that as the subpolar water becomes smaller and weaker its fauna retract north and that, as a result, the warmer and saltier subtropical waters occupy the available area, together with the associated fauna such as smaller copepod species (e.g. as happened in the mid-90s).

Euphausiids (krill) are also an important zooplankton group; they prey on phytoplankton and other zooplankton. Euphausiids species are also keystone species because they are an important part of the diet for higher predators including whales, but also fish such as cod, capelin, herring, and blue whiting (e.g. Bogstad et al., 2015; Christensen et al., 1992; Haug et al., 2002; Nøttestad et al., 2014; Melle et al., 2004 In: Øien and Bøthun, 2009; Ressler et al., 2015; Sigurjónsson and Víkingsson, 1997; Smout and Lindstrøm, 2007; Víkingsson, 1997; Víkingsson et al., 2015). Off southern Iceland, there have been long term changes in euphausiid distribution and abundance in oceanic and shelf areas (Silva et al., 2014). Spatially, krill seems to have decreased west to east and temporally, abundance seems to have decreased during 1958-2011, as inferred from CPR data. Temperature and phytoplankton biomass were the strongest predictors of krill. Additionally, changes in timing of the spring bloom may have affected the long-term changes in krill abundance by causing a temporal mismatch between young krill and the phytoplankton bloom, as mediated by recent climate warming. Changes have been also recorded in the Barents Sea, where the euphausiid community comprises six species. Historically of low abundance and importance, *Meganyctiphanes norvegica* has now become more common due to the recent warmer conditions (Zhukova et al., 2009).

Around Iceland, warmer and saltier water from the mid-1990s to 2010 has also been related to changes in the distribution of several fish species. During this period, rare and nomadic species have been seen more frequently and 31 species have been recorded for the first time in Icelandic waters. In a similar pattern to that of zooplankton, capelin (*Mallotus villosus*), an Arctic species, has retracted to colder northern waters from its previous nursery and feeding areas around northern Iceland leading to a reduction in stock size (Valdimarsson et al., 2012). On the other

hand, southern commercial fish species have reached more northern areas; the most evident changes have been in haddock (*Melanogrammus aeglefinus*), monkfish (*Lophius piscatorius*) and mackerel (*Scomber scombrus*) (Valdimarsson et al., 2012). Mackerel biomass has changed significantly in Icelandic waters; its occurrence had been recorded every year since 1996 but since 2007 in large numbers (Astthorsson et al., 2012). The cause of this increase is not clear; it is likely a result of a combination of factors, including the increase in water temperature and ecological relationships such as competition (Astthorsson et al., 2012). Its current occurrence, importance and impacts on the area mean that mackerel could be an indicator of the water mass changes in the area.

In contrast to mackerel, the biomass of sand eel has decreased markedly since 2005 (Marine Research Institute, 2015), affecting the trophic web at higher levels (Lilliendahl et al., 2013; Vigfusdottir et al., 2013 In: Víkingsson et al., 2015). There is no evidence that such changes in sand eel are linked to oceanographic and/or atmospheric processes, but their decrease could be an indirect result of multiple factors including interaction with other species (Frederiksen et al., 2007). Another commercially important fish species for which changes have been reported in Icelandic and Faroese waters is the blue whiting (*Micromesistius poutassou*). Changes in spawning distribution and stock size have been related to changes in the North Atlantic gyre and the associated water masses (Huse et al., 2015; Trenkel et al., 2014). The suggested mechanism is that a weak gyre (warmer regime) has a direct influence through an increase in recruitment, possibly due to a larger spawning area, broader dispersion, and higher growth/survival, and an indirect influence through changes in food availability; the opposite situation has been suggested for a stronger gyre (colder regime) (Hátún et al., 2009).

In the Norwegian Sea, fish species distribution, abundance and composition have also changed in recent years. The reasons for these fluctuations is uncertain, however an increase in SST and a reduction of zooplankton biomass have been described for the last 20 years (Skjoldal et al., 2004 In: Nøttestad et al., 2015). The Norwegian Sea is the feeding ground of two of the largest fish stocks in the world, Norwegian spring-spawning (NSS) herring and blue whiting. Mackerel also spend the summer feeding in the area (Bachiller et al., 2016), where its biomass has increased, as in Icelandic waters and the North East Atlantic in general (ICES, 2019a; Nøttestad et al., 2016). The combined abundance/biomass of mackerel, herring, and blue whiting has

increased since the late 1980s, but most of this increase has been linked to mackerel with historically high biomass between 2008-2014 (ICES, 2019a).

The Barents Sea plays a key role in the life history of several fish stocks: Northeast Arctic cod (*Gadus morhua*), Northeast Arctic haddock (*Melanogrammus aeglefinus*), Northeast Arctic saithe (*Pollachius virens*), herring (Norwegian Spring Spawning, NSS), and capelin (Olsen et al., 2010). They are important for fisheries but also as part of the diet of several cetacean species (Olsen et al., 2010; Ressler et al., 2015). Capelin has gone through three collapses in the last 30 years: 1985-1989, 1993-1997, and 2003-2006 (Gjøsæter et al., 2009). The main cause of the collapses is believed to be poor recruitment, and this could be the result of several factors including low growth, predation pressure from young herring, cod and haddock, and fishing (Gjøsæter et al., 2016). These events have had effects on the food web; its prey, zooplankton, have increased, and the predators have responded in different ways. Cod, sea birds and harp seals have suffered, for example, increased mortality and recruitment failure. However, in the recent collapses the effects were milder indicating the usage of other food sources (Gjøsæter et al., 2009).

Hátún et al. (2009) showed, in the Iceland-Faroes region, that weakening of the gyre around the mid-1990s matched changes in phytoplankton, zooplankton and blue whiting abundance and distribution, and linked these changes in the trophic web to long-finned pilot whale (*Globicephala melas*) catches in the Faroe Islands. There are some studies in the North Atlantic relating the long-term effects of large-scale environmental variations on top predators (Drinkwater et al., 2003; Greene and Pershing, 2004; Hátún et al., 2009; Nøttestad et al., 2015; Ottersen et al., 2001; Víkingsson et al., 2015; Williams et al., 2013). The availability of long-term ecological datasets is limited, but such datasets are needed to understand the drivers of top predator distribution.

1.4 Cetaceans in the North Atlantic

In northwest European waters, it has been suggested that around 33 species of cetaceans inhabit the area; some of them common year-round and others seasonal (Evans, 2009; Reid et al., 2003). In central and north-eastern waters of the North Atlantic, the area covered by the

North Atlantic Marine Mammal Commission (NAMMCO), to which Greenland, Iceland, the Faroe Islands and Norway are parties, 16 species of cetaceans are regularly seen. These include six baleen whales: blue (*Balaenoptera musculus*), fin (*Balaenoptera physalus*), sei (*Balaenoptera borealis*), humpback (*Megaptera novaeangliae*), bowhead (*Balaena mysticetus*), and common minke whale (*Balaenoptera acutorostrata*) and 10 species of toothed whales: beluga (*Delphinapterus leucas*), narwhal (*Monodon monoceros*), long-finned pilot whale (*Globicephala melas*), sperm whale (*Physeter macrocephalus*), northern bottlenose whale (*Hyperoodon ampullatus*), killer whale (*Orcinus orca*), white-sided dolphin (*Lagenorhynchus acutus*), white-beaked dolphin (*Lagenorhynchus albirostris*), bottlenose dolphin (*Tursiops truncatus*), and harbour porpoise (*Phocoena phocoena*).

These cetacean species have optimized their fitness in diverse ways by evolving different life-history strategies including the ways in which they exploit the available resources. Optimal acquisition and allocation of resources result in survival and reproductive success (Stearns, 1989). Two life history strategies that have evolved to achieve this are capital breeding and income breeding, which reflect how the organisms manage their resources (allocation and storage) (Jonsson, 1997; Stearns, 1989). Capital breeders store the resources that they will later use in reproduction, including raising offspring. Income breeders depend on the continual availability of resources including during periods of reproduction (Alerstam et al., 2003; Jonsson, 1997; Stephens et al., 2009). In cetaceans, baleen whales are generally capital breeders, while odontocetes are income breeders (e.g. Christiansen et al., 2014; Irvine et al., 2017; Oftedal, 1997). Species can be also grouped by the type and way they exploit their resources; such functional groupings, known as guilds, are central to our understanding of ecological communities. A guild has been defined as components of a community that exploit the same kind of resources in a similar way, where species overlap in their requirements regardless of their taxonomy (Simberloff and Dayan, 1991). The cetacean species of the North Atlantic, excluding the polar species, can be grouped into three guilds (deep diving cetaceans, baleen whales and Delphinidae).

Although the North Atlantic is not as densely populated with humans as the north-western European seaboard, animals are exposed to several direct and indirect anthropogenic pressures. In this area, and globally, these include: interactions with fisheries, collision with vessels,

pollution, direct impacts of whaling and climate change among others (Harwood, 2001). This is a wide range of pressures and this project includes several cetacean species inhabiting diverse habitats; hence the pressures do not affect them all equally. Global trends show an increase in fishing effort which translates to an increase in marine mammal - fisheries interactions, either "biological" (such as reduction in prey availability) or "operational" (such as incidental catches) (DeMaster et al., 2001). Incidental catches, or bycatch, in fishing gear is a problem that particularly affects small cetaceans; hundreds of thousands are taken every year worldwide (Bearzi, 2002; Read and Northridge, 2006; Reeves et al., 2013). Indirectly, commercial fisheries compete with marine mammals for the same (or linked) resources (DeMaster et al., 2001; Kaschner and Pauly, 2005). For example, in the Mediterranean Sea, overfishing has been suggested as one of the reasons for the decline of short-beaked common dolphins (Bearzi et al., 2008). Marine mammals can interact with fisheries in different ways; in the North Atlantic there is high fishing pressure making them particularly vulnerable (Kaschner and Pauly, 2005) and pressure could increase in both volume and extent as a result of climate change and the availability of 'new' areas. The cetaceans studied in this project could all interact with fisheries due to overlap in resources, bycatch, and entanglement (e.g. Bettridge et al., 2015; Esteban et al., 2016; Luque et al., 2006; Ryan et al., 2016).

Accidental collision with vessels is a well-documented direct threat in the North Atlantic for some whale species (Laist et al., 2001; Van Waerebeek et al., 2007). Fin whales seem to be the species most affected by ship strikes, and sperm whales are among the commonly struck species (Laist et al., 2001). Pollution is another threat that can affect marine mammals directly; this includes chemical pollutants and noise pollution. The main contaminants found in marine mammals are heavy metals, polycyclic aromatic hydrocarbons, and organochlorines (Aguilar et al., 2002; Das et al., 2003). The latter have been found at high levels in top predator marine mammals in temperate areas of Europe and North America (Jepson et al., 2016; O'Shea and Brownell, 1994); the pilot whale, together with the killer whale, has one of the highest levels of contaminants of any cetacean species (Dam and Bloch, 2000). The impact of chemical pollutants at the population level is still poorly known but endocrine and immune effects have been reported for different species (Jepson et al., 2016; Murphy et al., 2015). Sound waves travel very efficiently through water which makes underwater noise problematic for marine mammals in the short and long-term (Tyack, 2008; Weilgart, 2007). Underwater noise can be a serious threat,

especially to deep diving odontocetes and killer whales (Hooker et al., 2019; Isojunno et al., 2018; Kuningas et al., 2013; Miller et al., 2015, 2012; Rendell and Gordon, 1999; Sivle et al., 2012; Tyack et al., 2006).

Whaling activities globally decreased markedly in the second half of the last century, most recently since the International Whaling Commission (IWC) introduced the so-called moratorium (pause in commercial whaling) in 1986 (IWC, 2012). Currently, all countries that are members of NAMMCO catch marine mammals. This international organization's objectives include the management and sustainable exploitation of marine mammals. The cetacean species captured by NAMMCO countries are Iceland: minke and fin whales, Faroe Islands: pilot whales and Atlantic white-sided dolphins, Norway: minke whales, and Greenland: narwhal, harbour porpoise, beluga, sperm, minke, humpback, bowhead, and fin whales (IWC, 2020; NAMMCO, 2015). The number of animals caught by the Faroe Islands, Iceland, and Norway follow the quota limits based on abundance estimates mainly from time series of data from the North Atlantic Sightings Survey (NASS) series and the independent Norwegian line transect surveys (NILS). These large-scale surveys were initiated after the moratorium and have been conducted since 1987 over a large part of the central and north-eastern North Atlantic.

During the period covered by NASS and NILS, changes in the abundance and/or distribution of several species of cetacean have been documented (Houghton et al., 2020; NAMMCO, 2019a; Neyman, 2018; Pike et al., 2020a, 2020b, 2019a, 2019b, 2009a, 2009b; Víkingsson et al., 2015). The ecological impacts of the climatic changes described above go from phytoplankton through the trophic web to the top predators (Drinkwater et al., 2003; Hátún et al., 2009). Climate change is an indirect pressure that is expected to have large spatial scale impacts on marine mammal populations (Moore, 2008; Walther et al., 2002) because the availability and distribution of prey will also be affected (Moore, 2008; Moore and Huntington, 2008). Surveys under the NASS and NILS programmes are conducted during the summer months. Although odontocetes breed in summer, feeding is a primary activity of all species in the area at this time (e.g. Canning et al., 2008; Fall and Skern-Mauritzen, 2014; Martin and Rothery, 1993; Ressler et al., 2015; Sigurjónsson and Víkingsson, 1997; Skern-Mauritzen et al., 2011) and it is assumed that changes in abundance and distribution are linked to their prey (Laran and Drouot-Dulau, 2007; e.g. Moore et al., 2019; Øien, 1988; Víkingsson et al., 2015). Understanding how marine

mammals/top predators respond to changes in the ecosystem through interactions with their prey at lower trophic levels allows for a synoptic view of the ecosystem and the potential use of marine mammals as ecosystem indicators (Moore, 2008; Moore et al., 2019).

Several changes in cetacean distribution and/or abundance documented by NASS and NILS have been suggested to be related to variations in physical and biological components of the marine ecosystem. In Chapters 3, 4, and 5 a detailed introduction to each of the species is given, describing information regarding relationships with physical and biological oceanographic variables, distribution, prey, abundance and pressures. These include examples of decadal-scale changes in the abundance and/or distribution of cetaceans that have been revealed by the long-term surveys in the North Atlantic (NASS & NILS) showing evidence of the effects of environmental change on the populations (Hátún et al., 2009; Nøttestad et al., 2015; Víkingsson et al., 2015). As mentioned above, to understand long-term climatic effects at large spatial scales it is important to make comparisons using ecological data at similar scales. NASS and NILS datasets allow this project to make these types of comparison and to develop a synoptic view of some processes from 1987 to 2015.

The study period is divided into two periods, 1987-1989 and 1998-2015, to see the effects of climate change and to take into account any additional effects of the Atlantic Multi-decadal Oscillation (AMO) (see section 1.2). In addition, the division of the data in this way enables the extensive environmental data available more recently to be used in the later period, which are not available to be used for the earlier period. As described above, physical changes have been shown to affect the bottom of the trophic web up to higher trophic levels. Linking the mechanistic way in which the physical environment leads to biological responses and changes in population distribution is crucial to understand the effects of environmental change. Knowledge of the processes that determine distribution is a keystone in ecology that can also provide scientific advice relating to the conservation and management of species that are impacted by different human activities (Redfern et al., 2006).

1.5 Thesis overview

To improve understanding of cetacean distribution and habitat use, relationships with environmental variability need to be investigated. The main goal of this thesis is to improve understanding of the environmental factors that influence the distribution and habitat use of a

range of cetacean species in the central and north-eastern Atlantic over a period of three decades by modelling their relative abundance as a function of a series of static and dynamic variables. Some of these variables have not previously been considered in this area but have been shown to be important elsewhere. This project aims to provide a better understanding of the species ecology in the North Atlantic by identifying key factors that have influenced their distribution and habitat use in the last 30 years while also providing clues on how environmental changes may affect cetacean populations in the future.

This study is timely and important because of the clear evidence of changes at the ecosystem level in the North Atlantic. These changes, described above, include variations in the oceanography of the area and variations all through the food web from phytoplankton to top predators. It is of fundamental importance to understand how the top predators respond to these changes in order to understand better the mechanisms that link them to the ecosystem. Given the current climate change scenario and increasing anthropogenic pressures, understanding cetacean distribution and habitat use is essential to underpin advice on their conservation and management. As mentioned above, poorly managed impacts on species and their ecosystems could push them to their limits and climate change can strengthen these negative effects (Walther et al., 2002).

The species selected in this study are the most common cetacean species in the area and they have diverse life histories. However, despite this diversity, the species can be clustered into three groups: deep-diving cetaceans (sperm, pilot and northern bottlenose whale), baleen whales (fin, humpback and mike whale) and two Delphinidae species (killer whale and white-beaked dolphin). These groups represent three guilds of similar species, as described above. The Delphinidae grouping comprises two species with very diverse habits but they have in common feeding on high trophic level prey; they might however be considered as ‘other Delphinidae’. The static and dynamic variables used to understand the species distribution and habitat use include a series of relief variables that could help to explain, for example, the influence of prey aggregations through the link between topography and currents and the distribution of prey at certain depth. SST and related variables could be related to temperature gradients at the surface, prey aggregations and enhanced primary production. Plankton-related variables explain the presence of the lower tropic level and may help explain links with higher trophic levels. SSH and mixed layer depth variables could help to understand the influence of mesoscale activity in the water column that may also be linked to prey aggregations.

Chapter 2 describes the data and methods used in the subsequent Chapters 3, 4, and 5. It includes preparation and processing of the data from the NASS (Iceland-Faroes) and NILS (Norway) cetacean datasets, including estimation of detection probabilities for the different species studied. Acquisition and preparation of environmental covariate data for static and dynamic variables are described in this chapter. Steps in spatial modelling using Generalized Additive Models (GAMs) are also described; these models are flexible and have been widely used to investigate species-habitat relationships for cetaceans.

Chapters 3, 4 and 5 evaluate the distribution and habitat use of three cetacean guilds: deep-diving cetaceans, baleen whales and two Delphinidae species, respectively, in the central and north-eastern North Atlantic. The study period is divided into two periods, 1987-1989 and 1998-2015, and the models are fitted to investigate each species distribution in relation to environmental features (static and dynamic variables) in each of the periods. Comparisons of the model relationships and predicted distributions are made within species (between periods) and between species of the same guild, to understand the drivers of distribution and whether these have changed over time.

Chapter 6 is a general discussion comparing distribution and habitat use among the three cetacean guilds, deep diving cetaceans, baleen whales and Delphinidae. Such a comparison of multiple cetacean species over three decades has not previously been attempted for such an extensive area. This work provides a better understanding of cetacean species ecology in the North Atlantic by identifying key factors that have influenced their summer distribution and habitat use in the last 30 years, while also providing clues about how environmental changes may affect cetacean populations in the future. This information could also inform assessments of human pressures on these species for example in consideration of overlap with areas of anthropogenic activities.

2 METHODOLOGY

2.1 Data preparation and processing

2.1.1 Cetacean survey data

Data on cetaceans were made available from shipboard surveys conducted since 1987 over a large part of the central and eastern North Atlantic: the North Atlantic Sightings Surveys (NASS) and the Norwegian Independent Line transect Surveys (NILS). All surveys were conducted in the summer (June, July and August) aiming for simultaneous coverage of the area within each year. The NASS were conducted by Iceland and the Faroe Islands, and covered the period 1987-2015. The Norwegian NILS covered the period 1987-2013. Independently of the species of interest, surveys recorded sightings of all cetaceans encountered (Øien, 2009; Øien and Bøthun, 2009; Víkingsson et al., 2009). The eight consistently most recorded species over all survey years have been selected as a focus in this study, including three baleen whale species (fin, humpback, and minke whales) and five toothed whale species (sperm, pilot, northern-bottlenose and killer whales, and white-beaked dolphins).

During the late 1980s, several North Atlantic nations including Norway, Iceland and the Faroe Islands joined efforts to generate synoptic estimates of whale population abundance, motivated by the beginning of the International Whaling Commission's Moratorium on commercial whaling. The first survey was conducted in the summer of 1987. The second survey was in 1989 and extended farther south. The third and largest simultaneous survey was in 1995. After 1995, Norway introduced a protocol to survey parts of the northeastern Atlantic each year to cover the whole area every 6 years in a so-called mosaic survey (Pike, 2009; Víkingsson et al., 2009).

Since 1994, the primary motivation for the surveys has been to generate estimates of abundance of species subject to hunting for consideration by the International Whaling Commission (IWC) Scientific Committee in its work on the Revised Management Procedure for commercial whaling and Aboriginal Whaling Management Procedures. The Scientific Committee of the North Atlantic Marine Mammal Commission (NAMMCO) also reviews these estimates. Abundance estimates for species that are not hunted has not been a priority, and nor has using these data for other purposes such as distribution/habitat use modelling. However, the time series of cetacean data

collected from these surveys is arguably the most comprehensive in the world at such a large spatial and temporal scale and the data are valuable for investigating ecological questions that require information at such a scale.

Differences in data collection protocols between the two datasets (Iceland-Faroes and Norway) required several steps of data preparation, processing and preliminary analysis. In summary four steps were followed. First, survey data were standardized for differences among years in both datasets. Here, the Norwegian data required extra care because on-effort data and minke whale duplicates needed to be identified, and effort and observation data needed to be linked. At the end of this step, all data within each year and among years within a 6-year (mosaic) period were consistent. Second, data were processed prior to modelling detection probability. This included standardizing sighting and associated covariate data, as necessary, and identifying and fixing inconsistencies in data and measurement units. Third, data were prepared for modelling. All data within each dataset from all survey years and mosaic periods were joined. The Iceland-Faroes data required extra steps to process effort legs into segments of effort of a target length suitable for modelling. The fourth final step was to join the Icelandic-Faroes and Norwegian datasets together.

2.1.1.1 Iceland- Faroes

Data were available from the Iceland and Faroes shipboard surveys (NASS) conducted in 1987, 1989, 1995, 2001, 2007, and 2015 (Figure 2.1). The surveys have been described by Víkingsson et al. (2009) and Pike et al., (Pike et al., 2020a, 2019b); details relevant to the data processing and analysis are described below. Survey effort varied among years.

The surveys were designed to maximize effectiveness for the primary target species of the supporting countries. For Iceland, the primary target species have consistently been fin and minke whale; 1989 was the only year during which the sei whale was also a primary target. For the Faroes, the target species has consistently been the long-finned pilot whale and in some years also fin and minke whales. However, as mentioned above, sightings of all cetaceans were systematically recorded (Víkingsson et al., 2009).

Data collection followed standard line transect methods and all the standard data for abundance estimation were collected (Buckland et al., 2001). Víkingsson et al., (2009), summarized the technical information on the vessels and observation platforms used by Iceland and the Faroes in 1987, 1989, 1995 and 2001. Survey information for 2007 and 2015 can be found in Pike et al., (Pike et al., 2020a, 2019a, 2019b).

In Iceland, in 1995, 2001 and 2007, double platform surveys were conducted in so-called "tracker" configuration so that mark-recapture line transect methods could be used to estimate the proportion of animals missed on the transect line and potentially to account for any movement of animals in response to the survey vessel (Buckland and Turnock, 1992). In 2015, the survey was conducted in so-called "independent observer (IO)" configuration in which there was two-way independence between the two platforms (i.e. without communication).

Data on sightings of cetaceans were collected to allow detection probabilities to be estimated from perpendicular distances calculated from radial distances and angles. Radial distances were recorded in meters. Distances were estimated by eye or by binocular reticule and the angle was measured using an angle board. Data on group size were also collected (Table 2.1).

The Faroese surveys were generally conducted in the same way as the Icelandic surveys. However, in 1995, additional experimental steps were implemented to estimate pilot whale group size (Desportes et al., 1996 In: Víkingsson et al., 2009).

In all surveys, data from both platforms were combined into a single platform (excluding duplicate sightings seen from the second platform) and the Icelandic and Faroes data were joined into a single dataset. In total, 62,123 nm of transect lines were included for analysis (Table 2.1). Figure 2.1 shows the area covered in the six years of NASS. The whole survey area in each year was divided into blocks. Searching effort within blocks consisted of survey transects each comprising a number of effort legs (Figure 2.1). Data on sightings were included in the same records as effort. A new effort leg was initiated when survey conditions changed or after consecutive sightings. The weather variables available for use were Beaufort scale, a measure of wind speed as inferred from sea conditions (in 2015 wind speed (m/s) was measured directly and converted to Beaufort scale), visibility and a weather index. Searching effort included sea conditions up to Beaufort 7 on Icelandic surveys and up to Beaufort 4 on Faroese surveys. But, searching effort in Beaufort 7 was excluded. Beaufort was averaged when it was recorded as a range. Visibility was recorded in nm or on a scale of 0 (excellent) to 3 (very poor); missing values

(recorded as -1) were re-labeled as NA. All visibility data were standardized to the 0-3 scale: 0 (>5nm), 1 (2-5nm), 2 (1-2nm), and 3 (<1nm). The weather index (1-9) referred to rain, fog and cloud cover but these data were not consistently collected and were not considered further.

Table 2.1. Yearly summary of searching effort and the number of individuals detected of the focal species in Iceland and Faroes NASS shipboard surveys. BA- minke, BP- fin, MN- humpback, PM- sperm, GM- pilot, HA- northern bottlenose, OO- killer whale, and LL- white-beaked dolphins.

Year	**Effort (nm)**	**BA**	**BP**	**MN**	**PM**	**GM**	**HA**	**OO**	**LL**
1987	16653	209	352	115	107	3953	220	182	484
1989	10705	215	458	26	161	3488	53	198	445
1995	7862	182	454	400	90	1448	169	37	757
2001	9893	269	942	481	198	1240	386	309	1028
2007	7261	35	395	136	99	893	84	35	381
2015	9749	144	707	159	134	4235	188	164	243
Total	62123	1054	3308	1317	789	15257	1100	925	3338

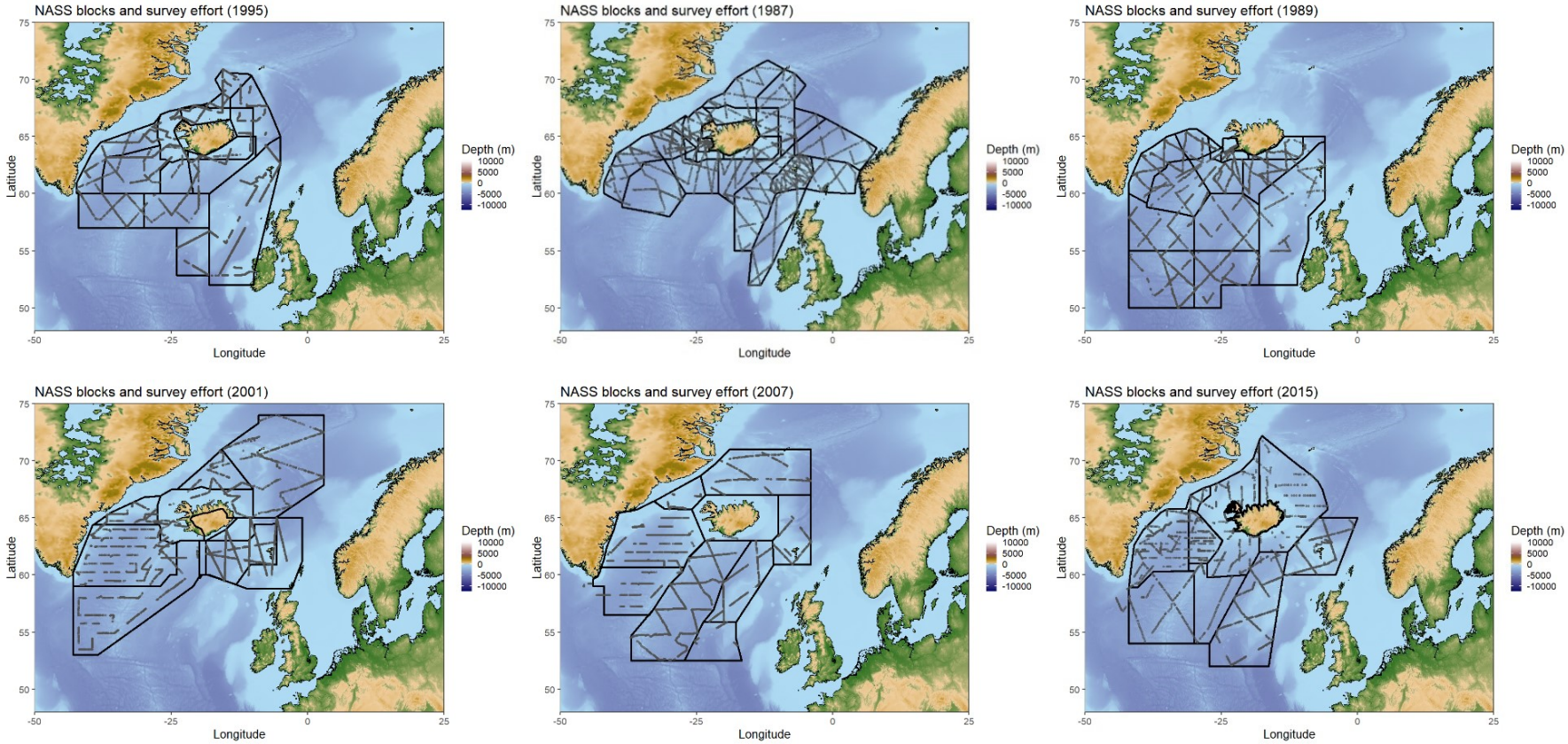

Figure 2.1. NASS survey effort in each year. Survey blocks are shown as black boxes and segment (see section 2.1.3.1) mid-points are shown as grey dots. Maps were plotted using the geographic coordinate system WGS84 and overlaid on the bathymetry of the area (ETOPO2).

2.1.1.2 Norway

The data from Norwegian surveys were broadly similar to those from Iceland and Faroes. The description (narrative) of the Norwegian surveys can be found in Øien and Bøthum (2009) and Solvang et al. (2015) and some generalities are also given in Víkingsson et al. (2009). All the surveys were run in mid-summer centred around July. The surveys in 1987, 1988, 1989, and 1995 covered the Norwegian and Barents Seas and adjacent waters synoptically; the area surveyed in 1995 was the largest. In 1996, a programme of "mosaic" surveys was initiated covering all parts of the area surveyed in 1995 over a period of 6 years (Øien and Bøthun, 2009). To date, three such mosaic surveys of the whole area have been completed in 1996-2001, 2002-2007, and 2008-2013 (Figure 2.2).

Single platforms were used on surveys in 1987, 1988, 1989 and some of the vessels in 1995 (Schweder et al., 1997). Two independent platforms were used on all surveys since 1996 and in 84% of the survey time in 1995 (Schweder et al., 1997; Skaug et al., 2004, 2002; Solvang et al., 2015). Primary effort data were collected while the vessel moved along the predefined transects at an average speed of 10 knots. Searching was done by naked eye.

Data per year and for each 6-year mosaic surveys were available in three separate datasets: observers, effort, and sightings. Here only the effort and sighting datasets were used. Effort data included a column describing the vessel's activity, indicating the type of effort: normal survey mode (predefined trackline and primary search effort); experiments; no primary effort; course change; unplanned transects conducted in primary search mode; speed change; closing mode; and end of day. R code developed in collaboration with Raul Martinez (Centro de Investigaciones Biológicas del Noroeste, CIBNOR, Mexico) selected only primary search mode effort for analysis and excluded closing mode, experiments and off primary search effort. Manual checking of the data was undertaken, and errors or inconsistencies rectified mainly due to different labeling among years. Once all the primary survey data (on-effort) were complete, the length in km of each piece of effort was calculated using the R package 'raster' and the function 'pointDistance' (version 2.6-7.; Hijmans 2017). In total 90,8387 nm of transect lines were included for analysis.

Data on sightings of cetaceans were collected to allow detection probabilities to be estimated from perpendicular distances calculated from radial distances and angles (degrees). Radial distances in the earlier years (1987, 1988, 1989)- were recorded in units of 1/100nm while from 1995 onwards they were in meters; all radial distances were standardized in meters. Distances

were estimated by eye and the angle was measured using an angle board. Data on group size were also collected (Table 2.2).

As two platforms were operated independently, the same group of cetaceans could have been seen by observers in both platforms (i.e. duplicate). Only minke whales' duplicates could be determined by using an algorithm developed in Norway, duplicates then were removed from the data. This could not be done for the other species so, to avoid duplicates being included, data only from one platform (main platform, A) were included.

Effort data have been processed for each of the survey years/ rotations to use only on-effort data. Sightings were associated with the effort data by linking three arguments between the two databases: vessel, date, and time -of the sighting and time interval (start-end) of the transect.

Following the processing described above, the Norwegian data consisted of a single table containing both effort and sightings data, equivalent to the Icelandic/Faroese data. Survey/mosaic areas were divided in blocks containing survey transects each comprising effort legs. Each effort leg started when sighting conditions changed, or when survey mode returned to on-effort mode. Sighting conditions such as sea state (Beaufort scale), visibility, weather, wind speed, wind direction and glare were recorded (Øien, 2009; Schweder et al., 1997). Searching effort generally ceased when Beaufort was above 4 and visibility was below 1 nm. Beaufort was averaged when it was recorded as a range. Visibility was converted to nm from the meteorological units given (1/100 nm). The weather index was given in 12 categories that included, cloud cover, fog, rain, snow or a combination of them. Wind speed was recorded in m/s and wind direction was given in degrees where north was given as 360. Glare was recorded on a scale of 0-3, where 0 is none, 1 (some), 2 (moderate), and 3 (severe). Most of the sighting condition variables were inconsistently recorded throughout and within the years hence only Beaufort was considered further.

Table 2.2. Yearly summary of searching effort and the number of individuals detected of the focal species on Norwegian NILS shipboard surveys. BA- minke, BP- fin, MN- humpback, PM- sperm, GM- pilot, HA- northern bottlenose, OO- killer whale, and LL- white-beaked dolphins.

Year	**Effort (nm)**	**BA**	**BP**	**MN**	**PM**	**GM**	**HA**	**OO**	**LL**
1987	4193	86	59	3	17	0	0	98	80
1988	7723	412	142	37	47	0	41	44	12
1989	15893	613	56	16	83	75	2	138	128
1995	14571	1193	157	46	54	326	0	121	241
1996	3910	262	7	7	78	0	0	42	0
1997	2577	206	90	62	12	0	0	30	0
1998	3450	172	10	0	4	30	0	8	26
1999	3461	250	75	19	5	0	4	1	86
2000	2942	86	9	0	10	31	0	14	10
2001	1767	99	15	2	16	0	8	32	0
2002	3287	156	23	16	80	0	1	153	55
2003	2363	165	70	129	22	0	2	2	365
2004	1978	40	4	0	2	0	11	14	114
2005	2138	101	33	42	20	0	9	43	52
2006	2260	101	11	3	53	0	0	160	52
2007	2243	135	25	14	0	0	0	0	151
2008	2760	186	120	68	2	0	34	0	356
2009	2347	60	0	0	0	0	0	23	6
2010	2521	48	44	36	27	0	2	64	47
2011	3717	102	35	0	45	20	1	157	83
2013	4736	229	22	40	10	0	0	0	420
Total	90837	4702	1007	540	587	482	115	1144	2284

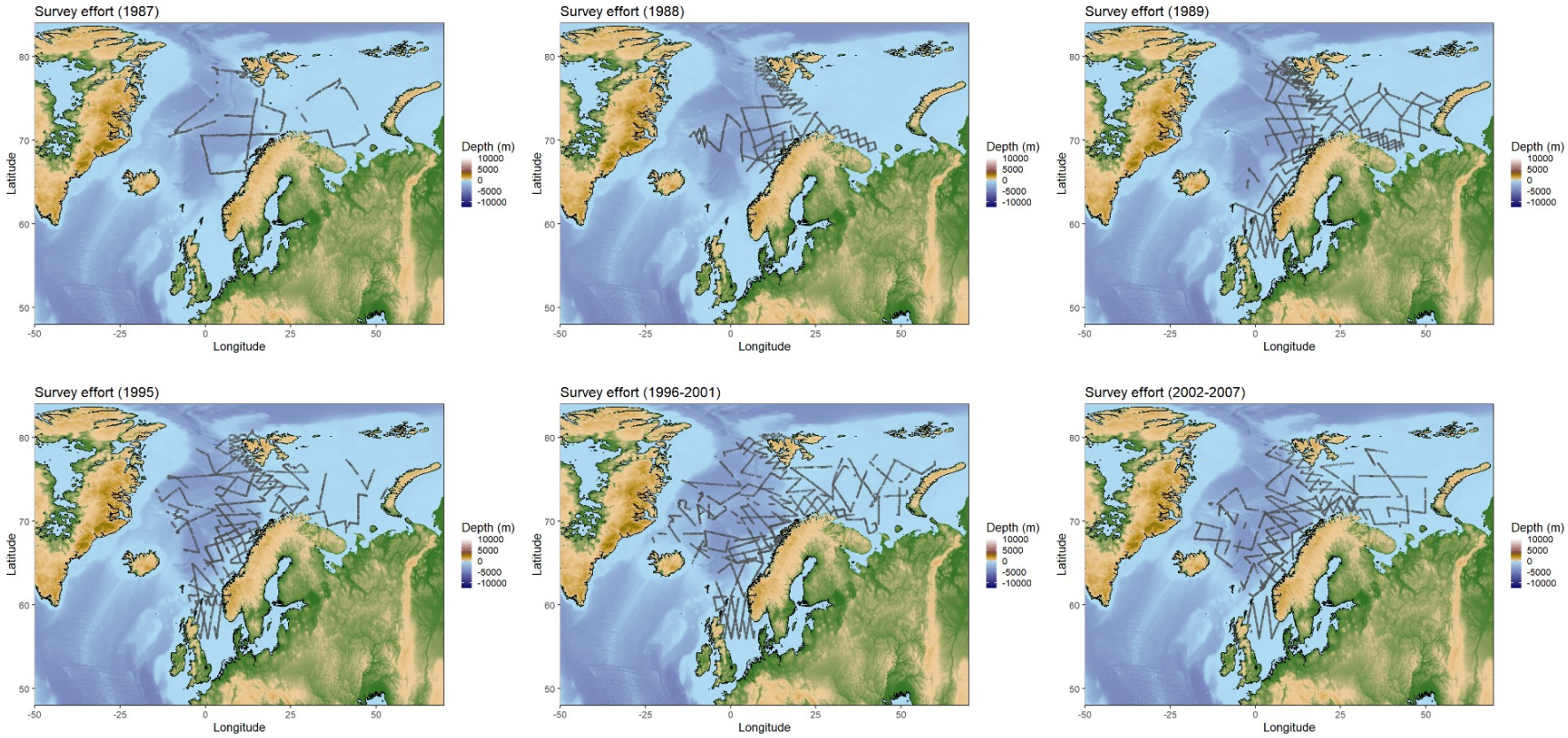
Survey effort (1987)
Survey effort (1988)
Survey effort (1989)
Survey effort (1995)
Survey effort (1996-2001)
Survey effort (2002-2007)
Latitude
Longitude
Depth (m)
10000
5000
0
-5000
-10000

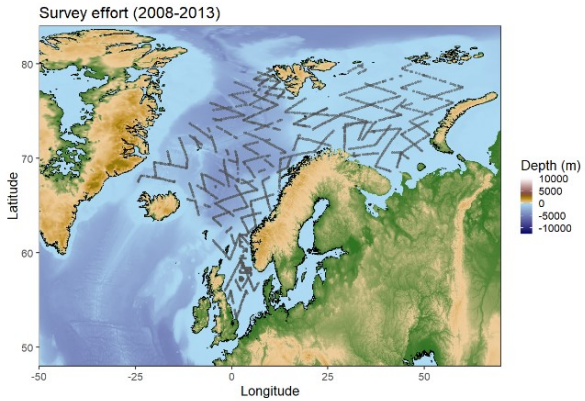

Figure 2.2. NILS survey effort in each year. Segment (see section 2.1.3.2) mid-points are shown as grey dots. Maps were plotted using the geographic coordinate system WGS84 and overlaid over the bathymetry of the area (ETOPO2).

2.1.2 Data preparation and processing for estimation of detection probabilities

The distance sampling data collected during the shipboard line transect surveys (angle and radial distance of each group of cetaceans sighted) were used to calculate perpendicular distance from the transect line. These data were used to estimate detection probabilities for the eight species. Prior to modelling detection probability (see section 2.2.1), some processing of the data was necessary.

2.1.2.1 Iceland- Faroes

Some measurements of radial distance were recorded as a range and in these cases the closest distance was used. If distance was recorded as not available (NA) sightings were excluded. Sightings were also excluded if the recorded angle did not fall within 0-360 or was given as a range. When group size was recorded as a range, the midpoint of the range (rounded up to a whole number) was used. Sightings with a low degree of certainty in species identification were excluded, as has been done in previous published studies using these data (Víkingsson et al., 2015, 2009); depending on which species these sightings actually were, it is possible that this led to an underestimation of density (Table 2.1).

Two covariates that could affect detection were considered. Beaufort was treated as a factor covariate ranging from 0-6. For some species, it was considered useful to group Beaufort into a smaller number of levels: two levels for northern bottlenose whales and white-beaked dolphins (Low 0-2 and High 2.5-6); three levels for minke, fin and pilot whales (Low 0-1, Medium 1.5-3, and High 3.5-6). Vessel was also considered as a factor covariate with 10 levels, corresponding to the 10 different vessels that had run surveys over the years. Other variables were assessed but not included due to missing data, for example: visibility was evaluated as a factor in the scale 0-3, but 37% of the data was missing.

2.1.2.2 Norway

As for the Icelandic and Faroese data, sightings were excluded if any of the basic data (radial distances, angle, and group size) were missing (labeled as 999 or 9999 in the original data). When group size was recorded as a range, the mid-point of the range (rounded up to a whole number) was used.

Again, as for the Icelandic and Faroese data, only Beaufort and vessel were evaluated as covariates that might affect detectability because these were the only covariates that were

consistent in the data. However, Beaufort was not recorded in 1988 and 1989, and was not consistently recorded in 1987. Because of the importance to consider Beaufort, Norwegian data were divided into 1987-1989 and 1995-2013 for distance sampling analysis. Only the vessel covariate was considered in 1987-1989. For 1995-2013 Beaufort was treated as a factor covariate ranging from 0-5. Grouping Beaufort into a smaller number of levels was also considered for some species: fin whales (Low 0, Medium 1-2, and High 3-5); pilot whales (Low 0-1, Medium 2, and High 3-5); and killer whales and white-beaked dolphins (Low 0, Medium 1-3, and High 4-5).

Vessel was evaluated as a factor with four levels for all years, which corresponded to the vessels grouped by their overall length (LOA): smaller than 30 m (1); 30 m - 40 m (2); 40 m - 50 m (3); and 50 m - 75.90 m (4) (Appendix 2-A).

The small number of sightings of pilot (3) and northern bottlenose (8) whales for the period 1987-1989 precluded estimation of the probability of detection for this period for these two species.

2.1.3 Data preparation and processing for habitat use modelling

The available cetacean data were used to model habitat use as a function of explanatory environmental covariates given in Table 2.3. The following sections describe the data processing necessary to prepare the data for habitat use modelling.

2.1.3.1 Iceland- Faroes

All data per year were organized and standardized as described above. Once all data was standardized, all the survey years were joined. Each effort leg was assigned a unique identifier.

Habitat modelling works most effectively if the sampling units are homogeneous, but in the Icelandic and Faroese data there was considerable variability in the length of the effort legs. Consequently, the data were processed to homogenize them as much as possible. In addition, it is important to match the length of the sample effort legs to the resolution of the environmental variables as far as possible. Based on the coarsest resolution of the environmental variables (Table 2.3), 0.25 degrees, the maximum leg was set to be no more than 25 km and longer legs were sub-divided (Figure 2.3). Matching the scale of the sampling unit (effort leg length) to the resolution of the covariate data, as far as possible, helps to ensure that the modelled

relationship accurately reflects the influence of the explanatory data on the response data. New unique identifiers were created, Sample.Label, which describes which original effort leg the new leg came from. Length, mid-latitude and mid-longitude were recalculated for each new leg.

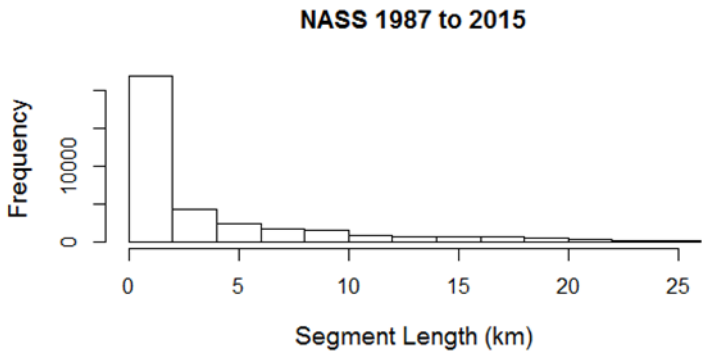

Figure 2.3. Distribution of effort legs lengths for the NASS data from 1987 to 2015.

The large majority of effort legs were small (Figure 2.3) because of the way the data were organized and made available. Small effort legs can lead to strong over-dispersion in the data to be modelled and are not desirable. To address this, small effort legs with the same conditions were joined, which involved a number of processing steps. First, it was necessary to identify if the survey effort has been continuous or if it stopped between adjacent transects. An index (laloindex) was developed to determine whether, within each transect, adjacent legs were contiguous based on their start and end latitude and longitude. Second, it was necessary to avoid mistakenly joining effort legs that were not contiguous (they could be from different dates, vessels, or transects). An identifier was created for this purpose as a combination of date, vessel name (vID), transect (nbl) and the index for latitude and longitude (laloindex).

This identifier allowed the use of a function called *segmentate* (developed by Sacha Viquerat, University of Veterinary Medicine Hanover, Germany) to join small effort legs if possible. The function was used to assign a new common identifier to effort legs that could be joined into segments of target length 18 km, with a maximum of 25 km. This process generated a new distribution of effort segments (Figure 2.4).

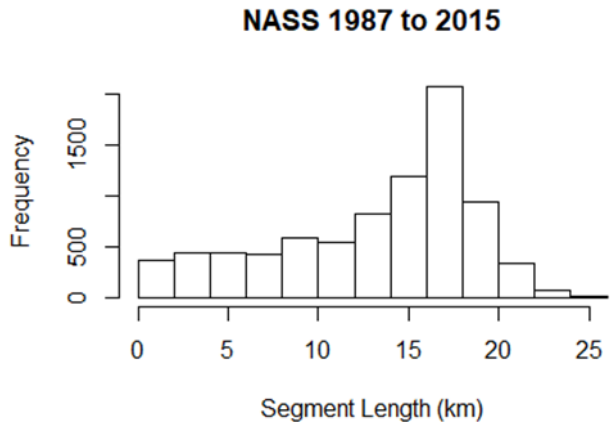

Figure 2.4. Distribution of processed segment lengths for the NASS data from1987 to 2015

The resulting data after running *segmentate* were evaluated for inconsistencies. This resulted in the deletion of 141 effort segments which had zero effort values and were not part of the previous effort segment. These reflected records that contained off-effort sightings or simply recorded the beginning of an effort leg.

Creating effort segments to use in modelling can accommodate the joining of effort legs with different conditions if the estimated effective strip half width (esw), and therefore the effective search area, is known for each leg so that the effective search area can be summed for each segment. The estimated effective strip half width (esw) from detection function modelling for each species (see section 2.2.1) was used to calculate effective search area for each effort leg as:

$$effective\ search\ area = (esw * 2) * effort\ leg\ length$$

which were added to the dataset. Segments were then grouped using the values of the common identifier resulting from running the *segmentate* function. New data columns were created for each of the new segments, including: average latitude and longitude, sum of survey effort (sum effort length), count of individuals seen in the segment (per species), occurrence as yes or no (per species), effective search area which (per species), and density which is the counts divided the effective search area (per species).

2.1.3.2 Norway

All data per year or mosaic were organized and standardized as described above. Each effort leg was assigned a unique identifier.

The lengths of the effort legs in the Norwegian data were distributed more homogeneously than for Iceland and the Faroes but needed some processing to limit the maximum length to 25 km (Figure 2.5). To keep consistency between the databases, the unique identifier among new legs Sample.Label was also created. For the new legs: lengths, mid-latitude, and mid-longitude were recalculated.

It was not necessary to use the *segmetate* function on the Norwegian data, hence effort legs and segments are the same but will here onwards be called segments for consistency between the two datasets.

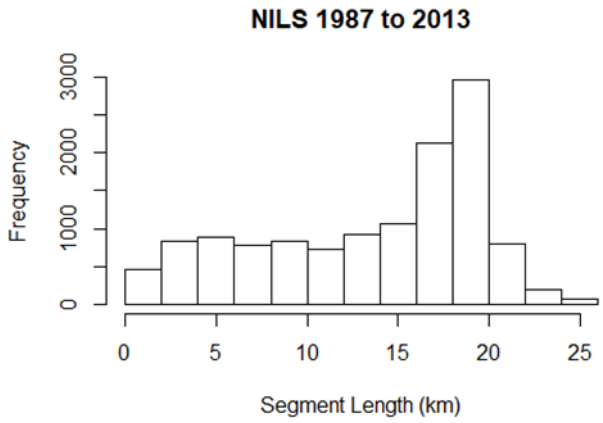

Figure 2.5. Distribution of segment lengths for the NILS data from 1987 to 2013.

The estimated effective strip half width (esw) from detection function modelling (see section 2.2.1) was used to calculate effective search area for each segment, as defined above, and added to the dataset, along with calculated density.

2.1.4 Environmental data preparation and processing

Environmental variables used in analysis included physiographic and oceanographic variables for the entire study area. Details of the description and source of each variable are given in Table 2.3. Physiographic data comprised depth and associated relief variables. Depth was extracted using R and the package 'marmap' (version 0.9.6.; Pante and Simon-Bouhet, 2013), which imports the 2-Minute Gridded Global Relief Data (ETOPO2). Derived from depth, the associated relief variables used for analysis were slope and aspect which were computed using the package 'raster' (version 2.6-7.; Hijmans, 2017).

Oceanographic variables were monthly composites of satellite-derived data processed by NEODAAS (https://www.neodaas.ac.uk/Home). The oceanographic data included sea level anomaly, sea surface temperature, ocean thermal front variables derived, chlorophyll *a*, primary productivity, and phytoplankton size class variables. Some of the data from NEODAAS come from COPERNICUS (https://www.copernicus.eu/en); NEODAAS provides additional quality control such as using region-specific algorithms for the ocean colour variables. Derived ocean thermal front variables and phytoplankton size class variables are a unique product developed by NEODAAS. Frontal data as maps are generated using SST values in a method developed by Dr Peter Miller. Oceanographic variables vary temporally, and lagged relationships were studied as far back as four months of lag, this included March – August comparisons. Lagged relationships were evaluated because some environmental conditions in the spring are the foundation for the summer when the surveys took place. Sea level anomaly was the exception where only June to August data were considered because this variable is representative of the water masses and lagged effect are not expected.

Additional oceanographic variables, also as monthly composites, processed by COPERNICUS were obtained from GLORYS2V4 (1993-2015) global ocean reanalysis for the Global Ocean and Sea Ice Physics. The reanalysis was performed with NEMOv3.1, the assimilated observations were satellite-derived and from in-situ profiles from the CORA4 data base (Gilles and Parent, 2017a, 2017b). The selected variables included mixed layer depth, sea surface height, sea floor potential temperature, and salinity. These variables also vary temporally, and lagged relationships were also evaluated from March - August.

As described above, the dynamic variables from both NEODAAS and COPERNICUS are provided as monthly composites, not as daily data. Regarding the lagged relationships, the same time lag was used for the whole area because the primary goal of the thesis is to evaluate the area holistically. However, there are regional differences over this wide area; using the same lags for the whole area assumes the same relative change over the seasons everywhere. The models thus attempt to capture these relative changes on average over this broad geographic scale.

Each of the covariate time series was quality checked. While doing this some issues were found that required NEODAAS to reprocess the sea surface temperature data. Specifically, the NASA algorithm used was problematic for the most northern area, generating high sea surface temperature values particularly for the month of April in 1996 (Figure 2.6). Calculations of the percentage of missing data for each month of each covariate were also necessary because more care must be taken during analysis if a substantial amount of data are missing. For example, the

high temperatures in 1995 occurred in a year with a considerable amount of missing data (Figure 2.7); these data were missing because of problematic data quality reported by NOAA particularly for that year (Selmes, 2018, personal communication, Nov 8th 2018). It is uncertain if the high temperatures occurred only because of the few data available or because 1995 was an anomalous year.

Different species are known to have different affinities for different depths (Table 2.3). Depth was used as a continuous variable and not as a factor describing broad ocean features (e.g. ocean-basin, shelf-edge, shelf); factor levels may conceal more complex relationships of interest that have been described in other studies. Using a continuous scale for depth allows inter and intraspecies comparisons as well as improving advice regarding conservation and management.

Regarding the variable mixed layer depth (mlp) the depths estimated by the model GLORYS2V4 are over-estimated in the North Atlantic Ocean deep convection areas (Gilles and Parent, 2017a; Våge et al., 2009), but the timing and the general trend is correct. Although the values are therefore not accurate for the area, for this thesis the variable was used for modelling because it can show the general tendency of the depth of the mixed layer. Interpretation of the modelled relationships for this variable was therefore limited to comparisons of deep versus shallow mixed layer depths.

Environmental variables were extracted for the mid-location of each segment (average latitude and longitude) using package 'raster' (version 2.6-7.; Hijmans, 2017). The extraction was a weighted mean over circular buffers of 10 km radius around the mid-location at each segment. The higher contribution 'weight' to the mean was given to the data points closer to the segment's mid-location. There were two exceptions to this process. First, due to the resolution of the data the circular buffers were 20 km radius for sea level anomaly and absolute dynamic topography variables (NEODAAS provided) and for mixed layer deep, sea surface height, sea floor potential temperature, and salinity (COPERNICUS provided). Second, median instead of weighted mean values were extracted for the variable temperature front side because values were either 0, 1 or -1.

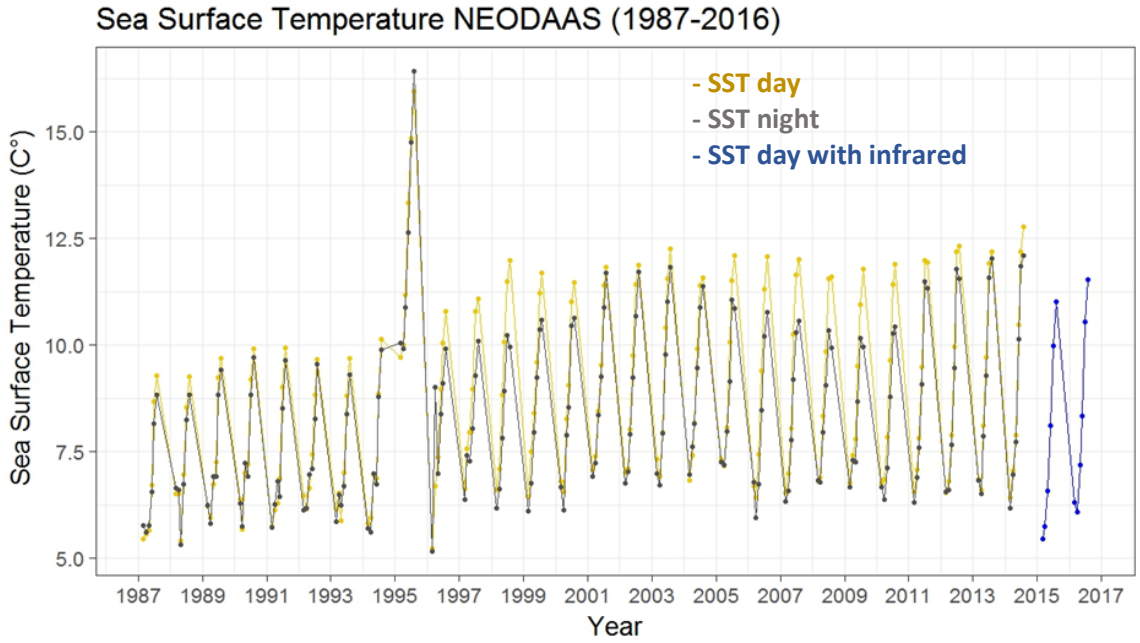

Figure 2.6. Monthly (March to August) time series of sea surface temperature data processed by NEODAAS from day and night satellites until 2014, and 2015 onwards by infrared, illustrating the problem encountered during quality checking for 1995 (first large peak) and April 1996 (small unique point peak).

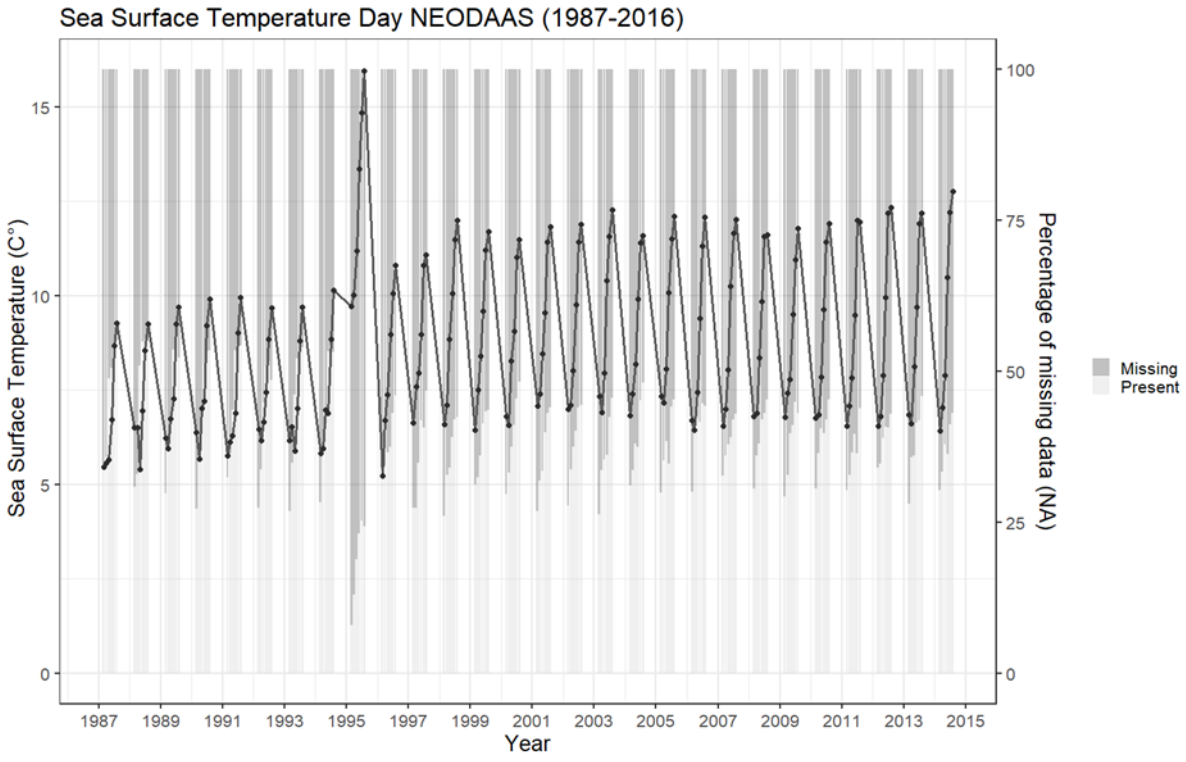

Figure 2.7. Monthly (March to August) time series of sea surface temperature data processed by NEODAAS from day satellites until 2014. Grey bars in the background show the total data, darker grey indicates the missing data (NA). The black dots joined by a line depict monthly mean temperature.

Table 2.3. Environmental covariates: description, source and any abbreviation used in species distribution modelling. Weighted means were calculated giving more weight to variable values close to the mid-grid point.

Name	Description	Source	Justification
Depth	Weighted mean of depth in meters	2-Minute Gridded Global Relief Data (ETOPO2). NOAA Satellite and Information Service. Extracted using 'marmap' R package.	Distribution of prey at certain depth. For example, deep divers feed on prey that inhabit deep waters. Minke and humpback whales feed on coastal-shelf prey, while fin whales feed offshore in deeper waters.
Slope	Weighted mean of slope of the sea floor in degrees	Derived from ETOPO2 bathymetric data. Extracted using 'marmap' R package. Computed using 'raster' R package, function terrain.	Associated with currents, slope gradients favour nutrient resuspension, increase of primary production and prey aggregation.
Aspect	Weighted mean of aspect of the sea floor in degrees	Derived from ETOPO2 bathymetric data. Extracted using 'marmap' R package. Computed using 'raster' R package, function terrain.	The angle that the sea floor is facing is associated with areas of upwelling or downwelling. Large scale signals of major currents which can be linked to a biogeographical signaling.

Sea level anomaly (SLA)	Sea level anomaly is the difference between sea surface height and a mean sea surface. Sea surface height is derived from satellite altimetry, and the mean sea surface is calculated from 20 years of these data. Weighted mean of SLA for the months of June to August 1994 to 2015, except 2006	Data were processed by NEODAAS from CMEMS L3 data. The altimetry data are produced by the Copernicus Marine Environment Monitoring Service (CMEMS) Sea Level-TAC multimission altimetry processing system. Altimeter missions: Jason-3, Sentinel-3A, HY-2A, Saral/AltiKa, Cryosat-2, Jason-2, Jason-1, T/P, ENVISAT, GFO, ERS1/2. Resolution: 0.25 degree, monthly composite.	Changes in SSH, show changes in mesoscale activity, influencing primary productivity, prey aggregation.
Sea surface temperature (SST)	Weighted mean sea surface temperature (°C) for the months of March to August 1987 to 2015	Data were processed by NEODAAS from NOAA L3 data. Sensor: Advanced Very High Resolution Radiometer (AVHRR); Resolution: 9km, monthly composite.	Related to surface gradients and temporal changes and seasonal progression linked with productivity.
Front gradient density (F.graden)	The gradient magnitude of detected fronts, spatially smoothed to give a continuous distribution of frontal activity. Given in units of °C per pixel distance (9 km). Sigma=5 pixels; sigma is link to the smoothing of the map, larger sigma will cause more severe smoothing to the front metric map. Weighted mean front density values for the months of March to August 1987 to 2015	Front gradient density is a derived covariate of SST. Data were processed by NEODAAS. Sensor: Advanced Very High Resolution Radiometer (AVHRR); Resolution: 9km, monthly composite.	Front metrics are associated with surface gradients, temporal changes and seasonal progression. Also linked with primary production, productivity prey aggregation and the presence of higher trophic levels.
Front persistence (F.pfden)	The fraction of cloud-free observations of a pixel for which a front was detected, spatially smoothed to give a continuous distribution. Sigma=5 pixels; sigma is link to the smoothing of the map, larger sigma will	Front persistence is a derived covariate of SST. Data were processed by NEODAAS. Sensor: Advanced Very High Resolution Radiometer (AVHRR); Resolution: 9km, monthly composite.	

	cause more severe smoothing to the front metric map. Weighted mean of front persistence values for the months of March to August 1987 to 2015		
Distance to major front (F.dist)	Distance to the closest major front, determined using a simplified version of the frontal strength map. Units are in pixels or km (by multiplying by 9). Sigma=4 pixels; sigma is link to the smoothing of the map, larger sigma will cause more severe smoothing to the front metric map. T- high=0.5; low values as 0.5, generate a more detailed map of simplified contour. Weighted mean of distance to major front values for the months of March to August 1987 to 2015	Distance to the major front is a derived covariate of SST. Data were processed by NEODAAS. Sensor: Advanced Very High Resolution Radiometer (AVHRR); Resolution: 9km, monthly composite.	
Temperature front side (F.side)	Whether the front is on the cold (-1) or warm (+1) side of the closest major front. Median of front persistence values for the months of March to August 1987 to 2015	Temperature front side is a derived covariate of SST. Data were processed by NEODAAS. Sensor: Advanced Very High Resolution Radiometer (AVHRR); Resolution: 9km, monthly composite.	

Chlorophyll *a* (chl*a*)	Weighted mean Chlorophyll *a* concentration [mg m^{-3}] for the months of March to August 1998 to 2015	Data products generated by the Ocean Colour component of the European Space Agency Climate Change Initiative project. Data were processed by NEODAAS (NERC Earth Observation Data Acquisition and Analysis Service) from ESA Ocean Colour CCI L3 data. Sensor: MERIS, MODIS Aqua, SeaWiFS LAC and GAC, VIIRS; Resolution: 9 km, monthly composite.	Plankton related variables explain the presence of the lower tropic level and give possible explanations of the links with higher trophic levels.
Primary production (PP)	Weighted mean primary production [mg C m^{-2} day^{-1}] for the months of March to August 1998 to 2015	Primary production is a derived covariate of Chlorophyll *a*. Data were processed by NEODAAS where chlorophyll profile parameters and photosynthesis parameters were used in conjunction with the remotely-sensed chlorophyll data from the OC-CCI v2.0 products (Sathyendranath et al., 2016). Average sea-surface irradiance (Photosynthetically-Active Radiation, PAR) for each month was taken from the NASA MODIS and SeaWiFS PAR products (OBPG, 2014). Resolution: 9km, monthly composite	Similar to Chlorophyll *a* is a proxy of prey availability.
Phytoplankton size class Chlorophyll	This comprises three sub-covariates giving the amount of chlorophyll present in three size class groups: • c02to2: Picoplankton (between 0.2 µm and 2 µm) • c2to20: Nanoplankton (between 2 µm and 20 µm) • c20to200: Microplankton (between 20 µm and 200 µm)	Phytoplankton size class Chlorophyll is a derived covariate of Chlorophyll *a.* Resolution: 9 km, monthly composite.	Phytoplankton size class is a proxy for prey availability. The division into plankton sizes allows inference of phytoplankton community succession in terms of concentration (size) and proportion (fraction) of the different groups.

	Weighted mean of the chlorophyll concentration for the months of March to August 1998 to 2015		
Phytoplankton size class fraction	This comprises three sub-covariates giving the proportion (0-1) of total chlorophyll present that is present in three size class groups: • f02to2: Picoplankton (between 0.2 µm and 2 µm) • f2to20: Nanoplankton (between 2 µm and 20 µm) • f20to200: Microplankton (between 20 µm and 200 µm) Weighted mean of the proportions for the months of March to August 1998 to 2015	Phytoplankton size class fraction is a derived covariate of Chlorophyll *a.* Resolution: 9 km, monthly composite.	
Density ocean mixed layer depth (mlp)	Weighted mean ocean mixed layer depth (m) for the months of March to August 1995 to 2015	Global reanalysis, GLORYS2V4. It relies in three main components, 1) the ocean model (including the surface atmospheric boundary condition, 2) the data assimilation method and 3) the assimilated observations. Resolution: 0.25 degree, monthly composite.	Associated with mesoscale gradients in the water column. Influencing nutrient aggregation which is linked with prey aggregations.

Sea surface height (ssh)	Weighted mean sea surface height (m) for the months of March to August 1995 to 2015	Global reanalysis, GLORYS2V4 as in mlp. Resolution: 0.25 degree, monthly composite.	Associated with changes in mesoscale activity, influencing primary productivity, prey aggregation
Sea floor potential temperature (bT)	Weighted mean bottom temperature (Kelvin) for the months of March to August 1995 to 2015	Global reanalysis, GLORYS2V4 as in mlp. Resolution: 0.25 degree, monthly composite.	Related to deep water horizontal gradients and temporal changes. Associated with changes in the water column, including warming.
Salinity (sal)	Weighted mean salinity (PSU) for the months of March to August 1995 to 2015	Global reanalysis, GLORYS2V4 as in mlp. Resolution: 0.25 degree, monthly composite.	Associated with water masses origin (horizontal gradients), influencing prey type.

2.2 Analytical methods

2.2.1 Modelling Detection Probability

Detection probability was modelled for each of the eight species including the evaluation of covariates that might affect detection. Packages 'Distance' (version 0.9.7.; Miller, 2017) and 'mrds' (version 2.1.18.; Laake et al., 2017) were used in R (version 3.4.3.; R Core Team, 2018).

For each species, whether or not to truncate the perpendicular distance data prior to modelling detection probability was investigated as a balance between removing distant observations to improve model fit and retaining as much as data possible (Buckland et al., 2001). Selection among models at different truncation distances was done using the unweighted Cramer-von Mises goodness of fit test.

Key detection functions evaluated were the half-normal and the hazard rate. Covariates evaluated were Beaufort (original data or grouped into fewer levels), and vessel.

Following any truncation of the data, the best models were selected using Akaike's Information Criterion (AIC). Q-Q plots and the results of the unweighted Cramer-von Mises test were also inspected. If the difference in AIC between models was less than 2 units and both models seemed adequate, the simplest model with fewest parameters was chosen.

The best models of detection probability for each species for the Iceland-Faroes data 1987-2015, the Norwegian data for 1987-1989, and the Norwegian data for 1995-2013 were used to estimate effective strip half width (esw) to be used to calculate effective search area (see section 2.1.3).

2.2.2 Species Distribution Modelling

2.2.2.1 Preparation of environmental data for modelling

Using all the environmental data described in Table 2.3 for modelling would lead to around 90% of the effort data being lost because of missing covariate data in some locations, especially in Norwegian waters, and in earlier years. To reduce data loss the number of covariates used in the modelling is a subset of those presented in Table 2.3.

To account for environmental changes including global warming in the region over the study period, effort data were split into two periods 1987-1989 and 1998-2015. Water temperature, typically

measured by sea surface temperature (SST), is a key regulator of the distribution and ecological interactions of cetacean populations, probably through indirect links with their prey and linked with the seasonal progression of summer. This temporal partition matches ecosystems changes described in the area (see section 1.2), and matches the most recent change from a cold to a warm phase of the Atlantic Multidecadal Oscillation (AMO), (e.g. Alexander et al., 2014; Carr et al., 2017). This may also help to elucidate anthropogenic warming within described phases of the AMO. The AMO relates to the whole North Atlantic (0°–70°N, 80°W–10°E), which is larger than and thus not totally representative of the study area. The AMO index was not used in the analysis for reasons described in section 1.2, but the partition of the study period reflects the change from a cold to a warm phase (see section 1.2). The number of years included in each period differed and the allocation of different periods could have been considered in various ways. Here it was decided to create a clear division between early years in the cold phase of the AMO and all more recent years combined in the warm phase of the AMO to maximize the amount of data available in the recent period and therefore maximize the ability of models to incorporate multiple explanatory covariates, as appropriate. Although 1995 was the year with the broadest survey coverage (Pike, 2009), it was not included in analysis because of the low quality / few environmental data available.

The variables included for modelling the 1987-89 data were depth, slope, aspect, and SST. For modelling the 1998-2015 data, the variables included were: depth, slope, aspect, SST, Chl*a*, PP, mlp, ssh, bT, and sal (Table 2.3). The use of the wider available range of covariates for the more recent period allows the potential for the models to reveal greater insight into the relationships between density and environmental variables. This does mean, however, that interpretation of any differences in results for the two periods is complicated by the potential for the relationships for the recent period for covariates common to both periods to be affected by relationships with the additional covariates. One way to investigate any such effects could be to run models for the recent period that only include covariates used in the early period (e.g. Houghton et al. 2020). However, this was not able to be done in the time available for this study (See also section 6.2).

Year was not included as a covariate because it is confounded with inter-annual changes in all the dynamic variables so including it as a covariate could conceal the fundamental relationships between relative density and the environmental variables. There were insufficient data to include interactions between all these variables and year in the models. SST residuals (anomalies) could have been used in lieu of SST; here, SST was used to allow temperature ranges to be described and to be able to compare results with those from studies in other areas. For the dynamic variables, March was not included for any variable in either period to avoid data loss greater than for other months; 25% of data

is available when March is included for the whole area including land Figure 2.7, this means approximately 10% of the survey data is lost if March was included in the analysis.

Prior to modelling, correlation/collinearity among environmental covariates was evaluated using Spearman's rank correlation test and pairplots. Correlation matrices were generated using package "ggcorrplot" (version 0.1.2.; Kassambra, 2018). Correlation was considered important when r > 0.7 between two covariates (e.g Bortolotto et al., 2017). If two covariates were correlated they were flagged, and their contribution re-evaluated during modelling as explained below in Section 2.2.2.4. 'Families' of covariates were defined as each dynamic variable and its monthly data, e.g. SST from April to August. Within each family, months were assumed to be correlated, hence only one covariate month was included in the full model as explained below in Section 2.2.2.4.

2.2.2.2 Model Framework

The relationship between animal count (response variable) and environmental variables (explanatory covariates – Table 2.3) was modelled using Generalized Additive Models (GAMs). Modelling was done in R using the package "mgcv" (version 1.8.22; Wood, 2017, 2011, 2004, 2003; Wood et al., 2016). The general formulation of the model was:

$$E[n_i] = \exp\left[\ln(a_i) + \beta_0 + \sum_k f_k\,(z_{ik})\right]$$

Here n_i is the number of individuals observed in the i^{th} segment, a_i is the effective area searched for the i^{th} segment (see section 2.1.3) serving as an offset, $\beta_0$is the intercept, f_k is the smooth function of the explanatory covariates, and z_{ik} is the value of the k^{th} explanatory covariate in the i^{th} segment. The offset, effective area searched (a_i) (see section 2.1.3), accounts for the variation in the length and width of the effort segments (e.g. Gilles et al., 2016; Hammond et al., 2013; Rogan et al., 2018). Modelling the number of individuals as the response variable and including the offset is equivalent to modelling relative density. As described above, the explanatory covariates used for modelling in the 1987-89 data were depth, slope, aspect, and SST. For modelling the 1998-2015 data, the variables included were depth, slope, aspect, SST, Chl*a*, PP, mlp, ssh, bT, and sal (Table 2.3) (see section 2.2.2.1).

2.2.2.3 Model Fitting

The first step in modelling was to determine the most appropriate error distribution for the response variable (count of individuals). The base error distribution for count data is the Poisson distribution. However, because over-dispersion in the data was likely, the Quasi-Poisson, negative binomial and

Tweedie distributions were also evaluated (e.g. Bortolotto et al., 2017; Gilles et al., 2011; Víkingsson et al., 2015). The link function used in all cases was log link.

The selected explanatory covariates (Table 2.3 and see section 2.2.2.1) were considered for modelling as smooth terms. The degree of smoothness was estimated as part of the model fitting procedure. Likelihood methods were used to find the most appropriate smoothness for each model term. Here models were fitted using REML (restricted maximum likelihood), in which the smooth functions are treated as random effects, so that variance parameters can be estimated. REML offer some improvement over the prediction criteria methods in most cases because they are less prone to severe under-smoothing; failures to which Akaike's Information Criterion and GCV (Generalized Cross Validation Score) are prone (Wood, 2011).

The smoothing parameter selection using prediction error criteria and/or likelihood methods penalizes the terms in a model but usually does not remove the smooth from the model (Wood, 2011). Automatic term selection extra penalization can be done using shrinkage or double penalization. Here double penalization was used, which leaves the original smooth un-touched but penalizes it only if the term is 'completely smooth' allowing smooth functions to become linear if warranted. Completely smooth means that the term is heavy penalized by the smoothness selection criteria, as explained above. Double penalization criteria operate using the original penalty matrix produced during the smoothing parameter selection (Wood, 2017). Double penalization can smooth any number of covariates within a model and the locations of the "knots" do not need to be specified (knots are where the different splines of the smooth join and is equivalent to degrees of freedom). The number of knots within a smooth were automatically decreased during model fitting (see above) and terms that ended up not contributing to explaining variability in the data were penalized to nothing, which was apparent as a smooth represented as a horizontal line (edf<0.5).

2.2.2.4 Model Selection and Evaluation

2.2.2.4.1 Model selection:

Model selection following an automatic stepwise approach cannot be implemented in the "mgcv" package so model selection was done manually. The covariate *survey*, which accounted for the differences between the two datasets (NASS and NILS) was always included in the base model.

First, a forward selection was run for each of the temporally varying oceanographic covariates (SST, PP, chl*a*, mlp, ssh, bT, and sal) to select the month that explained the most deviance in the data for each covariate. Each covariate was added to the base model one at a time. The month that resulted

in the best model improvement (AIC) was selected as representative of that covariate 'family', as explained above (section 2.2.2.1).

Second, the best representatives for each temporally varying family and non- temporally varying covariates were added to a full model even if they were collinear (see below). In this full model the smooths were penalized using double penalization (see section 2.2.2.3). The terms that were penalized to nothing (section 2.2.2.3) were removed from the full model and this 'reduced model' was then re-run.

Third, using the reduced model, concurvity was evaluated for the model terms. Concurvity is an analog of multicollinearity, which can similarly lead to parameter estimates with an upward bias and underestimation of standard errors (Amodio et al., 2014). Because concurvity and multicollinearity are analogs, and both were evaluated in the model terms (see section 2.2.2.1), all the pairs of terms that had collinearity and concurvity could be identified in the 'reduced model'. Each model was run with each of the terms within a collinear pair plus the rest of the terms already selected in the reduced model. Selection between these two models was made using AIC. Collinearity and concurvity step was not needed in the 1987-1989 models as, the relief variables and SST did not presented collinearity.

2.2.2.4.2 Model evaluation:

The fit of each model was evaluated by visual inspection of the QQ and residual plots. Here a QQ plot including the 95% confidence interval, and a randomized quantile residual versus linear predictor plot were generated; the latter helped to evaluate homoscedasticity (similar variance) across the data. Smooth plots were also inspected to evaluate evidence for under-smoothing, as illustrated by extremely 'wiggly' and unrealistic smooths. Prediction maps were visually compared with observations to check for evidence of edge effects or obvious mismatches that might indicate that the model was not a good description of the data.

Temporal autocorrelation of the residuals was evaluated by visual examination of auto-correlation function plots generated by the function 'acf' in the R package 'stats'.

2.2.2.5 Prediction

To predict the model results, the whole study area was overlaid by a spatial grid of resolution 25 km x 25 km, which was approximately the same resolution of the maximum segment length. This grid resolution was also selected because it was approximately the coarsest resolution of the covariates.

The grid was built using QGIS software using the 'vector grid' function (QGIS Desktop 2.18.15; QGIS Development Team, 2018).

Each grid cell was populated with the selected environmental covariates (Table 2.3) depth, slope, aspect, SST, Chl*a*, PP, mlp, ssh, bT, and sal (see section 2.2.2.1). They were extracted as described in section 2.1.4.

The predictions of animal densities were made for each grid cell using the function *predict* in R under package "mgcv" (version 1.8.22; Wood, 2017). The results were plotted on a map using the package 'ggplot2' (version 2.2.1; Wickham, 2016) in R. To avoid predicting outside the range of the data, the prediction grid area only included the survey area and a small additional edge in some places, and predictions were not made in grid cells in which one or more of the covariates was outside the range included in the models.

2.2.2.6 Estimation of prediction uncertainty

The uncertainty of the prediction was done by calculating the coefficients of variation (CV) using a posterior simulation as in Schleimer et al., (2019). A matrix that produces a vector of linear predictor values for each grid cell was generated using the R package *mgcv*, function predict (type='lpmatrix') (Wood, 2017). Model coefficients were extracted from the posterior distribution and 1000 samples were produced using the R package *MASS,* function 'mvrnorm' (Venables and Ripley, 2002). Then both calculations were used to generate 1000 predictions from which the CV was calculated and plotted. The plots of the CV of predicted density indicate relative confidence in the predictions across the study area. Areas with high CVs should be interpreted cautiously when used to advise conservation and management.

2.2.3 Summary of sources of bias and uncertainty in analysis

From data collection to prediction of estimated density, the data have gone through a series of processing and analytical steps (see previous sections in this chapter), each of which introduces known or possible bias and/or statistical error. In consideration of the impact of these on results and conclusions, it is important to reiterate that the aim of the research was to model the impact of environmental covariates on relative density through distribution and habitat use modelling, not to model absolute density or obtain estimates of absolute abundance. Thus, data processing and analysis

steps that result in positive or negative bias in estimated density that is constant across the whole study area do not affect results or conclusions.

Species identification errors could potentially lead to under or overestimation of density. Low certainty sightings were not included in the analysis and this may lead to underestimation of density. Conversely, including uncertain sightings that could have been from other species would lead to overestimation (Víkingsson et al., 2015, 2009).

Each covariate used in modelling is associated with some processing error. Information on this error is typically not available and typically not considered in habitat modelling research (e.g. Bortolotto et al., 2017; Gilles et al., 2009; Pirotta et al., 2011; Rogan et al., 2018; Virgili et al., 2019). If the processing error is approximately random, the impact on model results will simply be to introduce some additional uncertainty into the modelled relationships and predictions; that is, the CVs around the fitted relationships and the predictions will be underestimated. Given the fairly large uncertainty in model results, the impact of covariate processing error is likely small. If, however, there is a bias in the processing, this could lead to erroneous modelled relationships. As mentioned above, values of mixed layer depth (mlp), a covariate present in the recent models for all species, are overestimated; however, the timing and trend are correct (see section 2.1.4). The effect of this overestimation on model results is unknown but the effect is assumed to be similar across species.

Estimation of ESW did not account for animals missed on the transect line, which results in availability bias and perception bias. All estimates of density are thus underestimated. Availability bias is a feature of the diving/surfacing behaviour of species and can reasonably be assumed to be the same across the study area and thus have minimal effect on results. Perception bias is dependent on survey platform and observation conditions could thus have varied over space and time. The impact of this on results is unknown but consistent data collection protocols and similar survey conditions should have minimized spatio-temporal variation in perception bias.

Movement of animals in response to approaching survey ships before they are detected can lead to bias in estimated density. Attraction to the ship will generate overestimation while avoidance will lead to underestimation of abundance. A recent large-scale survey south of the study area found no evidence of responsive movement to the survey vessels in any of the species (Hammond et al., 2017). Previous surveys of the same type have found weak evidence of avoidance in minke whales and white-beaked dolphins (Hammond et al., 2013).

The statistical error in estimated effective strip width (ESW) has not been propagated through to the modelling of distribution and habitat use; the error (CV) associated with predicted density is thus

underestimated. However, given the generally rather large CVs of predicted densities from the modelling, statistical error in ESW would likely make only a minor contribution to the overall CV.

The uncertainty (CV) in the effect of each covariate is indicated by the 95% confidence interval about the fitted smooth relationships. The uncertainty in the spatial prediction of density is indicated by the maps of the CVs.

2.3 Appendix

Appendix 2-A. Norwegian vessel abbreviation name, vessel length overall (LOA) given by range, and level identification based on these ranges.

Level	LOA range	Vessel name (abbreviation)
1	< 30 m	ABR
		RGO
		RBU
		VFL
		FBA
		AAN
		OLE
2	30 m > LOA < 40 m	ULV
		LKJ
		HAV
		MER
		WSE
		PJA
		HKY
		THO
		SGU
		NYS
		SAF
3	40 m > LOA < 50 m	ASB
		VKA
		BHA
		STE
		HMO
		PBJ
		BGU
4	50 m > LOA < 75.9 m	SLO
		NBA
		HGU

	JHJ
	BHO
	ERO

Intentionally left blank

3 DISTRIBUTION AND HABITAT USE OF DEEP-DIVING CETACEANS IN THE CENTRAL AND NORTH-EASTERN NORTH ATLANTIC

3.1 Introduction

3.1.1 State of knowledge about sperm whales

The sperm whale (*Physeter macrocephalus*) is the most sexually dimorphic Odontocete species. Females are generally found in latitudes lower than 40° and commonly along the equator, in the company of other females; in sperm whale societies the basic family unit is around 10 females and their young (Whitehead, 2003). Young male sperm whales stay in the family unit in tropical and subtropical waters until moving gradually to higher latitudes between the age of 4 to 21 years. Mature male sperm whales are distributed at high latitudes up to the ice-edge in both hemispheres. They return to lower latitudes to breed but the exact timing is unknown (Whitehead, 2018). In the eastern part of the North Atlantic, there are no reports of females north of the Azores (Clarke, 1956 In: Christensen et al., 1992). Although no females were reported in the area from whaling, in the 1989 NASS survey females were believed to have been observed around 55° N (Gunnlaugsson et al., 2009). As this seems to be exceptional, in the study area it is assumed that mainly/only males were observed.

Globally, sperm whales of both sexes and all age classes are more commonly found in deep waters and along the continental slope (Christensen et al., 1992; Gunnlaugsson et al., 2009; Roberts et al., 2016; Rogan et al., 2017; Virgili et al., 2019; Whitehead, 2018). Females are found almost exclusively in waters deeper than 1000 m (Rice, 1989), while males are generally found in deep waters but in some areas such as off New York and Nova Scotia have been seen in waters less than 300 m (Whitehead, 2018). In the central and north-eastern North Atlantic, sperm whales have been observed most frequently in deep waters (Christensen et al., 1992; Gunnlaugsson et al., 2009; Rogan et al., 2017). In Icelandic waters (Denmark Strait), the species depth range, based on existing knowledge from whaling and some of its prey, is between 400 and 1200 m but can extend to depths of 2000-3000 m (Martin and Clarke, 1986). Rogan et al., (2017) found that sperm whale group abundance was highest in waters between 1000 and 4000 m, while group size was larger in waters <2000 m. Slope consistently seems to be an important feature influencing sperm whale distribution (Rogan et al.,

2017; Virgili et al., 2019), especially in Norwegian waters where most whales have been observed along the continental slope (Christensen et al., 1992; Øien, 2009).

Globally, the influence of sea surface temperature on sperm whale distribution varies between the sexes. Female and family unit occurrence seems to be concentrated around 15° C (Rice, 1989), while males occur in a wider range of temperatures because of their broader distribution (Baumgartner et al., 2001; Pirotta et al., 2011; Rogan et al., 2017). In the southern part of the central and north-eastern North Atlantic, estimated abundance was found to be highest between 10 °C and 20 °C, while group size was predicted to increase with increasing SST (Rogan et al., 2017). Overall, the relationship between sperm whale density and SST seems to be linked to the presence of thermal fronts. Some studies have found sperm whale occurrence to be related to upwelling zones but others have found a relationship with downwelling zones (Baumgartner et al., 2001; Pirotta et al., 2011). Fronts are areas with density gradients in physical features such as temperature; these favour the accumulation of nutrients and plankton which in turn attracts higher tropic level species such as sperm whales.

Sperm whale diet has been mainly described as consisting of squid and other cephalopods. In addition, males are more likely than females to consume demersal fish (Bjørke, 2001; Sigurjónsson and Víkingsson, 1997; Whitehead, 2018). Diet analysis from 221 sperm whales caught in the Denmark Strait had fish remains in 87% and cephalopods remains in 68% of stomachs - the main fish species contributing to the diet was lumpsucker (*Cyclopterus lumpus)* and the most important families of cephalopods were Histioteuthidae, Cranchiidae, Ommastrephidae and Gonatidae (Martin and Clarke, 1986). In Norwegian waters, studies have shown variation from a fish and squid diet, to mainly squid (Hjort and Ruud, 1929 In: Bjørke, 2001; Clarke, 1996; Santos et al., 1999). The squid *Gonatus fabricii* has been suggested to represent the main cephalopod species consumed and, in some studies, the main prey for sperm whales in the Norwegian Sea (Clarke, 1996; Santos et al., 1999). However, summer distribution of sperm whales in the Norwegian Sea in 2009, 2010 and 2012 was found not to be related to herring, mackerel, blue whiting, capelin, krill or *Gonatus* spp (Nøttestad et al., 2015).

Feeding is assumed to be the primary activity of male sperm whales in the central and north-eastern North Atlantic during the summer months, due to the availability of prey during this season and the absence of females. The modelled relationships are therefore likely to reflect environmental drivers related to finding prey. During this period, other behaviour could also include socializing to an unknown degree by males in the feeding areas (Whitehead, 2018, 2003) and some individuals will travel as part of their migration to northern locations (e.g. Azores to the Norwegian Sea (Steiner et al., 2012)) or between (unknown) feeding areas. However, most cetacean species are believed to be

opportunistic feeders and could take advantage of available prey, for example, while travelling. Covariates included in the models have been chosen because they may have the power to explain foraging behaviour (see also general justification of the included covariates in section 2.2.2.1 and Table 2.3). Other studies have found relationships between sperm whale density and depth, slope, aspect, presence of fronts and SST (see above). Covariates related to primary production may have a lagged relationship with sperm whale density because they feed high in the trophic web. Covariates linked with prey aggregation such as SSH and mlp are expected to be related to prey accumulation and to have little to no lag. Salinity is related to water masses and in the study area may explain the influence of Arctic versus temperate water on sperm whale distribution. Bottom water temperature relates to deep water horizontal gradients which are relevant for species diving deep to forage.

Sperm whale abundance in the central and north-eastern North Atlantic has most recently been estimated for Iceland/Faroes in 2015 and Norway in the 2014-2018 mosaic coverage (Table 3.1). There are no estimates available for Greenland waters because there have been very few sightings, 3 sightings in the East and 5 in the West (Hansen et al., 2018). However, estimates are likely negatively biased because the long diving time of sperm whales strongly restricts their availability (e.g. Gunnlaugsson et al., 2009; Hammond et al., 2017; Rogan et al., 2017). There are no sperm whale trend estimates available in the area, but Pike et al. (Pike et al., 2019b) summarizes estimates from different subareas in the central and eastern North Atlantic including Iceland-Faroes, Norway, Ireland, and from the southern European surveys SCANS and CODA, suggesting more than 30,000 whales are present in this area during the summer.

Table 3.1.Most recent abundance estimates of sperm whales during surveys.

Areas	Estimate	95% Confidence interval	Reference
Iceland/Faroe Islands	23,166	7,699 – 69,709	Pike et al., (2019b)
Norway (GL & NO seas) 2014-2018	5,522	3,325 – 9,170	NAMMCO (2019a)

Regarding the conservation status and management, sperm whales are listed as Vulnerable by the IUCN (Taylor et al., 2019).

Anthropogenic pressures on sperm whales could include (or have included): direct harvest, vessel collisions, entanglement, noise pollution, chemical pollution, debris, and oceanographic changes. Sperm whales were heavily exploited in the past, but are protected from hunting under the IWC moratorium on whaling (IWC, 2020). Whales are distributed mainly in offshore waters, however, vessel collisions in sperm whales seem to occur commonly (Laist et al., 2001). Sperm and killer whales are the main species at high latitudes known to interact strongly with fisheries, specifically longline

gear, putting them then at risk of entanglement (Hamer et al., 2012). Some sources of noise could be detrimental for sperm whales (Harris et al., 2015), for example, changes in sperm whale dive behaviour have been found in some animals after sonar exposure, which potentially affects foraging (Sivle et al., 2012). Pollutants in sperm whale blubber are found at higher concentrations than in baleen whales but lower than other odontocetes living closer to the coast (Whitehead, 2018). Debris is another type of pollution sperm whales are known to be exposed to. During a large stranding event in the North Sea, 41% of the whales stomachs contained a wide range of debris that included netting, ropes, foils, packaging material, and a part of a car (Unger et al., 2016). Although, the debris was not the cause of death of the animals it demonstrates the high level of exposure and potential impact on the animals. The effects of oceanographic changes, including those linked with climate change, on sperm whales are unknown but because of their wide distribution the effects may not be as detrimental as on some other species (MacLeod, 2009).

3.1.2 State of knowledge about pilot whales

The two pilot whale species, long-finned (*Globicephala melas*) and short-finned (*G. macrorhynchus*) pilot whale are wide ranging species found along coasts and far off-shore (Abend and Smith, 1999; Buckland et al., 1993; Olson, 2018; Pike et al., 2019a). They are among the largest members of the Delphinidae and among the most gregarious cetacean species. Pilot whales are believed to be nomadic; few resident populations have been identified (Abend and Smith, 1999). However, Alves et al (2013) and Servidio et al (2019) found evidence for different levels of site fidelity in short-finned pilot whales: transient, temporary migrants and resident (island associated) animals in Madeira and the Canary Islands, respectively. Photo-identification studies of long-finned pilot whales in the Strait of Gibraltar have suggested that some whales are seasonal (summer) residents (Verborgh et al., 2009). The two species are difficult to distinguish in the wild; the key morphological differences are the flipper length, skull shape and number of teeth. In terms of distribution, short-finned are tropical and long-finned anti-tropical, although there is some overlap in temperate waters of the North and South Atlantic, along the Peruvian coast, and off South Africa. In this study, the term pilot whale is used only to refer to long-finned pilot whales because short-finned inhabit warmer/more tropical waters than the ones of the study area. Specifically, the term refers to the subspecies *Globicephala melas melas* as *Globicephala melas edwardii* inhabits the Southern Hemisphere (Olson, 2018).

Pilot whale males are larger than females with a maximum length of 6.25 m and weight of 2.3 tonnes, while females can be 5.12 m and 1.3 tonnes (Bloch et al., 1993). Males have a higher mortality rate at

all ages, causing their life expectancy to be shorter than females at 46 years, compared to 59 years (Bloch et al., 1993; Olson, 2018).

Pilot whales (*G. melas melas)* are broadly distributed in coastal and oceanic waters in the west and east of the North Atlantic: in the western part from around 35° to 65° N and in the eastern part from around 40° to 75° N (Figure 3.1) (Abend and Smith, 1999; ICES, 1992; NAMMCO, 1998, 1997; Roberts et al., 2016). In Icelandic waters, data from whaling vessels during 1979 to 1988 reported an increase in pilot whale sightings after July 15th, occurring mostly in waters between 400 and 1000 m in depth and some in waters less than 400 m, although there may be some inaccuracies because reports of small cetaceans have less accuracy than those of other species (Sigurjónsson and Gunnlaugsson, 1990). More recently, Rogan et al., (2017) found that pilot whale summer distribution in the Northeast Atlantic peaked at depths >1000 m, and was strongly associated with the 2000 m depth contour and areas of moderate slope. Similarly, the summer distribution to the west of Scotland during 2004-2005 occurred primarily in depths between 1370 and 1951 m (MacLeod et al., 2007). In contrast, during the summer months of 2009, 2010 and 2012 in the Norwegian Sea, pilot whales were associated with shallow depths, especially waters shallower than 300 m (Nøttestad et al., 2015).

There is little information directly relating pilot whale occurrence to water temperature. Because they are considered deep divers, sea surface temperature is not thought to directly influence, or act as a direct proxy for, their presence. However, observations do seem to be associated with warmer water temperatures. For example, pilot whales west of Scotland were only recorded in warmer waters at temperatures >10.9°C (MacLeod et al., 2007). Whaling data from the north-eastern region of the Faroe Islands found larger catches with warmer water temperatures (Hátún et al., 2009), suggesting a possible relationship between the two.

Pilot whales are not known to migrate but their distribution does change seasonally. In the summer, whales in the North Atlantic occur more in slope, shelf, and shelf-slope waters, while in the winter it is believed that they move southward and into deeper waters (Abend and Smith, 1999; IWC, 1990; Nøttestad et al., 2015; Roberts et al., 2016; Rogan et al., 2017). Pilot whales in the central and northeast Atlantic occur in offshore and in coastal waters (Nøttestad et al., 2015; Pike et al., 2019a). In Icelandic waters, opportunistic sightings from whaling vessels during 1979 to 1988 occurred west-northwest of the island (Sigurjónsson and Gunnlaugsson, 1990). Abend and Smith (1999) compiled data from the 1950s to 1992; their summary of Icelandic sightings indicates that pilot whales regularly occurred off the southern coast and did not occur on the northern side of the island (Figure 3.1). Pike et al., (2019a) evaluated pilot whale relative abundance using the Icelandic and Faroese NASS data

(1987 to 2015), concluding that they were broadly spread offshore but that their distribution varied among survey years. The year with broadest southern coverage was 1989, revealing an area of high density south of 56 ˚N but this area was not covered by any other survey. The peak in the number of whale drives in July-August in the Faroe Islands is indicative of seasonal movements (Zachariassen, 1993). In Norwegian waters, pilot whales seem less common (Abend and Smith, 1999), but the catch history also showed a peak in July-August along the coasts of Lofoten and Møre (ICES, 1992). The most northerly records of pilot whales are opportunistic observations from whaling boats during the summer of 1973 to 1975 in the Barents Sea (Christensen, 1977 In: Abend and Smith, 1999).

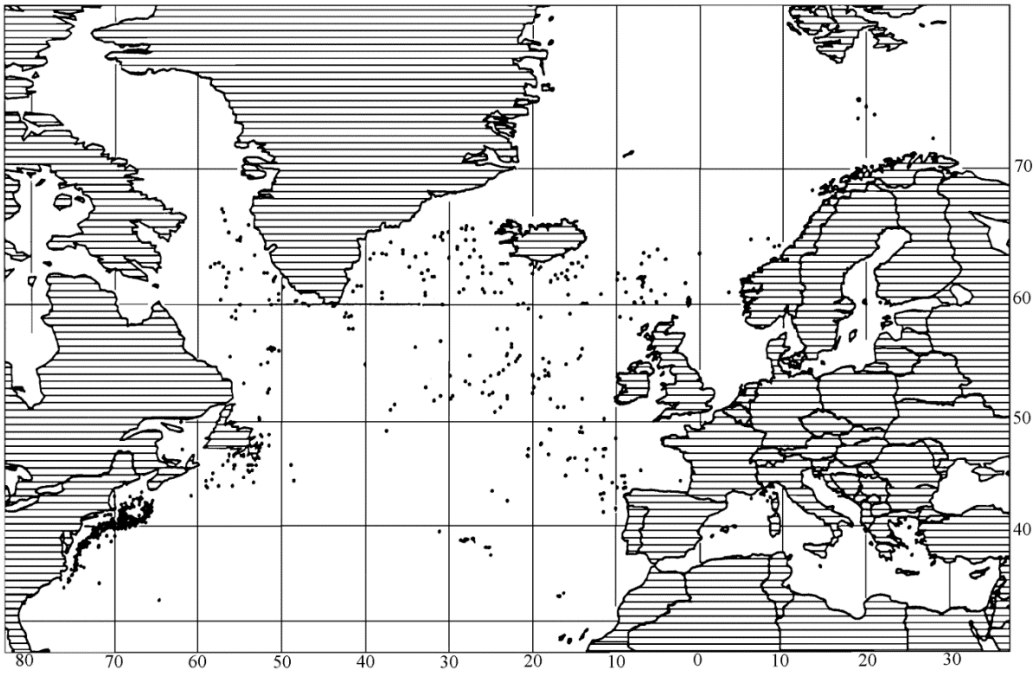

Figure 3.1. Distribution of long-finned pilot whales in the North Atlantic and Mediterranean Sea based on sighting data from 1952 to 1992 (Abend and Smith, 1999).

Changes in distribution and movements of pilot whales are assumed to be linked to the abundance of their prey, which are mainly different squid species (Méndez-Fernandez et al., 2013; Pike et al., 2019a; Santos et al., 2014; Sigurjónsson et al., 1993; Zachariassen, 1993). The species consumed seem to vary depending on the area, and small pelagic fish are also consumed. They are believed to be opportunistic feeders, exploiting any locally abundant prey in oceanic and coastal waters; ecological tracers show this dietary plasticity (Desportes and Mouritsen, 1993; Méndez-Fernandez et al., 2013; Santos et al., 2014).

In Faroese waters, their preferred prey seems to be the European flying squid (*Todarodes sagittatus*). If this species is abundant, the diet seems to be nearly mono-specific (Desportes and Mouritsen, 1993).

Other prey species around the Faroes include the harmhook squid (*Gonatus* spp.), fish such as greater argentine (*Argentina silus*), blue whiting (*Micromisistius poutassou*), Greenland halibut (*Reinhardtius hippoglossoides*), and pandalid shrimps. Other common fish species in the area are cod, herring, and mackerel but they have not been reported as prey despite being preyed upon by pilot whales in other areas (Desportes and Mouritsen, 1993). In other areas of the north-eastern and central Atlantic, specific information regarding pilot whale prey preferences is less complete than the Faroes. Limited stranding data from Iceland in the 1980s also indicated the European flying squid as the main prey (Sigurjónsson et al., 1993). In the Norwegian Sea, pilot whale summer distribution in 2009, 2010 and 2012 seemed to be highly correlated with high concentrations of Norwegian spring-spawning herring (Nøttestad et al., 2015).

Foraging is assumed to be a primary activity of pilot whales in the central and north-eastern North Atlantic during the summer months, due to the availability of abundant prey during this season. The modelled relationships are therefore likely to reflect environmental drivers related to finding prey. However, pilot whales inhabit the area year-round and there is substantial inter-annual variation in distribution (Pike et al., 2019a; Sigurjónsson and Víkingsson, 1997). Pilot whales are gregarious and social behaviour is also expected to influence distribution. Although information about reproduction is limited, it is known that calving peaks in spring and late summer (Martin and Rothery, 1993). However, pilot whales are income breeders so need to continue feeding during lactation. They are also believed to be opportunistic feeders and could take advantage of available prey, for example, while travelling.

Covariates included in the models have been chosen because they may have the power to explain foraging behaviour (see also general justification of the included covariates in section 2.2.2.1 and Table 2.3). Other studies have found relationships between pilot whale density and depth, slope, presence of fronts and SST (see above). Covariates related to primary production may have a lagged relationship with pilot whale density because they feed high in the trophic web. Covariates linked with prey aggregation such as SSH and mlp are expected to be related to prey accumulation and to have little to no lag. Salinity is related to water masses and in the study area may explain the influence of Arctic versus temperate water on pilot whale distribution. Bottom water temperature relates to deep water horizontal gradients which are relevant for species diving deep to forage.

In the North Atlantic pilot whales have been hunted in Greenland, Iceland, Faroe Islands, western Ireland, Scotland, Norway, USA and Canada (Abend and Smith, 1999; Faroe, 2019; Minton et al., 2018; NAMMCO, 2019b; Pike et al., 2019a). At the moment they are hunted by Greenland and Faroe Islands (Faroe, 2019; NAMMCO, 2019b; Zachariassen, 1993). Around Greenland, catches are opportunistic

and mainly in the southwest. For the period from 2000 to 2013 the yearly catch average was 204 animals (range 0-433 animals) (NAMMCO, 2019b). The Faroe Islands has a long whaling tradition dating back to the 9th century with catch statistics since 1584 and unbroken from 1709 to the present (Zachariassen, 1993). In the period from 2000 to 2013 the yearly catch average was 671 animals (range 0-1107 animals) (NAMMCO, 2019b).

Hoydal and Lastein (1993), using effort-corrected catch data from the Faroe Islands, showed a cyclic pattern with peaks in 1720-1730, 1840-1850 and 1935-1985, suggesting neither a long-term increase nor a decline. Abundance estimates from Icelandic and Faroese surveys in the north-eastern and central North Atlantic are summarized in Table 3.2, the same survey years included in this thesis. The abundance estimates are not totally comparable because the spatial coverage varied over the years. The most different survey was in 1989, which covered waters more to the south and west than the other years. The highest abundance estimate was in 1989, suggesting a wider part of the species range was covered. In general, the estimates for the different surveyed years may suggest that pilot whale occupation or the timing of occupation varies from year to year around the north-eastern and central North Atlantic; this was similarly suggested by the Faroes catch data.

Table 3.2. Abundance of pilot whales in the North Atlantic, from the NASS, FI – Faroe Island – Iceland area. Per. – perception bias; Avail. – availability bias; n – uncorrected (Pike et al., 2019a).

Survey	Year	Area (nm^2)	Effort (nm)	Corrections		Abundance	95% Confidence Interval	
				Per.	Avail.		L	U
NASS FI	1987	667,349	14,968	n	n	118,459	68,189	205,791
NASS FI	1989	874,659	8,093	n	n	553,389	354,246	864,482
NASS FI	1995	709,194	6,182	n	n	226,665	125,630	408,956
NASS FI	2001	799,754	8,058	n	n	95,056	46,549	194,110
NASS FI	2007	750,410	5,875	n	n	128,093	75,682	213,802

As mentioned above, the abundance estimates are not totally comparable. Pike et al (2019a) did make direct comparisons by restricting the estimates to an area that was common for all the survey years and also a larger common area covered only in 1989, 1995 and 2007. They also found variation in the abundance estimates (of the common areas), suggesting changes in the distribution year to year, and no evidence of any trend in pilot whale numbers.

At a regional level, the lack of trend in pilot whale abundance estimates seems to suggest that whaling in the Faroese waters is not causing a decline (Hoydal and Lastein, 1993; ICES, 1992; NAMMCO, 2019b, 1998, 1997; Pike et al., 2019a). Stock structure is uncertain; using pollutant concentrations and parasites suggests that more than one stock is being harvested around the Faroes and thus the impact

is not on a local population (ICES, 1992; NAMMCO, 1998, 1997). NAMMCO in (1997) performed the most recent assessment for long-finned pilot whales in the area (north-eastern and central North Atlantic), which suggested that Faroese whaling is likely sustainable with the current annual catch (NAMMCO, 1998, 1997). A new assessment is being planned by the NAMMCO Scientific Committee for 2020 (NAMMCO, 2019b).

Regarding the conservation status and management, the taxonomic uncertainty about long-pilot whales has led it to being listed as Data Deficient by the IUCN (Minton et al., 2018).

The pressures that long-finned pilot whales face are direct exploitation, contaminants, bycatch, competition with fisheries, oceanographic changes, and anthropogenic noise. As mentioned above, pilot whales in the North Atlantic have a long history of utilisation by humans. Faroese hunting has been carried out for centuries, which NAMMCO (1997) concluded is sustainable. Regarding contaminants, the pilot whale together with the killer whale (*Orcinus orca*), has one of the highest levels of contaminants of any cetacean species (Dam and Bloch, 2000). Studies from the Faroes reveal relatively high levels of PCBs (polychlorinated biphenyls) and heavy metals such as mercury (Hg) and cadmium (Cd) (Caurant et al., 1993; Caurant and Amiard-Triquet, 1995; Dam and Bloch, 2000). Bycatch in the eastern Atlantic is not a cause for concern (ICES, 2013, 2002; Minton et al., 2018). Pilot whales feed on some commercially important species but they seem less vulnerable to prey depletion than some other species because they can apparently adjust their diet in response to changes in prey abundance (Desportes and Mouritsen, 1993). Around the Faroes, high catches/observed abundance (not effort corrected) of pilot whales have been reported in warmer waters, probably linked by their main prey (Hátún et al., 2009; Hoydal and Lastein, 1993). Finally, anthropogenic noise, especially sonar, has been associated with changes in pilot whale behaviour causing changes in vocalizations, traveling, surfacing, diving, breathing rate and foraging (Isojunno et al., 2018; Miller et al., 2012; Rendell and Gordon, 1999; Sivle et al., 2012). Conversely, they seem less sensitive to sonar exposure compared to beaked and killer whales (Antunes et al., 2014; Miller et al., 2012; Sivle et al., 2012).

3.1.3 State of knowledge about northern bottlenose whales

The northern bottlenose whale (*Hyperoodon ampullatus*) is the least known among the three deep diving species studied here but is one of the best known species of beaked whale family (Ziphiidae). The northern bottlenose whale shares the genus *Hyperoodon* with the southern bottlenose whale (*H. planifronts*). It is medium-sized whale 7-9 m in length; mature females are approximately 1 m shorter than males (Benjaminsen and Christensen, 1979; Mead, 1989). Life expectancy is around 27 years in

females and 37 years in males (Christensen, 1973 In: Benjaminsen and Christensen, 1979; Mead, 1989).

Northern bottlenose whales are found in temperate, subarctic and Arctic waters of the North Atlantic, extending from the ice edge to approximately 30° N (Taylor et al., 2008). They are usually found in waters deeper than 500 m with the highest occurrences at depths between 750 and 1800 m and along the continental shelf edge (Figure 3.2) (Benjaminsen and Christensen, 1979; Compton, 2004; Hooker et al., 1999; Whitehead and Hooker, 2012a, 2010). In the northwest Atlantic, Compton (2004) found the core predicted area to be characterised by an aspect of 142^{o} (south, south-east facing slopes). The broad latitudinal occurrence implies a wide temperature range for the species. Benjaminsen and Christensen (1979), summarized reports from whaling data in the north-eastern Atlantic, where animals were reported in surface water temperatures from -2 ^{o}C to + 17 ^{o}C, but in the northwest Atlantic the core predicted area had an average surface temperature of 2.7 ^{o}C (Compton, 2004).

Northern bottlenose whales in the north-eastern Atlantic are the only deep diving species for which a summer north-south migration has been suggested (Benjaminsen and Christensen, 1979; Benjaminsen, 1979 In: NAMMCO, 2019c; Reeves et al., 1993). However, the limited knowledge of this species means that the evidence for the whole north-eastern Atlantic is unclear. Some information from whaling and tagged animals suggests that August is the month when animals are moving south (Benjaminsen and Christensen, 1979; Bloch et al., 1996; Miller et al., 2015; Reeves et al., 1993). However, there are also records of animals year-round in Faroese and Norwegian waters (Bloch et al., 1996; IWC, 2012). An alternative hypothesis is that there is an inshore-offshore movement (Whitehead and Hooker, 2012a).

Several studies suggest that the main prey of northern bottlenose whales is *Gonatus* spp. In the Norwegian Sea, *Gonatus fabricii* and northern bottlenose whales have a similar distribution (Bjørke, 2001). In the western Atlantic off Baffin-Labrador, the primary prey is also *G. fabricii* (Mead, 1989) while on the Scotian Shelf it is *G. steenstrupi* (Hooker et al., 2001). In the North Sea, stomach content analysis of two stranded whales showed that *Gonatus* spp. comprised greater than 98% of the estimated prey weight (Santos et al., 2001). Other squid species also taken include *Teuthowenia* spp., *Taonius pavo* and *Histioteuthis reversa* (Hooker et al., 2001). Fernández et al. (2014), analysing the stomach contents of 10 stranded whales from the North Sea, found *Gonatus* spp., *Teuthowenia* spp. and *Taonius pavo* to comprise greater than 90% of the total prey weight and number. Fish and occasionally benthic organisms have also been found in stomachs (Benjaminsen and Christensen, 1979; Reeves et al., 1993; Taylor et al., 2008). From whaling data, there appear to be differences in the amount of fish consumed between areas: 53% of stomachs off Labrador but only 13% off Iceland

(Benjaminsen and Christensen, 1979). There is also evidence of a mixed diet in the northwest Atlantic where the core predicted area depth (1780 m) matched with the maximum depth of Greenland halibut (Compton, 2004).

Summer is the peak abundance of northern bottlenose whales in the central and north-eastern North Atlantic and feeding is assumed to be a primary activity due to the availability of abundant prey during this season. The modelled relationships are therefore likely to reflect environmental drivers related to finding prey. Northern bottlenose whales are usually encountered in groups, so social behaviour may be expected to have some influence on distribution. Although northern bottlenose whales can be found in the area year-round, a north-south migration has been suggested in the late summer (Benjaminsen and Christensen, 1979; Bloch et al., 1996; Miller et al., 2015; Benjaminsen, 1979 In: NAMMCO, 2019c; Reeves et al., 1993), although it is unknown how much this north-south 'migration' is linked to prey movement. Nevertheless, the models may also reflect the influence of environmental variability on, for example, the use of certain relief features or water masses to facilitate travel unrelated to foraging.

Covariates included in the models have been chosen because they may have the power to explain foraging behaviour (see also general justification of the included covariates in section 2.2.2.1 and Table 2.3). Other studies have found relationships between northern bottlenose whale density and depth, slope, aspect and SST (see above). Covariates related to primary production may have a lagged relationship with northern bottlenose whale density because they feed high in the trophic web. Covariates linked with prey aggregation such as SSH and mlp are expected to be related to prey accumulation and to have little to no lag. Salinity is related to water masses and in the study area may explain the influence of Arctic versus temperate water on northern bottlenose whale distribution. Bottom water temperature relates to deep water horizontal gradients which are relevant for species diving deep to forage.

Whaling (during the period 1880s-1973) occurred throughout the northern North Atlantic Figure 3.2 (Benjaminsen and Christensen, 1979; Whitehead and Hooker, 2012a). There is ecological and genetic evidence separating the two western populations: Scotian Shelf (1) and Labrador−Baffin Bay (2) (Compton, 2004; Dalebout et al., 2006; Whitehead and Hooker, 2012a). In contrast, genetic evidence indicates linkages between Labrador-Baffin and Icelandic animals (Dalebout et al., 2006) but there is no other evidence of interactions among whales from the other historical catching areas (Whitehead and Hooker, 2012a).

There are no abundance estimates for the pre-whaling period or when whaling ceased, but it has been estimated that prior to whaling there may have been around 100 000 whales (Whitehead and Hooker,

2012a). Northern bottlenose whales were the focus of two periods of intense whaling, one in the 1880s to 1920 and the second from 1937 to 1973. Estimates of trends based on catch per unit effort analysis show declines in northern bottlenose whale populations through time, the last decline due to whaling ended at the end of the second phase of whaling. It is believed that after the second phase there were probably only a few tens of thousands (Whitehead and Hooker, 2012a). Since commercial whaling ended, northern bottlenose whales are occasionally taken off Greenland and the Faroe Islands (Whitehead and Hooker, 2012a).

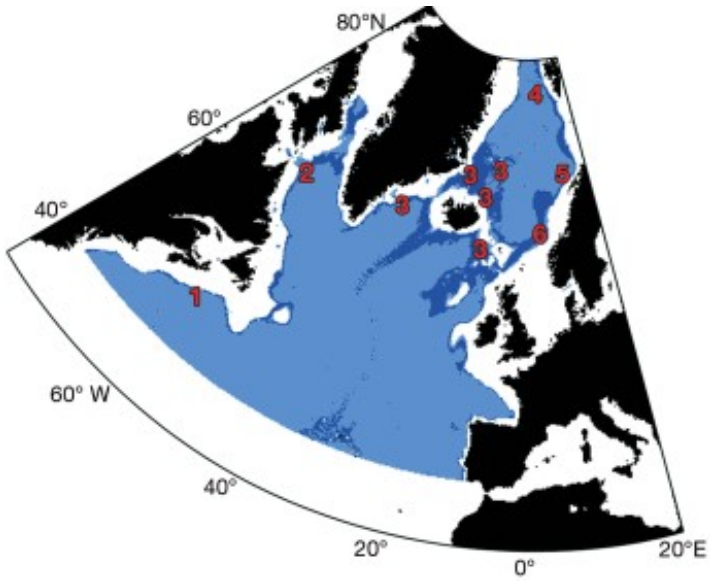

Figure 3.2. General distribution of northern bottlenose whales in the North Atlantic (light blue), defined as waters greater than 500 m deep and north of 37.5°N. Preferred habitat (800– 1800 m deep) is shown in dark blue. The six centres of whaling operations are shown: (1) Scotian Shelf; (2) Labrador and southern Baffin Bay; (3) East Greenland, Iceland, Jan Mayen and the Faroe Islands; (4) Svalbard; (5) Andenes; and (6) Møre (Whitehead and Hooker, 2012a).

There are population estimates for this species in some parts of the central and north-eastern North Atlantic study area but not for the whole area. These estimates show an apparent increase in Icelandic and Faroes waters over the years from 1987-1989, 4,925 (CV = 0.16) off Iceland and 902 (CV = 0.45) off the Faroes, to 1995, 27,900 (CV =0.67), and 2001, 28,000 (CV = 0.22) (Gunnlaugsson and Sigurjónsson,1990; Pike et al., 2003 In: NAMMCO, 2019c). For Faroes waters in 2007, abundance was estimated as 16,284 (CV = 0.41), based upon 12 sightings (Cañadas et al., 2011 In: Whitehead and Hooker, 2012a). There are no abundance estimates from Norwegian waters, but in two whaling areas off mainland Norway, Andenes and Møre, there seems to be no indication of recovery since whaling ceased (Whitehead and Hooker, 2012a). Around Svalbard, there are reports of sightings (IWC, 2012).

The lack of knowledge about this species has led to it being listed as Data Deficient by the IUCN (Taylor et al., 2008).

Currently, in some areas the pressures that northern bottlenose face are bycatch, entanglement with fishing gear, and contaminants (Fisheries and Oceans Canada, 2016), but the main pressure overall is anthropogenic noise. Underwater anthropogenic noise is seen as the primary pressure, given the sensitivity of other species from the family Ziphiidae, to noise disturbance (Hooker et al., 2019; Tyack et al., 2006), especially disturbance as a result of exposure to mid-frequency sonar which has been linked to mass strandings of beaked whales (Hooker et al., 2019). Behavioural response experiments have shown that beaked whales appear to cease foraging and delay the return to foraging or leave the area associated with sound exposure (Hooker et al., 2019). Miller et al., (2015), found high sensitivity of northern bottlenose whales to acoustic disturbance. They are at risk due to the increase in ship traffic, especially in newly ice-free high latitude areas in the North Atlantic where they have not been exposed before.

3.2 Methods

3.2.1 Estimation of effective strip width

Distance sampling methods were applied as described in Chapter 2 (see section 2.2.1).

For the earlier period (1987-1989), there was insufficient data to fit a detection function for northern bottlenose whales and pilot whales. This was done using only the NASS data (Iceland and Faroe Islands) because there were too few sightings of these species in Norwegian waters in this period.

3.2.2 Modelling distribution and habitat use

Distribution and habitat modelling methods were applied as described in Chapter 2. The effort and sightings used for modelling the three deep diving species are shown in Figure 3.3. The number of sighted animals made during this effort is summarized in Table 2.1 and Table 2.2. For the earlier period (1987 - 1989), modelling of northern bottlenose whales and pilot whales was done using only the NASS data (Iceland and Faroe Islands) because there were too few sightings of these species in Norwegian waters, as mentioned above.

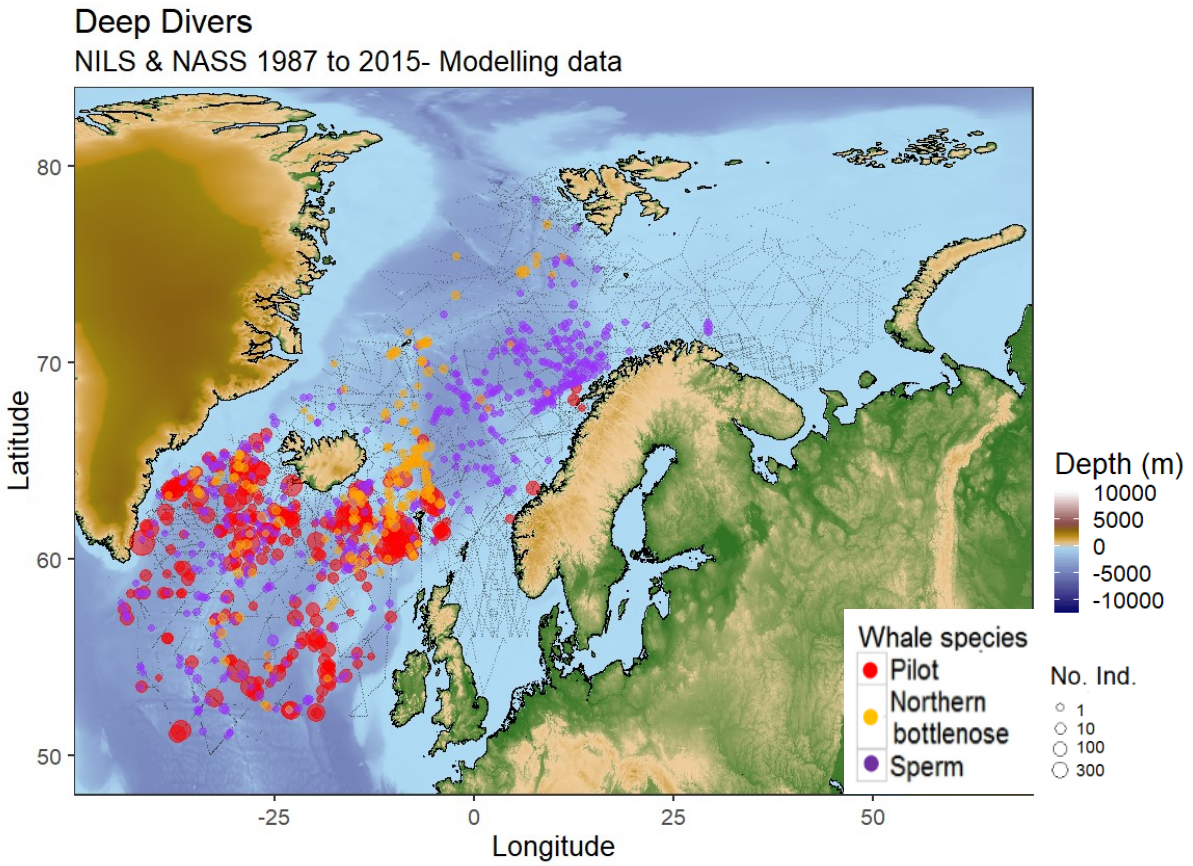

Figure 3.3. Summary of 1987 to 2015 NILS (Norway) & NASS (Iceland and Faroes) survey effort and sightings of pilot, northern bottlenose and sperm whales used for modelling. Effort is depicted by segment mid-points as grey-dots. Sightings are shown as coloured dots, the size of which indicates the number of individuals (No. Ind.). The map was plotted using the geographic coordinate system WGS84 & overlaid over the bathymetry of the area (ETOPO2).

3.3 Results

3.3.1 Sperm whales

3.3.1.1 Effective strip width – NASS (Iceland-Faroes) 1987-2015

The best detection function for the 1987-2015 sperm whale NASS (Iceland and Faroese) data was a half normal model with a 3000 m truncation distance which included 564 sightings (Appendix 3-A). Only vessel ID (ten levels) was retained in the selected model. The fitted model is shown in Figure 3.4. The model fitted the data well as shown in the Q-Q plot Figure 3.4 and by the goodness of fit test Cramer-von Mises test [unweighted] p = 0.148. The average probability of detection *p* was 0.581 (CV = 0.036). The estimated effective strip width for the ten covariate levels is given in Appendix 3-E.

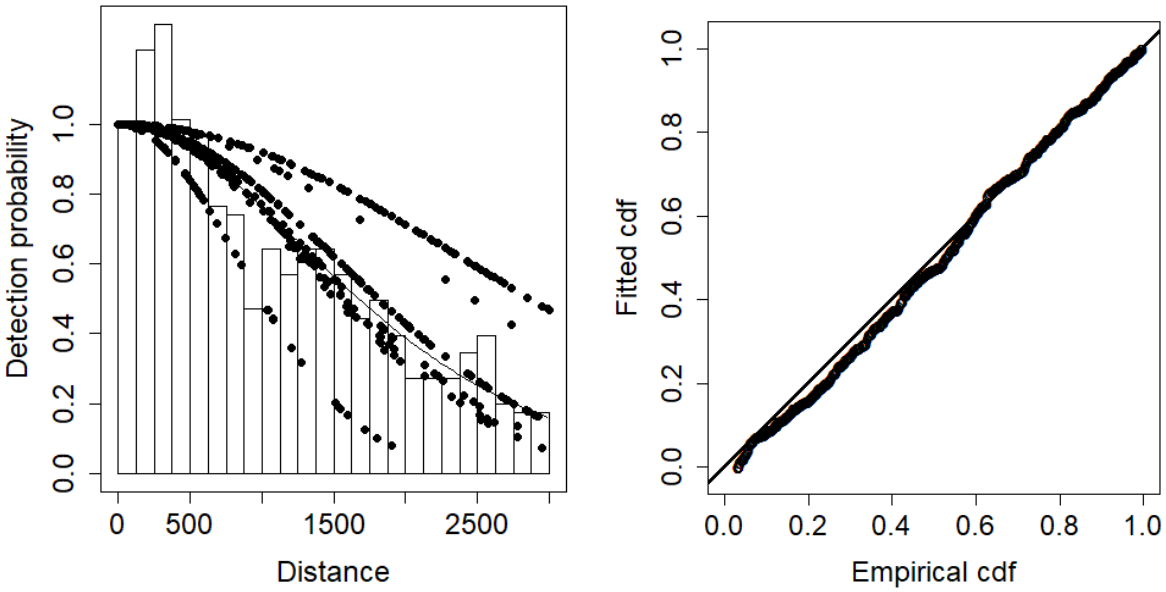

Figure 3.4. Detection probability (left) and Q-Q (right) plots for sperm whale 1987-2015 NASS data. For detection probability, the circles represent fitted values of the data, the line is the fitted model and the frequency histogram represents the observed data. In the Q-Q plot (right) the points are the fitted values while the solid line represents the expected data distribution.

3.3.1.2 Effective strip width – NILS (Norway) 1987-1989

The best detection function for the 1987-1989 sperm whale NILS (Norwegian) data was a hazard rate model with a 2000 m truncation distance which included a total of 107 sightings (Appendix 3-A). Vessel ID (three levels) was retained in the selected model. The fitted model is shown in Figure 3.5. As shown in the Q-Q plot Figure 3.5 and by the goodness of fit test Cramer-von Mises test [unweighted] p = 0.795, the model fitted the data well. The average probability of detection *p* was 0.418 (CV = 0.148). The estimated effective strip width for the three covariate levels is given in Appendix 3-F.

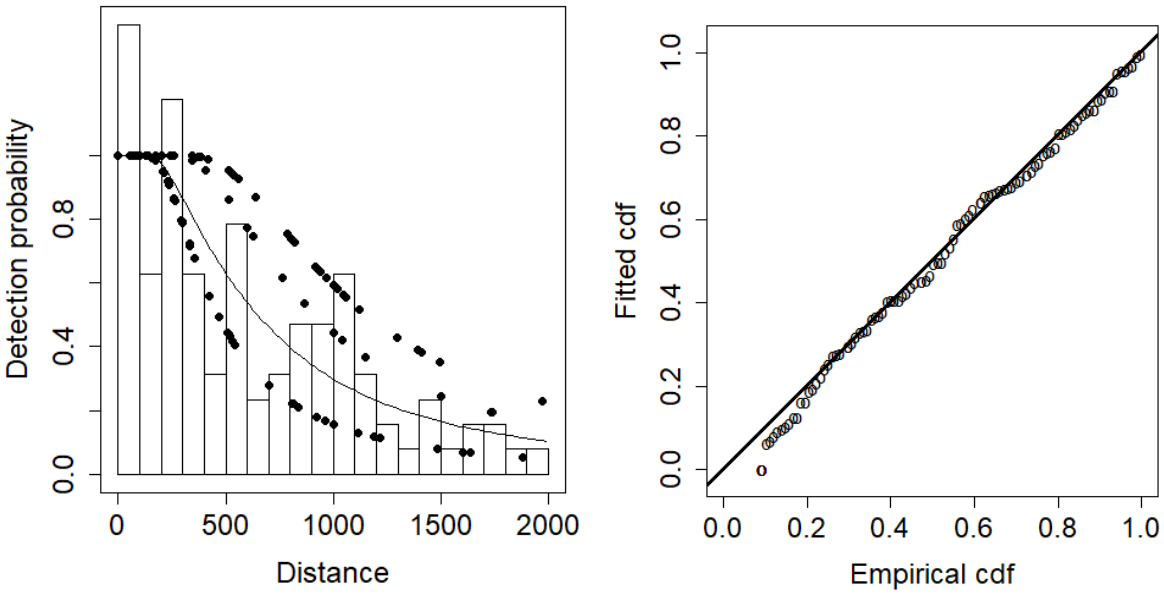

Figure 3.5. Detection probability (left) and Q-Q (right) plots for sperm whale 1987-1989 NILS data. For detection probability, the circles represent fitted values of the data, the line is the fitted model and the frequency histogram represents the observed data. In the Q-Q plot (right) the points are the fitted values while the solid line represents the expected data distribution.

3.3.1.3 Effective strip width – NILS (Norway) 1995-2013

The best detection function for the 1995-2013 sperm whale NILS (Norwegian) data was a hazard rate model with a 3000 m truncation distance which included a total of 811 sightings (Appendix 3-A). No variables were retained in the selected model. The fitted model is shown in Figure 3.6. The model fitted the data well as shown in the Q-Q plot Figure 3.6 and by the goodness of fit test Cramer-von Mises test [unweighted] p = 0.576. The average probability of detection *p* was 0.41 (CV = 0.042). The estimated effective strip width for models was 1230 m.

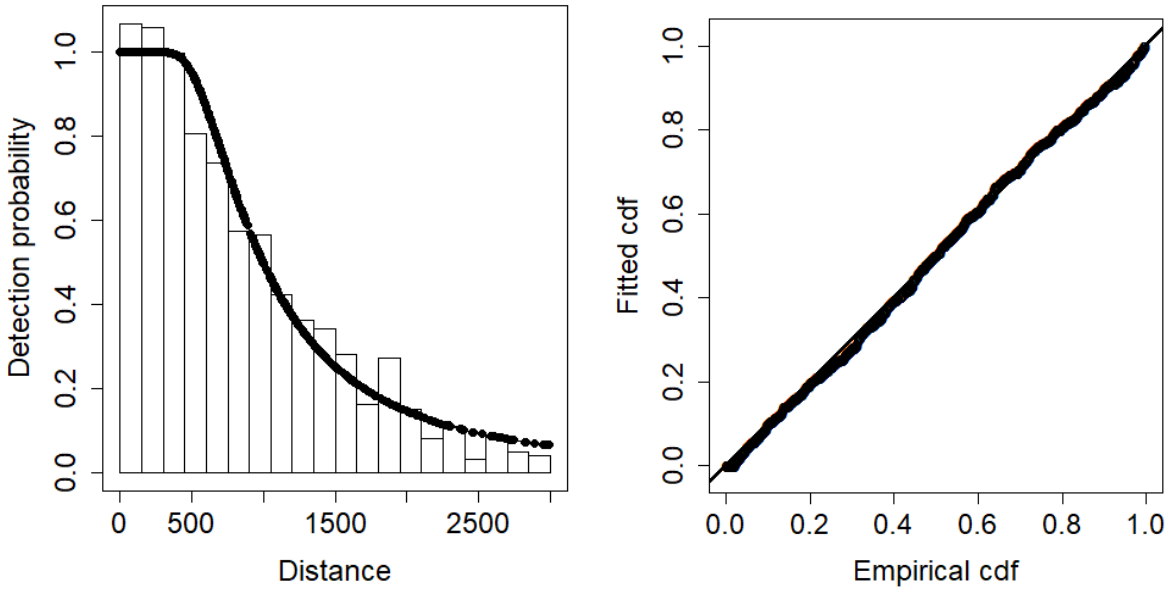

Figure 3.6. Detection probability (left) and Q-Q (right) plots for sperm whale 1995-2013 NILS data. For detection probability, the circles represent fitted values of the data, the line is the fitted model and the frequency histogram represents the observed data. In the Q-Q plot (right) the points are the fitted values while the solid line represents the expected data distribution.

3.3.1.4 Distribution and habitat use models: 1987-1989

The negative binomial was determined to be the best error distribution for the 1987-1989 spatial models for sperm whales (Appendix 3-G). A summary of all the fitted single variable models is given in Appendix 3-H. The correlation evaluation between static variables and SST months is shown in Appendix 3-B, where none of the pairs had a Pearson's correlation coefficient greater than 0.7. As for other species, concurvity was not evaluated in the 1980s models (see methods section 2.2.2.4.1).

After fitting models to determine the best month for SST, the covariates selected in the best model included: depth, slope, aspect, and April SST. The model fitted the data well as shown in Figure 3.7. The best model had a deviance explained of 32.3% (Table 3.3).

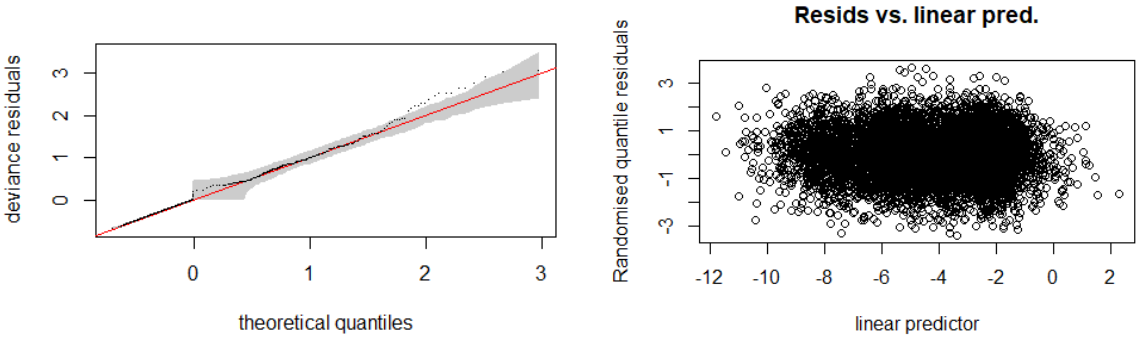

Figure 3.7. GAM diagnostics for the sperm whale 1987-1989 best model. In the Q-Q plot (left) the shaded area represents 95% confidence interval, the circles represent the data, the line is the expected data distribution if the model fits the data perfectly. The residual versus linear predictor (right) does not show any patterns or presence of heteroscedasticity.

Table 3.3. Summary of sperm whale 1987-1989 models at different SST months. The best error structure for all models was the negative binomial distribution. The model included the standard covariates survey and depth, and aspect plus the stated month for SST.

Model:	Deviance	Deviance explained (%)	AIC	REML	n
April	630.72	32.33	2064.24	1038.77	6695
May	612.55	32.01	2070.12	1042.60	
June	617.99	31.01	2077.17	1045.20	
July	610.63	29.72	2090.26	1051.89	
August	605.54	29.35	2093.64	1053.21	

The smooth functions show a predicted positive effect on sperm whale density of depths greater than 800 m and a negative effect in waters 500 m or shallower. Slopes below 1˚ had a negative effect, while slopes of 1.5˚ to 9˚ had a positive effect. Aspect did not show a clear signal. Cold SST in April from -2 ˚C to 2 ˚C T had a negative effect while warmer waters between 4˚C to around 8˚C had a positive effect (Figure 3.8).

Predictions of sperm whale density (from 1987-1989) are shown in Figure 3.9. Comparing with the observed whale sightings, the model predicted well the high occurrence in the Norwegian Sea, Denmark Strait, Irminger Sea and around Charlie-Gibbs fracture zone. The map of the coefficient of variation (CV) of the predictions shows the highest precision in the areas were sperm whales are generally present. Less confidence was in the Barents and Greenland Sea, south of the North Sea and at the south eastern Atlantic in all were where not or very few sperm whale sightings (Figure 3.10).

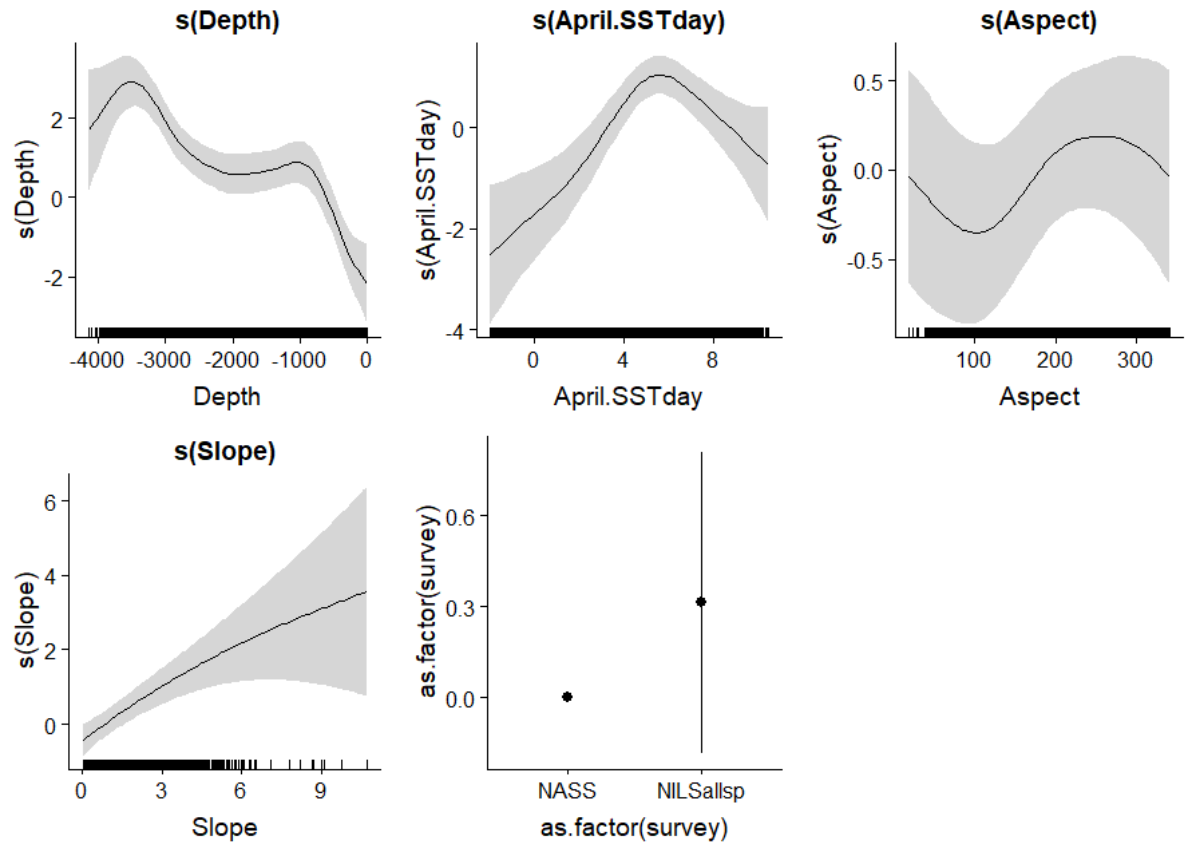

Figure 3.8. Relative density of sperm whales as a smooth function of depth, April SST, aspect, and slope for 1987-1989. Zero on the vertical axes corresponds to no effect of the covariate on the relative density of sperm whales. Shaded areas represent 95% confidence intervals. The scales on each vertical axis vary among plots. Data points are represented as rug plots on the horizontal axes.

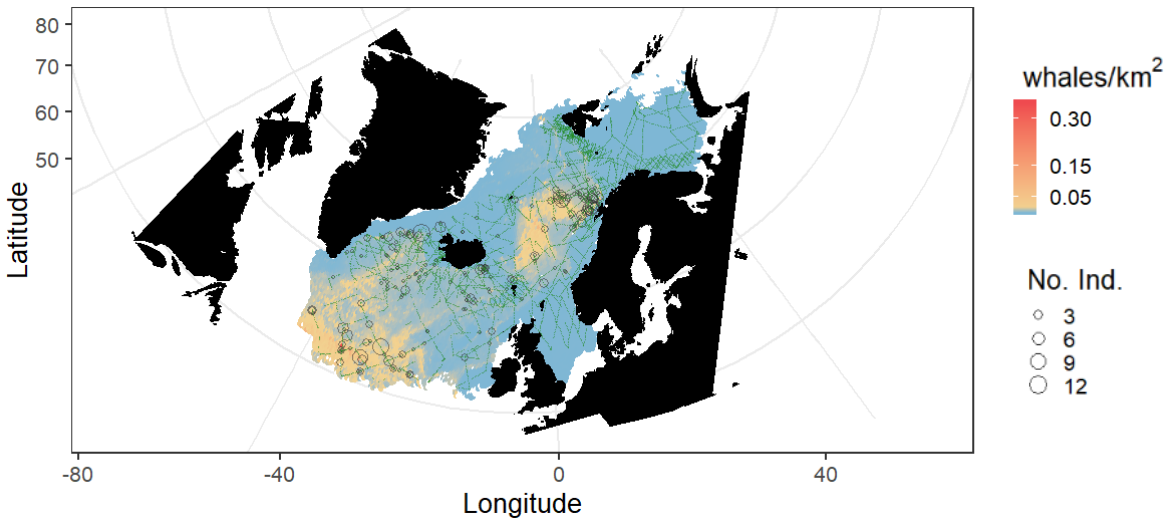

Figure 3.9. Predicted density of sperm whales for the best-fitting model for 1987-1989, which included depth, slope, aspect and April SST. The map shows sperm whale observations as grey circles, the size of which indicates the number of individuals (No. Ind.), the small green dots represent the effort.

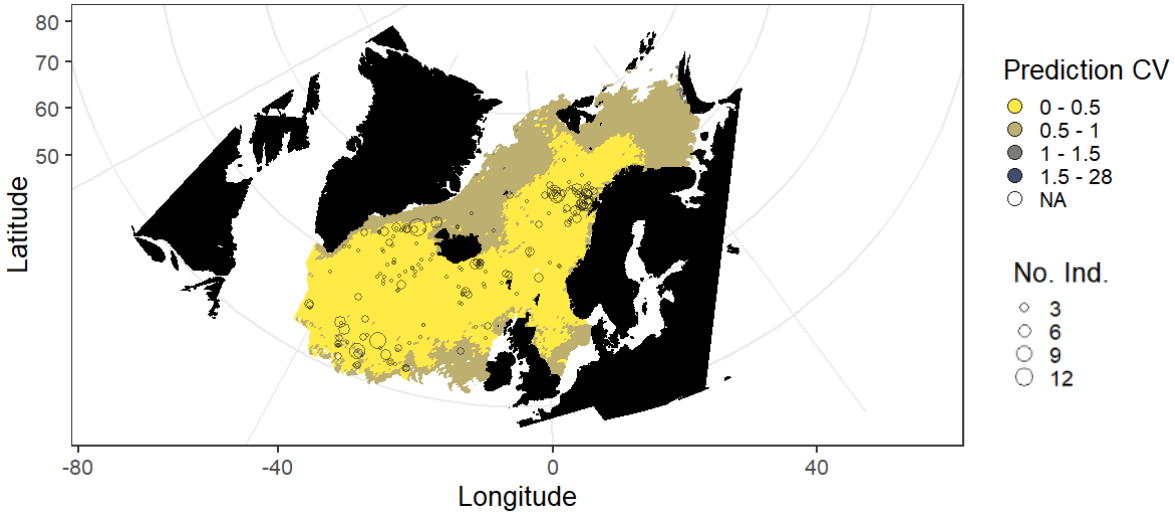

Figure 3.10. Coefficient of variation of the average predicted density of the best-fitting sperm whale model for 1987-1989. Yellow areas show the highest precision. Sperm whale observations are indicated as grey circles and scaled to the number of individuals (No. Ind.).

3.3.1.5 Distribution and habitat use models: 1998-2015

The negative binomial was determined to be the best error distribution for the sperm whale spatial model for 1998-2015 (Appendix 3-I). A summary of all the fitted single variables models can be found in the Appendix 3-J. The best covariate for each variable family that were part of the candidate full model were: depth, aspect, slope, April bT, April SST, May salinity, August SSH, July mixed layer depth, May chlorophyll *a*, and July primary productivity. The terms that were removed by penalization were April bT, May salinity, and May chlorophyll *a*. No further penalization due to collinearity and concurvity was needed (Appendix 3-K).

The covariates selected in the best model included: depth, aspect, slope, April SST, August SSH, July mixed layer depth, and July primary productivity. The model fitted the data well Figure 3.11. The best model had a deviance explained of 33.91% (Table 3.4) (see methods section 2.2.2.4.1).

Table 3.4. Summary of the fitted models for sperm whales 1998-2015 using a forward full model and double penalization. The best error structure for all models was the negative binomial distribution. All the models included the standard covariate survey.

Model:	Deviance	Deviance explained (%)	AIC	REML	n
Penalized full model	1024.78	33.91	2957.69	1496.16	7361
Full model	1021.28	35.35	2945.43	1493.03	

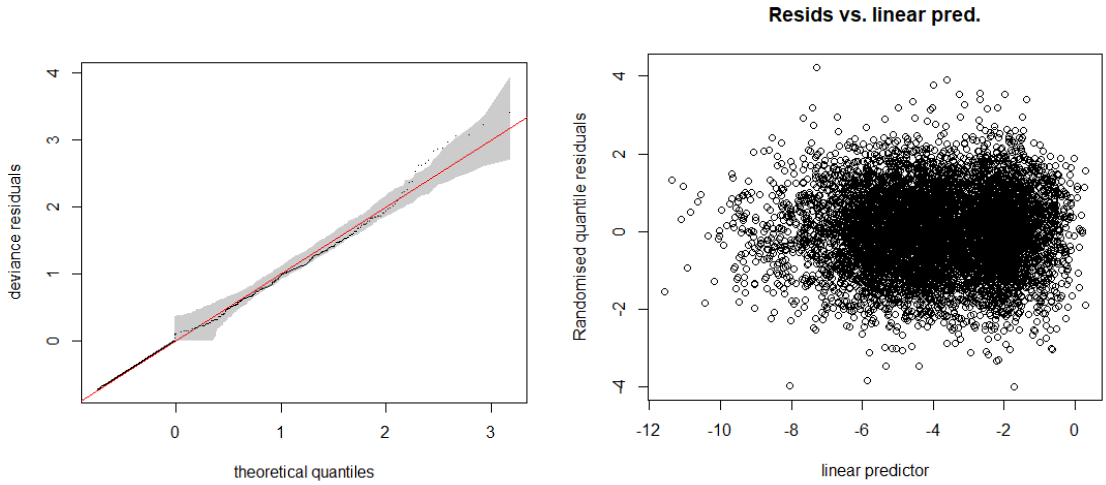

Figure 3.11. GAM diagnostics for the best sperm whale model for 1998-2015. In the Q-Q plot (left) the shaded area represents 95% confidence interval, the circles represent the data, the line is the expected data distribution if the model fits the data perfectly. The residual versus linear predictor (right) does not show any patterns or presence of heteroscedasticity.

The model predicted a positive effect on sperm whale density at depths greater than 800 m and a negative effect in waters of 500 m or shallower. Slope and aspect did not show a clear signal. April SST had a negative effect between -1°C and 1°C and also greater than 8°C, and a positive effect between 3°C and 7°C. Mixed layer depth showed positive peaks around 12 m and 18 m, with a dip in between around 15 m. August SSH had a negative effect between -1 m and -0.7 m and a positive effect at less negative values between -0.7 m and -0.4 m. Primary productivity did not show a clear signal (Figure 3.12).

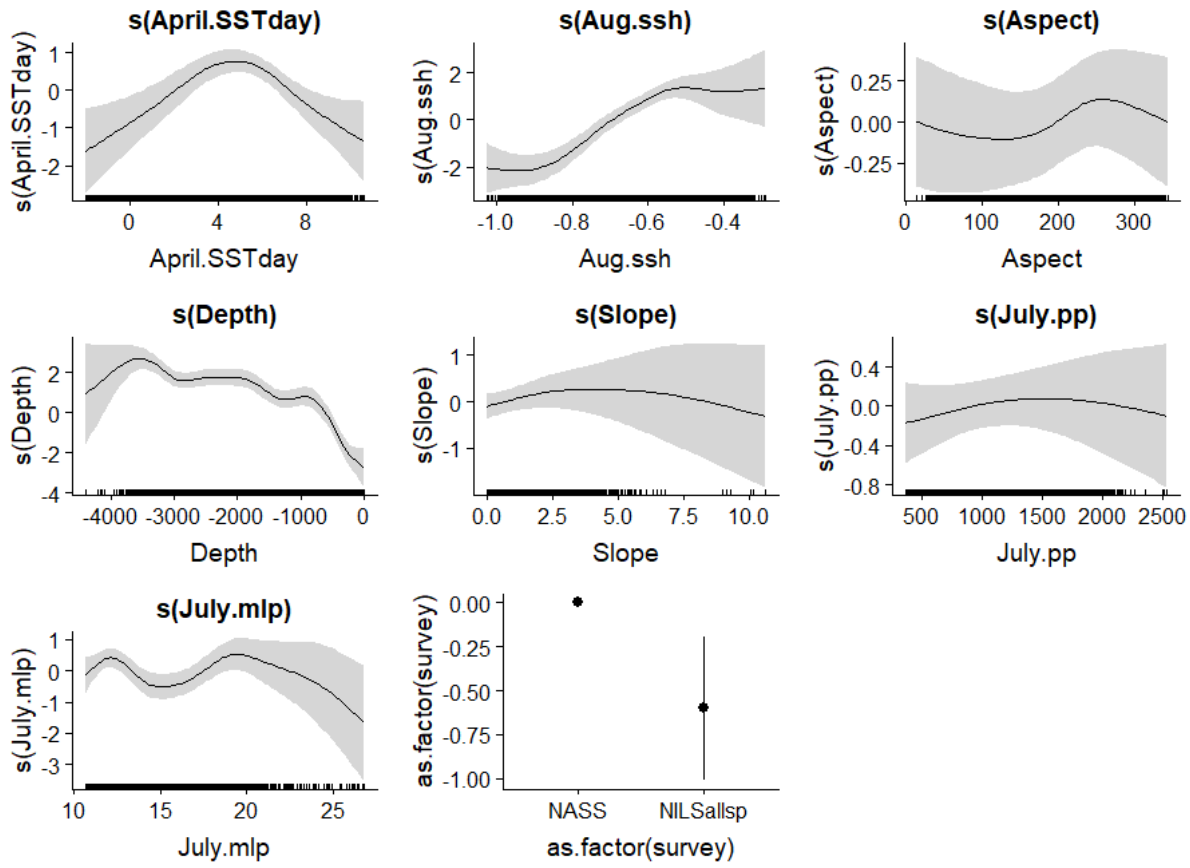

Figure 3.12. Relative density of sperm whales as a smooth function of April SST, August SSH, aspect, depth, slope, July pp, and July mlp for 1998-2015. Zero on the vertical axes corresponds to no effect of the covariate on the relative density of sperm whales. Shaded areas represent 95% confidence intervals. The scales on each vertical axis vary among plots. Data points are represented as rug plots on the horizontal axes.

Predicted sperm whale density for average values of the covariates (across 1998-2015) are shown in Figure 3.13. Comparing with the observed whale sightings, the model predicted well the high occurrence in the Norwegian Sea, the Irminger Sea and Icelandic Basin, and around the Denmark Strait. High predicted density also occurred around the Rockall Trough and Charlie-Gibbs fracture zone, where there were fewer observations. The CV of predicted density showed the highest precision in the areas were sperm whales are generally present. In the Atlantic at the southern edge of the study area including the Charlie-Gibbs fracture zone although few sperm whale sightings, the confidence is lower than in the other areas. Less confidence was also in the Barents, Greenland and North Sea were there were not sperm whale sightings (Figure 3.14).

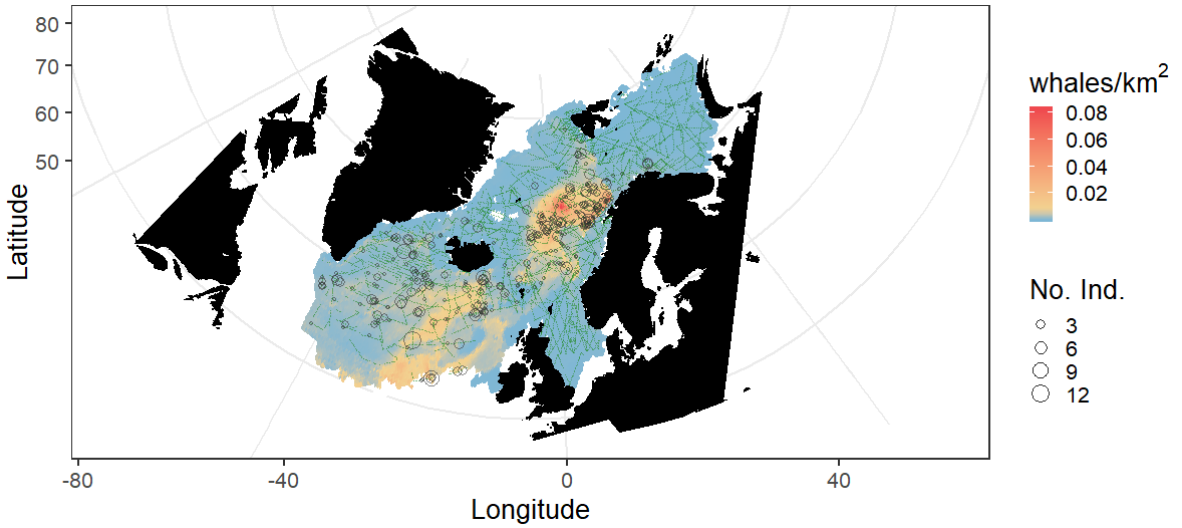

Figure 3.13. Predicted density of sperm whales for the best-fitting model for 1998-2015 including aspect, April bT, April SST, July salinity, and July mixed layer depth. Sperm whale observations are shown as grey circles, the size of which indicates number of individuals (No. Ind.). Small green dots represent the effort.

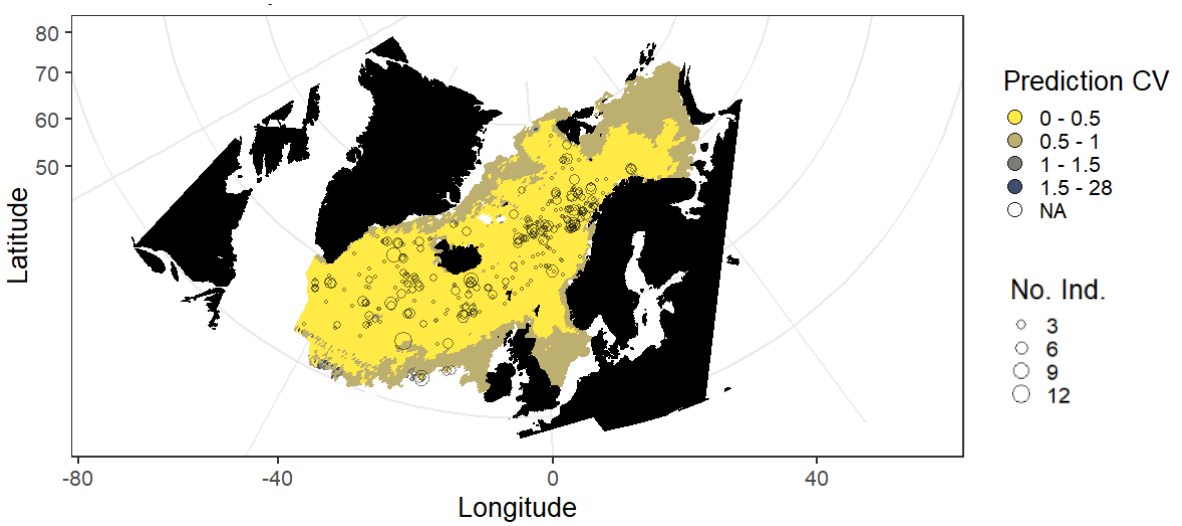

Figure 3.14. Coefficient of variation of the average predicted density of the best-fitting sperm whale model for 1998-2015. Yellow areas show the highest precision. Sperm whale observations are indicated as grey circles and scaled to the number of individuals (No. Ind.).

3.3.2 Pilot whales

3.3.2.1 Effective strip width – NASS (Iceland-Faroes) 1987-2015

The best detection function for the 1987-2015 pilot whale NASS (Iceland and Faroese) data was a hazard rate model with an 1800 m truncation distance which included 558 sightings (Appendix 3-A). Only Beaufort (two levels) was retained in the selected model. The fitted model is shown in Figure 3.15. The model fitted the data well as shown in the Q-Q plot Figure 3.15 and by the goodness of fit

test Cramer-von Mises test [unweighted] p = 0.577. The average probability of detection *p* was 0.296 (CV = 0.086). The estimated effective strip width for the two covariate levels is given in Appendix 3-L.

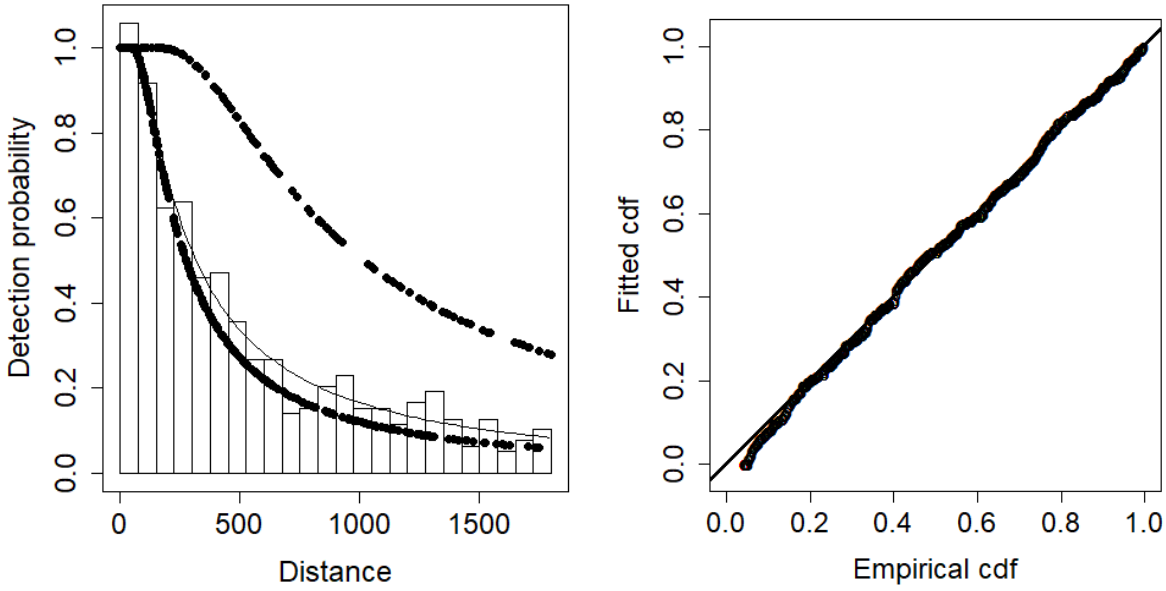

Figure 3.15. Detection probability (left) and Q-Q (right) plots for pilot whale 1987-2015 NASS data. For detection probability, the circles represent fitted values of the data, the line is the fitted model and the frequency histogram represents the observed data. In the Q-Q plot (right) the points are the fitted values while the solid line represents the expected data distribution.

3.3.2.2 Effective strip width – NILS (Norway) 1995-2013

The best detection function for the 1995 - 2013 pilot whale NILS (Norwegian) data was a hazard including a total of 35 sightings (Appendix 3-A). Beaufort (three levels) was retained in the selected model. The fitted model is shown in plots Figure 3.16. The model fitted the data fairly as shown by the Q-Q plot Figure 3.16 and by the goodness of fit test Cramer-von Mises test [unweighted] p = 0.845. The average probability of detection *p* was 0.484 (CV = 0.095). The estimated effective strip width for the three covariate levels is given in Appendix 3-M.

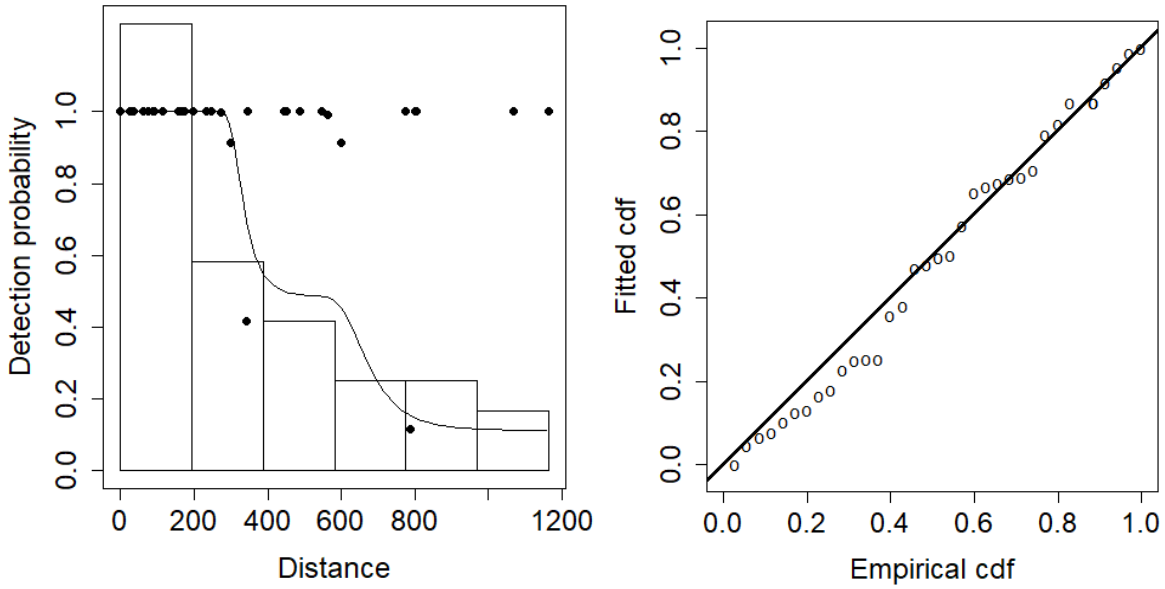

Figure 3.16. Detection probability (left) and Q-Q (right) plots for pilot whale 1995-2013 NILS data. For detection probability, the circles represent fitted values of the data, the line is the fitted model and the frequency histogram represents the observed data. In the Q-Q plot (bottom) the points are the fitted values while the solid line represents the expected data distribution.

3.3.2.3 Distribution and habitat use models: 1987-1989

The Tweedie was determined to be the best error distribution for the 1987-1989 spatial models for pilot whales (Appendix 3-N). A summary of all the fitted single variable models is given in Appendix 3-O. The correlation evaluation between static variables and SST months is shown in Appendix 3-D, where none of the pairs had a Pearson's correlation greater than 0.7. As for the other species concurvity was not evaluated in the 1980s models (see methods section 2.2.2.4.1).

After fitting models to determine the best month for SST, the covariates selected in the best model included: depth, slope, and May SST. Aspect was penalized out of the best model and in all monthly models tested. The model fitted the data well as shown in Figure 3.17. The best model had a deviance explained of 14% (Table 3.5).

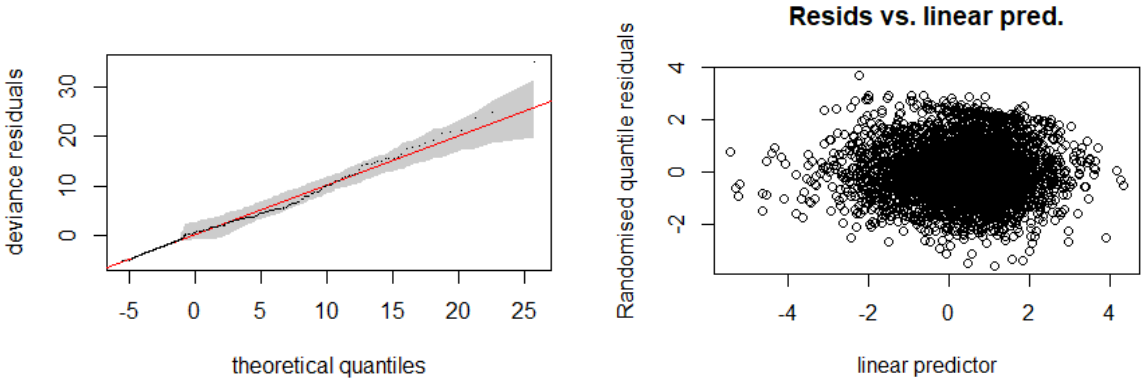

Figure 3.17. GAM diagnostics for the pilot whale 1987-1989 best model. In the Q-Q plot (left) the shaded area represents 95% confidence interval, the circles represent the data, the line is the expected data distribution if the model fits the data perfectly. The residual versus linear predictor (right) does not show any patterns or presence of heteroscedasticity.

Table 3.5. Summary of pilot whale 1987-1989 models at different SST months. The best error structure for all models was the Tweedie distribution. The model included depth, and slope plus the stated month for SST. In all the monthly models' aspect was penalized.

Model:	Deviance	Deviance explained (%)	AIC	REML	n
May	33375.02	14.01	4892.05	1297.34	3491
April	35325.94	9.20	4898.30	1298.53	
August	34164.12	12.10	4899.73	1301.34	
July	34084.71	12.33	4901.87	1301.93	
June	35736.83	8.34	4902.43	1299.60	

The model predicted a positive effect on pilot whale density of depths greater than 1500 m and a negative effect in waters shallower than that. Slopes below 1˚ had a negative effect, while slopes of 1˚ to 6˚ had a positive effect. There was a generally increasing positive effect as temperature increased for May SST, with peaks around 8 ˚C and around 11 ˚C (Figure 3.18).

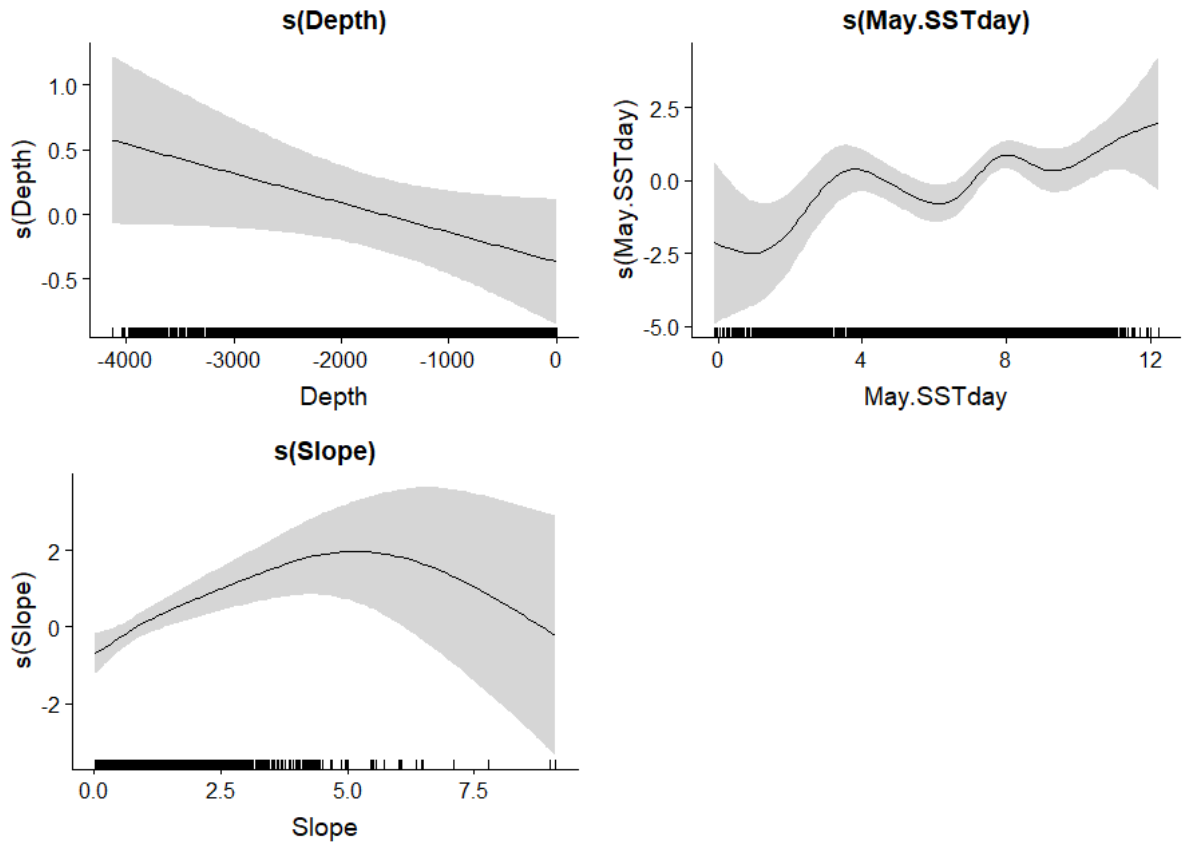

Figure 3.18. Relative density of pilot whales as a smooth function of depth, slope, and May SST for 1987-1989. Zero on the vertical axes corresponds to no effect of the covariate on the relative density of pilot whales. Shaded areas represent 95% confidence intervals. The scales on each vertical axis vary between plots. Data points are represented as rug plots on the horizontal axes.

Predictions of pilot whale density (from 1987 and 1989) are shown in Figure 3.19. Comparing with the observed whale sightings the model predicted well the high occurrence around the Faroe Islands. The model also predicted high densities in areas in the southern part of the studied area, some of which were without any sightings, such as west of Ireland (Rockall Basin), and around the Charlie-Gibbs fracture zone. The CV of the predicted density showed the highest precision in the areas were pilot whales are present. Less confidence was in general around the edge of the study area and in north eastern Iceland (between Iceland and Jan Mayen) where no animals were recorded (Figure 3.20).

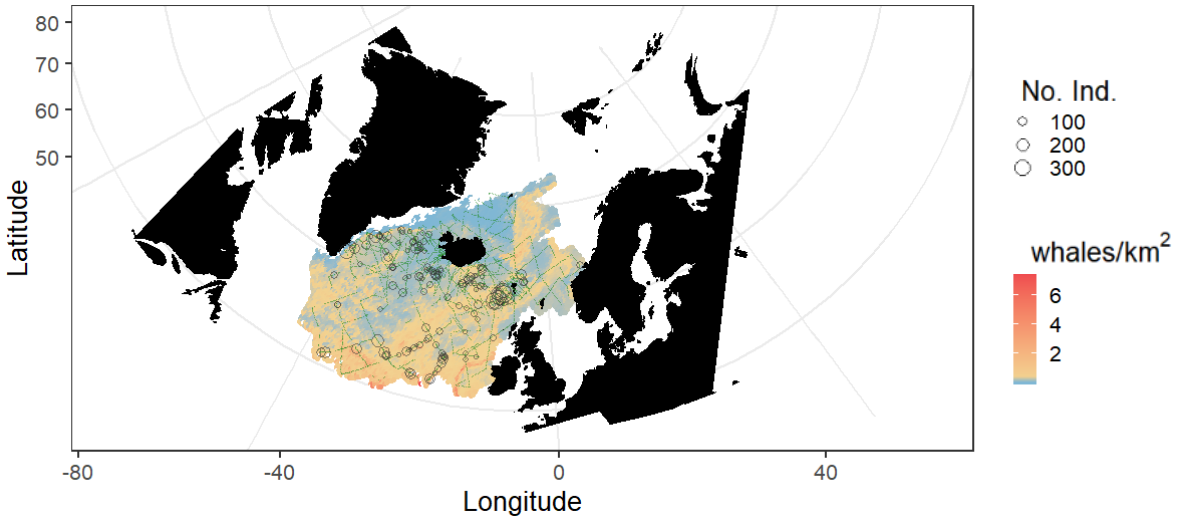

Figure 3.19. Predicted density of pilot whales for the best-fitting model in 1987 and 1989 including depth, slope, and May SST. The map shows pilot whale observations as grey circles, the size of which indicates the number of individuals (No. Ind.). The small green dots represent the effort.

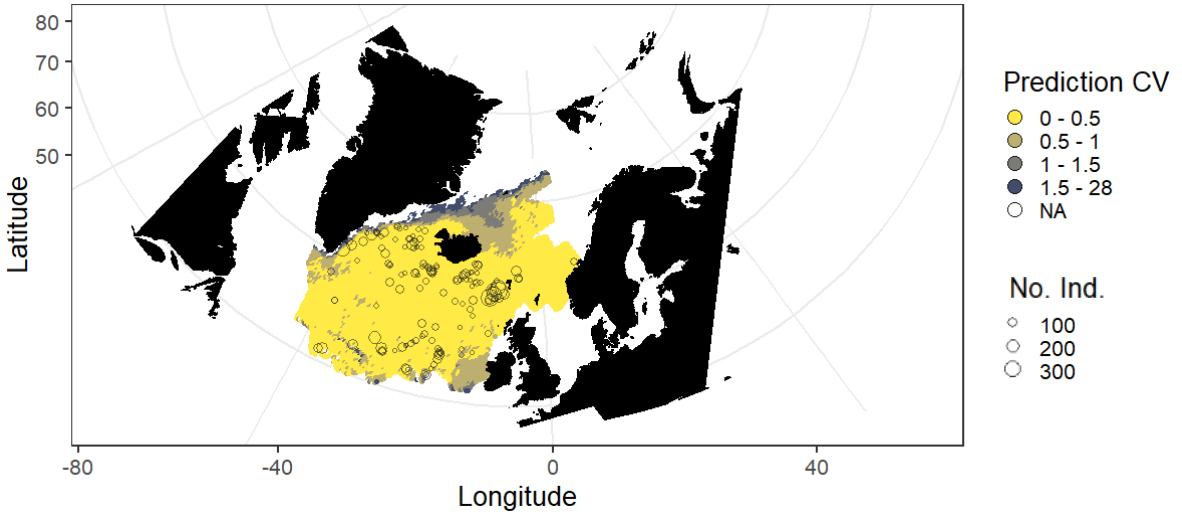

Figure 3.20. Coefficient of variation of the average predicted density of the best-fitting pilot whale model for 1987 and 1989. Yellow areas show the highest precision. Pilot whale observations are indicated as grey circles and scaled to the number of individuals (No. Ind.).

3.3.2.4 Distribution and habitat use models: 1998-2015

The negative binomial was determined to be the best error distribution for the pilot whale spatial models for 1998-2015 (Appendix 3-P). A summary of all the fitted single variables models can be found in the Appendix 3-Q. The best covariates for each variable family that were included for consideration in the full model were: depth, aspect, slope, April bT, April SST, July salinity, July SSH, July mixed layer depth, July chlorophyll *a*, and July primary productivity. The terms that were removed by penalization

were slope, July SSH, July chlorophyll *a*, and July primary productivity. In the remaining full model, after double penalization, collinearity and concurvity were found between bT and depth (Appendix 3-C and Appendix 3-R) (see methods section 2.2.2.4.1).

The covariates selected in the best model thus included: aspect, April bT, April SST, July salinity, and July mixed layer depth. The model fitted the data well Figure 3.21. The best model had a deviance explained of 50.4% (Table 3.6).

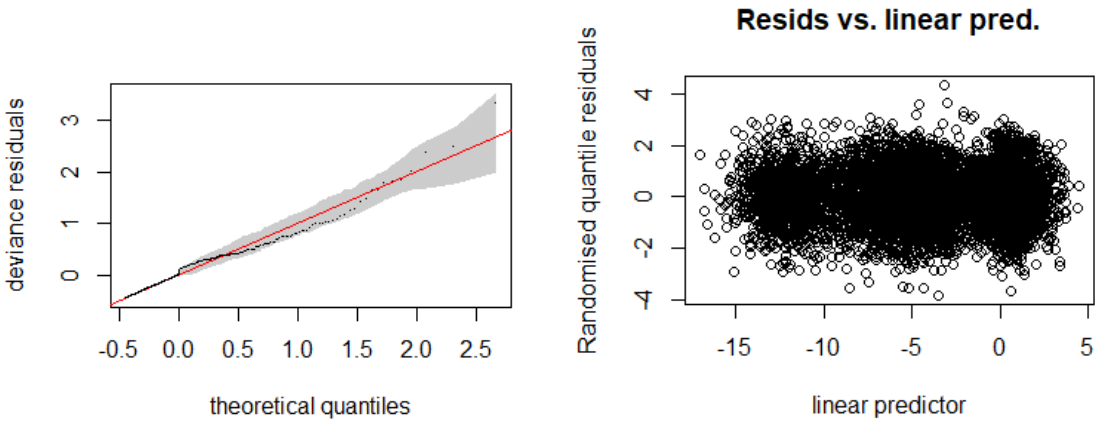

Figure 3.21. GAM diagnostics for the pilot whale 1998-2015 best model. In the Q-Q plot (left) the shaded area represents 95% confidence interval, the circles represent the data, the line is the expected data distribution if the model fits the data perfectly. The residual versus linear predictor (right) does not show any patterns or presence of heteroscedasticity.

Table 3.6. Summary of the fitted models for pilot whales 1998-2015 using a forward full model, double penalization and concurvity penalization. The best error structure for all models was the negative binomial distribution. All the models included the standard covariate survey.

Model:	Deviance	Deviance explained (%)	AIC	REML	n
Best model (concurvity)	397.06	50.39	2844.14	1424.62	7361
Penalized full model	394.84	51.98	2838.75	1421.82	
Full model	394.83	51.98	2838.76	1421.82	
Concurvity Model	399.62	49.53	2849.03	1425.99	

The best model predicted a positive effect on pilot whale density at aspects towards the west/northwest around 275°. A negative effect was found at angles around 180° (south). April bT had a negative effect at warmer temperatures around 280 °K (7 °C) and a tendency to have a positive effect, but no clear signal, at greater temperatures. April SST had a positive effect at temperatures greater than 4 C° and a negative effect below this temperature. Saltier waters greater than 35 PSU in

July had a negative effect while waters between 32 and 34 PSU had a positive effect. Mixed layer depths between 17 and 25 m had a positive effect while shallower depths did not show a clear signal (Figure 3.22).

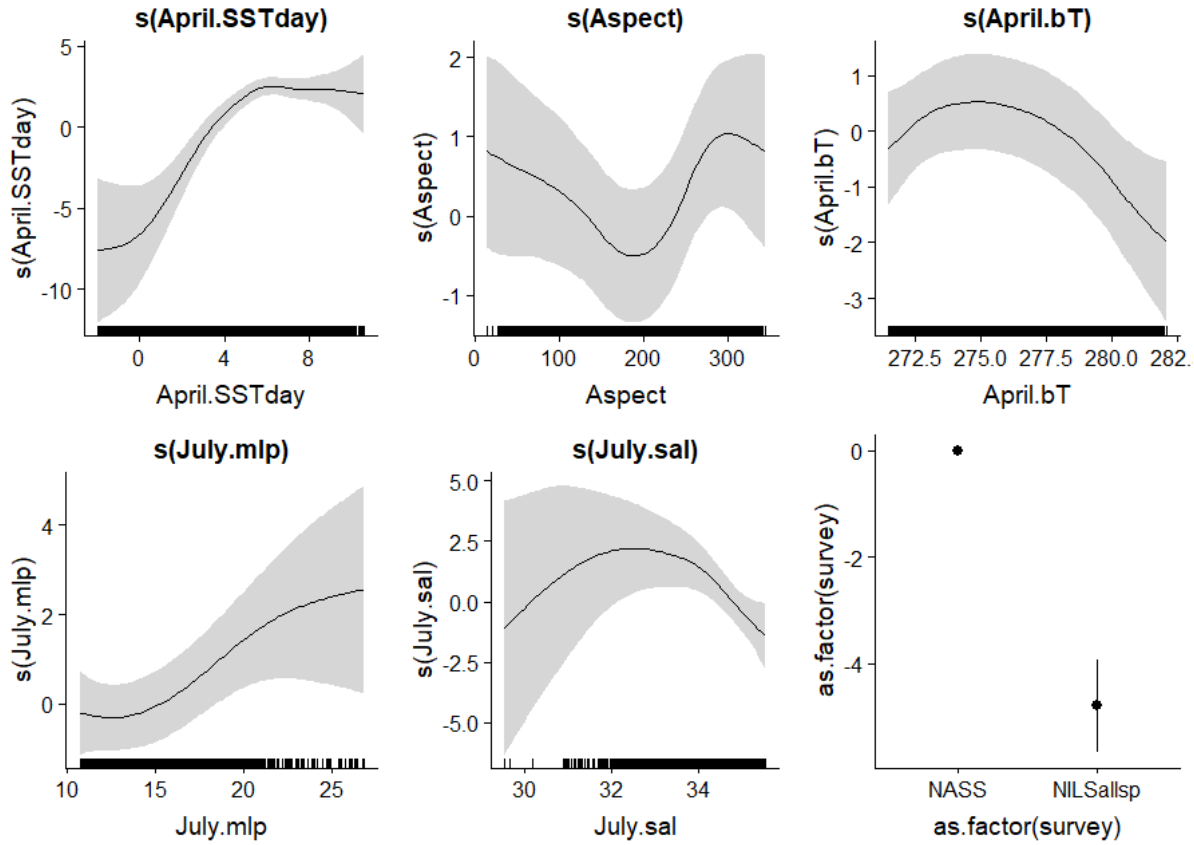

Figure 3.22. Relative density of pilot whales as a smooth function of April SST, aspect, April bT, July mlp, and July sal for 1998-2015. Zero on the vertical axes corresponds to no effect of the covariate on the relative density of pilot whales. Shaded areas represent 95% confidence intervals. The scales on each vertical axis vary between plots. Data points are represented as rug plots on the horizontal axes.

Predictions of pilot whale density for average values across 1998-2015 are shown in Figure 3.23. Comparing with the observed whale sightings, the model predicted well the high occurrence around the Denmark Strait, Faroe Islands, the Irminger Sea and the Icelandic Basin. There were high predictions with few observations in some Norwegian waters. High predictions also occurred along the eastern side of the North Sea, where there are no observations. The CV predicted density in Figure 3.24 shows high precision in the areas were most of the pilot whales are present. Less confidence was in general around the edge of the study area, and at the Greenland and Barents Sea. Also, low confidence is found along the eastern side of the North Sea where high predictions were found but not observations (Figure 3.23 and Figure 3.24).

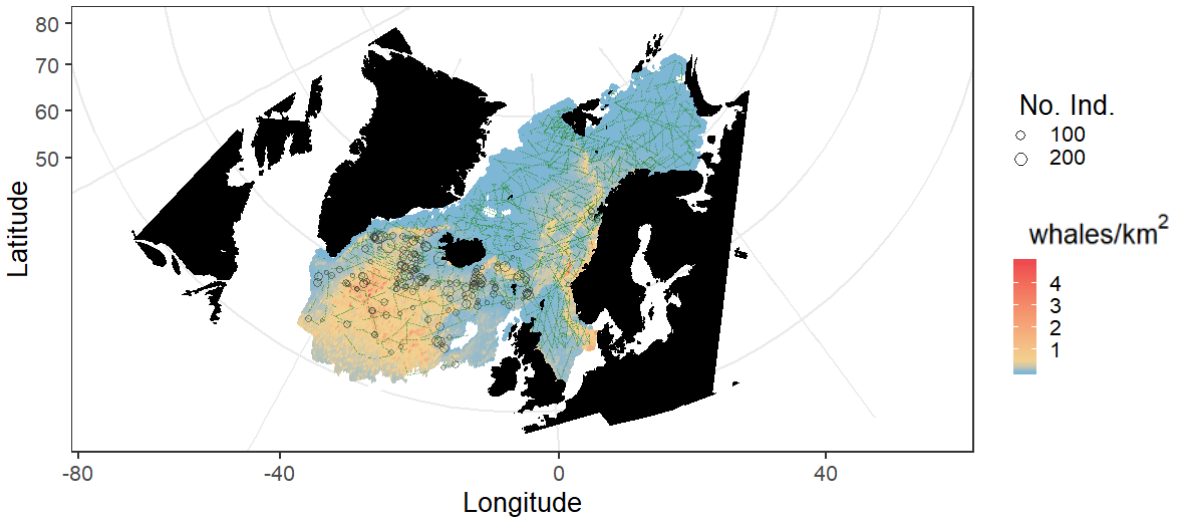

Figure 3.23. Predicted density of pilot whales for the best-fitting model across 1998-2015 including aspect, April bT, April SST, July salinity, and July mixed layer depth. Pilot whale observations are shown as grey circles, the size of which indicates the number of individuals (No. Ind.). Small green dots represent the effort.

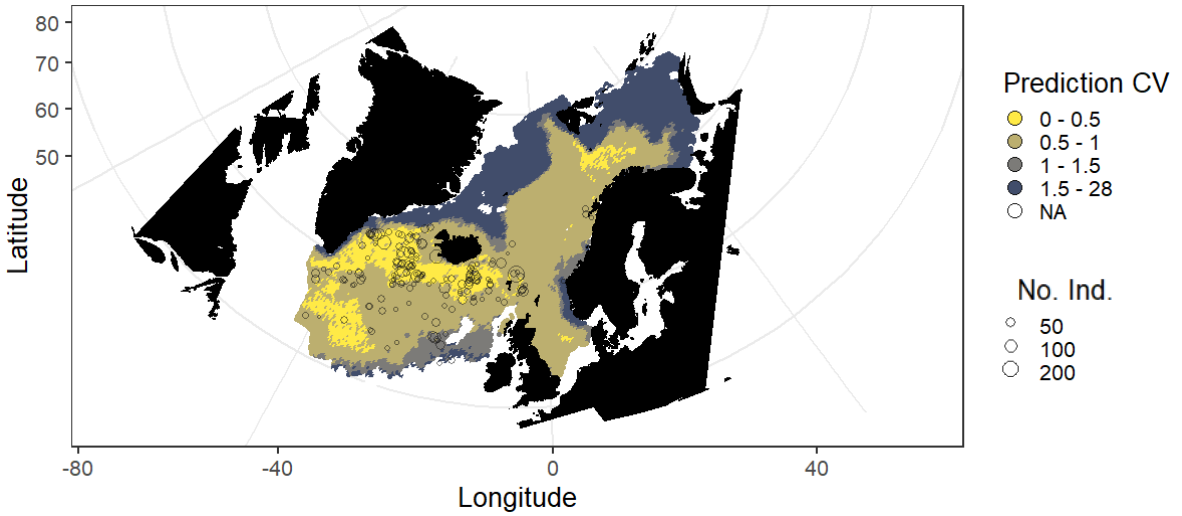

Figure 3.24. Coefficient of variation of the average predicted density of the best-fitting pilot whale model for 1998-2015. Yellow areas show the highest precision. Pilot whale observations are indicated as grey circles and scaled to the number of individuals (No. Ind.).

3.3.3 Northern bottlenose whales

3.3.3.1 Effective strip width – NASS (Iceland-Faroes) 1987-2015

The best detection function for the 1987-2015 northern bottlenose whale NASS (Iceland and Faroese) data was a hazard rate model with a 2000 m truncation distance which included 313 sightings (Appendix 3-A). Two factor covariates were retained in the selected model: vessel (ten levels) and Beaufort (three levels). The fitted model is shown in Figure 3.25. The model fitted the data well as

shown in the Q-Q plot Figure 3.25 and the goodness of fit test Cramer-von Mises test [unweighted] p = 0.784. The average probability of detection *p* was 0.226 (CV = 0.261). The estimated effective strip width for all combinations of covariate levels is given in Appendix 3-S.

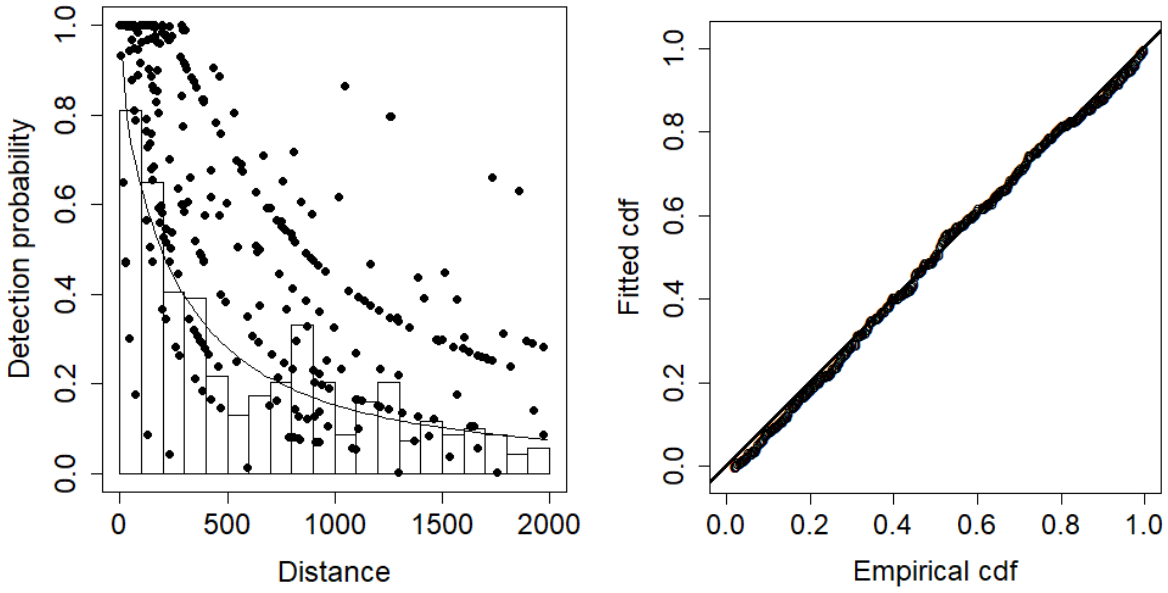

Figure 3.25. Detection probability (left) and Q-Q (right) plots for northern bottlenose whale 1987 - 2015 NASS data. For detection probability, the circles represent fitted values of the data, the line is the fitted model and the frequency histogram represents the observed data. In the Q-Q plot (right) the points are the fitted values while the solid line represents the expected data distribution.

3.3.3.2 Effective strip width – NILS (Norway) 1995-2013

The best detection function for the 1995-2013 northern bottlenose whale NILS (Norwegian) data was a hazard rate model without additional covariates fitted to untruncated data including a total of 48 sightings (Appendix 3-A). The model fitted the data well as shown in the detection probability, Q-Q plot Figure 3.26 and the goodness of fit test Cramer-von Mises test [unweighted] p = 0.822. The average probability of detection *p* was 0.286 (CV = 0.235). The estimated effective strip width for all the data was 494 m.

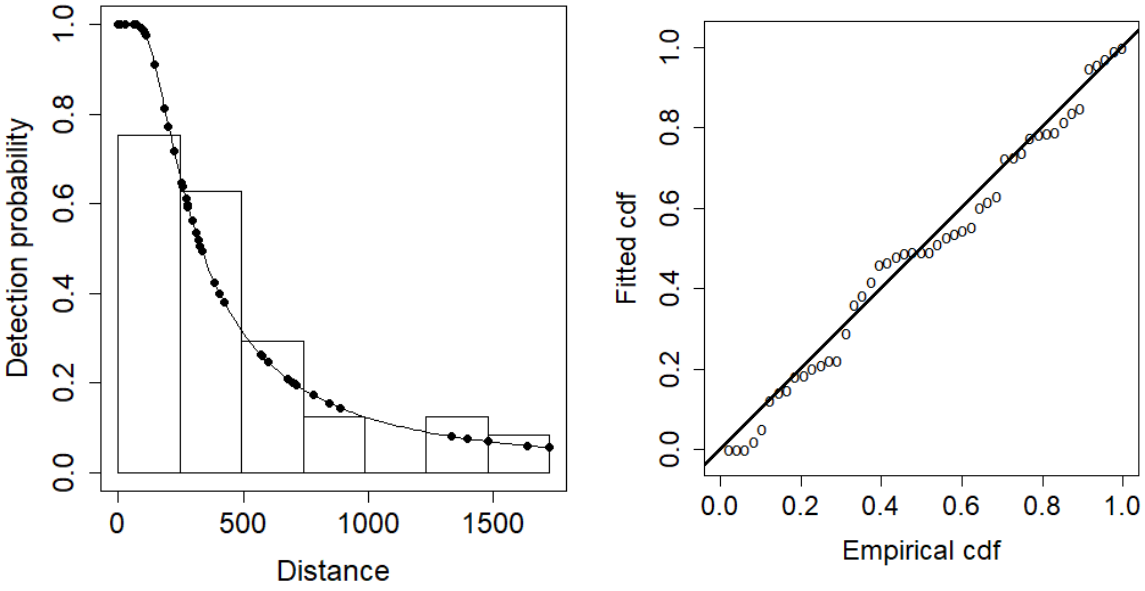

Figure 3.26. Detection probability (left) and Q-Q (right) plots for northern bottlenose whale 1995-2013 NILS data. For detection probability, the circles represent fitted values of the data, the line is the fitted model and the frequency histogram represents the observed data. In the Q-Q plot (bottom) the points are the fitted values while the solid line represents the expected data distribution.

3.3.3.3 Distribution and habitat use models: 1987-1989

The negative binomial was determined to be the best error distribution for the 1987-1989 spatial models for northern bottlenose whales (Appendix 3-T). A summary of all the fitted single variable models is given in Appendix 3-U. The correlation evaluation between static variables and SST months is shown in Appendix 3-D, where none of the pairs had a Pearson's correlation greater than 0.7. As mentioned for the other species, concurvity was not evaluated in the 1980s models (see methods section 2.2.2.4.1).

After fitting models to determine the best month for SST, the covariates selected in the best model included: depth, aspect, and August SST. Slope was penalized out of the best model and in all monthly models tested. The model fitted the data well as shown in Figure 3.27. The best model had a deviance explained of 24.2% (Table 3.7).

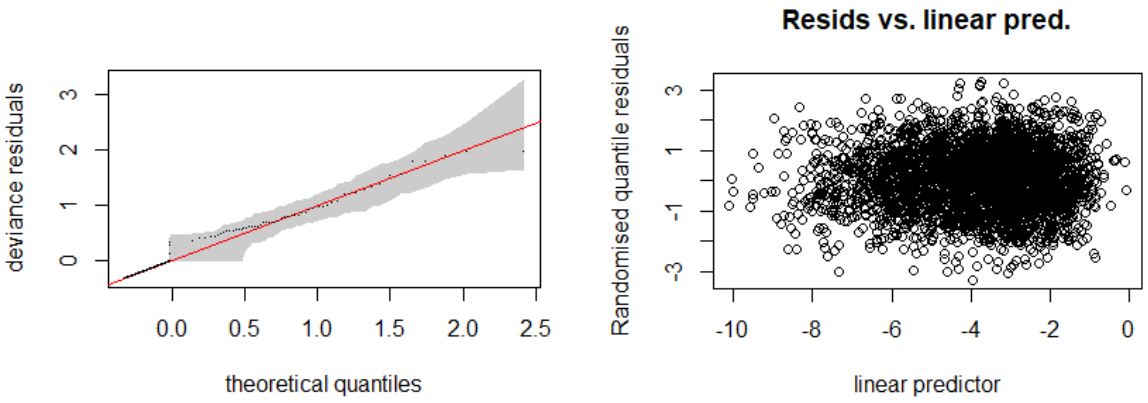

Figure 3.27. GAM diagnostics for the northern bottlenose whale 1987-1989 best model. In the Q-Q plot (left) the shaded area represents 95% confidence interval, the circles represent the data, the line is the expected data distribution if the model fits the data perfectly. The residual versus linear predictor (right) does not show any patterns or presence of heteroscedasticity.

Table 3.7. Summary of northern bottlenose whale 1987-1989 models at different SST months. The best error structure for all models was the negative binomial distribution. The model included depth and aspect plus the stated month for SST. In all the monthly models' slope was penalized.

Model:	Deviance	Deviance explained (%)	AIC	REML	n
August	161.82	24.18	826.27	416.88	3491
July	160.94	19.52	832.73	419.01	
June	161.78	19.32	833.48	419.65	
April	161.04	15.80	838.10	420.48	
May	161.21	14.37	838.99	420.55	

The model predicted a positive effect on northern bottlenose whale density at depths between 1000 m and 2000 m and a much greater positive effect in waters greater than 3500 m, and a negative effect in waters of 500 m or shallower. There was no clear signal for aspect. August SST was predicted to have a positive effect at temperatures between 9 C° to 11 C° (Figure 3.28).

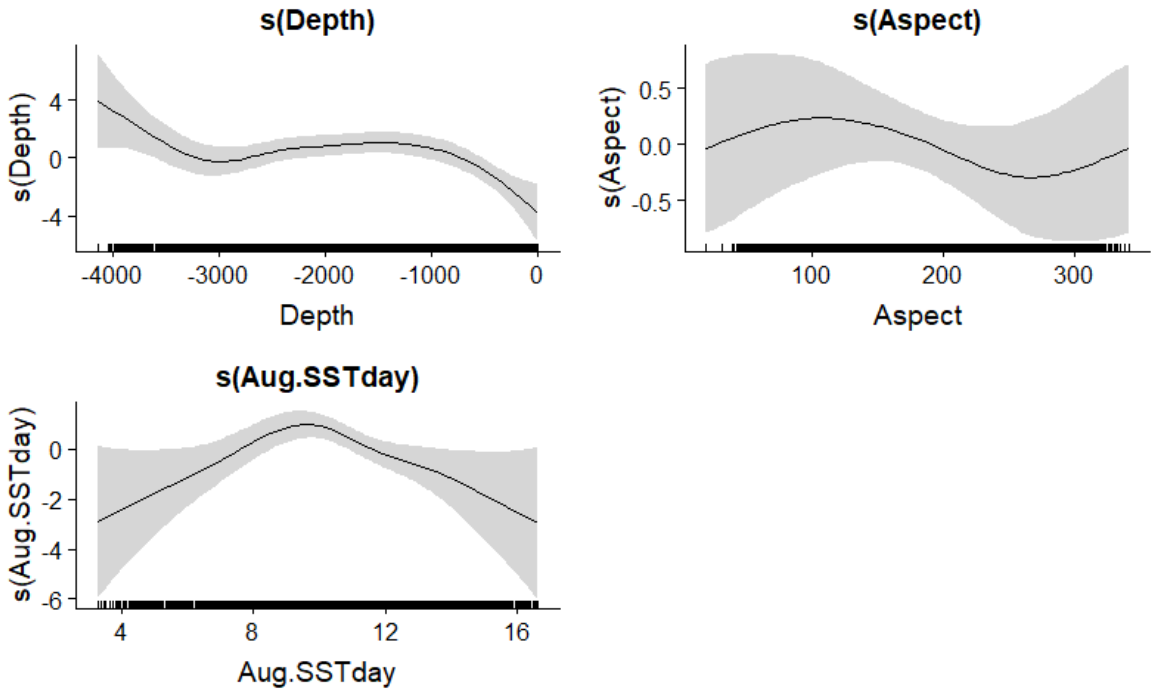

Figure 3.28. Relative density of northern bottlenose whales as a smooth function of depth, aspect, and August SST for 1987-1989. Zero on the vertical axes corresponds to no effect of the covariate on the relative density of northern bottlenose whales. Shaded areas represent 95% confidence intervals. The scales on each vertical axis vary between plots. Data points are represented as rug plots on the horizontal axes.

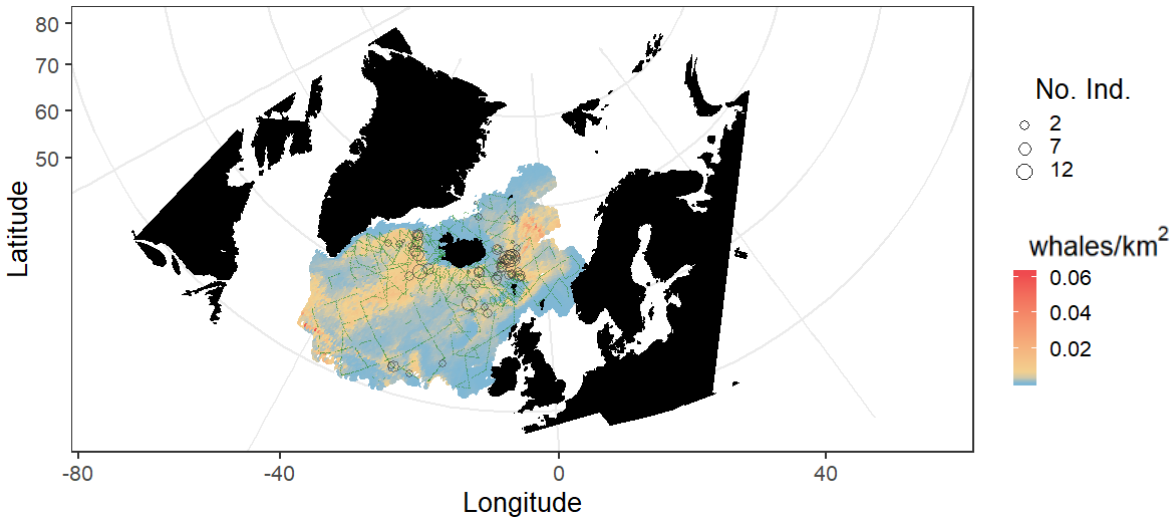

Figure 3.29. Predicted density of northern bottlenose whales for the best-fitting model in 1987 and 1989 including depth, aspect, and August SST. The map shows northern bottlenose whale observations as grey circles, the size of which indicates the number of individuals (No. Ind.). The small green dots represent the effort.

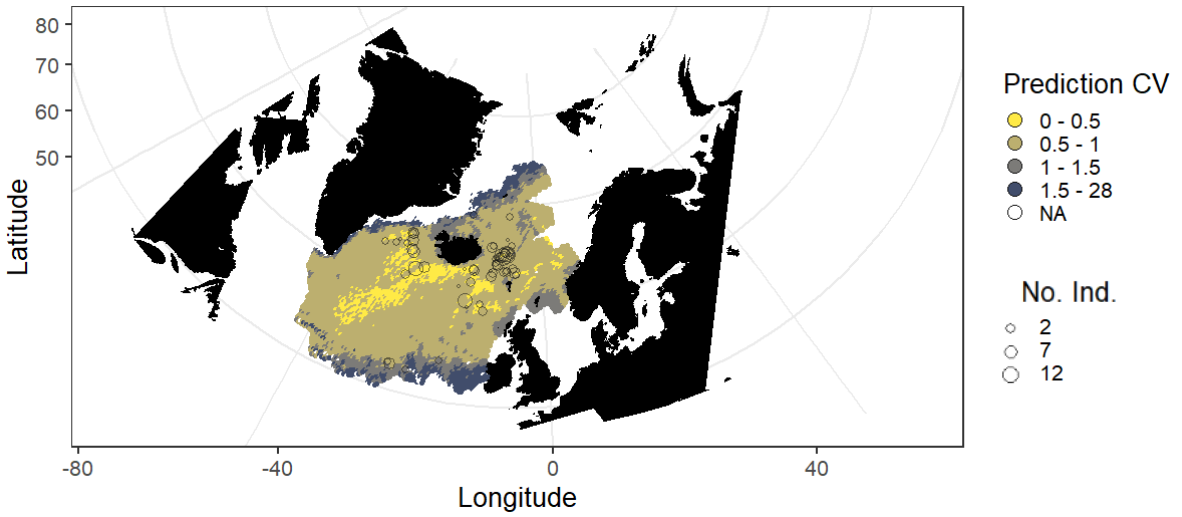

Figure 3.30. Coefficient of variation of the average predicted density of the best-fitting northern bottlenose whale model for 1987 and 1989. Yellow areas show the highest precision. Northern bottlenose whale observations are indicated as grey circles and scaled to the number of individuals (No. Ind.).

Predictions of northern bottlenose whale density from 1987 and 1989 are shown in Figure 3.29. Comparing with the observed whale sightings, the model predicted well the high occurrence north of the Faroe Islands, in the Irminger Sea and Icelandic Basin and in the mid-Atlantic (eastern Charlie-Gibbs fracture zone). The model also predicted high densities in areas which were without any sightings such as southeast of Jan Mayen, along the Reykjanes ridge and western Charlie-Gibbs fracture zone. The CV of the predicted density in Figure 3.30 shows high or medium precision in the central area were most of the northern bottlenose whales are present. High predictions and precision were found along the Reykjanes ridge, an area with some sightings (Figure 3.29 and Figure 3.30). Less confidence was in general around the edge of the study area, and in southeast of Jan Mayen and western Charlie-Gibbs fracture zone which are areas without or very few observations (Figure 3.30).

3.3.3.4 Distribution and habitat use models: 1998-2015

The negative binomial was determined to be the best error distribution for the northern bottlenose whale spatial models for 1998-2015 (Appendix 3-V). A summary of all the fitted single variables models can be found in the Appendix 3-W. The best covariate for each variable family that were included for consideration in the full model were: depth, aspect, slope, April bT, June SST, August salinity, July SSH, June mixed layer depth, April chlorophyll *a*, and April primary productivity. The terms that were removed by penalization were slope and April primary productivity. In the remaining full model, after double penalization, collinearity and concurvity were found between bT and depth (Appendix 3-C and

Appendix 3-X) (see methods section 2.2.2.4.1).

The covariates selected in the best model included: depth, aspect, June SST, August salinity, July SSH, June mixed layer depth and April chlorophyll *a*. The model fitted the data well Figure 3.31. The best model had a deviance explained of 53.7% (Table 3.8).

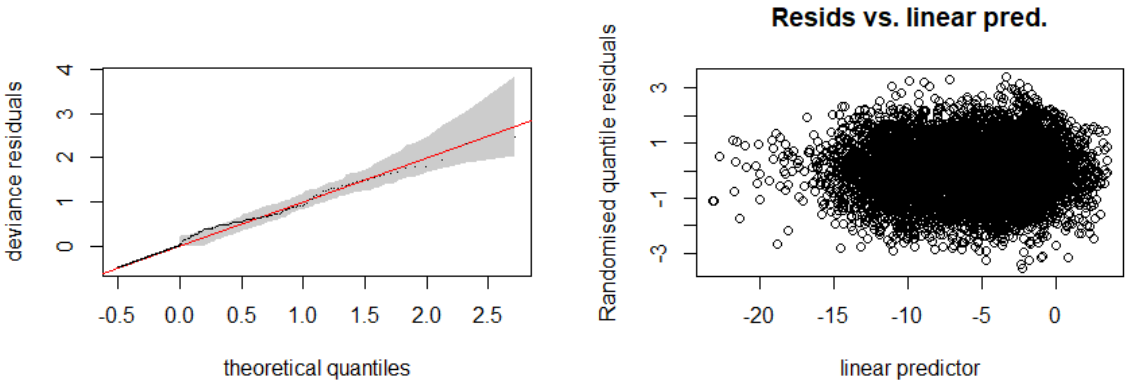

Figure 3.31. GAM diagnostics for the northern bottlenose whale 1998-2015 best model. In the Q-Q plot (left) the shaded area represents 95% confidence interval, the circles represent the data, the line is the expected data distribution if the model fits the data perfectly. The residual versus linear predictor (right) does not show any patterns or presence of heteroscedasticity.

Table 3.8. Summary of the fitted models for northern bottlenose whales 1998-2015 using a forward full model, double penalization and concurvity penalization. The best error structure for all models was the negative binomial distribution. All the models included the standard covariate survey.

Model:	Deviance	Deviance explained (%)	AIC	REML	n
Best model (concurvity)	343.65	53.72	1880.67	949.91	7361
Penalized full model	343.84	53.78	1881.31	949.70	
Full model	344.52	53.48	1883.52	950.26	
Concurvity Model	349.57	50.01	1898.92	955.06	

The model predicted a positive effect on northern bottlenose whale density at depths between 2000 m and 800 m, shallow waters from 500 m had a negative effect. For aspect, the effects were weak, but angles from 90° to 120° (east) had a positive effect while angles between 250° to 310° (west) had a negative effect on density. June SST had a positive effect for temperatures around 5 C° but a negative effect in warmer waters around 12.5 C°. Saltier waters around 35 PSU in August had a slight positive effect while waters around 34 PSU had a slight negative effect. July SSH showed a negative effect around -1 m but a positive effect around -0.85 m. Mixed layer depths did not show a clear signal,

mainly due to the limited amount of data at depths greater than 100 m. April chlorophyll *a* had a clear negative effect as the concentration increased (Figure 3.32).

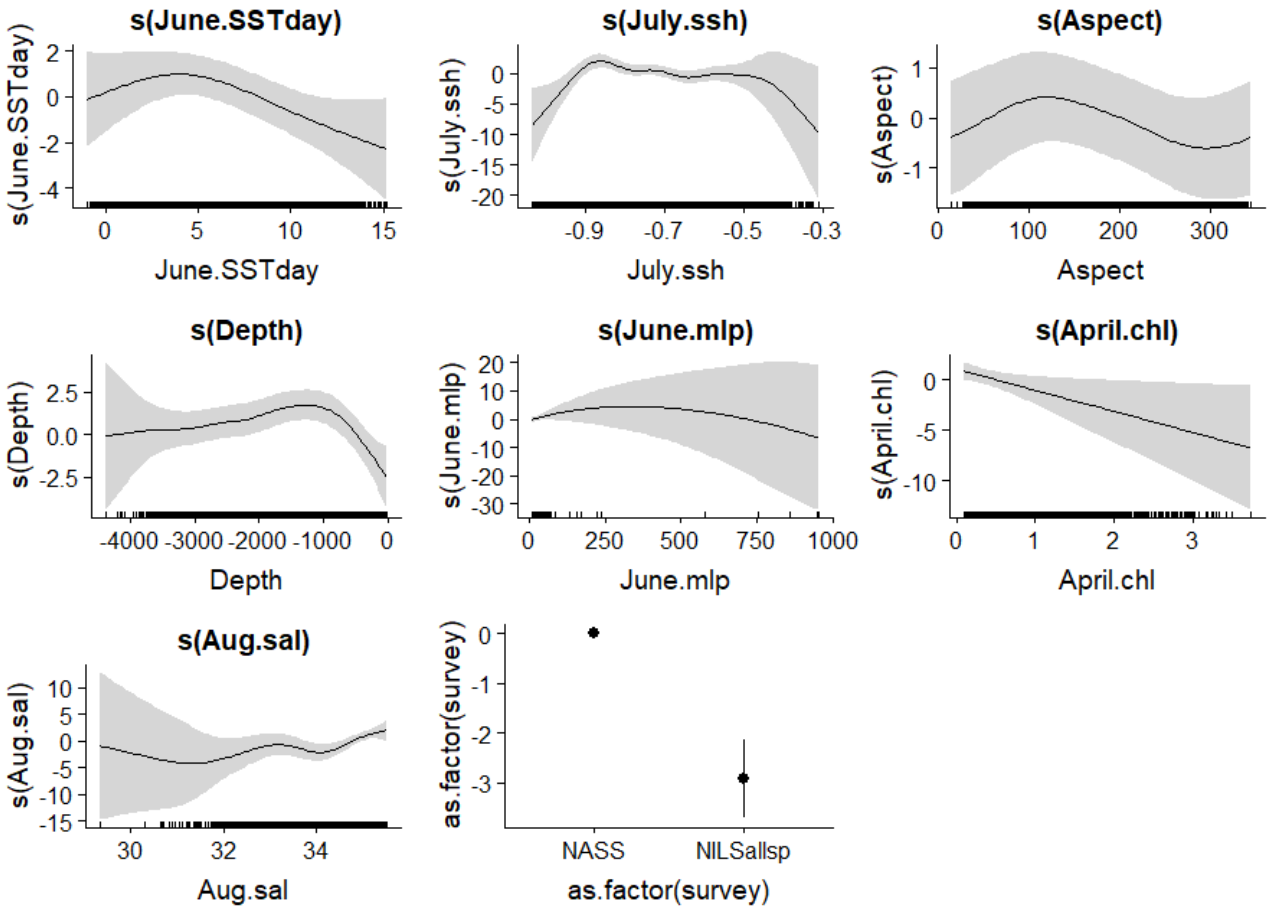

Figure 3.32. Relative density of northern bottlenose whales as a smooth function of June SST, July ssh, aspect, depth, April chl, June mlp, and Aug sal for 1998-2015. Zero on the vertical axes corresponds to no effect of the covariate on the relative density of northern bottlenose whales. Shaded areas represent 95% confidence intervals. The scales on each vertical axis vary among plots. Data points are represented as rug plots on the horizontal axes.

Predictions of northern bottlenose whale density for average values across 1998-2015 are shown in Figure 3.33. Comparing with the observed whale sightings, the model predicted well the high occurrence around west of Svalbard, Jan Mayen, Faroe Islands, East Greenland in the Irminger Sea and Icelandic Basin, and along the Reykjanes ridge. There were high predictions with few observations close to southwest Svalbard. The CV of the predicted density Figure 3.34 shows high or medium precision in the central area were most of the northern bottlenose whales are present. High predictions and precision were found along the Reykjanes ridge and Irminger Sea (by the East Greenland Current), areas with sightings all along (Figure 3.33 and Figure 3.34). Less confidence was

in general around the edge of the study area, the North Sea and around UK and Ireland which are areas without or very few observations (Figure 3.34).

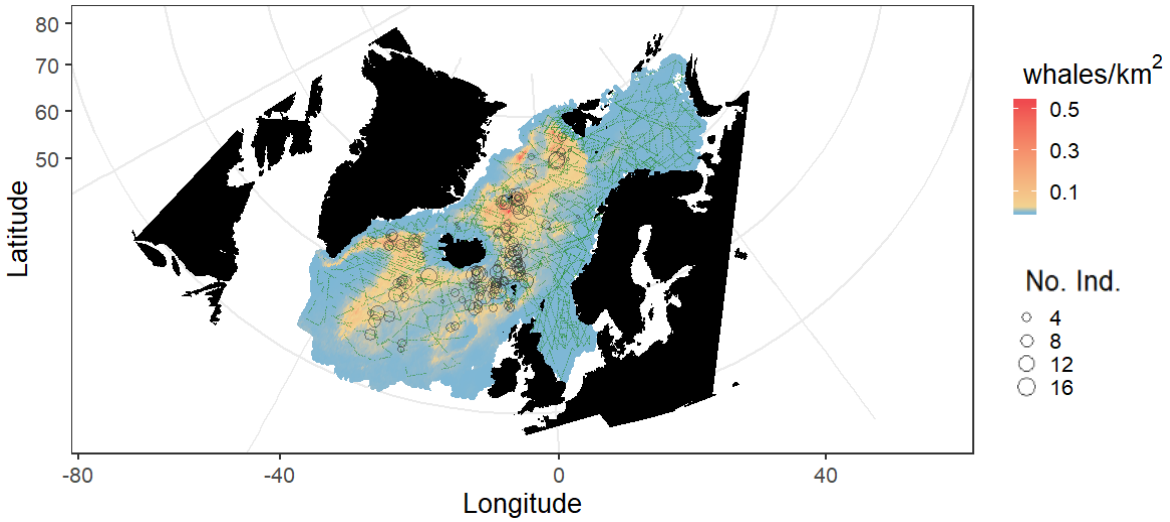

Figure 3.33. Predicted density of northern bottlenose whales for the best-fitting model across 1998-2015 including depth, aspect, June SST, August salinity, July SSH, June mixed layer depth, and April chlorophyll a. The map shows northern bottlenose whale observations as grey circles, the size of which indicates the number of individuals (No. Ind.). Small green dots represent the effort.

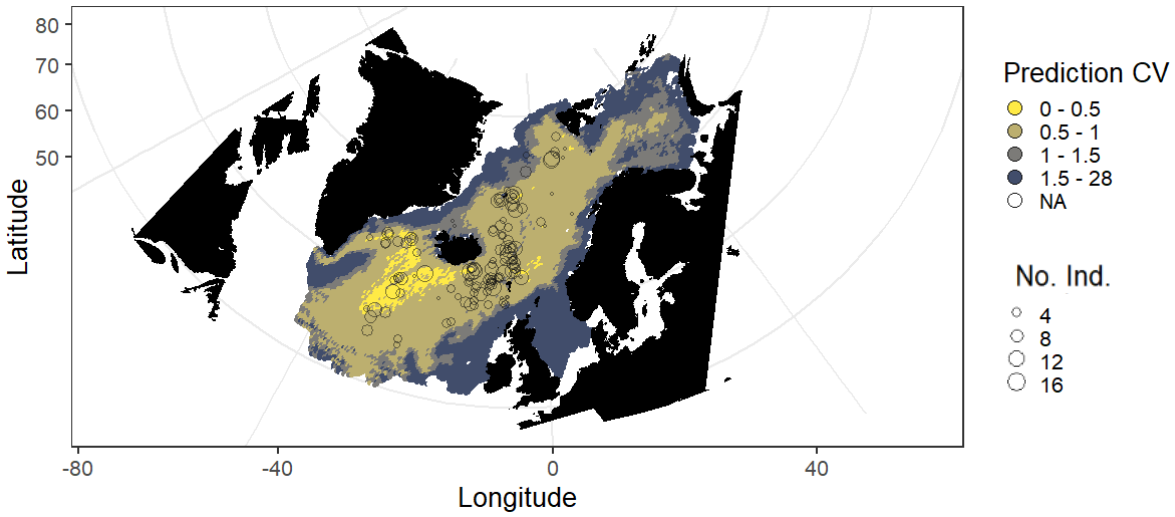

Figure 3.34. Coefficient of variation of the average predicted density of the best-fitting northern bottlenose whale model for 1998-2015. Yellow areas show the highest precision. Northern bottlenose whale observations are indicated as grey circles and scaled to the number of individuals (No. Ind.).

3.4 Discussion

3.4.1 Sperm whales

Relationships between sperm whale density and oceanographic features

Male sperm whales have been suggested to have a wide distribution but in general occur in deep water and along the continental shelf (Christensen et al., 1992; Gunnlaugsson et al., 2009; Rogan et al., 2017). Modelling results between the two periods evaluated, 1987-1989 and 1998-2015, show a consistent relationship between sperm whale densities and depth. Shallower waters of ≤500 m seem to have a negative effect on density, while waters >800 m had a positive effect. Slope and aspect did not show this consistency or a clear signal over time, thus suggesting that these variables have a weaker influence over area and time. The clear and unchanged relation with depth indicates that it is likely a strong proxy for sperm whale prey occurrence. However, in light of ocean warming and changes in some pelagic fish distribution in the area (Astthorsson et al., 2012; Hátún et al., 2009; Huse et al., 2015; Trenkel et al., 2014), this might seem questionable and it is possible that sperm whales are adapting to environmental change by staying in the same area but consuming different prey.

The relationship of sperm whales with SST has been suggested to have a broad range due to the species' wide distribution, especially for males (Baumgartner et al., 2001; Pirotta et al., 2011; Rogan et al., 2017). Because sperm whales are known to dive deeply to find their prey (Whitehead, 2018), SST is not expected to be a strong proxy of their relationship with their prey. However, the modelling results from the two periods, 1987-1989 and 1998-2015, show a similar and consistent signal over the whole area. In both periods the SST in April best explained sperm whale densities, and the smooth relations are also similar in the study area for both periods. Very cold temperatures of -1° to 2°C and the warmest temperatures ≥8 °C had a negative effect on sperm whale density. In both sets of years, a temperature range between 4°C to 7°C had a positive effect. These temperatures are within the range found by Rogan et al., (2017) in the southern part of the area. In summary, SST show a consistent signal and seem a good predictor of sperm whale densities in the area.

What further information can be obtained by considering the additional covariates retained in the 1998-2015 model? Looking at the physical variables, SST was the only one with a spring signal, while mixed layer depth and SSH both had summer signals in July and August, respectively. SST is expected to have a more lagged relationship, because it is assumed to affect the subsequent seasonal progression of productivity up the trophic levels. Mixed layer depth and SSH are expected to have shorter lagged relationships because they may be more related to water masses and prey aggregation. Generally, SSH values are negative in the North Atlantic. Negative values are associated with cyclonic

circulation or cold-core rings (Leterme and Pingree, 2008) and, in the model, the least negative SSH values from approximately -0.7 m to -0.4 m had a positive effect on sperm whale densities. The strongest negative SSH anomaly was in the Irminger Sea, where sperm whales are observed and predicted but not in great densities. The highest whale densities were predicted around the Norwegian Sea where the SSH seems on average to be less negative; here anticyclonic eddies are known to form. Anticyclonic eddies, where the mixed layer depth is shallow and there are high nutrient levels, can support phytoplankton blooms (Hansen et al., 2010), which attract higher trophic levels including the prey of sperm whales. The biological covariate primary productivity did not show a clear signal, which was expected of the several trophic level difference between this and sperm whales, which feed high in the trophic web (Whitehead, 2018).

Changes in sperm whale distribution

Sperm whales were predicted to be widely distributed in the area and no major change in distribution was seen between the two periods (Figure 3.35). In the later period, the model predicted a slightly higher density than in 1987-1989 along the Norwegian coast, west of Svalbard, along the Denmark Strait, and north of Iceland. This could indicate a slight expansion in distribution in areas such as the Denmark Strait where sperm whales were previously caught (Martin and Clarke, 1986).

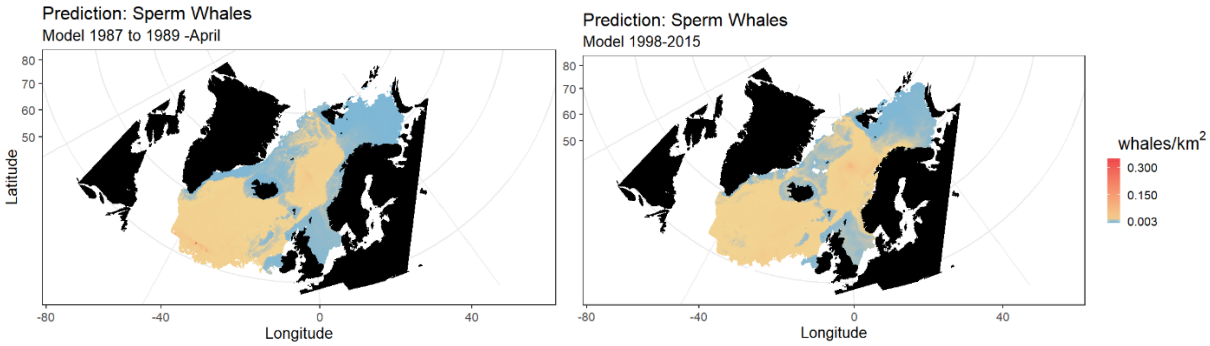

Figure 3.35. Predicted density of sperm whales from the best-fitting models for 1987-1989 (left), and 1998-2015 (right). The coloured prediction scale (right) whales/km^2, is standardized to be the same for both maps.

Overall, these summer models for sperm whales show some clear and consistent relationships with depth and SST over the area during the two periods studied. Moreover, it seems that sperm whale distribution has not changed but rather has slightly expanded over time, including into areas where it was previously caught. It is unknown if the prey of sperm whales in the entire central and north-

eastern North Atlantic is the same. Therefore, two alternate hypotheses about the consistency of the influential variables in the model and their use as proxy for the sperm whale prey arise. Firstly, sperm whales are feeding on the same prey over the entire study period and study area, meaning that sperm whales from Iceland to Norway feed on a mixture of fish and cephalopod species such as lumpsucker and *Gonatus* sp, respectively (Bjørke, 2001; Clarke, 1996; Martin and Clarke, 1986; Santos et al., 1999; Sigurjónsson and Víkingsson, 1997). Secondly, the distribution of the prey may have changed as reported for some pelagic fish species in the area (Astthorsson et al., 2012; Hátún et al., 2009; Huse et al., 2015; Trenkel et al., 2014; Valdimarsson et al., 2012) and sperm whales are now feeding on different prey. Future research could use whaling samples and current biopsy samples to understand the foraging ecology of the animals better and how well this reflects the results of the present models.

3.4.2 Pilot whales

Relationships between pilot whale density and oceanographic features

Pilot whales seem to do not have an extensive migration and their distribution during the summer in the North Atlantic seems to be highly variable year to year (Nøttestad et al., 2015; Pike et al., 2019a). As with the other species analysed, we assume pilot whales summer distribution is a reflection of their prey abundance but keeping in mind their dietary plasticity (Desportes and Mouritsen, 1993; Pike et al., 2019a; Sigurjónsson et al., 1993; Zachariassen, 1993). We expect that as both temporal models are an evaluation of several years together the yearly variation is not captured in the overall predictions but instead a broad distribution being captured. However, it is important to have in mind that there were not enough sightings to be used in modelling for the earlier years in the Norwegian data as for the northern bottlenose whales.

Modelling results show the expected effect of relief variables; pilot whales generally are associated with deeper water because they dive deeply for their prey (MacLeod et al., 2007; Rogan et al., 2017). But this expected effect was not completely clear nor found consistently between the models for the two time periods. In the 1987-1989 model, depth and slope were selected as the best covariates. Depth did show the expected relationship with a positive effect in deeper waters and a negative effect in shallower waters, but this relationship had high variability. Slope also had the expected effect with steeper slopes having a positive effect. But in the 1998-2015 model, the only covariate selected from the relief variables was aspect with positive west/northwest effects and negative effect in southerly angles, also with high variability. These findings support the previously suggested high annual variation in pilot whale distribution and foraging plasticity (Desportes and Mouritsen, 1993; Nøttestad et al.,

2015; Pike et al., 2019a; Sigurjónsson et al., 1993; Zachariassen, 1993). But they also show that combining several years together leads to high variability and lack of a clear signal.

Spring sea surface temperature was selected in both models, and the relationship generally described a positive effect of warmer waters and a negative effect of colder waters. Although the general pattern was similar, the slightly greater 'wiggliness' in the fitted smooth relationship in the 1998-2015 model could be due to the inclusion of Norwegian waters, where pilot whales may respond differently to temperature. A similar general relationship was also described for pilot whales in Scottish and Faroes waters where higher sightings/catches were associated with warmer summer waters (Hátún et al., 2009; MacLeod et al., 2007). Although it is not expected that SST is a direct influence on pilot whales, the pattern found in this study appears similar to those previously found. The previous studies did not evaluate lagged relationships, but it is possible that temperature in the spring months was also important. This relationship with temperature in general could be related to warmer water favouring early stages of planktonic production that link with higher trophic levels such as fish and squid.

What further information can be obtained by considering the additional covariates retained in the 1998-2015 model? Of the physical covariates, SST and bottom temperature showed a spring signal while mixed layer depth and salinity showed a summer signal. This may be related to foraging and the trophic level at which pilot whales feed. As described above, temperature most likely influences phytoplankton productivity, which would thus lead to a lagged relationship with pilot whale density. Summer mixed layer depth and salinity relate to water masses that could be linked to summer prey availability/aggregation. The biological covariate chlorophyll *a* concentration was not retained in the final model, which could be expected because pilot whales feed at a higher trophic level web.

Changes in pilot whale distribution

There seems to be no major change in the predicted distribution between the two modelled periods (1987-1989 and 1998-2015) (Figure 3.36). A wide distribution is predicted in the studied area in both periods, notwithstanding that there is no prediction in Norwegian waters in the earlier period because of small sample size. During the earlier years predicted density was higher in the south compared with the later years when high density was predicted in more central areas. It is possible that this difference could reflect differences in survey effort rather than a shift in distribution because the area surveyed in 1989 was the most southerly of all the years (Pike et al., 2013 In: NAMMCO, 2019b). One problematic area in the 1998-2015 model is the North Sea, where pilot whales are not commonly seen and where the model predicts presence in the eastern part where pilot whales have not been reported

either historically (Figure 3.1) or from this study (Figure 3.3). This unsupported prediction could be part of the model trying to capture the high yearly variability previously mentioned, furthermore the CV of the predicted density shows a low precision for this area Figure 3.24.

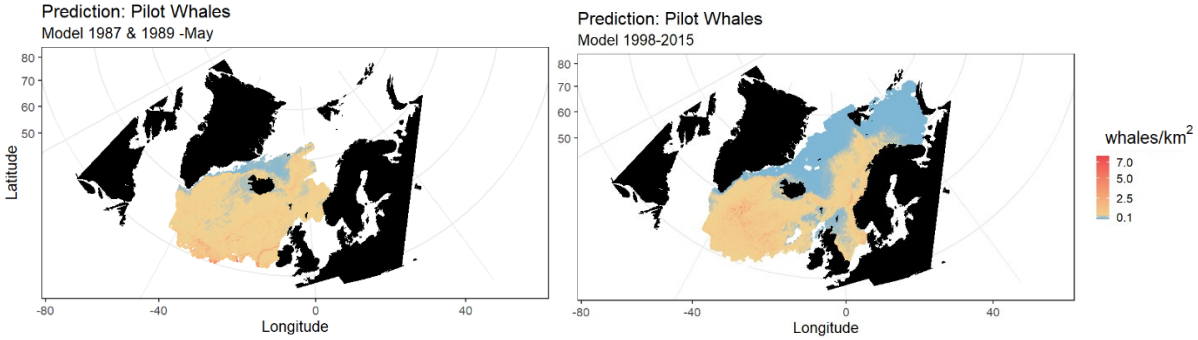

Figure 3.36 Predicted density of pilot whales for the best-fitting models for 1987-1989 (left), and 1998-2015 (right). The coloured prediction scale (right) whales/km², is standardized to be the same for both maps.

Overall, relating the summer distribution of pilot whales to information about their prey appears difficult with the available covariates. The main reason seems to be the inter-annual variation in distribution (Hoydal and Lastein, 1993; Pike et al., 2019a). Changes in pilot whale distribution could be linked to changes in their prey distribution. Pilot whales are plastic in their diet and hence opportunistic feeders (Desportes and Mouritsen, 1993) and their main prey may vary among areas (Desportes and Mouritsen, 1993; Nøttestad et al., 2015; Sigurjónsson et al., 1993). The most consistent feature in the models over time and over the whole studied area was the spring SST signal where warmer water had a positive effect on pilot whale density, a feature that has also been described in the area and in Scotland (Hátún et al., 2009; MacLeod et al., 2007) but the mechanisms underlying these relationships are unknown. Future research could focus on investigating this relationship in the context of ocean warming. The best way to understand pilot whale summer distribution in the central and north-eastern North Atlantic in relation to their prey may be to develop models for annual data instead of for periods of time and to develop separate models for different regions, such as around Iceland, the Faroes and Norway. This may uncover distribution patterns that were hidden using only two periods of time.

3.4.3 Northern bottlenose whales

Relationships between northern bottlenose whale density and oceanographic features

Northern bottlenose whales have a different summer behaviour from the other whale species investigated here. Although the evidence is mixed, it seems that overall the number of northern

bottlenose whales in the northern part of the study area may have decreased, as a result of southward movement -southward migration- (Benjaminsen and Christensen, 1979; Bloch et al., 1996; Miller et al., 2015; Reeves et al., 1993; Whitehead and Hooker, 2012a). Although we would expect that signals related to prey are evident, the predicted patterns may also be related to the movement or 'migration' of animals. In considering this, it is important to have in mind that there were not enough sightings to be used in modelling the Norwegian data in the earlier years.

As expected, the effect of depth on northern bottlenose whale density did not change between the periods 1987-1989 and 1998-2015. The positive effects were in deeper waters around 1000-2000 m and beyond 3500 m and negative effects were found in shallower waters from 500 m or less (Figure 3.28 and Figure 3.32). These relationships and approximate ranges support the findings in other studies in the West Atlantic (Compton, 2004; Whitehead and Hooker, 2012a) and from whaling data in the East Atlantic (Benjaminsen and Christensen, 1979), which suggest that this whale species is quite restricted in the habitat it uses in terms of depth. Slope was not included in the final model of both studied periods. Aspect signal was not clear on either period, although the smooths follow a similar pattern for both periods (Figure 3.28 and Figure 3.32).

Focusing only on the relationship with depth, it is known that bottlenose whales prey on different deep-water fishes and squid (Mead, 1989); *Gonatus* spp seem one of the most common prey species (Bjørke, 2001; Fernández et al., 2014; Mead, 1989; Whitehead et al., 2003) especially in the Northeast Atlantic (Benjaminsen and Christensen, 1979; Bjørke, 2001; Santos et al., 2001). For example, in the Norwegian Sea their distribution seems to match the distribution of *Gonatus fabricii* (Bjørke, 2001). Prey is a primary driver of distribution and depth seems to be the best covariate explaining this relationship for this species. Regarding the two other static variables, no inferences can be made.

For SST, the month selected for the 1980s was August with positive effects between 9 C° and 11 C°, while the month selected for the period 1998-2015 was June with positive effects around 5 C° (Figure 3.28 and Figure 3.32). The difference in both the month selected and the temperature exerting a positive effect are not readily explained. The 1980s model includes a later summer signal compared to the 1998-2015 model. An explanation may lie in the combination of the southward 'migration' movement of the animals as summer progresses and the fact that Norwegian (north-eastern) data were not included in the 1980s model. The late summer signal in SST in 1998-2015 may be partially reflecting the difference in coverage between the studied periods combined with a decline in the number of whales in the northern areas. A way to evaluate difference in both the month selected and the effect of different coverage could be to model only the NASS data for both periods.

What further information does consideration of the additional covariates from the 1998-2015 model show? Looking in general at the physical covariates, all of them show a summer signal. It is expected that some of this may be related to foraging, although it is uncertain if the southward/offshore movement of the animals is due to foraging as well. Regarding the biological covariates, specifically chlorophyll *a* concentration, the signal was from spring and there is no logical explanation for the apparent negative effect of increasing chlorophyll *a* concentration.

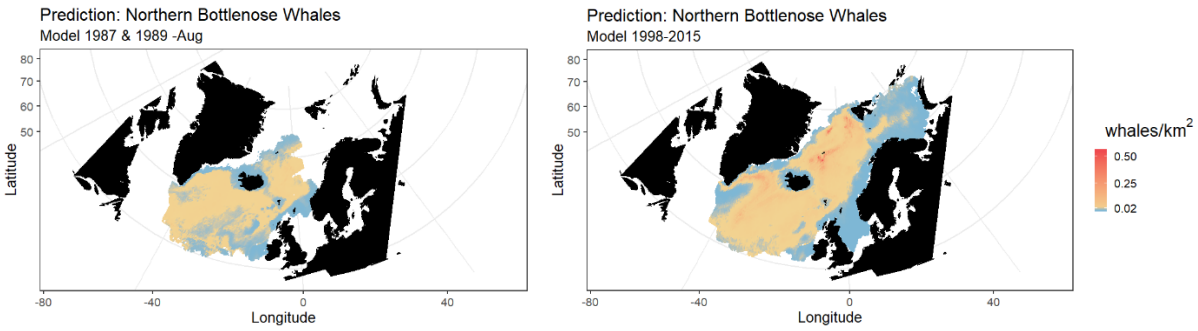

Figure 3.37. Predicted density of northern bottlenose whales for the best-fitting models for 1987-1989 (left), and 1998-2015 (right). The coloured prediction scale (right) whales/km^2, is standardized to be the same for both maps.

Changes in northern bottlenose whale distribution

In terms of predicted distribution, in north-eastern waters in 1998-2015 there were high density areas southwest of Svalbard and around Jan Mayen. In the 1980s there were few sightings in these areas, which may indicate an increase in abundance in more recent years. Such an increase may raise some questions regarding the quality of the data and survey methods for this species. But there is no reason to believe that northern bottlenose whales would have been missed by the Norwegian surveys in the 1980s. The "missing" animals in the earlier years are more likely a result of low densities.

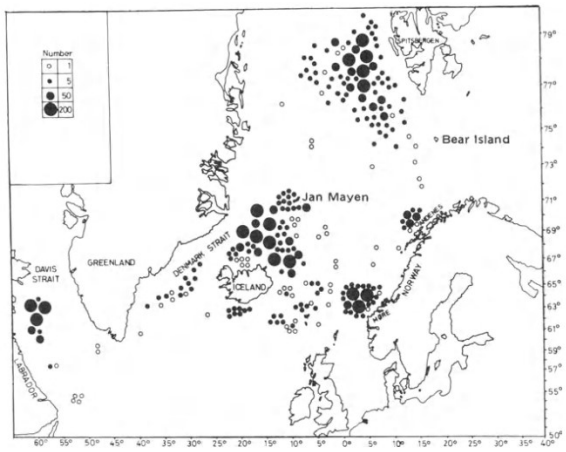

Figure 3.38. Localities of bottlenose whale caught by Norwegian whalers in the period 1938-1972 (Modified from Benjaminsen, 1972 In: Benjaminsen and Christensen, 1979)

The predicted lower densities in the 1980s may be a result of whaling activities on the species, which continued until 1972 (Whitehead and Hooker, 2012a). Data from the whaling period in 1938-1972 show that northern bottlenose whales historically occupied waters southwest of Svalbard and around Jan Mayen (Figure 3.38). Thus, the higher densities predicted in these areas in 1998-2015 may reflect an increase in density since whaling ceased almost 50 years ago. However, there is very low predicted density in waters off the coast of Andenes (around 69.3° N) and Møre (around 62.9° N) where whales were previously hunted, so it appears that whales have not returned to these areas following former exploitation (Figure 3.37 and Figure 3.38) (Benjaminsen and Christensen, 1979). This study thus indicates, in general, an increase in density through the study period (post-whaling) perhaps caused by the return of whales to some areas, but not to others as mentioned above.

Regarding the southern areas, whales occurred and were predicted in both periods studied. It seems there has been an increase in the density over time, particularly between Greenland and Iceland. Indeed, the available abundance estimates for the species show an increase from the initial estimates in the 1980s of 4,925 (CV = 0.16) off Iceland and 902 (CV = 0.45) off the Faroes (Gunnlaugsson and Sigurjónsson, 1990 In: NAMMCO, 2019c) to the latest combined estimates for Iceland and the Faroes of 28,000 (CV = 0.22) in 2001 (Pike et al. 2003 In: NAMMCO, 2019c).

It is difficult to describe a clear explanation of the northern bottlenose whale habitat use and the relationship with its prey. It is expected that prey is one of the main drivers of distribution and depth seem to be the best covariate explaining this relationship for northern bottlenose whales. But the extent to which possible “migration” is also driver of distribution is unclear, as is how such possible ”migration” may be related to prey distribution. The models predicted an overall increase in density

over time, including areas where animals were previously whaled, except in the waters off the coast of Norway by Andenes and Møre.

3.5 Comparison among species

The common covariates that best explained these three species' distributions in both periods were relief variables and SST. The selected dynamic temperature-related covariates for sperm and pilot whales were for spring, but for bottlenose whales were for summer. Summer relationships were also found for the three species for the other dynamic variables, except spring chlorophyll-*a* for bottlenose whales (Figure 3.8, Figure 3.12, Figure 3.18, Figure 3.22, Figure 3.28, and Figure 3.32). The difference in seasonal relationships for bottlenose whales may be related to a previously suggested north-south summer migration (Benjaminsen and Christensen, 1979; Bloch et al., 1996; Miller et al., 2015; Reeves et al., 1993; Whitehead and Hooker, 2012a). As expected, the predicted high-use areas for all three species were deep waters (Christensen et al., 1992; Gunnlaugsson et al., 2009; Hooker et al., 1999; MacLeod et al., 2007; Roberts et al., 2016; Rogan et al., 2017; Virgili et al., 2019; Whitehead, 2018; Whitehead and Hooker, 2012b, 2010), with some overlap among them in the central Norwegian Sea (e.g. Nøttestad et al., 2015), and the Central North Atlantic (e.g. Rogan et al., 2017), including the Irminger Sea (Abend and Smith, 1999; Gunnlaugsson et al., 2009; Whitehead and Hooker, 2012a) (Figure 3.9, Figure 3.13, Figure 3.19, Figure 3.23, Figure 3.29 and Figure 3.33). Differences in distribution likely reflect differences in prey preferences and the variation of these preferences according to the area (Benjaminsen and Christensen, 1979; Bjørke, 2001; Desportes and Mouritsen, 1993; Fernández et al., 2014; Martin and Clarke, 1986; Méndez-Fernandez et al., 2013; e.g. Nøttestad et al., 2015; Santos et al., 2014; Sigurjónsson and Víkingsson, 1997; Zachariassen, 1993). Changes in distribution between the two periods appear more as a range expansion than a shift, with generally higher predicted densities in northern waters in recent years (Figure 3.13, Figure 3.23, and Figure 3.33), which could result from an increase in suitable habitat due to warming waters (e.g. Nøttestad et al., 2015; Víkingsson et al., 2015).

3.6 Appendix

3.6.1 All species

3.1.1.1 Distance sampling

Appendix 3-A. HR= hazard-rate, HN= Half-normal. p = average probability of detection, No. obs= number of observations, CV= coefficient of variation, SE= standard error, Goodness of fit= Cramer-von Mises

Species	Truncation	Key function	Covariates	No. obs	*p*	CV	SE	Goodness of fit (p-value)	AIC	Survey & Period
Sperm whale	3000	HR	~1	564	0.502	0.081	0.041	0.766	8887.088	NASS 1987-2015
		HN	~1		0.603	0.034	0.021	0.031	8894.313	
		HR	~group size		0.512	0.077	0.040	0.785	8886.642	
		HN	~group size		0.601	0.034	0.021	0.036	8893.063	
		HR	~ vessel ID		0.584	0.055	0.032	0.225	8885.596	
		HN	**~ vessel ID**		**0.581**	**0.036**	**0.021**	**0.148**	**8876.979**	
		HR	~beaufort(3)		0.500	0.081	0.040	0.712	8887.533	
		HN	~beaufort(3)		0.601	0.034	0.021	0.036	8895.100	
		HR	~group size + vessel ID		0.583	0.054	0.032	0.239	8885.627	
		HN	~group size + vessel ID		0.579	0.036	0.021	0.162	8877.658	
		HR	~vessel ID + beaufort(3)		0.584	0.054	0.031	0.244	8885.004	
		HN	~vessel ID + beaufort(3)		0.578	0.036	0.021	0.178	8878.283	
		HR	~group size + vessel ID + beaufort(3)		0.584	0.054	0.031	0.244	8885.004	
		HN	~group size + vessel ID + beaufort(3)		0.578	0.036	0.021	0.178	8878.283	
Pilot whale	1800	HR	~1	558	0.281	0.095	0.027	0.675	8022.528	NASS 1987-2015
		HN	~1		0.501	0.028	0.014	0.000	8100.886	
		HR	~group size		0.278	0.095	0.027	0.740	8023.374	
		HN	~group size		0.497	0.028	0.014	0.000	8091.851	
		HR	~ vessel ID		0.192	0.159	0.030	0.461	8020.285	
		HN	~ vessel ID		0.484	0.029	0.014	0.000	8086.011	
		HR	~beaufort(2)		0.296	0.086	0.026	0.577	7999.264	
		HN	~beaufort(2)		0.485	0.028	0.014	0.000	8067.430	

		HR	~group size + vessel ID		0.191	0.158	0.030	0.500	8021.757	
		HN	~group size + vessel ID		0.480	0.029	0.014	0.000	8077.174	
		HR	~vessel ID + beaufort(2)		0.270	0.098	0.026	0.660	8067.430	
		HN	~vessel ID + beaufort(2)		0.470	0.029	0.014	0.000	8056.636	
		HR	~group size + beaufort(2)		0.293	0.087	0.025	0.616	7999.636	
		HN	~group size + beaufort(2)		0.480	0.028	0.014	0.000	8057.701	
Northern bottlenose whale	2000	HR	~1	313	0.269	0.144	0.039	0.598	4595.549	NASS 1987-2015
		HN	~1		0.525	0.040	0.021	0.000	4631.242	
		HR	~group size		0.266	0.146	0.039	0.577	4596.797	
		HN	~group size		0.525	0.041	0.021	0.000	4632.321	
		HR	~ vessel ID		0.219	0.267	0.058	0.715	4590.275	
		HN	~ vessel ID		0.500	0.044	0.022	0.000	4624.237	
		HR	~beaufort(3)		0.219	0.267	0.058	0.715	4590.275	
		HN	~beaufort(3)		0.500	0.044	0.022	0.000	4624.237	
		HR	~group size + vessel ID		0.217	0.264	0.057	0.694	4591.730	
		HN	~group size + vessel ID		0.498	0.046	0.023	0.000	4624.134	
		HR	~vessel ID + beaufort(3)		0.226	0.261	0.059	0.784	4587.811	
		HN	~vessel ID + beaufort(3)		0.494	0.044	0.022	0.000	4622.457	
		HR	~group size + beaufort(3)		0.257	0.150	0.039	0.695	4596.333	
		HN	~group size + beaufort(3)		0.519	0.042	0.022	0.000	4628.629	
Sperm whale	2000	HR	~1	107	0.386	0.174	0.067	0.691	1578.432	NILS 1987-1989
		HN	~1		0.506	0.070	0.035	0.154	1578.996	
		HR	~ vessel ID		0.418	0.148	0.062	0.795	1575.770	
		HN	~ vessel ID		0.498	0.070	0.035	0.218	1580.026	
Sperm whale	3000	HR	~1	814	0.410	0.042	0.017	0.576	12475.421	NILS 1995-2013
		HN	~1		0.441	0.024	0.010	0.007	12482.255	
		HR	~1	813	0.409	0.042	0.017	0.570	12460.695	NILS 1995-2013
		HN	~1		0.441	0.024	0.011	0.006	12467.460	
		HR	~group size		0.409	0.042	0.017	0.572	12462.675	

		HN	~group size		0.441	0.024	0.011	0.006	12469.457	
		HR	~ vessel ID		0.409	0.042	0.017	0.489	12462.550	
		HN	~ vessel ID		0.439	0.024	0.011	0.009	12465.606	
		HR	~beaufort		0.411	0.042	0.017	0.533	12469.514	
		HN	~beaufort		0.438	0.026	0.012	0.010	12473.947	
Pilot whale	No truncation	HR	~1	35	0.396	0.307	0.122	0.991	481.557	NILS 1995-2013
		HN	~1		0.532	0.116	0.062	0.398	482.396	
		HR	~group size		0.346	0.369	0.128	0.967	483.811	
		HN	~group size		0.531	0.122	0.065	0.391	484.340	
		HR	~ vessel ID		0.521	0.126	0.066	0.410	474.088	
		HN	~ vessel ID		0.402	0.214	0.086	0.629	471.762	
		HR	~beaufort(3)		0.484	0.095	0.046	0.845	465.250	
		HN	~beaufort(3)		0.361	0.197	0.071	0.586	465.359	
Northern bottlenose whale	No truncation	HR	~1	48	0.286	0.235	0.067	0.822	679.246	NILS 1995-2013
		HN	~1		0.460	0.079	0.036	0.029	688.102	
		HR	~pod.best.av		0.348	0.199	0.069	0.667	680.345	
		HN	~pod.best.av		0.443	0.081	0.036	0.053	686.834	
		HR	~beaufort(2)		0.248	0.273	0.068	0.885	678.015	
		HN	~beaufort(2)		0.460	0.082	0.038	0.030	690.089	
		HR	~vessel ID		0.279	0.226	0.063	0.781	679.403	
		HN	~vessel ID		0.445	0.111	0.049	0.045	689.095	

3.1.1.2 Modelling

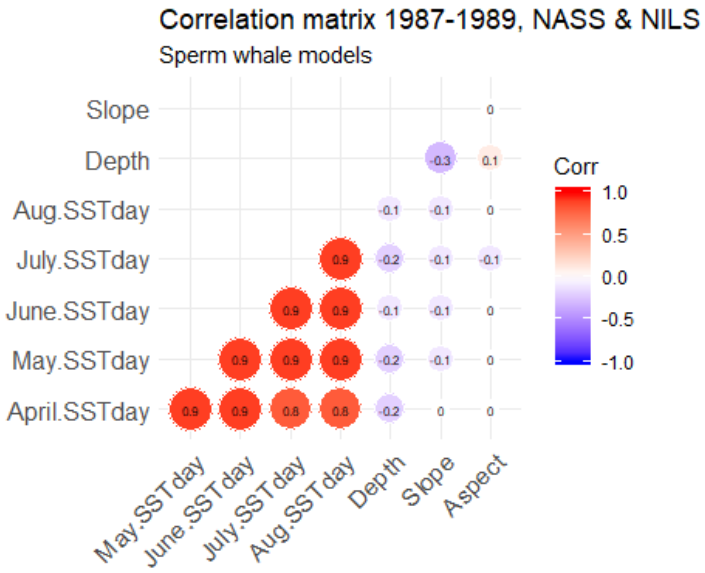

Appendix 3-B. Correlation matrix for sperm whales 1987 to 1989 models.

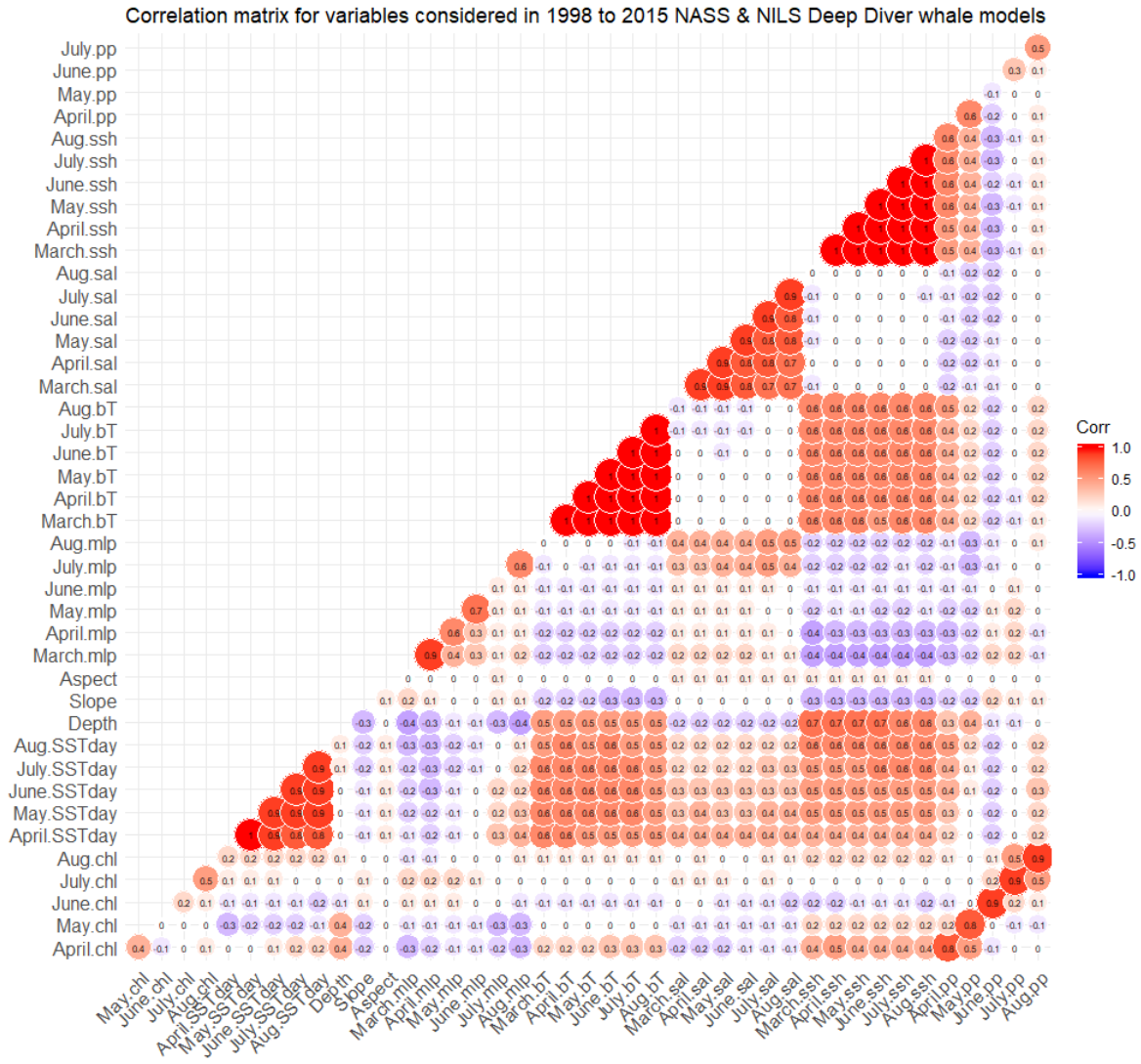

Appendix 3-C. Correlation matrix for sperm, pilot and northern bottlenose whales 1998 to 2015 models.

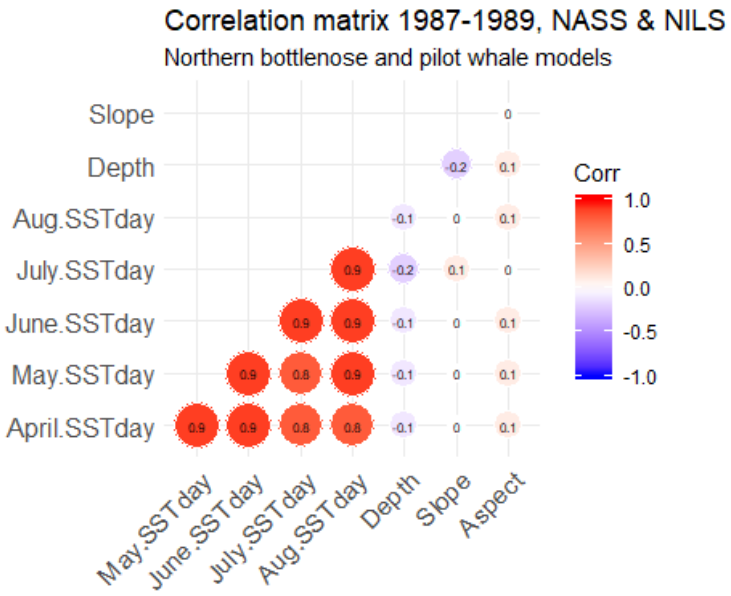

Appendix 3-D. Correlation matrix for pilot and northern bottlenose whales 1987 to 1989 models.

3.6.2 Sperm whales

3.6.2.1 Distance sampling

Appendix 3-E. ESW, effective strip width for the NASS sperm whales at all levels of the covariate vessel. Vessel name is given as an abbreviation of the vessel's name.

Vessel (ID)	ESW (m)
F	1646.23
G	1838.29
K	2532.53
S	1687.20
I	1641.14
J	1597.46
A	2385.41
B	2225.18
V	1828.04
H	1055.01

Appendix 3-F. ESW, effective strip width for the NILS 1987-1989 sperm whales at all levels of the covariate vessel. Vessel name is given as an abbreviation of the vessel's grouping base of vessel size (see methods).

Vessel (ID)	ESW (m)
1	627.98
2	1073.26
3	1256.29

3.6.2.2 Modelling

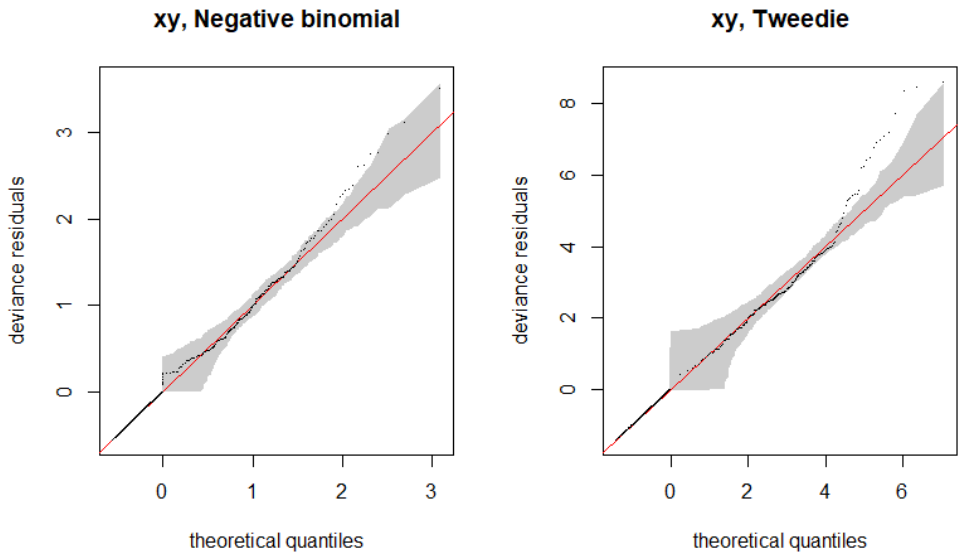

Appendix 3-G. Q-Q plots for error distribution selection for sperm whale 1987-1989 models. Spatial models (xy) for negative binomial and tweedie distributions. The shaded area represents 95 % confidence interval, the circles represent the data, the line is the expected data distribution if the data fits precisely the model.

Appendix 3-H.Single model variables fitted models for sperm whales 1987-1989 using double penalization. The best error structure for all models was the negative binomial distribution.

Model	Deviance	Deviance explained (%)	AIC	REML	n
Depth	600.15	24.17	2125.27	1067.86	6695
April.SSTday	623.51	12.77	2211.11	1107.47	
May.SSTday	605.42	10.40	2228.86	1116.73	
June.SSTday	607.06	7.39	2246.10	1123.79	
Aug.SSTday	596.47	5.03	2259.49	1129.54	
Slope	619.28	3.97	2264.73	1131.90	
July.SSTday	599.30	4.03	2266.15	1132.87	
Aspect	595.81	2.63	2276.64	1138.12	

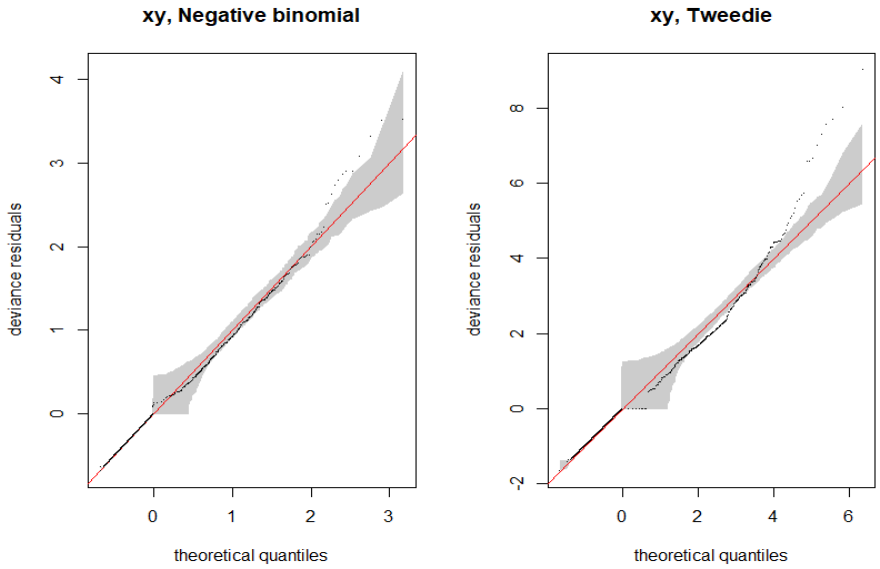

Appendix 3-I.Q-Q plots for error distribution selection for sperm whale 1998 to 2015 models. Spatial models (xy) for negative binomial and Tweedie distributions. The shaded area represents 95 % confidence interval, the circles represent the data, the line is the expected data distribution if the data fits precisely the model.

Appendix 3-J.Single model variables fitted models for sperm whales 1998-2015 using double penalization. The best error structure for all models was the negative binomial distribution. The best covariate by each variable family is in bold letters.

Model: Survey +	Deviance	Deviance explained (%)	AIC	REML	n
Depth	1014.19	18.95	3139.32	1575.55	7361
April.bT	994.46	15.73	3183.54	1601.34	
May.bT	998.09	15.48	3185.47	1601.89	
July.bT	1001.15	15.38	3185.56	1602.00	
Aug.bT	1001.53	15.33	3185.56	1601.48	
June.bT	1000.46	15.32	3186.52	1602.20	
April.SSTday	1004.20	14.08	3200.84	1607.30	
May.sal	1005.42	13.27	3210.48	1612.63	
June.sal	999.66	12.38	3219.45	1613.32	
May.SSTday	1005.97	11.57	3225.81	1615.73	
Aug.sal	1026.41	12.07	3225.99	1621.95	
July.sal	1014.25	11.00	3232.59	1618.37	
July.mlp	1004.78	10.83	3242.20	1630.89	
June.SSTday	1010.57	9.29	3251.57	1628.23	
April.sal	1006.56	9.54	3252.33	1631.67	
Aug.SSTday	1007.66	9.31	3255.85	1632.30	
July.SSTday	996.31	8.87	3260.38	1633.82	
Slope	1019.69	6.91	3283.18	1647.24	
Aug.ssh	998.25	6.66	3285.43	1646.62	
May.chl	1007.22	5.56	3292.01	1647.88	
June.ssh	1002.07	5.72	3293.32	1649.94	

July.ssh	999.30	5.69	3294.16	1650.98	
May.ssh	1002.14	5.38	3297.30	1651.42	
July.pp	1007.61	4.49	3304.83	1654.78	
April.ssh	999.91	4.67	3304.85	1655.03	
July.chl	1014.56	3.88	3311.13	1658.10	
April.pp	1009.86	4.00	3312.53	1660.16	
Aspect	1003.86	3.15	3316.42	1658.81	
May.pp	1009.40	3.18	3318.17	1660.53	
Aug.mlp	1019.50	2.60	3318.32	1659.84	
April.mlp	1003.26	3.43	3318.99	1664.83	
June.pp	1004.79	2.85	3320.58	1661.69	
May.mlp	1013.37	2.77	3323.39	1666.38	
June.mlp	1014.16	2.48	3323.77	1663.22	
April.chl	1002.58	2.33	3325.15	1663.17	
June.chl	1003.67	2.45	3327.48	1665.89	
Aug.pp	1003.07	2.66	3328.99	1669.13	

Appendix 3-K Concurvity values for sperm whales 1998-2015 variables in remaining full model after double penalization. Key pairs evaluated are highlighted within coloured squares.

$`worst`

	para	s(April.SSTday)	s(Aug.ssh)	s(Aspect)	s(Depth)	s(Slope)	s(July.pp)	s(July.mlp)
para	1.000000e+00	1.972272e-28	2.297264e-28	7.876014e-32	3.228737e-27	1.616859e-28	7.208924e-28	6.192704e-24
s(April.SSTday)	1.786150e-28	1.000000e+00	2.650415e-01	2.399695e-02	1.929277e-01	5.331083e-02	1.469668e-01	2.312713e-01
s(Aug.ssh)	2.928819e-28	2.650415e-01	1.000000e+00	5.691339e-02	5.379606e-01	3.000158e-01	7.711057e-02	1.024268e-01
s(Aspect)	3.115334e-31	2.399695e-02	5.691339e-02	1.000000e+00	4.613535e-02	2.020570e-02	2.618325e-02	1.452347e-02
s(Depth)	3.909991e-27	1.929277e-01	5.379606e-01	4.613535e-02	1.000000e+00	5.091917e-01	4.467460e-02	1.626304e-01
s(Slope)	1.749755e-28	5.331083e-02	3.000158e-01	2.020570e-02	5.091917e-01	1.000000e+00	5.874107e-02	5.469282e-02
s(July.pp)	8.862244e-28	1.469668e-01	7.711057e-02	2.618325e-02	4.467460e-02	5.874107e-02	1.000000e+00	2.480880e-02
s(July.mlp)	6.192489e-24	2.312713e-01	1.024268e-01	1.452347e-02	1.626304e-01	5.469282e-02	2.480880e-02	1.000000e+00

$observed

	para	s(April.SSTday)	s(Aug.ssh)	s(Aspect)	s(Depth)	s(Slope)	s(July.pp)	s(July.mlp)
para	1.000000e+00	1.448104e-31	7.508069e-32	2.684028e-34	3.527704e-30	5.816376e-31	6.877518e-31	1.250271e-26
s(April.SSTday)	1.786150e-28	1.000000e+00	2.402683e-01	2.084724e-02	8.802142e-02	1.862041e-02	5.966444e-02	3.999520e-02
s(Aug.ssh)	2.928819e-28	6.294573e-02	1.000000e+00	3.891655e-02	4.697271e-01	2.127627e-01	4.811233e-02	1.966058e-02
s(Aspect)	3.115334e-31	5.855685e-03	2.504102e-02	1.000000e+00	2.812539e-03	1.162979e-02	9.934363e-03	1.327262e-03
s(Depth)	3.909991e-27	1.006719e-01	4.304621e-01	1.604875e-02	1.000000e+00	2.924656e-01	1.968118e-02	1.756867e-02
s(Slope)	1.749755e-28	1.162536e-02	2.347270e-01	5.001299e-03	4.371919e-01	1.000000e+00	5.199507e-02	1.176377e-02
s(July.pp)	8.862244e-28	1.024408e-01	2.631103e-02	2.244517e-02	2.613327e-02	3.952280e-02	1.000000e+00	1.521781e-02
s(July.mlp)	6.192489e-24	1.154165e-01	3.480590e-02	1.271364e-02	1.473774e-01	4.131893e-02	1.345640e-02	1.000000e+00

$estimate

	para	s(April.SSTday)	s(Aug.ssh)	s(Aspect)	s(Depth)	s(Slope)	s(July.pp)	s(July.mlp)
para	1.000000e+00	2.241471e-31	3.167305e-31	6.219906e-33	9.107996e-31	7.320919e-30	1.787162e-31	4.481448e-26
s(April.SSTday)	1.786150e-28	1.000000e+00	2.100428e-01	6.961632e-03	1.030449e-01	1.472431e-02	4.181907e-02	1.021700e-01
s(Aug.ssh)	2.928819e-28	1.916654e-01	1.000000e+00	1.025663e-02	3.607348e-01	6.274163e-02	4.377724e-02	4.901205e-02
s(Aspect)	3.115334e-31	5.386089e-03	1.548589e-02	1.000000e+00	1.010739e-02	4.384704e-03	6.299727e-03	3.583316e-03
s(Depth)	3.909991e-27	4.703158e-02	4.157378e-01	6.554564e-03	1.000000e+00	1.179156e-01	1.906777e-02	9.789903e-02
s(Slope)	1.749755e-28	2.832656e-02	1.919761e-01	3.974873e-03	2.137308e-01	1.000000e+00	2.873448e-02	3.361990e-02
s(July.pp)	8.862244e-28	6.455013e-02	2.421195e-02	5.161474e-03	2.573557e-02	1.297495e-02	1.000000e+00	1.049035e-02
s(July.mlp)	6.192489e-24	1.737155e-01	4.166376e-02	3.725170e-03	9.694799e-02	1.244418e-02	1.484337e-02	1.000000e+00

3.6.3 Pilot whales

3.6.3.1 Distance sampling

Appendix 3-L. ESW, effective strip width for the NASS pilot whales at the two Beaufort levels: high (H), and low (L).

Beaufort	ESW (m)
H	457.64
L	1095.07

Appendix 3-M. ESW, effective strip width for the NILS 1995-2013 pilot whales at the three Beaufort levels: high (H), medium (M) and low (L).

Beaufort	ESW (m)
H	343.76
M	690.04
L	1164.36

3.6.3.2 Modelling

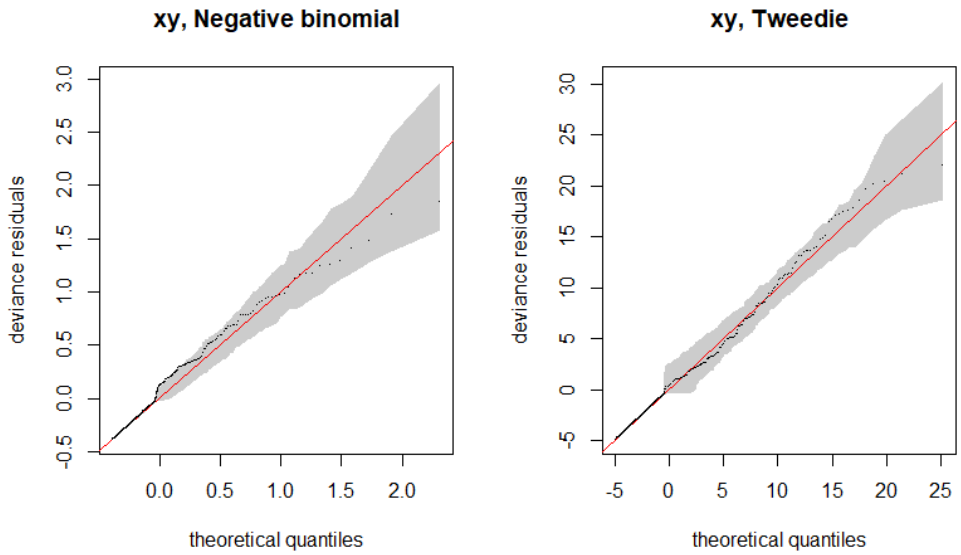

Appendix 3-N. Q-Q plots for error distribution selection for pilot whale 1987-1989 models. Spatial models (xy) for negative binomial and tweedie distributions. The shaded area represents 95 % confidence interval, the circles represent the data, the line is the expected data distribution if the data fits precisely the model.

Appendix 3-O. Single model variables fitted models for pilot whales 1987 and 1989 using double penalization. The best error structure for all models was the Tweedie distribution.

Model	Deviance	Deviance explained (%)	AIC	REML	n
Depth	35910.71	7.99	4907.14	1305.31	3491
May.SSTday	36273.92	7.30	4912.55	1307.03	
Slope	37283.54	4.76	4912.96	1304.81	
April.SSTday	37972.16	2.98	4918.13	1309.12	
June.SSTday	38381.53	2.23	4920.04	1309.02	
Aug.SSTday	37247.69	5.05	4920.67	1310.34	
July.SSTday	37328.31	4.98	4921.79	1310.09	
Aspect	39415.95	0.00	4928.45	1312.24	

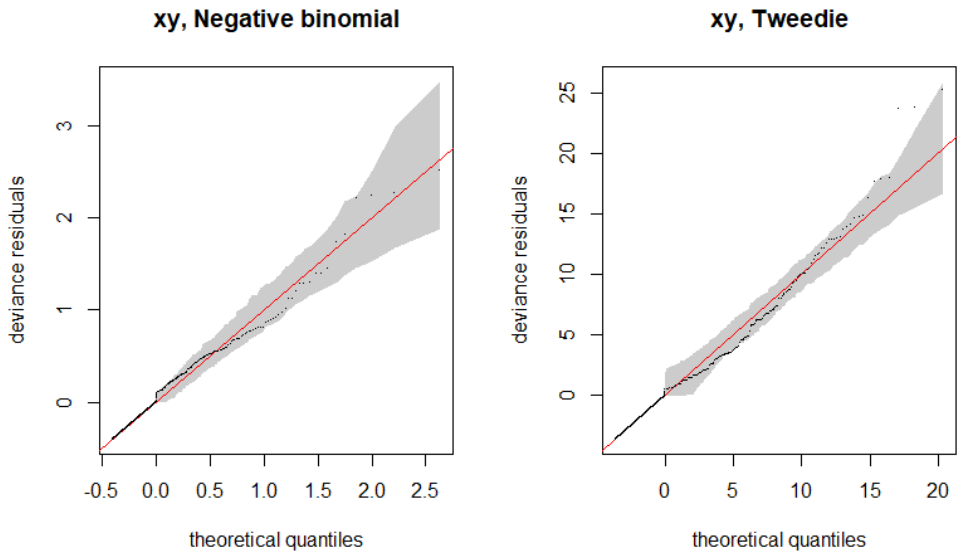

Appendix 3-P. Q-Q plots for error distribution selection for pilot whale 1998 to 2015 models. Spatial models (xy) for negative binomial and Tweedie distributions. The shaded area represents 95 % confidence interval, the circles represent the data, the line is the expected data distribution if the data fits precisely the model.

Appendix 3-Q. Single model variables fitted models for pilot whales 1998-2015 using double penalization. The best error structure for all models was the negative binomial distribution. The best covariate by each variable family is in bold letters.

Model: Survey +	Deviance	Deviance explained (%)	AIC	REML	n
April.SSTday	408.73	43.72	2869.95	1436.23	7361
May.SSTday	406.12	43.91	2871.33	1438.15	
July.chl	398.59	42.93	2881.01	1446.51	
July.SSTday	410.13	41.53	2886.67	1444.69	
June.SSTday	409.64	40.93	2889.04	1445.57	
Aug.SSTday	414.04	39.99	2895.50	1448.78	
Aspect	407.21	40.43	2897.53	1455.30	
July.pp	403.25	40.06	2899.11	1453.15	
Slope	405.47	39.71	2903.23	1460.14	
April.bT	410.17	38.63	2910.77	1463.02	
July.mlp	424.75	34.80	2927.38	1462.95	
July.ssh	415.70	34.73	2930.13	1465.75	
Aug.mlp	413.56	34.82	2930.21	1466.15	
May.chl	423.32	33.07	2932.68	1465.48	
Depth	421.46	33.54	2932.69	1465.20	
May.pp	423.42	32.75	2934.60	1466.33	
May.ssh	422.00	32.37	2936.73	1467.24	
Aug.ssh	421.18	32.48	2938.59	1467.61	
April.ssh	422.21	32.02	2939.07	1468.18	
June.ssh	420.90	32.40	2939.08	1467.86	
Aug.chl	424.38	31.57	2942.87	1469.76	
April.mlp	423.39	31.27	2943.08	1469.78	
April.pp	425.37	30.85	2943.78	1470.19	

April.chl	425.37	30.85	2943.78	1470.19	
July.sal	425.37	30.85	2943.78	1470.19	
April.sal	425.37	30.85	2943.78	1470.19	
Aug.sal	425.37	30.85	2943.78	1470.19	
May.mlp	425.37	30.85	2943.78	1470.19	
May.sal	425.37	30.85	2943.79	1470.19	
June.chl	425.37	30.85	2943.80	1470.19	
June.sal	425.37	30.85	2943.80	1470.19	
June.mlp	425.37	30.85	2943.80	1470.19	
June.pp	425.36	30.85	2943.81	1470.19	
May.bT	423.73	31.25	2943.92	1469.92	
June.bT	423.82	31.21	2943.95	1469.95	
July.bT	424.24	31.08	2944.26	1470.09	
Aug.bT	424.09	31.12	2944.30	1470.08	
Aug.pp	425.24	31.27	2944.31	1470.05	

Appendix 3-R. Concurvity values for pilot whales 1998-2015 variables in remaining full model after double penalization. Key pairs evaluated are highlighted within coloured squares.

$`worst`

	para	s(April.SSTday)	s(July.ssh)	s(Aspect)	s(April.bT)	s(Depth)	s(July.mlp)	s(July.sal)
para	1.000000e+00	1.972272e-28	4.627694e-28	7.876014e-32	1.232322e-27	3.228737e-27	6.192704e-24	1.745005e-27
s(April.SSTday)	1.786150e-28	1.000000e+00	3.015049e-01	2.399695e-02	4.589301e-01	1.929277e-01	2.312713e-01	4.523649e-01
s(July.ssh)	4.175566e-28	3.015049e-01	1.000000e+00	5.484135e-02	6.491278e-01	5.138991e-01	8.018170e-02	1.639251e-01
s(Aspect)	1.022128e-31	2.399695e-02	5.484135e-02	1.000000e+00	4.630615e-02	4.613535e-02	1.452347e-02	1.601446e-02
s(April.bT)	1.535522e-27	4.589301e-01	6.491278e-01	4.630615e-02	1.000000e+00	6.429678e-01	1.342035e-01	1.166658e-01
s(Depth)	3.709593e-27	1.929277e-01	5.138991e-01	4.613535e-02	6.429678e-01	1.000000e+00	1.626304e-01	1.342153e-01
s(July.mlp)	6.201439e-24	2.312713e-01	8.018170e-02	1.452347e-02	1.342035e-01	1.626304e-01	1.000000e+00	4.861265e-01
s(July.sal)	1.918901e-27	4.523649e-01	1.639251e-01	1.601446e-02	1.166658e-01	1.342153e-01	4.861265e-01	1.000000e+00

$observed

	para	s(April.SSTday)	s(July.ssh)	s(Aspect)	s(April.bT)	s(Depth)	s(July.mlp)	s(July.sal)
para	1.000000e+00	5.254480e-32	1.826130e-31	1.143749e-32	9.525444e-31	9.077288e-32	3.704791e-29	2.179333e-30
s(April.SSTday)	1.786150e-28	1.000000e+00	2.656967e-01	1.298432e-02	2.759051e-01	1.135161e-01	7.150907e-02	3.037600e-01
s(July.ssh)	4.175566e-28	1.532361e-01	1.000000e+00	3.593479e-02	6.068321e-01	3.196652e-01	4.959229e-02	8.313009e-02
s(Aspect)	1.022128e-31	5.382354e-03	3.603418e-03	1.000000e+00	6.211879e-03	1.807542e-02	2.235612e-03	5.579618e-03
s(April.bT)	1.535522e-27	3.866740e-01	5.749560e-01	3.917377e-02	1.000000e+00	5.594072e-01	4.338382e-02	1.060351e-01
s(Depth)	3.709593e-27	3.605802e-02	3.959222e-01	4.034669e-02	2.735113e-01	1.000000e+00	8.664818e-02	1.000216e-01
s(July.mlp)	6.201439e-24	2.150266e-01	3.179557e-02	1.781837e-03	2.794056e-02	5.953408e-02	1.000000e+00	4.555306e-01
s(July.sal)	1.918901e-27	2.534633e-01	1.107677e-01	4.263096e-03	6.407188e-02	5.474152e-02	8.740707e-02	1.000000e+00

$estimate

	para	s(April.SSTday)	s(July.ssh)	s(Aspect)	s(April.bT)	s(Depth)	s(July.mlp)	s(July.sal)
para	1.000000e+00	2.241471e-31	5.488704e-31	6.219906e-33	1.758264e-31	9.107996e-31	4.481448e-26	2.262928e-30
s(April.SSTday)	1.786150e-28	1.000000e+00	2.482829e-01	6.961632e-03	3.163980e-01	1.030449e-01	1.021700e-01	1.093891e-01
s(July.ssh)	4.175566e-28	2.172728e-01	1.000000e+00	9.418110e-03	4.721169e-01	3.616410e-01	4.745386e-02	5.345732e-02
s(Aspect)	1.022128e-31	5.386089e-03	1.273520e-02	1.000000e+00	1.577837e-02	1.010739e-02	3.583316e-03	7.770239e-03
s(April.bT)	1.535522e-27	3.803568e-01	4.658568e-01	1.076396e-02	1.000000e+00	5.518076e-01	5.653694e-02	5.992319e-02
s(Depth)	3.709593e-27	4.703158e-02	4.195580e-01	6.554564e-03	2.906255e-01	1.000000e+00	9.789903e-02	3.974009e-02
s(July.mlp)	6.201439e-24	1.737155e-01	3.943152e-02	3.725170e-03	2.040493e-02	9.694799e-02	1.000000e+00	2.395121e-01
s(July.sal)	1.918901e-27	3.217546e-01	1.049616e-01	3.913815e-03	3.777570e-02	7.159733e-02	1.572255e-01	1.000000e+00

3.6.4 Northern bottlenose whales

3.6.4.1 Distance sampling

Appendix 3-S. ESW, effective strip width for the NASS northern bottlenose whales at all covariate/level combination. Levels of the covariate vessel relate to the abbreviation of the vessel's name. Covariate Beaufort has three levels: high (H), medium (M) and low (L).

Vessel (ID)	Beaufort	ESW (m)	Vessel (ID)	Beaufort	ESW (m)
A	H	842.86	I	H	417.72
A	L	1702.62	I	L	1109.12
A	M	1102.33	I	M	581.76
B	H	42.69	J	H	523.25
B	L	152.68	J	L	1297.50
B	M	63.74	J	M	717.55
F	H	426.79	K	H	470.97
F	L	1126.50	K	L	1207.93
F	M	593.59	K	M	650.81
G	H	790.51	S	H	312.39
G	L	1651.55	S	L	889.76
G	M	1042.14	S	M	442.05
H	H	283.06	V	H	609.57
H	L	822.64	V	L	1430.10
H	M	402.39	V	M	825.45

3.6.4.2 Modelling

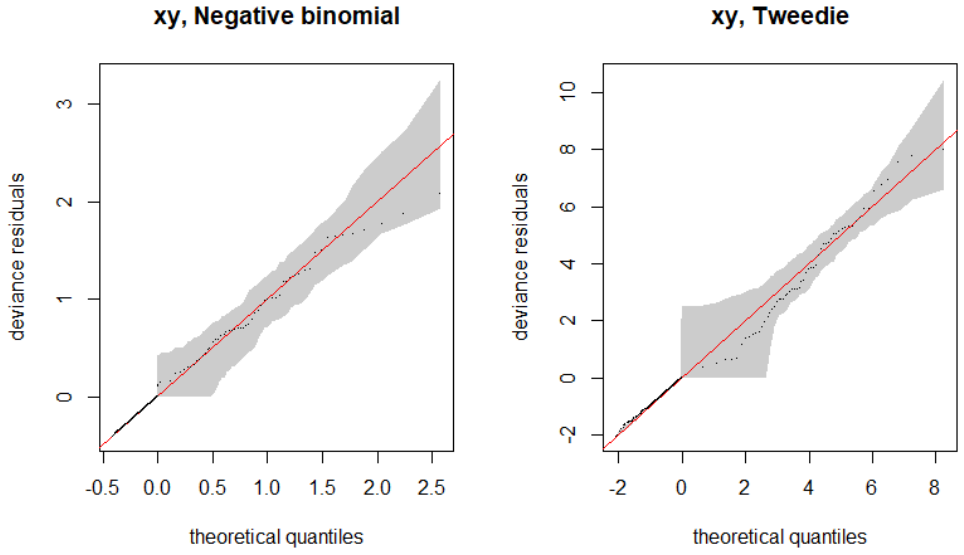

Appendix 3-T. Q-Q plots for error distribution selection for northern bottlenose whale 1987-1989 models. Spatial models (xy) for negative binomial and tweedie distributions. The shaded area represents 95 % confidence interval, the circles represent the data, the line is the expected data distribution if the data fits precisely the model.

Appendix 3-U. Single model variables fitted models for northern-bottlenose whales 1987 and 1989 using double penalization. The best error structure for all models was the negative binomial distribution.

Model	Deviance	Deviance explained (%)	AIC	REML	n
Depth	162.29	12.16	838.00	420.66	3491
Aug.SSTday	163.94	6.19	846.15	422.62	
July.SSTday	162.43	3.84	848.50	423.06	
June.SSTday	162.63	2.44	849.79	423.19	
Slope	162.87	0.83	850.60	423.58	
April.SSTday	162.57	0.33	850.60	423.65	
May.SSTday	162.35	1.06	850.65	423.51	
Aspect	162.13	1.12	850.96	423.61	

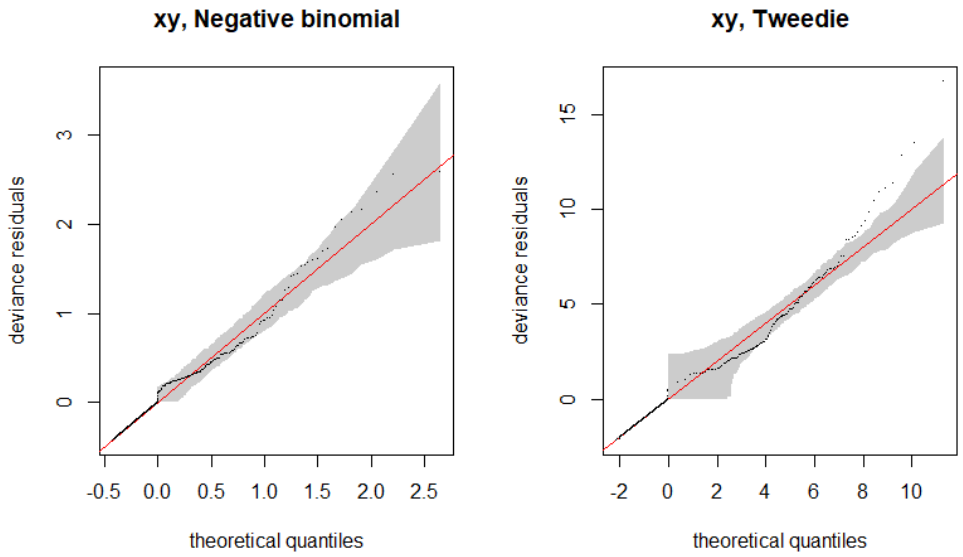

Appendix 3-V. Q-Q plots for error distribution selection for northern bottlenose whale 1998 to 2015 models. Spatial models (xy) for negative binomial and tweedie distributions. The shaded area represents 95 % confidence interval, the circles represent the data, the line is the expected data distribution if the data fits precisely the model.

Appendix 3-W. Single model variables fitted models for northern-bottlenose whales 1998-2015 using double penalization. The best error structure for all models was the negative binomial distribution. The best covariate by each variable family is in bold letters.

Model: Survey +	Deviance	Deviance explained (%)	AIC	REML	n
July.ssh	351.65	40.47	1940.04	975.71	7361
Aug.ssh	355.44	40.40	1940.46	977.18	
Depth	349.07	39.25	1946.84	977.47	
April.bT	358.05	38.64	1950.37	979.51	
Aug.bT	358.11	38.18	1950.58	978.66	
April.pp	361.06	36.96	1953.07	976.39	
July.bT	358.07	37.79	1953.25	979.88	
April.chl	359.53	36.98	1953.79	976.48	

May.bT	359.52	37.79	1954.20	980.06	
June.bT	358.97	37.55	1954.67	980.09	
May.pp	355.79	37.39	1957.04	981.89	
April.ssh	351.78	37.45	1957.54	982.42	
June.ssh	353.93	36.01	1960.36	979.84	
May.ssh	354.87	35.60	1965.72	983.94	
May.chl	361.11	32.92	1975.54	986.99	
June.SSTday	363.47	32.66	1979.72	989.95	
Aug.sal	361.96	33.21	1981.00	995.61	
Aug.SSTday	364.18	32.43	1982.60	991.88	
July.SSTday	365.79	31.69	1983.30	990.84	
May.SSTday	361.96	31.29	1988.09	994.63	
Slope	372.45	30.04	1990.14	993.69	
July.sal	364.78	30.94	1991.62	998.82	
June.mlp	364.45	35.00	1995.21	995.55	
June.sal	364.27	30.12	1995.23	1000.06	
July.mlp	365.82	30.72	1995.81	1002.50	
Aspect	361.48	30.14	1997.08	1000.38	
May.mlp	367.40	28.62	1999.39	999.69	
April.SSTday	367.13	28.34	1999.99	998.95	
April.mlp	367.62	27.75	2002.87	1000.38	
Aug.mlp	365.16	26.44	2005.92	1001.71	
Aug.chl	366.44	26.62	2008.03	1002.44	
June.pp	365.83	26.02	2008.06	1002.59	
Aug.pp	366.76	26.52	2008.79	1003.03	
May.sal	368.01	26.31	2009.30	1002.93	
July.pp	367.82	25.71	2009.54	1003.16	
June.chl	366.35	25.61	2011.74	1003.58	
April.sal	368.31	25.38	2012.11	1003.90	
July.chl	368.83	24.98	2012.24	1004.13	

Appendix 3-X. Concurvity values for northern bottlenose whales 1998-2015 variables in remaining full model after double penalization. Key pairs evaluated are highlighted within coloured squares.

$`worst`

	para	s(June.SSTday)	s(July.ssh)	s(Aspect)	s(April.bT)	s(Depth)	s(April.chl)	s(June.mlp)	s(Aug.sal)
para	1.000000e+00	3.604740e-29	4.627694e-28	7.876014e-32	1.232322e-27	3.228737e-27	1.273271e-27	2.746177e-23	3.079595e-28
s(June.SSTday)	3.282930e-29	1.000000e+00	4.999994e-01	2.300414e-02	4.383307e-01	2.378928e-01	2.045644e-01	1.660332e-01	2.395991e-01
s(July.ssh)	3.920149e-28	4.999994e-01	1.000000e+00	5.484135e-02	6.491278e-01	5.138991e-01	3.555584e-01	1.019604e-01	1.400218e-01
s(Aspect)	1.527005e-31	2.300414e-02	5.484135e-02	1.000000e+00	4.630615e-02	4.613535e-02	1.452810e-02	9.981672e-03	1.253567e-02
s(April.bT)	9.646844e-28	4.383307e-01	6.491278e-01	4.630615e-02	1.000000e+00	6.429678e-01	2.411816e-01	1.285925e-01	1.235110e-01
s(Depth)	3.171641e-27	2.378928e-01	5.138991e-01	4.613535e-02	6.429678e-01	1.000000e+00	3.405314e-01	1.440876e-01	1.247481e-01
s(April.chl)	1.283416e-27	2.045644e-01	3.555584e-01	1.452810e-02	2.411816e-01	3.405314e-01	1.000000e+00	1.410524e-01	1.031072e-01
s(June.mlp)	2.747330e-23	1.660332e-01	1.019604e-01	9.981672e-03	1.285925e-01	1.440876e-01	1.410524e-01	1.000000e+00	4.061466e-01
s(Aug.sal)	4.476476e-28	2.395991e-01	1.400218e-01	1.253567e-02	1.235110e-01	1.247481e-01	1.031072e-01	4.061466e-01	1.000000e+00

$observed

	para	s(June.SSTday)	s(July.ssh)	s(Aspect)	s(April.bT)	s(Depth)	s(April.chl)	s(June.mlp)	s(Aug.sal)
para	1.000000e+00	3.079931e-34	5.274864e-29	1.491499e-33	7.741875e-33	3.095790e-31	5.144711e-34	3.193312e-27	2.202281e-30
s(June.SSTday)	3.282930e-29	1.000000e+00	1.332140e-01	2.040686e-02	3.367508e-01	1.139445e-01	6.395278e-02	5.971955e-02	1.781420e-01
s(July.ssh)	3.920149e-28	4.207677e-01	1.000000e+00	5.135528e-02	4.718288e-01	3.407335e-01	1.944203e-01	4.303568e-02	8.426945e-02
s(Aspect)	1.527005e-31	5.188147e-03	2.811658e-03	1.000000e+00	1.654355e-02	1.313875e-02	1.962390e-03	2.203384e-03	6.231743e-03
s(April.bT)	9.646844e-28	3.823984e-01	2.079155e-01	3.158716e-02	1.000000e+00	4.288731e-01	1.357489e-01	5.334437e-02	1.101075e-01
s(Depth)	3.171641e-27	9.971645e-02	1.104558e-01	2.808446e-02	3.052836e-01	1.000000e+00	2.308826e-01	7.131982e-02	1.099769e-01
s(April.chl)	1.283416e-27	1.398169e-01	5.848447e-02	6.659679e-03	1.236045e-01	2.901777e-01	1.000000e+00	6.981561e-02	7.038619e-02
s(June.mlp)	2.747330e-23	1.794442e-02	1.664359e-02	4.469293e-03	6.601104e-03	1.223842e-01	7.280664e-02	1.000000e+00	3.527592e-01
s(Aug.sal)	4.476476e-28	1.375634e-01	1.965287e-02	5.583782e-03	2.978867e-02	1.091023e-01	5.783986e-02	1.502009e-01	1.000000e+00

$estimate

	para	s(June.SSTday)	s(July.ssh)	s(Aspect)	s(April.bT)	s(Depth)	s(April.chl)	s(June.mlp)	s(Aug.sal)
para	1.000000e+00	9.347483e-32	5.488704e-31	6.219906e-33	1.758264e-31	9.107996e-31	2.870267e-30	1.674092e-27	1.574089e-30
s(June.SSTday)	3.282930e-29	1.000000e+00	3.394556e-01	5.777279e-03	3.192183e-01	4.246769e-02	3.987480e-02	1.261975e-02	9.330384e-02
s(July.ssh)	3.920149e-28	3.306455e-01	1.000000e+00	9.418110e-03	4.721169e-01	3.616410e-01	7.062958e-02	1.709959e-02	5.533935e-02
s(Aspect)	1.527005e-31	5.854593e-03	1.273520e-02	1.000000e+00	1.577837e-02	1.010739e-02	1.482425e-03	2.154132e-03	6.452371e-03
s(April.bT)	9.646844e-28	3.670103e-01	4.658568e-01	1.076396e-02	1.000000e+00	5.518076e-01	6.034950e-02	1.208823e-02	4.788463e-02
s(Depth)	3.171641e-27	5.824028e-02	4.195580e-01	6.554564e-03	2.906255e-01	1.000000e+00	8.949932e-02	1.982791e-02	2.982285e-02
s(April.chl)	1.283416e-27	8.367564e-02	2.755092e-01	3.595482e-03	1.241995e-01	1.715847e-01	1.000000e+00	1.251882e-02	2.331682e-02
s(June.mlp)	2.747330e-23	3.977640e-02	3.691601e-02	2.638870e-03	1.112290e-02	7.053845e-02	2.476005e-02	1.000000e+00	1.444063e-01
s(Aug.sal)	4.476476e-28	1.698875e-01	8.095650e-02	3.037207e-03	3.111869e-02	6.982670e-02	3.123674e-02	3.162306e-02	1.000000e+00

4 DISTRIBUTION AND HABITAT USE OF BALEEN WHALES IN THE CENTRAL AND NORTH-EASTERN NORTH ATLANTIC

4.1 Introduction

In the central and north-eastern Atlantic fin, humpback and minke whales are the most commonly found baleen whales. In Icelandic and adjacent waters, fin and minke whales are two of the four greatest (cetacean) consumers in the area together with pilot and northern bottlenose whales (Sigurjónsson and Víkingsson, 1997). This is also true in Norwegian waters in Norwegian waters, where minke whales are even more numerous than in the Central North Atlantic (Icelandic and adjacent waters) (Moore et al., 2019; Nøttestad et al., 2015; Øien and Bøthun, 2009; Solvang et al., 2015; Vacquié-Garcia et al., 2017).

During the summer, fin, humpback and minke whales feed in the central and north-eastern Atlantic where they must find dense patches of prey. They have diverse diets that range from macro-zooplankton to various fish species and vary spatially and temporally with some evidence of prey preference (e.g. Nøttestad et al., 2015; Ressler et al., 2015; Sigurjónsson and Víkingsson, 1997; Skern-Mauritzen et al., 2011; Víkingsson et al., 2015). At the regional level some changes in baleen whale prey are due to changes in availability and this is likely linked to changes in the environment (Nøttestad et al., 2015; Víkingsson et al., 2015). Oceanographic conditions are changing in the central and north-eastern Atlantic (e.g. Carr et al., 2017; Häkkinen et al., 2013; Hátún et al., 2009; Havforskningsinstituttet, 2020; Sundby et al., 2016); this is affecting baleen whale prey species but the extent to which baleen whales are responding is unknown (e.g. Moore et al., 2019; Nøttestad et al., 2015; Ressler et al., 2015; Silva et al., 2014; Skern-Mauritzen et al., 2011; Vacquié-Garcia et al., 2017; Víkingsson et al., 2015).

4.1.1 State of knowledge about fin whales

The fin whale (*Balaenoptera physalus*) is the second largest species of baleen whale or Mysticeti. It has a worldwide distribution ranging from tropical to polar regions; however it may be absent

in the most extreme latitudes, such as polar (ice-cover) or tropical seas (Aguilar and García-Vernet, 2018). Worldwide, three broad populations are recognized: Southern Hemisphere, North Atlantic, and North Pacific. Taxonomically, fin whales from the Northern Hemisphere are classified as the subspecies *B. p. physalus*, while *B. p. quoyi,* and *B.p. patachonica (*pygmy) inhabit the Southern Hemisphere (Committee on Taxonomy, 2018).

Males and females are very similar in appearance; females are slightly longer than males. In the Northern Hemisphere, adult females average around 20.5 m and males 19 m in length. Longevity is approximately 80-90 years (Lockyer, 1984 In: IWC, 1984). In Iceland, the oldest fin whale captured was 94 years old (Konráðsson & Gunnlaugsson, 1990 In: IWC, 1989).

In the North Atlantic, fin whales are widely distributed during summer, most commonly off Nova Scotia and Newfoundland, in the Davis Strait off Western Greenland, in the East Greenland/Iceland/Jan Mayen area, and west of the Iberian Peninsula. They have not been reported north of Novaya Zemlya or Franz Josef Land. They are mostly pelagic but are sometimes found in waters as shallow as 30 m (Aguilar and García-Vernet, 2018). Víkingsson et al., (2009) described fin whales to be mainly distributed in 1987-1989 along the continental slope of the Iceland/East Greenland shelf, while Víkingsson et al., (2015) found a relationship with the 2000 m isobath. In Norwegian waters, Nøttestad et al., (2015) found that sightings of fin whales in the Norwegian Sea between 2009-2012 were highly correlated with shallow bottom depths, while in the Norwegian high Arctic during late summer 2015, fin whales were mainly observed offshore along shelf/slope margins west and north of Svalbard (Vacquié-Garcia et al., 2017).

In the East Greenland/Iceland area, fin whale density increases with water temperature in deep waters (around 200 m) of the Irminger Sea (Víkingsson et al., 2015, 2009). There has been a shift in the distribution and abundance of fin whales in the East Greenland/Iceland area, which may be linked to oceanographic changes, such as temperature, in deep waters (Figure 4.1). Specifically, the highest probability of encounter was found at surface temperatures between 5-11 °C, with a peak between 6-7 °C (Víkingsson et al., 2015). In the Norwegian Sea 2009-2012, fin whale relative abundance was significantly correlated with low temperatures (Nøttestad et al., 2015). The exact mechanisms are unknown but what is evident is that there has been changes in the water temperatures in the area as well as changes in fin whale distribution (Moore et al., 2019; Nøttestad et al., 2015; Víkingsson et al., 2015, 2009).

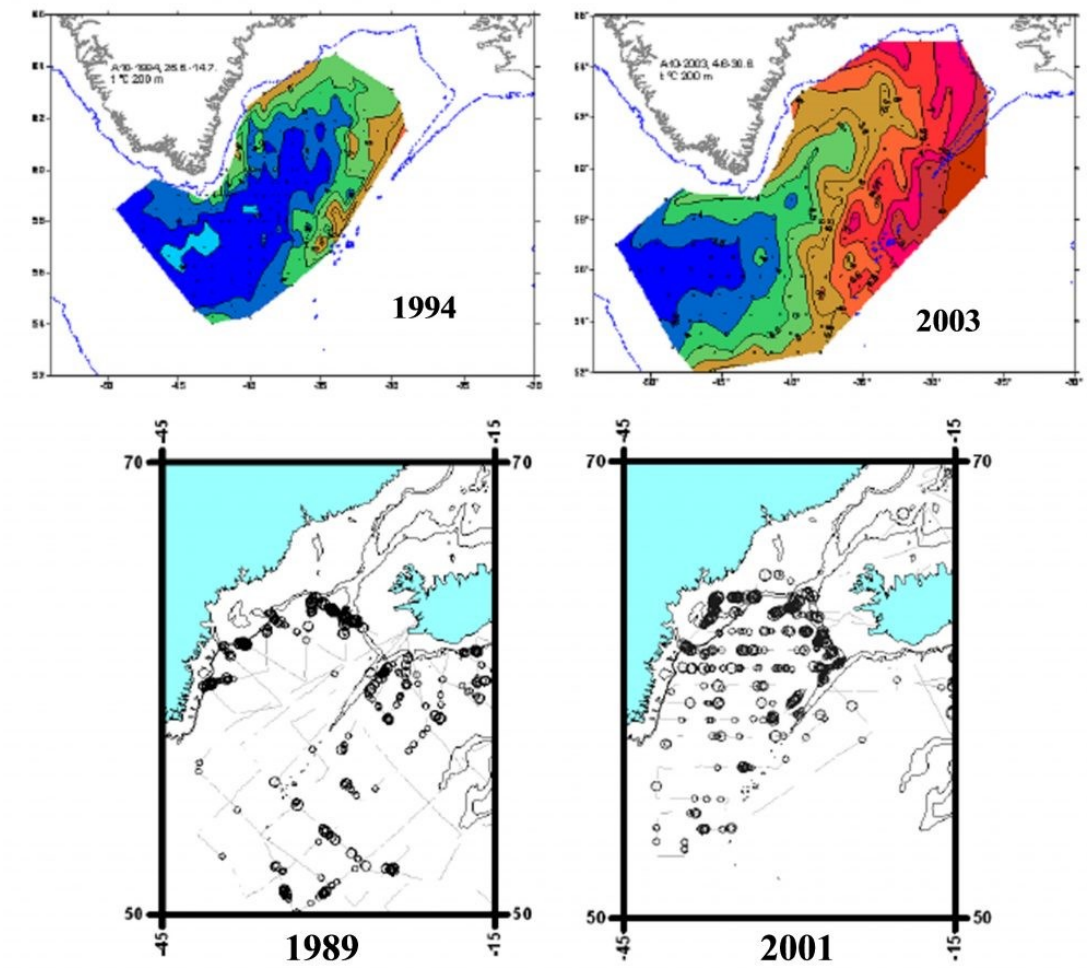

Figure 4.1. Changes in sea temperature (200 m depth) between 1994 and 2003 and changes in the distribution of fin whales between 1989 and 2001.The temperature gradient goes from blue through green to red with increasing temperature (Víkingsson et al., 2015).

Fin whales in general are believed to be migratory, having seasonal south-north movements; wintering at warm waters in low latitudes for breeding and summering at cold waters for feeding. But this migration description is not a rule, for example there are fin whale resident populations as in the Mediterranean (e.g. Laran and Drouot-Dulau, 2007; Laran and Gannier, 2008; Mizroch et al., 2009). An alternative hypothesis is that whales disperse more in open waters during winter and therefore detecting them is difficult. In the North Atlantic, fin whales may be present throughout the year (Clark, 1995 In: NAMMCO, 2019d), but the densities may vary seasonally. Acoustic data from Fram Strait and Greenland Sea have detected fin whales from August to March/May (Klinck et al., 2012; Moore et al., 2012); this is longer and later in the season than expected for fin whales migrating in northern latitudes. Similar findings were made in the western Atlantic where acoustic activity of fin whales was reported in the Davis Strait

(between Canada and Greenland); whales were recorded at least until the end of December (Simon et al., 2010). These could be examples of migratory changes linked to less sea ice for example, as also described below for humpback whales.

Fin whale diet is diverse and flexible depending on prey availability and seasonality (Kawamura, 1980). In the North Atlantic the main prey is krill (*Meganyctiphanes norvegica*). Other species consumed include planktonic crustaceans (*Thysanoessa inermis* and *Calanus finmarchicus*), pelagic schooling fish such as capelin (*Mallotus villosus*), juvenile herring (*Clupea harengus*), mackerel (*Scomber scombrus*), and blue whiting (*Micromesistius poutassou*), and in some areas small squids may be eaten (e.g. Aguilar and García-Vernet, 2018; Ressler et al., 2015; Sigurjónsson and Víkingsson, 1997; Skern-Mauritzen et al., 2011; Woodley and Gaskin, 1996). Between Iceland and East Greenland (Irminger Sea) fin whales stomach contents has shown them feeding almost exclusively on euphasiids (>95%), specifically krill (*M. norvegica*) (Sigurjónsson and Víkingsson, 1997; Víkingsson, 1997). An increase in abundance in this area, linked to an increase of water temperatures (see above) but a decrease in euphasiids (Silva et al., 2014) have led to the suggestion that there may have been a switch in prey (Víkingsson et al. 2015) but this is inconclusive.

Around the Norwegian Sea, the dominant prey species have been krill (*M. norvegica*) and amphipods (Nøttestad et al., 2015, Jonsgard, 1966 In: Nøttestad et al., 2014; Øien, 2009). Nøttestad et al (2014) found fin whale presence (summer 2006-2007) to be correlated with the presence of macro-zooplankton (krill and amphipods) in the cold Arctic waters; no correlations were found in the area with Calanoid biomass and similarly other studies have. However, Nøttestad et al., (2015), found significant correlation between capelin and fin whale presence (summer 2009, 2010 and 2012). Fin and humpback whales at the Barents Sea (2003-2012) are generalist, but for both whale species modelling exercises have shown positive associations with krill (Ressler et al., 2015). It seems that whales and capelin are competing for the same prey, but whales appear to be foraging ahead of capelin migration (Moore et al., 2019; Ressler et al., 2015; Skern-Mauritzen et al., 2011).

As a capital breeder, feeding is assumed to be the primary activity of fin whales in the central and north-eastern North Atlantic during the summer months, due to the availability of abundant prey during this season. The modelled relationships are therefore likely to reflect environmental drivers related to finding prey. During this period, some individuals may also travel as part of their migration to northern locations (e.g. to the Barents Sea or Svalbard (e.g. Ressler et al.,

2015; Vacquié-Garcia et al., 2017)) or between (unknown) feeding areas. However, most cetacean species are believed to be opportunistic feeders and could take advantage of available prey, for example, while travelling.

Covariates included in the models have been chosen because they may have the power to explain foraging behaviour (see also general justification of the included covariates in section 2.2.2.1 and Table 2.3). Other studies have found relationships between fin whale density and depth, slope, SST, and prey (see above). Covariates related to primary production may only have a small lagged relationship with fin whale density because they typically feed low in the trophic web (e.g. Nøttestad et al., 2015, 2014; Øien, 2009; Ressler et al., 2015; Víkingsson et al., 2015). Covariates linked with prey aggregation such as SSH and mlp are expected to be related to prey accumulation and to have little to no lag. Salinity is related to water masses and in the study area may explain the influence of Arctic versus temperate water on fin whale distribution.

Abundance in the central and eastern North Atlantic has most recently been estimated in 2015 (Table 4.1). Some of the estimates have not been fully corrected for perception or availability biases and number of fin whales in the area could be larger.

Table 4.1. Abundance estimates of fin whales during surveys in 2015.

Areas 2015	Estimate	95% Confidence interval	Reference
West Greenland	2,215	1,017-4,823	Hansen et al., (2018)
East Greenland (coastal)	6,440	3,901-10,632	Hansen et al., (2018)
Iceland/Faroe Islands	36,773	25,811-52,392	Pike et al., (Pike et al., 2019b)
Norway (GL & NO seas) 2014-2018	11,387	8,072-16,063	NAMMCO (2019a)

The North Atlantic was also simultaneously covered during the summer of 2007, fin whale abundance estimates from the whole North Atlantic suggest a total abundance of over 50,000, however these have not been fully corrected for perception or availability biases either (NAMMCO, 2019a, 2019d, 2011; Øien, 2009; Pike et al., 2020a). Estimates of abundance from earlier years (2007 for example) cannot be fully compared with the most recent estimates because of differences in methodology (2007 was BT and 2015 was IO) and coverage in the areas surveyed. However, fin whale abundance appears to have increased between 2007 and 2015 possibly because of movement of animals from other areas, or an intrinsic increase, or a

combination of both scenarios (NAMMCO, 2019d). Víkingsson et al., (2009) reported rapid changes in abundance and distribution of fin whales in the Central North Atlantic. In this area, an increase of about 12% was found from 1987 to 2001, and a further increase was found between 2007-2015 (Pike et al., 2019b; Víkingsson et al., 2009). Changes in distribution in the Central North Atlantic have been related to oceanographic changes in SST and SSH, as mentioned above (Víkingsson et al., 2015). In Norwegian waters, fin whale abundance since 1996 is estimated to be around 10,000 animals, but was around half that in 1995 (NAMMCO, 2019a; Øien, 2009). Estimated abundance in waters to the south has not changed (Hammond et al., 2017, 2009) so the increase in abundance in northern waters is not because of movement from the south. In conclusion, the available evidence is that fin whale abundance in the North Atlantic is increasing (NAMMCO, 2019d).

The fin whale globally is listed as Vulnerable by the IUCN (Cooke, 2018a). In the North Atlantic, "Assessments of the population status [of fin whales] in the central North Atlantic and off West Greenland have shown populations there to be in a healthy state" (IWC, 2019)**.**

Anthropogenic pressures on fin whales could include: direct harvest, vessel collisions, entanglement, acoustic pollution, prey depletion, water pollution, harassment due to tourism (whale watching), and oceanographic changes. Fin whales have been target of commercial whaling since the late 1800s (Kalland and Sejersen, 2005; Tønnessen and Johnsen, 1982 In: NAMMCO, 2019d), several declines in the past have lead to moratoriums in the past (IWC, 1989; NAMMCO, 2000). Currently, only Greenland and Iceland harvest fin whales in the North Atlantic and West Greenland whales under IWC 'subsistence whaling' with a quota of 19 animals per year. Iceland resumed whaling in 2006, and since then catches range from 0-155 per year (IWC, 2020). Among threats, fin whales seem most susceptible to vessel collisions; compared to other whale species they are stuck more frequently (Laist et al., 2001). In the central and eastern North Atlantic, only one animal has been reported by NAMMCO nations to have been killed due to a collision. Incidental catches seem very rare globally (Aguilar and García-Vernet, 2018). Seismic exploration and increased shipping noise can cause changes in vocalizations or avoidance or by reducing the range of vocalizations, which could affect reproductive success (Castellote et al., 2012) but impacts are unknown. Prey depletion and overfishing do not seem problematic because fin whales in general feed low in the food web. Hence, the contaminant load in fin whales is low compared with other marine mammals. North Atlantic concentrations of organochlorines (DDTs and PCBs) are higher than in the Southern Hemisphere but still low

(O'Shea and Brownell, 1994). Low concentrations of heavy metals such as cadmium, zinc, and cooper have also been found (Das et al., 2003; Sanpera et al., 1996). Oceanographic changes caused by climate change could lead to changes in prey availability and distribution, which could affect body condition and distribution (Moore et al., 2019; Williams et al., 2013).

4.1.2 State of knowledge about humpback whales

The humpback whale (*Megaptera novaeangliae*) is widely distributed found in all the oceans except the high Arctic. Taxonomically, some classify humpback whales into three subspecies: *M. n. australis* or Southern humpback, *M. n. kuzira* or North Pacific humpback, and *M. n. novaeangliae* North Atlantic humpback (Committee on Taxonomy, 2018). Adults typically measure 14-15 m and females are around 1-1.5 m longer than males. Longevity is at least 50 years may be up to 70 years (Clapham, 2018; NAMMCO, 2019e).

Humpback whales migrate between feeding grounds at high latitudes in spring to fall and breeding and calving grounds in the tropics in winter (Dawbin, 1966 In: Clapham, 2018). The main feeding areas in the eastern North Atlantic extend from Arctic waters in northern Norway, to Jan Mayen and Iceland (Stevick et al., 2006). In general, humpbacks exhibit site fidelity at the feeding grounds; in Iceland and Norway this has been maintained on an evolutionary timescale (Larsen et al., 1996; Palsbøll et al., 1997). Not all humpback whales migrate to winter breeding grounds and overwintering whales have been recorded singing in Icelandic waters (Magnúsdóttir and Lim, 2019). In the fjords of northern Norway, humpback whales have been recorded only in the last decade (NAMMCO, 2019e; Rikardsen, 2020). These demonstrate not only that migration can vary amongst individuals but also that there have been changes in migration patterns of baleen whales in the study area (e.g. Klinck et al., 2012; Moore et al., 2012).

Humpback whales are mainly found in coastal waters, shelf waters, and close to islands or reefs in their feeding grounds but also offshore (Clapham, 2018; Jefferson et al., 1993). In Icelandic waters, humpback whales are associated with shallower waters and slopes >1˚ (Neyman, 2018; Paxton et al., 2009); similarly, in British Columbia there is a preference for waters between 50-200 m, depth contours of 100 m and a positive relation with the shelf break (Dalla Rosa et al., 2012). In feeding grounds, relationships with water temperature are more varied. Paxton et al., (2009) found that in Icelandic waters between 1995 and 2001 the highest probability of

encounter was in waters between 6-8 ˚C, similarly Neyman (2018) analysing 2015 data found the highest encounters in waters cooler than 8 ˚C. In the North Pacific, humpback whales off Washington State were found in water temperatures with a mean of 13.9 ˚C (Calambokidis et al., 2004), and off British Columbia negative effects of temperature were found in temperatures below 8 ˚C and slight higher encounter rates between 8-11 ˚C (Dalla Rosa et al., 2012). Overall, the higher occurrence of humpback whales in shallower waters could indicate that relationships with SST are likely to be linked to prey presence.

Globally, humpback whales have a diverse diet; depending the area and season they have been recorded feeding on euphausiids (sometimes almost exclusively), amphipods, capelin, sardines, herring, sand lance (sand eels) and mackerel (Clapham, 2018; Cooke, 2018b). Humpback whale distribution has been shown to be positively related with oceanic frontal systems (which concentrate prey) in the study area (NAMMCO, 2019a; Ressler et al., 2015; Skern-Mauritzen et al., 2011) and elsewhere (e.g. Dalla Rosa et al., 2012). Observations in Icelandic and East Greenland waters suggest that the whales mainly forage on euphausiids, capelin and sand lance (Heide-Jørgensen and Laidre, 2007; Magnúsdóttir et al., 2014). However, unlike minke and fin whales, humpback whale diet in Icelandic waters has not been validated with stomach content data (Sigurjónsson and Víkingsson, 1997; Víkingsson et al., 2015). The temporal changes in distribution of humpbacks in Icelandic waters are thought to be associated with changes in capelin distribution because whales have been observed following the fish migration (Víkingsson et al., 2015). In Norwegian waters humpback whale presence has been associated with different types of prey such as macro-zooplankton (krill and amphipods), capelin, and herring (Christensen et al., 1992; NAMMCO, 2019a; Nøttestad et al., 2015, 2014; Ressler et al., 2015), but these associations with different prey types are variable depending on the area and season. For example, since 2008 distribution has changed likely due to the association with the overwintering herring in northern Norway (NAMMCO, 2019a). In summary, in the study area humpbacks seem to be very plastic in their feeding behaviour.

As a capital breeder, feeding is assumed to be the primary activity of humpback whales in the central and north-eastern North Atlantic during the summer months, due to the availability of abundant prey during this season. The modelled relationships are therefore likely to reflect environmental drivers related to finding prey. During this period, individuals may also travel as part of their migration to northern locations (e.g. from the tropics to the Barents Sea or Svalbard (e.g. Ressler et al., 2015; Stevick et al., 2006, 2003; Vacquié-Garcia et al., 2017)) or between

(unknown) feeding areas. However, most cetacean species are believed to be opportunistic feeders and could take advantage of available prey, for example, while travelling.

Covariates included in the models have been chosen because they may have the power to explain foraging behaviour (see also general justification of the included covariates in section 2.2.2.1 and Table 2.3). Other studies have found relationships between humpback whale density and depth, slope, presence of fronts, SST, and prey (see above). Covariates related to primary production may have a small to medium lagged relationship with humpback whale density because they feed fairly low in the trophic web (e.g. Christensen et al., 1992; Heide-Jørgensen and Laidre, 2007; Huse et al., 2015; Magnúsdóttir et al., 2014; Nøttestad et al., 2015, 2014; Ressler et al., 2015). Covariates linked with prey aggregation such as SSH and mlp are expected to be related to prey accumulation and to have little to no lag. Salinity is related to water masses and in the study area may explain the influence of Arctic versus temperate water on humpback whale distribution.

In the North Atlantic, Icelandic and Norwegian waters have the largest abundance of humpback whales in the study area and in the whole North Atlantic (NAMMCO, 2019e) (Table 4.2). Humpback whale abundance in the study area and in the whole North Atlantic has increased over time; the best available estimate for the entire North Atlantic population is 11,570 (95% CI 10,290-13,390), based on mark-recapture analysis of photo-id data from 1992-1993 (Stevick et al., 2003). In Icelandic-Faroese waters a substantial change in abundance has been estimated from 1970s to 2001. Sigurjónsson and Gunnlaugsson (1990) found a 14% annual increase in the relative abundance of humpback whales in 1979-1988, while Pike et al., (2009a) found a 12% annual increase in abundance in 1987-2001. The increase rate during these periods are too high to be biologically feasible, so the increases in abundance must incorporate changes in distribution (Stevick et al., 2003; Zerbini et al., 2010). In the most recent years abundance seems to have levelled off or possibly even decreased (NAMMCO, 2019a; Pike et al., 2019b; Víkingsson et al., 2015). In Norwegian waters, estimated abundance has increased from 1,059 (CV=0.248) and 1,450 (CV=0.29) in 1995 and 1996-2001, respectively (Øien, 2009). In a new stratum north of Iceland included since the 1996-2001 survey period, abundance was estimated as 3,246 (CV=0.51). Abundance increased through the most recent survey periods (2002-2007, 2008-2013 and 2014-2018) to more than 10,000 in the latest period (2014-2018) (NAMMCO, 2019a), as shown in Table 4.2.

Table 4.2. Abundance estimates of humpback whales during surveys in 2015.

Areas 2015	Estimate	95% Confidence interval	Reference
West Greenland	993	434-2,272	Hansen et al., (2018)
East Greenland (coastal)	4,223	1,845-9,666	Hansen et al., (2018)
Iceland/Faroe Islands (shipboard)	9,867	4,854-20,058	Pike et al., (2019b)
Norway (2014-2018)	11,662	15,225-26,027	NAMMCO (2019a)

Globally, the humpback whale is listed as Least Concern by the IUCN; the Arabian Sea sub-population is listed separately as Endangered (Cooke, 2018b). This listing has been given since 2008 as the species recovers from the whaling pressure of the past (Reilly et al., 2008a).

Humpback whales have a mainly coastal distribution and thus may be more susceptible to pressure from human activities than species inhabiting offshore waters. Such pressures may include: harvest, vessel collisions, entanglement, acoustic pollution, prey depletion, water pollution, harassment due to tourism (whale watching), and oceanographic changes. Humpbacks have been commercially hunted in the past (Clapham, 2018; Greenland, 2012; Smith and Reeves, 2010; Stevick et al., 2003). Currently, under the IWC Aboriginal Subsistence Whaling management program humpback whales are hunted in Greenland (feeding ground) and in St Vincent and the Grenadines (breeding ground) (IWC, 2020). Humpbacks are one of the most vulnerable whale species to vessel collisions and entanglement with fishing gear (Bettridge et al., 2015; Clapham, 2018). In Scottish waters, a study from 1992 to 2006 found that although humpback whales were not very frequent, when whales are present the entanglement rate per day is so high that it would not be sustainable if they regularly fed in the area (Ryan et al., 2016). In Norwegian waters, entanglement has increased because whales in the fjords overlap with the herring fisheries; as mitigation, the local government has started giving training in entanglement response (Øien and Haug, 2018). Not all entanglement events lead to mortality, but it may have an effect on reproduction as described in whales from the Gulf of Maine, where females that had been entangled produced fewer calves (IWC, 2002).

Regarding acoustic pollution, there is contradictory information about the effects of sonar noise on humpback whales in the Gulf of Maine. While Risch et al (2012) found effects, Gong et al

(2014) did not find changes in vocalizations. Prey depletion is believed not to have a significant effect at the population level (Avila et al., 2018; Clapham, 2018; Cooke, 2018b). Chemical pollutants are found in low concentrations below the estimated toxicity threshold in humpback whales and are not expected to cause negative effects in the species (Ryan et al., 2013). Humpback whales are one of the primary targets of whale-watching because of their coastal distribution and their behaviour and approachability. The practice is generally considered sustainable but further and more detailed studies addressing the long-term effects on humpback populations have been suggested (Scheidat et al., 2004; Weinrich and Corbelli, 2009).

Humpback whales have historically seemed to adapt to large-scale environmental variation by changing their distribution, as in the examples given above in the Icelandic and Norwegian waters (Nøttestad et al., 2015; Ressler et al., 2015; Víkingsson et al., 2015). Similar responses have also been observed in the western North Atlantic where, as a result of climate change, whales have been seen further north than before at the Canadian Eastern Arctic (Higdon and Ferguson, 2011) and were shown to be arriving at the Gulf of St Lawrence feeding ground four weeks earlier in 2010 than in 1984 (Ramp et al., 2015).

4.1.3 State of knowledge about minke whales

The common minke whale (*Balaenoptera acutorostrata*) is the smallest species in the Balaenopteridae family but the most commonly found and with a worldwide distribution. The common minke whale is taxonomically subdivided into two subspecies: North Atlantic minke whale (*B. a. acutorostrata*) and North Pacific minke whale (*B. a. scammoni*) (Committee on Taxonomy, 2018). In the Southern Hemisphere there is an overlap between common minke whales, Antarctic minke whales (*Balaenoptera bonaerensis*) and dwarf minke whales (Perrin et al., 2018). Although, an Antarctic minke whale and hybrids (maternal and paternal) between North Atlantic and Antarctic minke whales have been found in the North Atlantic (Glover et al., 2013, 2010), in this study it is assumed that these are rare exceptions and that all sightings are of North Atlantic minke whales, henceforth referred to as 'minke whale'. In the North Atlantic, full-grown minke whales measure between 8-9 m and females are slightly larger (Perrin et al., 2018). The lifespan is suggested to be approximately up to 60 years (NAMMCO, 2019f), however a study using eye lenses of 176 Icelandic minke whales estimated a maximum age of 42 years (Auðunsson et al., 2013).

Minke whales distribution during winter is poorly known but it is assumed that animals migrate to lower latitudes and/or disperse (Víkingsson and Heide-Jørgensen, 2015) although it is possible that part of the population also spends winter in the summer range area while others move south (Cooke, 2018c; Risch et al., 2014). In the summer, minke whales are common in the North Atlantic and could reach northern areas such as Greenland Sea, Svalbard, Franz Josef Land and Novaya Zemlya (Cooke, 2018c; Ressler et al., 2015; Skern-Mauritzen et al., 2011; Vacquié-Garcia et al., 2017) and as far south along the European coast as the North Sea, English Channel (Hammond et al., 2017), and along the mid-Atlantic by 50˚ N (Sigurjónsson et al., 1991 In: NAMMCO, 2019f). The migration north appears to be segregated in West Greenland and Iceland, where different migration based on sex has been reported; females seem to arrive earlier to the feeding grounds and also move to northern areas earlier than males as the season progressed (Laidre et al., 2009; Pampoulie et al., 2013). Changes in distribution between years have also been recorded. In some areas, minke whales also seem to be extending the their summer range further north, for example, in Canadian and Norwegian waters they have been recorded in areas that had no recordings before (Higdon and Ferguson, 2011; NAMMCO, 2019a; Storrie et al., 2018).

Globally, minke whales occur frequently in coastal waters; in the North Atlantic they are also found in offshore waters. The Icelandic continental shelf has usually been the most important summer feeding ground for minke whales in the Central North Atlantic (Pike et al., 2009a; Víkingsson et al., 2014). In Norwegian waters minke whales are mainly found in coastal waters along the continental shelf (Storrie et al., 2018; Vacquié-Garcia et al., 2017). In the Barents Sea where the average depth is around 230 m, minke whales are found in shallow waters in the north and along the shelf edge to the west and south west (Haug et al., 2002; Skern-Mauritzen et al., 2011). Around Svalbard, Storrie et al., (2018) used a 'citizen science' database from 2002-2013 to show that minke whales occurred at depths between >20 m and <4000 m, with median depth of 188 m. In the central and northeast Atlantic, minke whales occur from the ice edge and the polar front in Svalbard and the Barents Sea (Skern-Mauritzen et al., 2011; Storrie et al., 2018) to the southern part (Víkingsson and Heide-Jørgensen, 2015). Around Svalbard during June-September, they were observed in water temperatures between 1.8-8 ˚C, with a median of 4.5 ˚C (Storrie et al., 2018), while minke whales off western Scotland showed a preference for water temperatures around 11.5-12 °C in June and 13-14 °C in August-September (Anderwald et al., 2012).

Distribution is presumably closely linked with diet and minke whales consume a wide range of prey and can vary between areas, seasons, and years, ranging from macro-zooplankton to large gadoid fish (e.g. Cooke, 2018c; Ressler et al., 2015; Skern-Mauritzen et al., 2011; Vacquié-Garcia et al., 2017; Víkingsson et al., 2014). In Icelandic waters in 1977 to 1997, in the south and west the main prey was sand eel, while in the north there were two main prey items: euphausiids (58%) (*Thysanoessa raschii* and *Meganyctiphanes norvegica*) and capelin (42%) (Sigurjónsson et al., 2000). Although stable isotopes results should be taken with care, an example of exchangeable distribution is in Icelandic waters where stable isotope analysis on minke whales' δ13C showed spatial-temporal changes: in 2003-2004 larger importance was on prey from coastal origin (south-west), while in 2006 it was pelagic diet (north-east) (Pampoulie et al., 2013). In the period 2003-2007, an overall decrease in the previous three main prey items and an increase in herring and haddock (*Melanogrammus aeglefinus*) were observed (Pampoulie et al., 2013; Víkingsson et al., 2014). In the north and east, cod comprised around 29% of the diet (Pampoulie et al., 2013) but capelin decreased to 22% (Víkingsson et al., 2015). These changes in prey composition are consistent with changes at the ecosystem level in the continental shelf around Iceland, where water temperatures have increased around 1-2 ˚C in the south and west (Valdimarsson et al., 2012), and fish composition has also changed with the intrusion of southern mackerel (Astthorsson et al., 2012) and the summer retreat of capelin (Pálsson et al., 2012). In the Northeast Atlantic it has been calculated annually (based on 1995) that minke whales consume more than 1.8 million tons of prey (NAMMCO, 1998). The prey consumed, although could be highly variable yearly and by area, comprises of several commercial important species could be around 70% or more of the total fishery (NAMMCO, 1998). In Icelandic shelf waters, minke whales consumed more than 1 million ton of fish (Sigurjónsson and Víkingsson, 1997), early stage modelling exercises suggested that these amounts of minke whale fish consumption could have implications on fish stocks (hence commercial fisheries) (NAMMCO, 1998; Stefánsson et al., 1997). Although, Lindstrøm et al., (2009), multi-species modelling approach showed that the effects from whale predation on fish stocks is variable depending the whale density and number, the effect among fish species could be indirect, such as the case where a minke whale increase predation on cod can result in increase of capelin.

In Norwegian waters there is also diversity in minke whale diet and some suggested spatial-temporal changes. In the early 2000s, krill was the main prey around Svalbard capelin around Bear island, capelin, herring and haddock along the north coast of continental Norway and herring in the Norwegian Sea (Windsland et al., 2007). Different studies at the Norwegian

Sea minke whales have been often identified herring as the main prey (Nøttestad et al., 2015; Olsen and Holst, 2001). In the Barents Sea the diet is also variable (e.g. Bogstad et al., 2015). In the south, the main prey was immature herring (0-3 years) but in low recruitment years whales switched to krill, capelin and/or gadoid fish. In the north, capelin was the main prey but following its collapse (1992/1993) the diet switched to krill (*Thysanoessa* sp. and *Meganyctiphanes norvegica*) (Haug et al., 2002). In the North Sea, the southern limit of the study area, minke whale diet was dominated by sand eels and mackerel (Windsland et al., 2007).

As a capital breeder, feeding is assumed to be the primary activity of minke whales in the central and north-eastern North Atlantic during the summer months, due to the availability of abundant prey during this season. The modelled relationships are therefore likely to reflect environmental drivers related to finding prey. During this period, some individuals may travel as part of their migration to northern locations (e.g. to the Greenland Sea, Svalbard, Franz Josef Land and Novaya Zemlya (Cooke, 2018c; Ressler et al., 2015; Skern-Mauritzen et al., 2011; Vacquié-Garcia et al., 2017)) or between (unknown) feeding areas. However, most cetacean species are believed to be opportunistic feeders and could take advantage of available prey, for example, while travelling.

Covariates included in the models have been chosen because they may have the power to explain foraging behaviour (see also general justification of the included covariates in section 2.2.2.1 and Table 2.3). Other studies have found relationships between minke whale density and depth, slope, SST, and prey (see above). Covariates related to primary production may have variable lagged relationships with minke whale density because they feed at several levels in the trophic web which has also changed over time (e.g. Haug et al., 2002; Nøttestad et al., 2015; Olsen and Holst, 2001; Sigurjónsson and Víkingsson, 1997; Víkingsson et al., 2015; Windsland et al., 2007). Covariates linked with prey aggregation such as SSH and mlp are expected to be related to prey accumulation and to have little to no lag. Salinity is related to water masses and in the study area may explain the influence of Arctic versus temperate or coastal water on minke whale distribution.

Recent abundance estimates show that Norwegian waters have the highest abundance of minke whales in the central and north-eastern Atlantic Table 4.3. Trends in abundance over time have been examined. In Icelandic coastal waters, abundance appears constant from 1986 to 2001 but then decreased in 2007 by around 75% and has remained steady through 2016 (Figure 4.2) (NAMMCO, 2019a; Pike et al., 2019b). For the whole area the decrease rate in density from 1986

to 2016 was estimated to be -0.04 (95% CI: -0.05; -0.02) (NAMMCO, 2019a). In Norwegian waters no statistically significant changes in abundance have been found between 1989 and 2013 (NAMMCO, 2019e). Some changes in abundance and distribution have been suggested but not yet published for the most recent survey rotation of 2014-2018 (NAMMCO, 2018). Around Jan Mayen, minke whale abundance estimates have been variable over time; abundance increased from 1989 to 1997, then estimates were stable until 2005, and then decreased during the period 2008-2013, but the most recent survey in 2015 shows higher abundance (NAMMCO, 2018).

Table 4.3.BA. Abundance estimates of minke whales during surveys in 2015 or most recent estimates up to date.

Areas 2015	Estimate	95% Confidence interval	Reference
West Greenland	5,095	2,171-11,961	Hansen et al., (2018)
East Greenland (coastal)	2,762	1,160-6,574	Hansen et al., (2018)
Iceland coastal aerial*	13,497	5,377-33,882	NAMMCO (2019a)
Iceland shipboard	42,515	22,896-78,942	Pike et al., (2019b)
Norway (2008-2013)**	89,623	N/A (CV = 0.18)	IWC (2016)

* partial estimate as un-flown areas (due to bad conditions) were removed.

** results of the last cycle (2014-2018) will not be available until IWC 2021 (NAMMCO, 2019a).

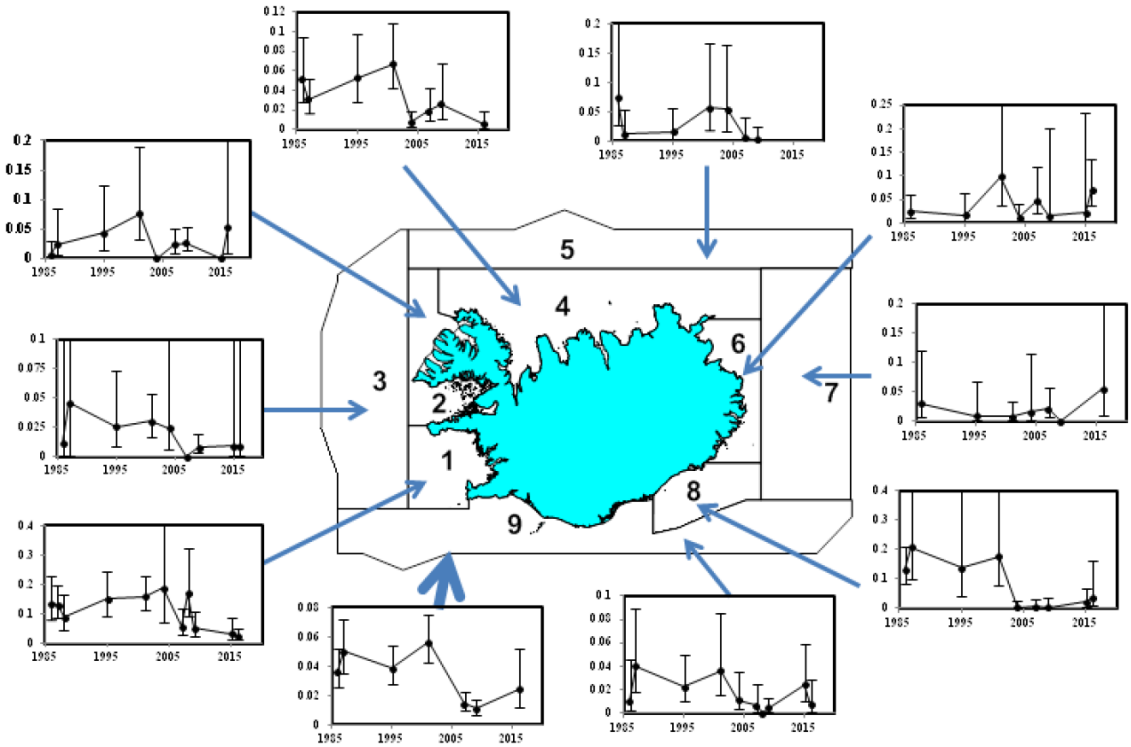

Figure 4.2. Trends in the relative abundance (uncorrected line transect density, whales nm^{-2}) of common minke whales by stratum and for the entire survey area (thick arrow) (Pike et al., 2020b).

Globally, minke whales have been listed as “Least Concern” since 2008 by the IUCN Red List (Cooke, 2018c).

The status of minke whales in the North Atlantic seems stable (Cooke, 2018c) despite diverse pressures including whaling. Pressures include: direct harvesting, vessel collisions, entanglement, acoustic pollution, prey depletion/overlap of resources, water pollution, harassment due to tourism (whale watching), and environmental changes. Minke whales have been caught in the North Atlantic for centuries but at a small local scale and became a direct target more recently in the early 20th century (Kalland and Sejersen, 2005; Sigurjónsson,1989 In: NAMMCO, 2019f). Currently in the study area Norway (annual quota 500-600 animals), Iceland (annual quota 40-80 animals) and Greenland (annual quota 12 animals) are harvesting minke whales in the central and north-eastern Atlantic (Greenland, 2012; IWC, 2020; Víkingsson et al., 2014). Few vessel strikes have been reported but this may be because collisions are underreported due to their smaller size compare to other whales (Northridge et al., 2010). Bycatch occurs in the North Atlantic, and minke whales are graded at level 2 on the ‘Pots and Traps’ risk category of the ICES Working Group on Bycatch, where 2 is the middle level within the risk classification (ICES, 2019b).

The increase of anthropogenic noise such as shipping, seismic, drilling, and naval activities can interfere with whales sounds or can generate displacement (e.g. Martin et al., 2015; Oswald et al., 2016). Regarding minke whales’ prey and possible conflict with humans due to prey depletion/overlap of resources, in the Northeast Atlantic minke whale fish consumption is large (see above) and could have implications on fish stocks hence commercial fisheries, generating an overlap of resources between whales and humans (NAMMCO, 1998; Stefánsson et al., 1997). Regarding chemical pollutants in minke whales, in the Northeast Atlantic some organochloride (DDT) concentrations were found to be higher in minke whales than, for example, harbour porpoises, which are primarily fish eaters (Kleivane and Skaare, 1998). In the central and north-eastern Atlantic and the North Sea the concentration of contaminants PCB, DDT, and CHL (Chlordane) in minke whale blubber increased west to east (Hobbs et al., 2003; Kleivane and Skaare, 1998). Whale watching is not as common or species targeted as is the case for humpback whales, but it does occur in Icelandic and Norwegian waters (Hoyt, 2013). Environmental changes such as rising ocean temperatures and/or loss of sea ice in some areas could be driving

the changes in minke whale distribution/densities and diets as described above (e.g. Hansen et al., 2018; Moore et al., 2019; NAMMCO, 2019a; Storrie et al., 2018; Víkingsson et al., 2015).

4.2 Methods

4.2.1 Estimation of effective strip width

Distance sampling methods are described in Chapter 2 (see section 2.2.1).

4.2.2 Modelling distribution and habitat use

Distribution and habitat modelling methods were applied as described in Chapter 2. The effort and sightings used for modelling the three baleen species is shown in Figure 4.3. The number of sighted animals made during this effort is summarized in Table 2.1 and Table 2.2.

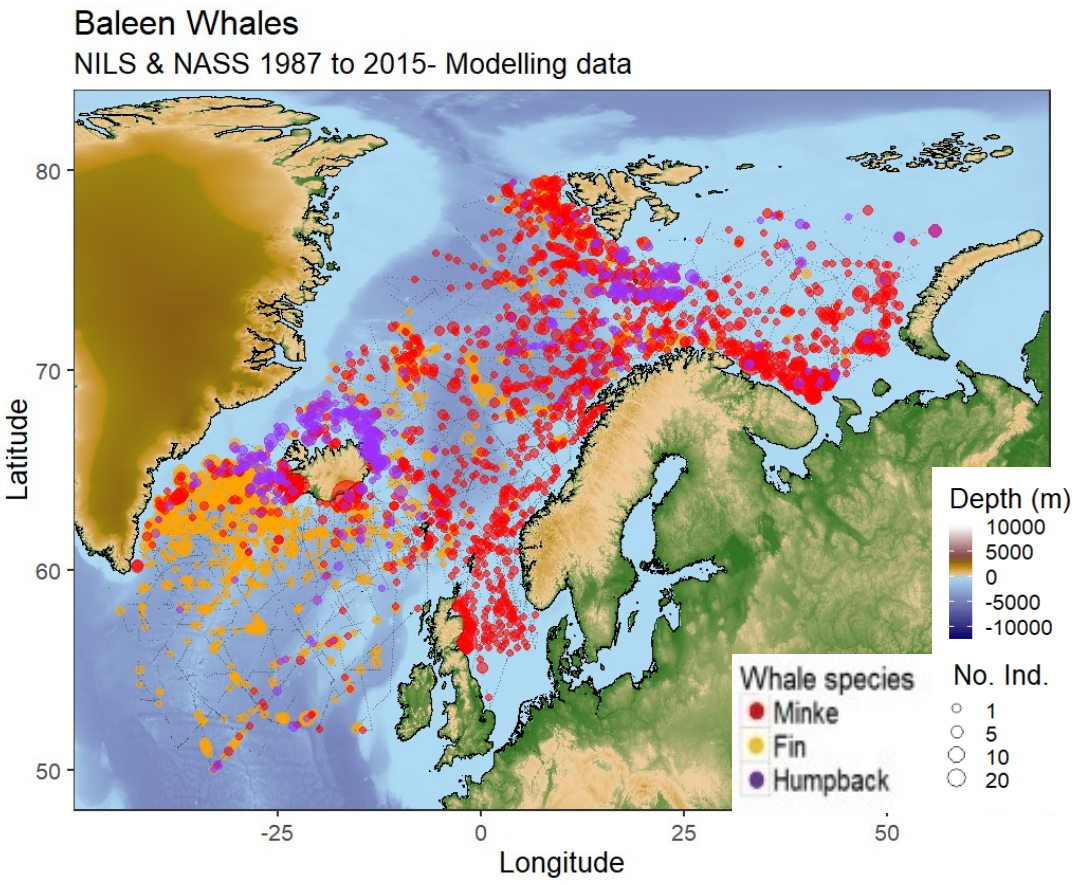

Figure 4.3. Summary of 1987 to 2015 NILS (Norway) & NASS (Iceland and Faroes) survey effort and sightings of fin, humpback and minke whales used for modelling. Effort is depicted by segment mid-points as grey-dots. Sightings are shown as coloured dots, the size of which indicates the number of individuals (No. Ind.). The map was plotted using the geographic coordinate system WGS84 & overlaid over the bathymetry of the area (ETOPO2).

4.3 Results

4.3.1 Fin whales

4.3.1.1 Effective strip width – NASS (Iceland-Faroes) 1987-2015

The best detection function for the 1987-2015 fin whale NASS (Iceland and Faroese) data was a hazard rate model with a 3800 m truncation distance which included 2073 sightings (Appendix 4-A). Vessel ID (ten levels) and Beaufort (three levels) were retained in the selected model. The fitted model is shown in Figure 4.4. The model fitted the data well as shown in the Q-Q plot Figure 4.4 and the Cramer-von Mises [unweighted] goodness of fit test p = 0.273. The average probability of detection *p* was 0.483 (CV = 0.029) and the estimated effective strip width for the combination of ten vessel ID covariate levels and three Beaufort is given in Appendix 4-D.

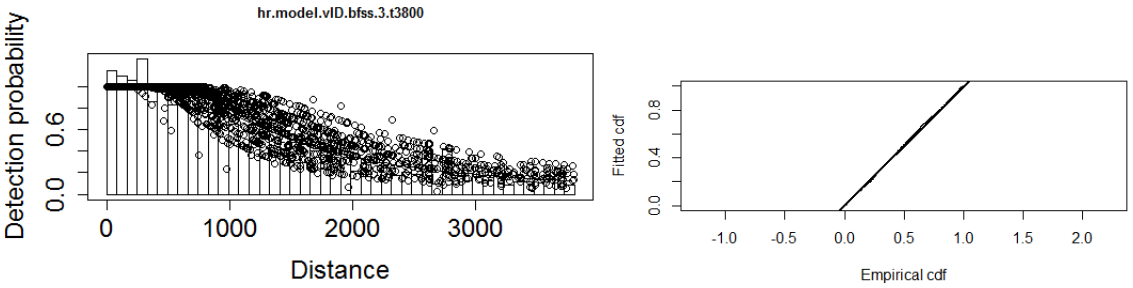

Figure 4.4. Detection probability (left) and Q-Q (right) plots for fin whale 1987-2015 NASS data. For detection probability, the circles represent fitted values of the data, the line is the fitted model and the frequency histogram represents the observed data. In the Q-Q plot (right) the points are the fitted values while the solid line represents the expected data distribution.

4.3.1.2 Effective strip width – NILS (Norway) 1987-1989

The best detection function for the 1987-1989 fin whale NILS (Norwegian) data was a half normal model with a 2500 m truncation distance which included a total of 147 sightings (Appendix 4-A). There were no covariates retained in the model. The fitted model is shown in Figure 4.5. The model fitted the data well, as shown in the Q-Q plot (Figure 4.5) and the Cramer-von Mises [unweighted] goodness of fit test p = 0.931. The average probability of detection *p* was 0.508 (CV = 0.066) and the estimated effective strip width was 1269 m.

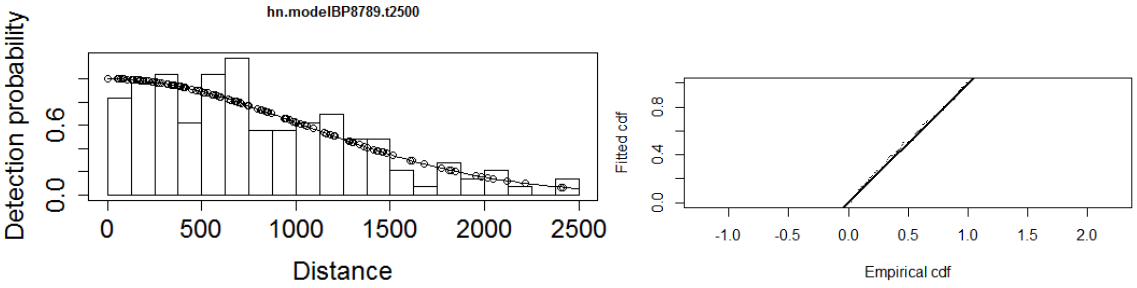

Figure 4.5. Detection probability (left) and Q-Q (right) plots for fin whale 1987-1989 NILS data. For detection probability, the circles represent fitted values of the data, the line is the fitted model and the frequency histogram represents the observed data. In the Q-Q plot (right) the points are the fitted values while the solid line represents the expected data distribution.

4.3.1.3 Effective strip width – NILS (Norway) 1995-2013

The best detection function for the 1995-2013 fin whale NILS (Norwegian) data was a hazard rate model with a 3200 m truncation distance which included a total of 1106 sightings (Appendix 4-A). Vessel ID (four levels) and Beaufort (three levels) were retained in the selected model. The fitted model is shown in Figure 4.6. The model fitted the data well, as shown in the Q-Q plot (Figure 4.6) and the Cramer-von Mises [unweighted] goodness of fit test p = 0.845. The average probability of detection *p* was 0.41 (CV = 0.037) and the estimated effective strip width for the three covariate levels is given in Appendix 4-E.

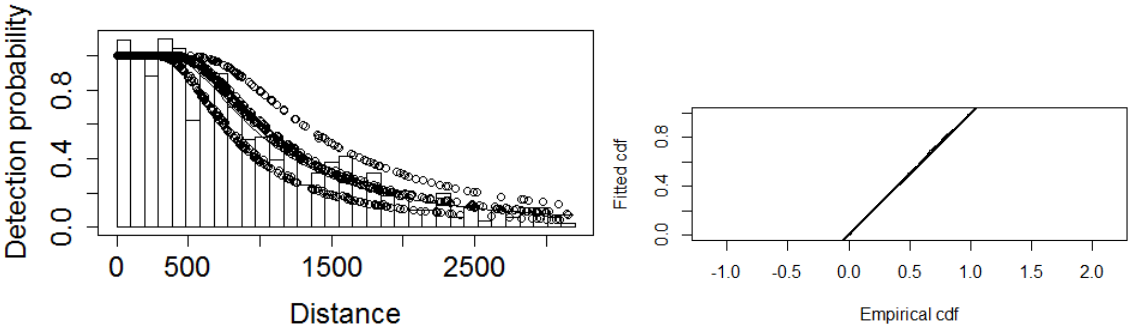

Figure 4.6. Detection probability (left) and Q-Q (right) plots for fin whale 1995-2013 NILS data. For detection probability, the circles represent fitted values of the data, the line is the fitted model and the frequency histogram represents the observed data. In the Q-Q plot (right) the points are the fitted values while the solid line represents the expected data distribution.

4.3.1.4 Distribution and habitat use models: 1987-1989

The negative binomial was determined to be the best error distribution for the 1987-1989 spatial models for fin whales (Appendix 4-F). A summary of all the fitted single variable models is given in Appendix 4-G. The correlation evaluation between static variables and SST months is shown

in Appendix 4-B, where none of the pairs presented a Pearson's correlation greater than 0.7. As mentioned previously, concurvity was not evaluated in the 80s models (see methods section 2.2.2.4.1).

After fitting models to determine the best month for STT, the covariates selected in the best model included: depth, slope, aspect, and July SST. The model fitted the data quite well as shown in Figure 4.7. The best model had a deviance explained of 27.8% (Table 4.4).

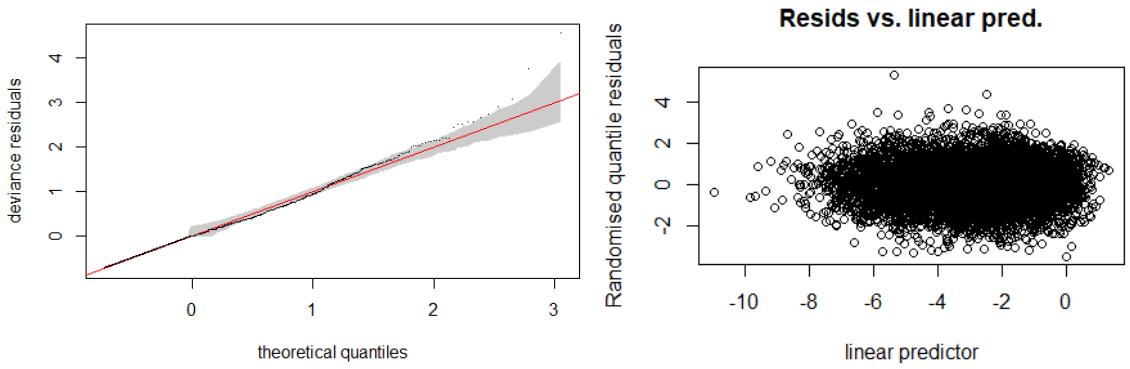

Figure 4.7. GAM diagnostics for the fin whale 1987-1989 best model. In the Q-Q plot (left) the shaded area represents 95% confidence interval, the circles represent the data, the line is the expected data distribution if the model fits the data perfectly. The residual versus linear predictor (right) does not show any patterns or presence of heteroscedasticity.

Table 4.4. Summary of fin whale 1987-1989 models at different SST months. The best error structure for all models was the negative binomial distribution. The model included the standard covariate survey and depth, slope, and aspect plus the stated month for SST.

Model:	Deviance	Deviance explained (%)	AIC	REML	n
July	1134.32	27.84	3916.81	1981.31	6697
May	1122.06	25.50	3950.10	1991.86	
August	1120.33	25.36	3952.44	1993.22	
April	1110.98	25.24	3957.44	1996.97	
June	1122.42	24.84	3961.83	2000.01	

The smooth functions show a predicted positive effect on fin whale density of depths greater than 800 m and a negative effect in shallower depths. Aspect did not show a strong signal, however a clear signal of higher densities at slopes facing southeast around 150˚. Slopes greater than 3˚ had a positive effect. July SST between 4-9 C˚ had a mostly positive effect while cooler and warmer waters had a negative effect in fin whale density (Figure 4.8).

Prediction of fin whale density from 1987 to 1989 is show in Figure 4.9. The model predicted well the high observed occurrence in the northern part of the Irminger Sea, around the Charlie-Gibbs fracture zone, east of Iceland, around Jan Mayen, north-east of the Norwegian Sea, and south of Svalbard. The coefficient of variation (CV) of the predictions shows overall high precision in the predictions, except at the north-west edge of the area at the limit of the cold Arctic waters (Figure 4.10). There were no sightings and very little effort in these areas.

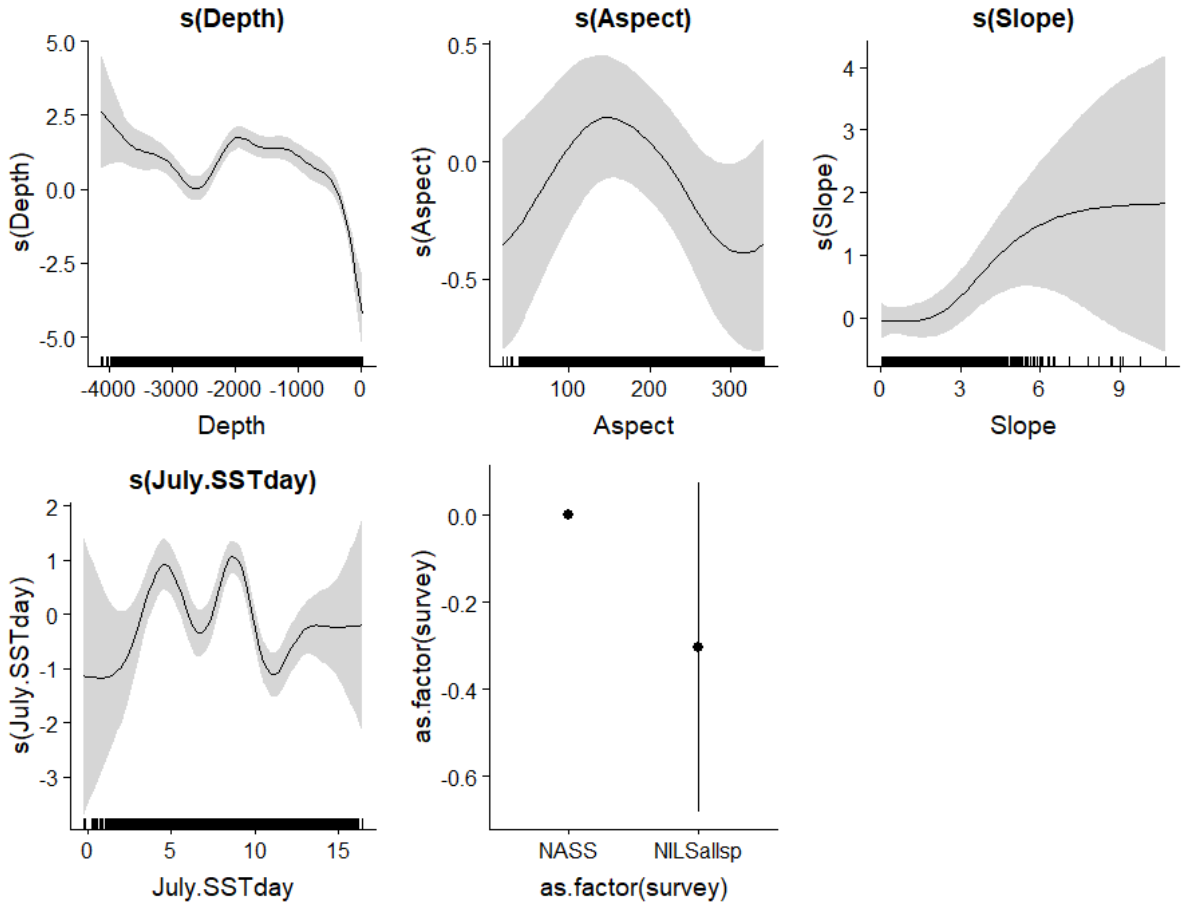

Figure 4.8. Relative density of fin whales as a smooth function of depth, aspect, slope, and July SST for 1987-1989. Zero on the vertical axes corresponds to no effect of the covariate on the relative density of fin whales. Shaded areas represent 95% confidence intervals. The scales on each vertical axis vary among plots. Data points are represented as rug plots on the horizontal axes.

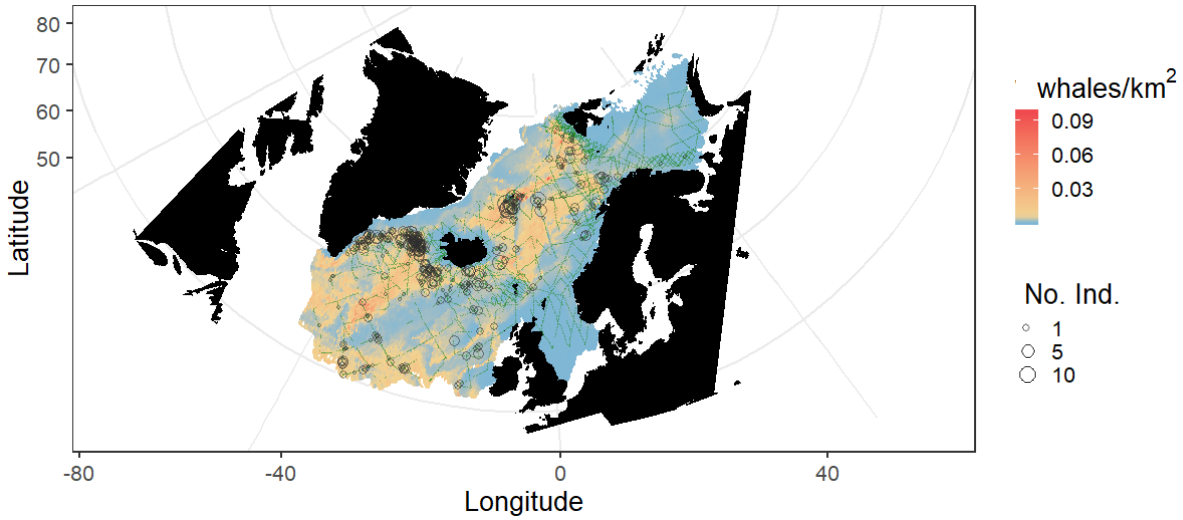

Figure 4.9. Predicted density of fin whales for the best-fitting model for 1987-1989, which included depth, slope, aspect and July SST. The map shows fin whale observations as grey circles, the size of which indicates the number of individuals (No. Ind.), the small green dots represent the effort.

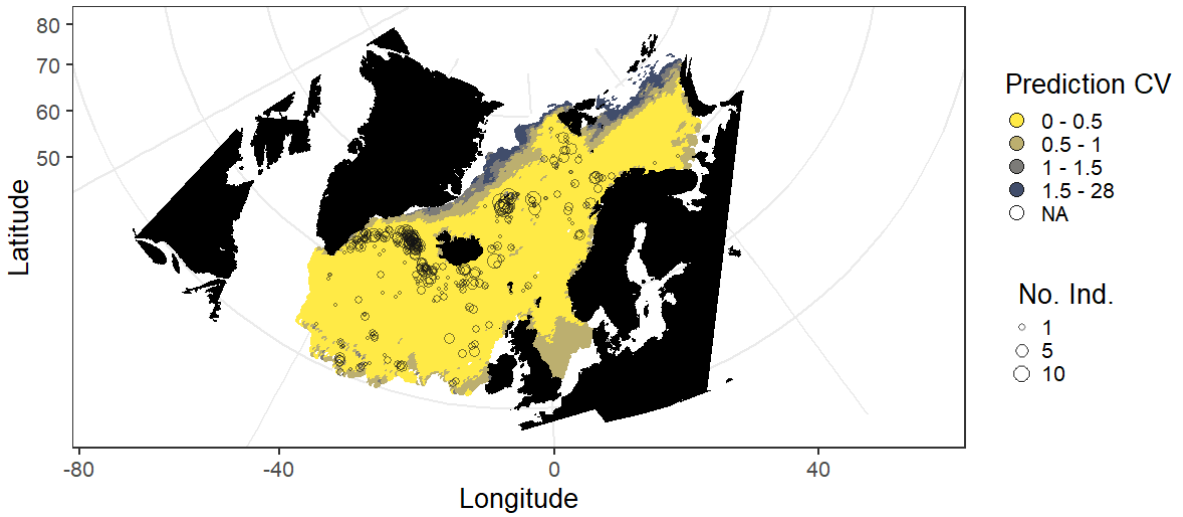

Figure 4.10. Coefficient of variation of the average predicted density of the best-fitting fin whale model for 1987-1989. Yellow areas show the highest precision. Fin whale observations are indicated as grey circles and scaled to the number of individuals (No. Ind.).

4.3.1.5 Distribution and habitat use models: 1998-2015

The negative binomial was determined to be the best error distribution for the fin whale spatial model for 1998-2015 (Appendix 4-H). A summary of all the fitted single variable models can be found in the Appendix 4-I. The best covariate for each variable family that were part of the candidate full model were: depth, aspect, slope, July bT, August SST, Aug salinity, August SSH, April mixed layer depth, April chlorophyll *a*, and April primary productivity. The terms that were removed by penalization were slope, April mixed layer depth, and aspect. In the remaining full

model, after double penalization, collinearity and concurvity were found between July bT/depth, July bT/Aug SSH and April chlorophyll/April primary productivity. After this penalization July bT and April chlorophyll *a* were removed (Appendix 4-C and Appendix 4-J).

The covariates selected in the best model included: depth, August SST, August SSH, August salinity, and April primary productivity. The model fitted the data reasonably well but the error structure was not well described Figure 4.11. The best model had a deviance explained of 30.14% (Table 4.5).

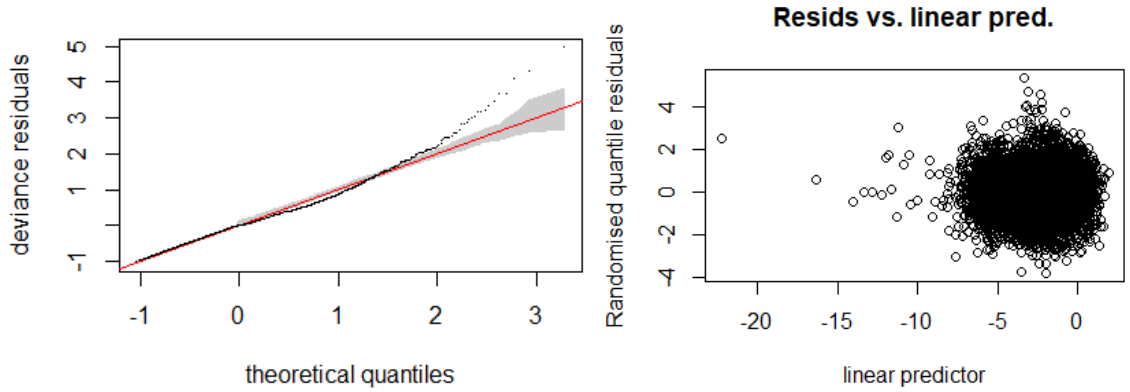

Figure 4.11. GAM diagnostics for the fin whale 1998-2015 best model. In the Q-Q plot (left) the shaded area represents 95% confidence interval, the circles represent the data, the line is the expected data distribution if the model fits the data perfectly. The residual versus linear predictor (right) does not show presence of heteroscedasticity.

Table 4.5. Summary of the fitted models for fin whales 1998-2015 using a forward full model, double penalization and concurvity penalization. The best error structure for all models was the negative binomial distribution. All the models included the standard covariate survey.

Model:	Deviance	Deviance explained (%)	AIC	REML	n
Best model (concurvity)	2050.01	30.14	6520.66	3299.02	7361
Penalized full model	2075.84	33.08	6433.81	3247.18	
Full model	2076.47	33.05	6435.34	3247.19	

The model predicted a positive effect on fin whale density at depths between 3000-500 m approximately, and a negative effect in shallower or deeper waters. August SST had a positive effect at temperatures around 6°C and 12°C, and a negative effect at warmer temperatures. August salinity had in general a negative effect on fin whale density at lower salinities and a positive effect around 35 PSU. August SSH had a positive effect between -1 m and -0.7 m and thereafter a negative effect, especially around -0.6 m. April primary productivity had a positive

effect at lower concentrations from 0-200 mg C m^{-2} day^{-1}, and above 1500 mg C m^{-2} day^{-1} but with higher variability and fewer data points (Figure 4.12).

Prediction of fin whale density for average values across 1998-2015 is shown in Figure 4.13. The model predicted well the high observed occurrence in the Irminger Sea, around the Faroes Islands, north-west Iceland and Jan Mayen, in the central Norwegian Sea, south of Svalbard, around Bear Island and in the western part of the Barents Sea. The CV of the predictions shows the highest precision in the areas where fin whales were where fin whales were predicted at higher densities. The lowest precision in the prediction was at the north-western edge of the study area close to Greenland. There was also low precision in the North Sea where there were no fin whale sightings (Figure 4.14).

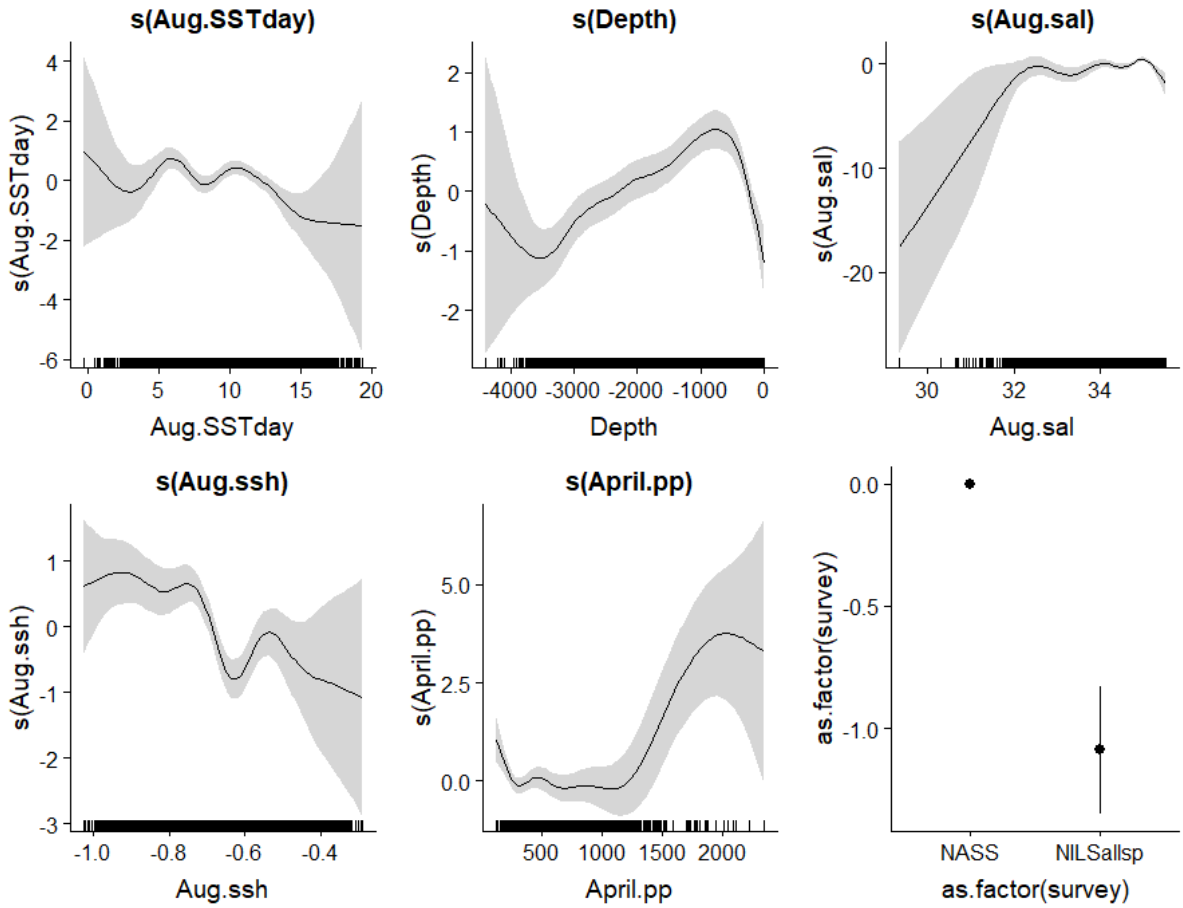

Figure 4.12. Relative density of fin whales as a smooth function of August SST, August SSH, depth, April primary productivity, and August sal for 1998-2015. Zero on the vertical axes corresponds to no effect of the covariate on the relative density of fin whales. Shaded areas represent 95% confidence intervals. The scales on each vertical axis vary between plots. Data points are represented as rug plots on the horizontal axes.

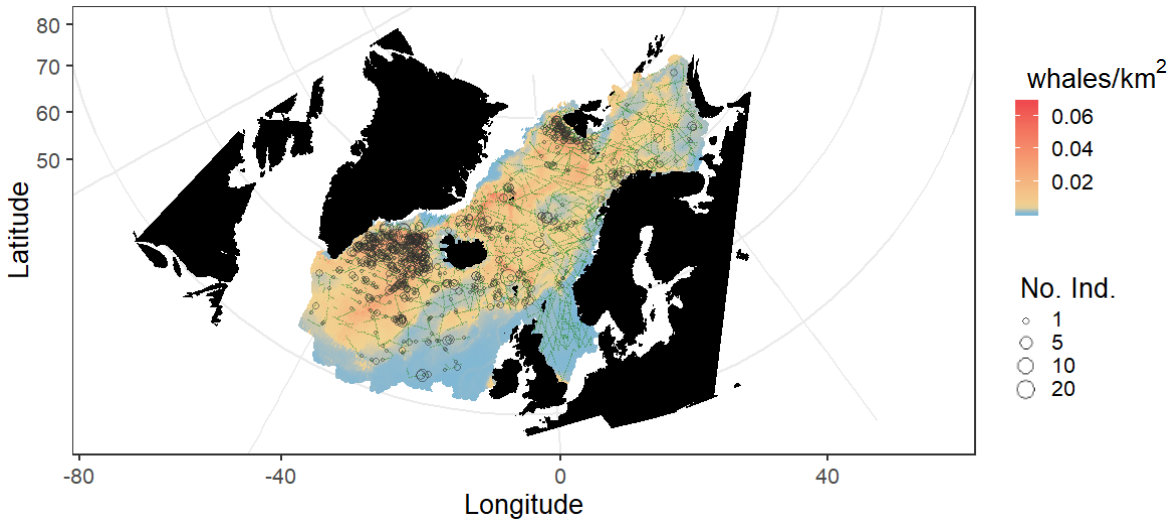

Figure 4.13. Predicted density of fin whales for the best-fitting model across 1998-2015 including August SST, August SSH, depth, April primary productivity, and August sal. Fin whale observations are shown as grey circles, the size of which indicates the number of individuals (No. Ind.). Small green dots represent the effort.

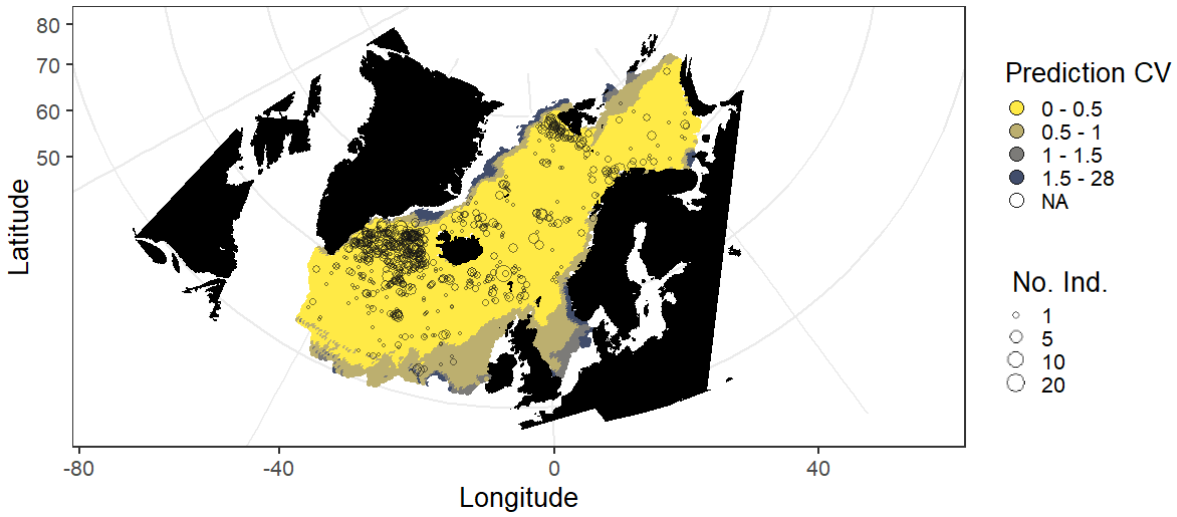

Figure 4.14. Coefficient of variation of the average predicted density of the best-fitting fin whales model for 1998-2015. Yellow areas show the highest precision. Fin whale observations are indicated as grey circles and scaled to the number of individuals (No. Ind.).

4.3.2 Humpback whales

4.3.2.1 Effective strip width – NASS (Iceland-Faroes) 1987-2015

The best detection function for the 1987-2015 humpback whale NASS (Iceland and Faroese) data was a hazard rate model with a 3300 m truncation distance which included 731 sightings (Appendix 4-A). No covariates were retained in the selected model. The fitted model is shown

in Figure 4.15. The model fitted the data well, as shown in the Q-Q plot (Figure 4.15) and the Cramer-von Mises [unweighted] goodness of fit test p = 0.452. The average probability of detection *p* was 0.535 (CV = 0.051). The estimated effective strip width was 1767 m.

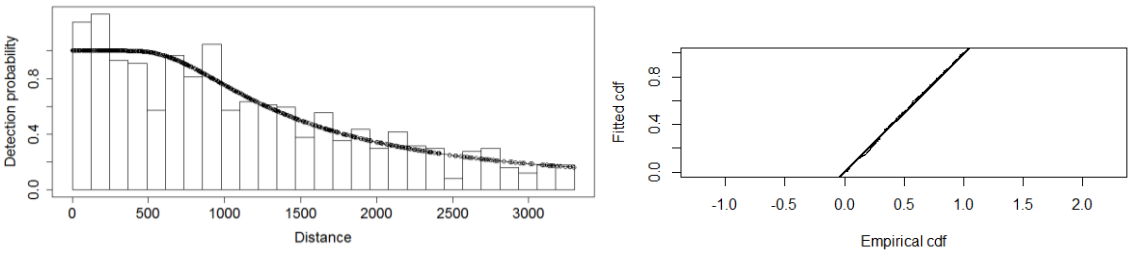

Figure 4.15. Detection probability (left) and Q-Q (right) plots for humpback whale 1987-2015 NASS data. For detection probability, the circles represent fitted values of the data, the line is the fitted model and the frequency histogram represents the observed data. In the Q-Q plot (right) the points are the fitted values while the solid line represents the expected data distribution.

4.3.2.2 Effective strip width – NILS (Norway) 1987-1989

The best detection function for the 1987-1989 humpback whale NILS (Norwegian) data was a hazard rate model with a 2500 m truncation distance which included a total of 39 sightings (Appendix 4-A). No covariates were retained in the selected model. The fitted model is shown in Figure 4.16. The model fitted the data well as shown in the Q-Q plot (Figure 4.16) and the Cramer-von Mises [unweighted] goodness of fit test p = 0.983. The average probability of detection *p* was 0.427 (CV = 0.191) and the estimated effective strip width was 1069 m.

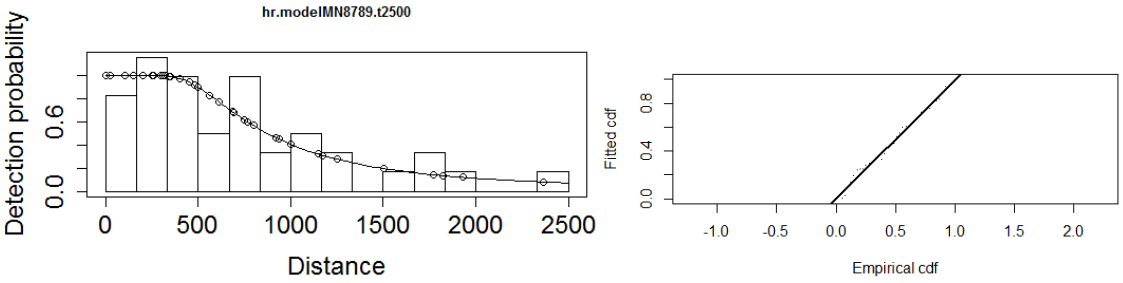

Figure 4.16. Detection probability (left) and Q-Q (right) plots for humpback whale 1987-1989 NILS data. For detection probability, the circles represent fitted values of the data, the line is the fitted model and the frequency histogram represents the observed data. In the Q-Q plot (right) the points are the fitted values while the solid line represents the expected data distribution.

4.3.2.3 Effective strip width – NILS (Norway) 1995-2013

The best detection function for the 1995-2013 humpback whale NILS (Norwegian) data was a hazard rate model with a 3500 m truncation distance which included a total of 695 sightings

(Appendix 4-A). Vessel ID (three levels) was retained in the selected model. The fitted model is shown in Figure 4.17. The model fitted the data well, as shown in the Q-Q plot (Figure 4.17) and the Cramer-von Mises [unweighted] goodness of fit test p = 0.887. The average probability of detection *p* was 0.441 (CV = 0.039) and the estimated effective strip width for the three covariate levels is given in Appendix 4-K.

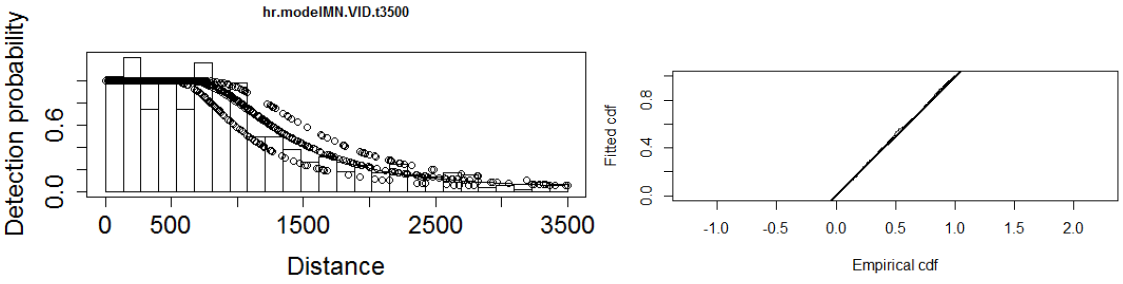

Figure 4.17. Detection probability (left) and Q-Q (right) plots for humpback whale 1995-2013 NILS data. For detection probability, the circles represent fitted values of the data, the line is the fitted model and the frequency histogram represents the observed data. In the Q-Q plot (right) the points are the fitted values while the solid line represents the expected data distribution.

4.3.2.4 Distribution and habitat use models: 1987-1989

The negative binomial was determined to be the best error distribution for the 1987-1989 spatial models for humpback whales (Appendix 4-L). A summary of all the fitted single variable models is given in Appendix 4-M. The correlation evaluation between static variables and STTday months is shown in Appendix 4-B, where none of the pairs presented a Pearson's correlation greater than 0.7. As mentioned previously, concurvity was not evaluated in the 1980s models.

After fitting models to determine the best month for STT, the covariates selected in the best model included: depth, aspect, and May SST. The covariate slope was penalized and removed from the final model. The model fitted the data well as shown in Figure 4.18. The best model had a deviance explained of 25.4% (Table 4.6).

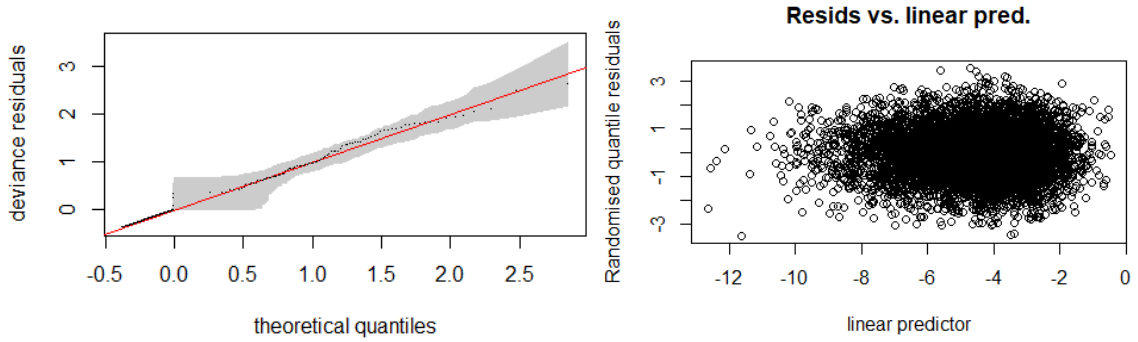

Figure 4.18.GAM diagnostics for the humpback whale 1987-1989 best model. In the Q-Q plot (left) the shaded area represents 95% confidence interval, the circles represent the data, the line is the expected data distribution if the model fits the data perfectly. The residual versus linear predictor (right) does not show any patterns or presence of heteroscedasticity.

Table 4.6. Summary of humpback whale 1987-1989 models at different SST months and unpenalized bathymetric variables. The model included the standard covariate survey, plus aspect for all the stated months. The best error structure for all models was the negative binomial distribution. Depth was only present in May and June models and penalized in the other months.

Model:	Deviance	Deviance explained (%)	AIC	REML	n
May + Depth	317.66	25.40	1167.38	592.61	6697
June + Depth	320.25	17.85	1192.29	595.84	
July	321.35	16.96	1194.21	598.00	
April	316.00	16.07	1197.06	598.21	
August	311.25	12.70	1209.69	604.30	

The smooth functions show a predicted positive effect on humpback whale density of May SST between 0 ˚C to 7 ˚C, with a negative effect in colder and warmer waters. Depth and aspect showed weak signals where, higher densities were found at shallow waters and slopes facing west/southwest (Figure 4.19).

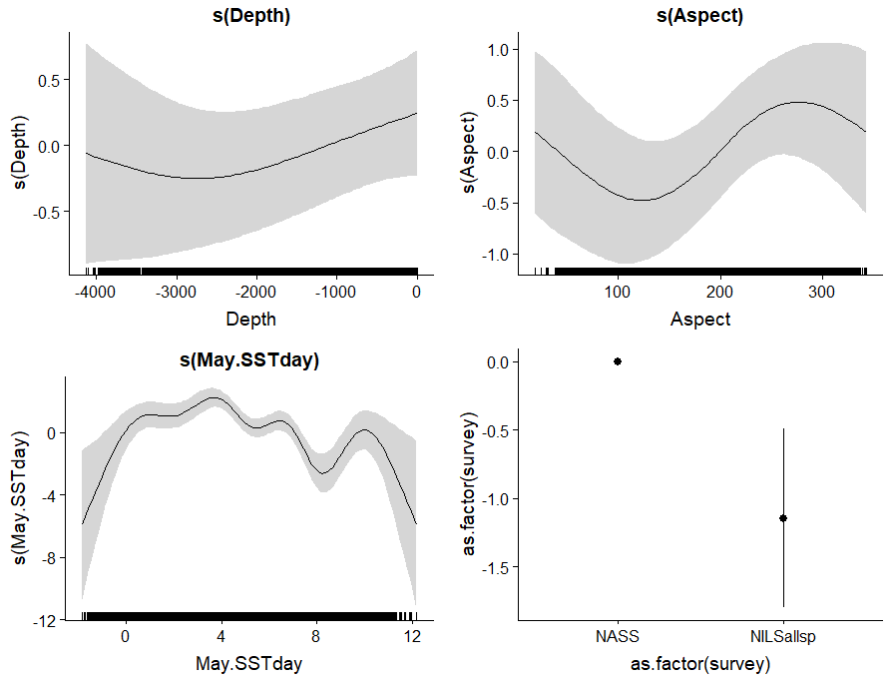

Figure 4.19. Relative density of humpback whales as a smooth function of depth, May SST, and aspect for 1987-1989. Zero on the vertical axes corresponds to no effect of the covariate on the relative density of humpback whales. Shaded areas represent 95% confidence intervals. The scales on each vertical axis vary among plots. Data points are represented as rug plots on the horizontal axes.

Prediction of humpback whale density from 1987-1989 is shown in Figure 4.20. The model predicted well the areas of observed occurrence around west and north Iceland, around Jan Mayen, Mohn Ridge (between Greenland and Norwegian Sea), Bear Island and the north coast of Norway/ south-west Barents Sea, however some other areas with no observations also have high predicted density. Predicted densities overall in this period are low (note the scale in Figure 4.20). The CV of the predictions shows the highest precision through the centre of the study area where almost all sightings occurred. The south-western part of the study area, south of Greenland, has relatively high predicted density and precision although there are no sightings and low coverage. The highest CVs are around edge of the study area edges especially in the north and north-west off Greenland and in the Barents Sea. There are also high CVs west of Ireland; all the areas with very high CV had no humpback sightings in this period (Figure 4.21).

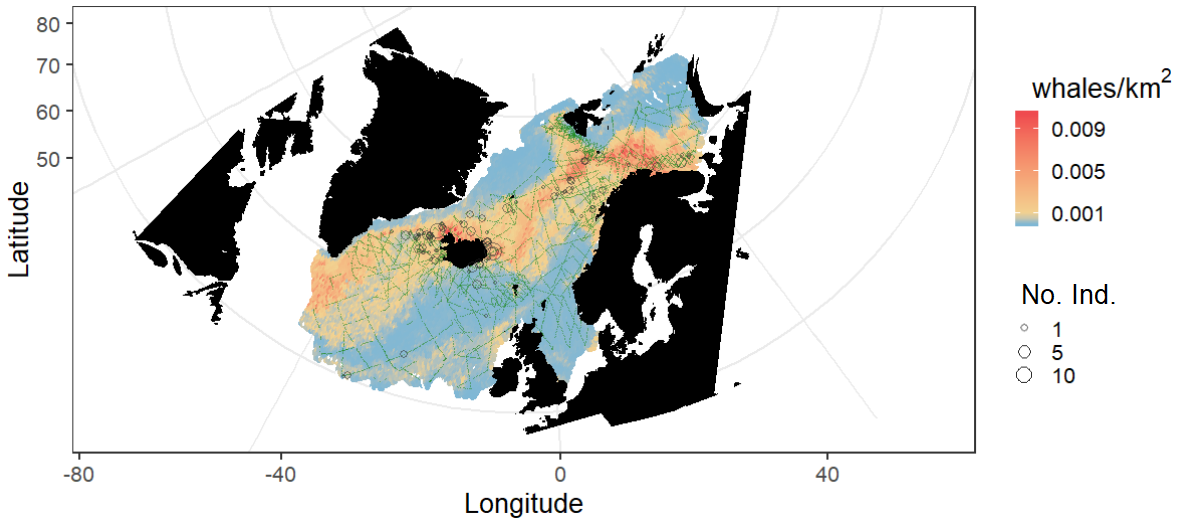

Figure 4.20. Predicted density of humpback whales for the best-fitting model for 1987-1989, which included depth, aspect and May SST. The map shows humpback whale observations as grey circles, the size of which indicates the number of individuals (No. Ind.), the small green dots represent the effort.

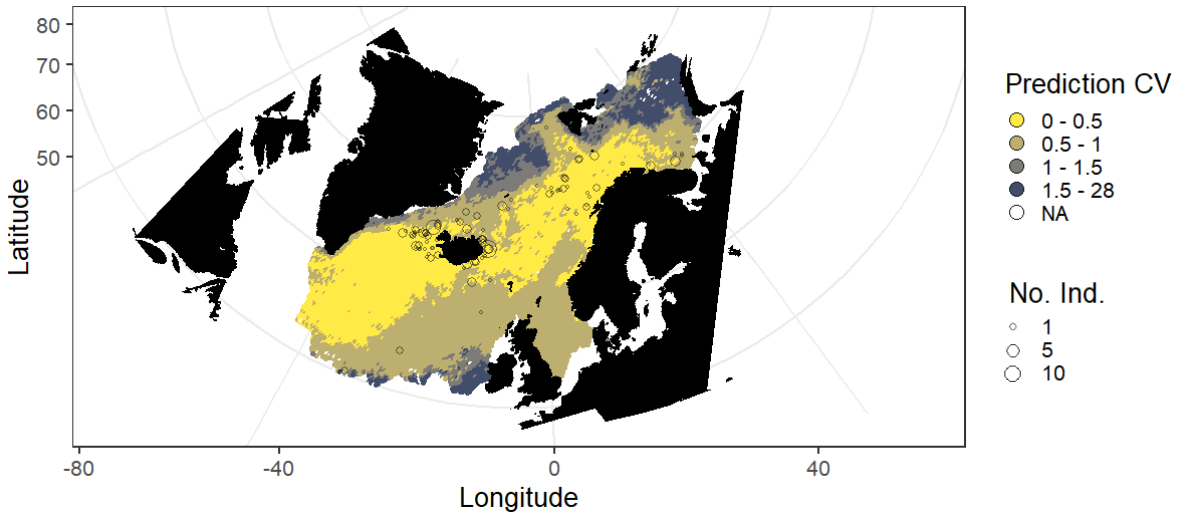

Figure 4.21. Coefficient of variation of the average predicted density of the best-fitting model humpback whales for 1987-1989. Yellow areas show the highest precision. Humpback whale observations are indicated as grey circles and scaled to the number of individuals (No. Ind.).

4.3.2.5 Distribution and habitat use models: 1998-2015

The negative binomial was determined to be the best error distribution for the humpback whale spatial model between 1998-2015 (Appendix 4-N). A summary of all the fitted single variable models can be found in the Appendix 4-O. The best covariates for each variable family that were included for consideration in the full model were: depth, aspect, slope, July bT, June SST, August salinity, August SSH, July mixed layer depth, April chlorophyll *a*, and August primary productivity. The term removed by penalization was slope. In the remaining full model, after double

penalization, collinearity and concurvity were found between bT/depth and bT/ssh (Appendix 4-C and Appendix 4-P) (see methods section 2.2.2.4.1).

The covariates selected in the best model thus included: depth, aspect, June SST, August salinity, August SSH, July mixed layer depth, April chlorophyll *a*, and August primary productivity. The model fitted the data well Figure 4.22. The best model had a deviance explained of 52.3 % (Table 4.7).

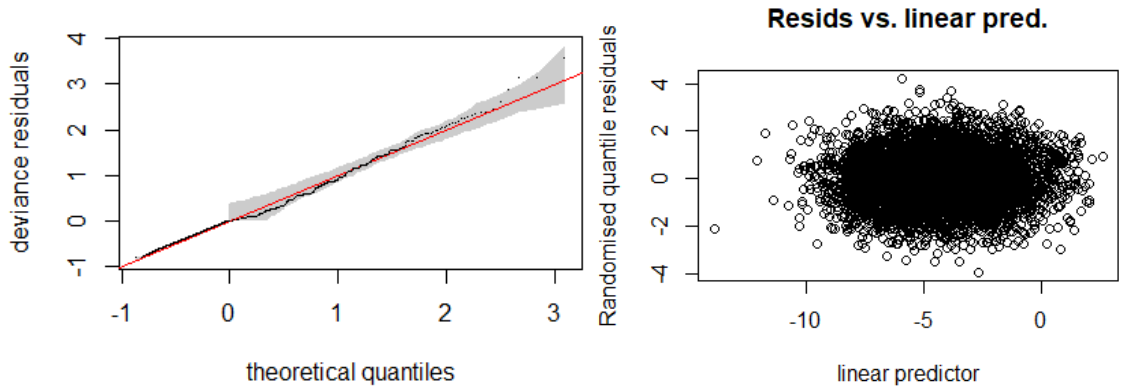

Figure 4.22. GAM diagnostics for the humpback whale 1998-2015 best model. In the Q-Q plot (left) the shaded area represents 95% confidence interval, the circles represent the data, the line is the expected data distribution if the model fits the data perfectly. The residual versus linear predictor (right) does not show any patterns or presence of heteroscedasticity.

Table 4.7. Summary of the fitted models for humpback whales 1998-2015 using a forward full model, double penalization and concurvity penalization. The best error structure for all models was the negative binomial distribution. All the models included the standard covariate survey.

Model: Survey +	Deviance	Deviance explained (%)	AIC	REML	n
Best model (concurvity)	740.89	52.31	2439.65	1238.60	7361
Penalized full model	730.60	55.03	2408.68	1230.38	
Full model	730.50	55.03	2408.79	1230.38	

The model predicted a positive effect on humpback whale density in depths shallower than 1000 m and a negative effect in deeper waters. Aspect had a positive effect above slopes facing west/southwest. June SST had a positive effect in cold waters less than 8 °C and a negative effect above this temperature. Saltier waters around 35 UPS in August had a positive effect. Mixed layer depths in July around 11-12 m had a positive effect; also between 22-25 m but with a higher variability and less data to support the relationship. August SSH had a positive effect between -0.8 and -0.6 m and a negative effect between -1 and -0.8 m. April chlorophyll *a* had a

weak effect, a decrease in predicted density was observed around 1 mg m^{-3}. August primary productivity did not show a clear effect except for a negative effect at low concentrations below 500 mg C m^{-2} day^{-1} and a positive around 750 mg C m^{-2} day^{-1} (Figure 4.23).

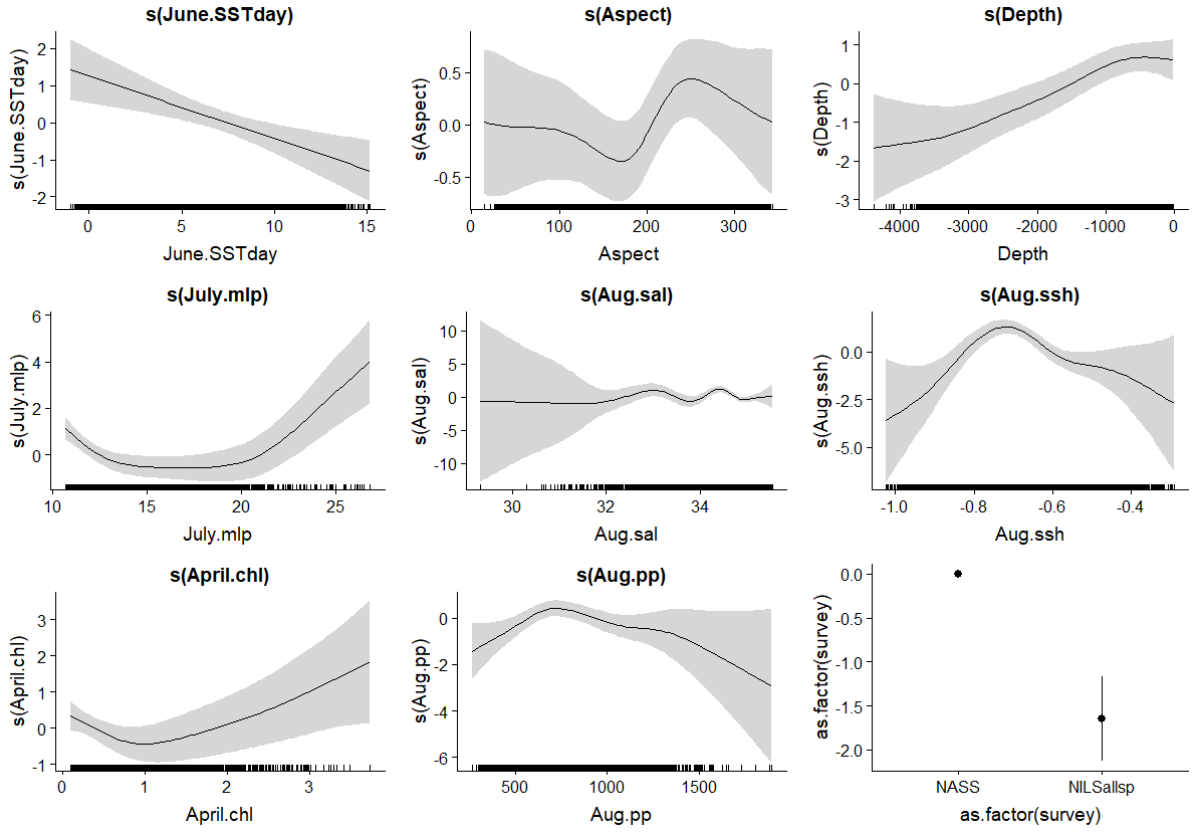

Figure 4.23. Relative density of humpback whales as a smooth function of depth, aspect, April chlorophyll a, June SST, July mixed layer depth, August salinity, August SSH, and August primary productivity for 1998-2015. Zero on the vertical axes corresponds to no effect of the covariate on the relative density of humpback whales. Shaded areas represent 95% confidence intervals. The scales on each vertical axis vary among plots. Data points are represented as rug plots on the horizontal axes.

Prediction of humpback whale density for average values across 1998-2015 is shown in Figure 4.24. The model predicted well the high observed occurrences south, west and north of Iceland, north-west of the Faroe Islands, in the Iceland Basin, south and east of Svalbard, around Bear Island, off the north coast of Norway and in the Barents Sea. High density was predicted along the edge of the study area off Greenland and in the far northwest where there were no observations. The CV of the predictions showed the highest precision in the central part of the study area where most of the sightings occurred. At the northern edge of the Barents Sea predicted density was high and relatively precise with some observations close by. The highest CV (lowest precision) was in general on the studied area edges in the Greenland Sea, south

Irminger Sea, west of Ireland and in the North Sea; all areas where there were no humpback whale observations (Figure 4.25).

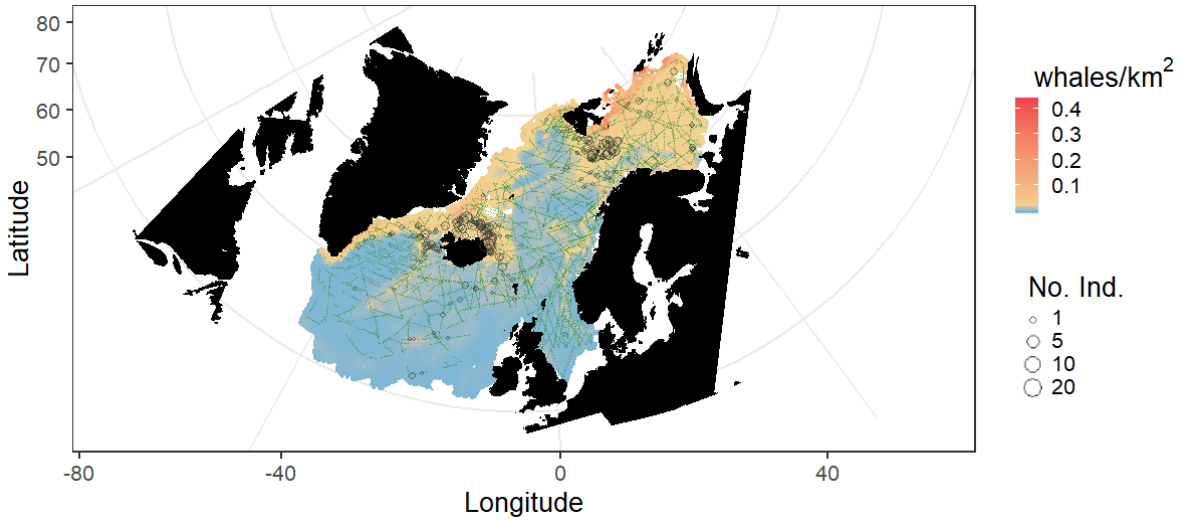

Figure 4.24. Predicted density of humpback whales for the best-fitting model for 1998-2015, which included depth, aspect, June SST, August salinity, August SSH, July mixed layer depth, April chlorophyll a, and August primary productivity. The map shows humpback whale observations as grey circles, the size of which indicates the number of individuals (No. Ind.), the small green dots represent the effort.

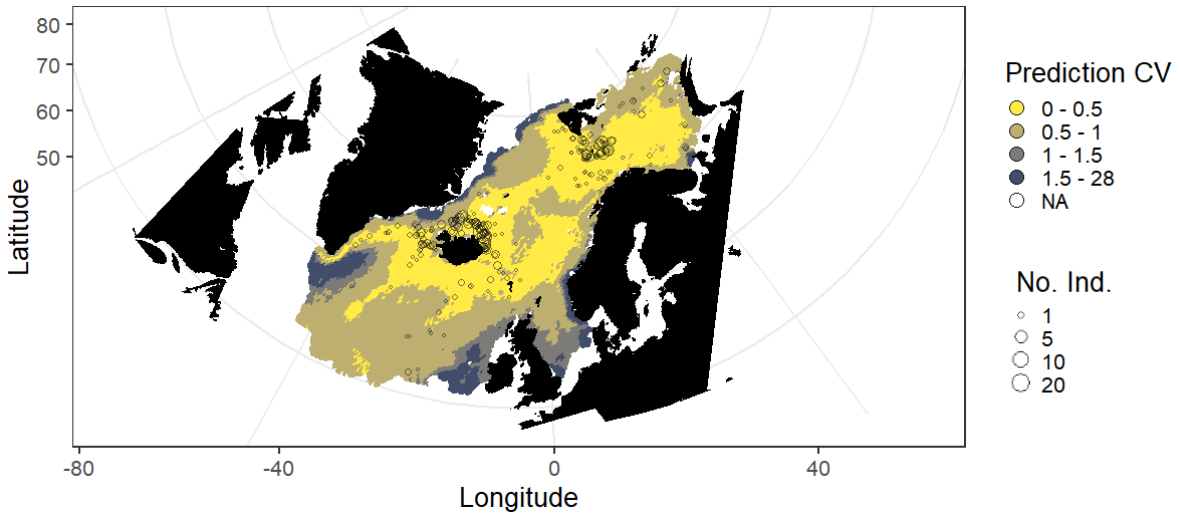

Figure 4.25. Coefficient of variation of the average predicted density of the best-fitting humpback whale model for 1998-2015. Yellow areas show the highest precision. Humpback whale observations are indicated as grey circles and scaled to the number of individuals (No. Ind.).

4.3.3 Minke whales

4.3.3.1 Effective strip width – NASS (Iceland-Faroes) 1987-2015

The best detection function for the 1987-2015 minke whale NASS (Iceland and Faroese) data was a hazard rate model with a 1500 m truncation distance which included 898 sightings (Appendix 4-A). Vessel ID (ten levels) and Beaufort (three levels) were retained in the selected

model. The fitted model is shown in Figure 4.26. The model fitted the data well as shown in the Q-Q plot (Figure 4.26) and the Cramer-von Mises [unweighted] goodness of fit test p = 0.404.. The average probability of detection *p* was 0.238 (CV = 0.061) and the estimated effective strip width for the combination of ten vessel ID covariate levels and three Beaufort is given in Appendix 4-Q

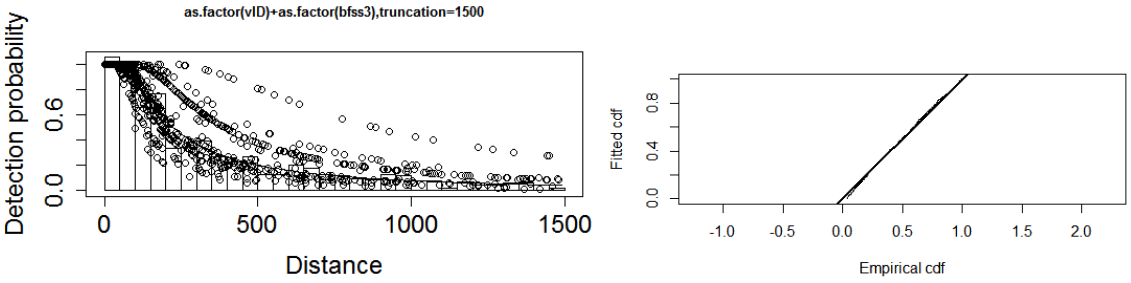

Figure 4.26. Detection probability (left) and Q-Q (right) plots for minke whale 1987-2015 NASS data. For detection probability, the circles represent fitted values of the data, the line is the fitted model and the frequency histogram represents the observed data. In the Q-Q plot (right) the points are the fitted values while the solid line represents the expected data distribution.

4.3.3.2 Effective strip width – NILS (Norway) 1987-1989

The best detection function for the 1987-1989 minke whale NILS (Norwegian) data was a hazard rate model with a 1000 m truncation distance which included a total of 999 sightings (Appendix 4-A). Vessel ID (four levels) was retained in the selected model. The fitted model is shown in Figure 4.27. The model fitted the data well as shown in the Q-Q plot (Figure 4.27) and the Cramer-von Mises [unweighted] goodness of fit test p = 0.249. The average probability of detection *p* was 0.489 (CV = 0.041) and the estimated effective strip width for the vessel ID levels is given in Appendix 4-R.

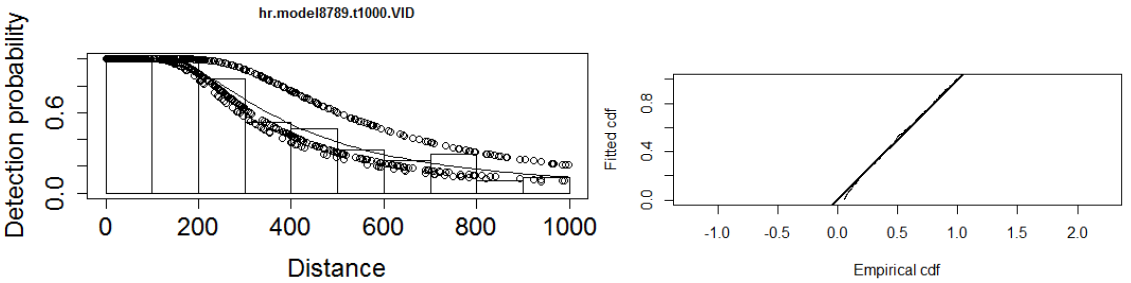

Figure 4.27. Detection probability (left) and Q-Q (right) plots for minke whale 1987-1989 NILS data. For detection probability, the circles represent fitted values of the data, the line is the fitted model and the frequency histogram represents the observed data. In the Q-Q plot (right) the points are the fitted values while the solid line represents the expected data distribution.

4.3.3.3 Effective strip width – NILS (Norway) 1995-2013

The best detection function for the 1995-2013 minke whale NILS (Norwegian) data was a hazard rate model with a 1500 m truncation distance which included 3551 sightings (Appendix 4-A). Vessel ID (four levels) and Beaufort (six levels) were retained in the selected model. The fitted model is shown in Figure 4.28. The model fitted the data well as shown in the Q-Q plot (Figure 4.28) and the Cramer-von Mises [unweighted] goodness of fit test p = 0.202. The average probability of detection *p* was 0.442 (CV = 0.015) and the estimated effective strip width for the combination of four vessel ID covariate levels and six Beaufort is given in Appendix 4-S.

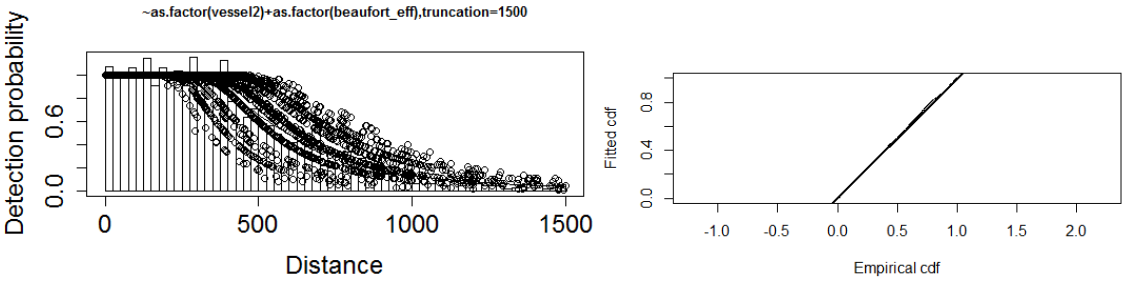

Figure 4.28. Detection probability (left) and Q-Q (right) plots for minke whale 1995-2013 NILS data. For detection probability, the circles represent fitted values of the data, the line is the fitted model and the frequency histogram represents the observed data. In the Q-Q plot (right) the points are the fitted values while the solid line represents the expected data distribution.

4.3.3.4 Distribution and habitat use models: 1987-1989

The negative binomial was determined to be the best error distribution for the 1987-1989 spatial models for minke whales (Appendix 4-T). A summary of all the fitted single variable models is given in Appendix 4-U. The correlation evaluation between static variables and STTday months is shown in Appendix 4-B , where none of the pairs presented a Pearson's correlation greater than 0.7. As mentioned previously, concurvity was not evaluated in the 1980s models (see methods section 2.2.2.4.1).

After fitting models to determine the best month for STT, the covariates selected in the best model included: depth, aspect, slope, and June SST. The model fitted the data quite well as shown in Figure 4.29. The best model had a deviance explained of 18.5% (Table 4.8).

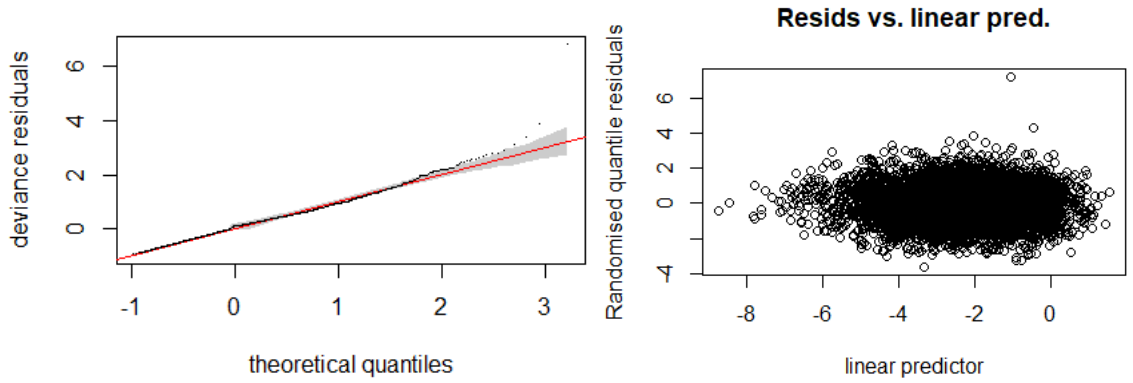

Figure 4.29. GAM diagnostics for the minke whale 1987-1989 best model. In the Q-Q plot (left) the shaded area represents 95% confidence interval, the circles represent the data, the line is the expected data distribution if the model fits the data perfectly. The residual versus linear predictor (right) does not show any patterns or presence of heteroscedasticity.

Table 4.8. Summary of minke whale 1987-1989 models at different SST months. The best error structure for all models was the negative binomial distribution. The model included the standard covariate survey and depth, slope, and aspect plus the stated month for SST.

Model:	Deviance	Deviance explained (%)	AIC	REML	n
June	1903.70	18.48	5642.28	2846.84	6695
May	1914.09	18.41	5642.93	2842.82	
July	1908.55	17.81	5653.32	2844.05	
April	1909.73	17.45	5664.33	2854.69	
August	1909.23	17.31	5666.91	2853.42	

The smooth functions show a predicted positive effect on minke whale density of depths greater than approximately 3500 m or shallower than 300 m. Water depths between these values had a negative effect on minke whale density. Slopes above 1˚ had a positive effect although the prediction for slopes greater than 6˚ has high variability and few supporting data. A negative effect was found above slopes facing towards the northeast and a positive effect towards the south. June SST had a positive effect at temperatures peaks around 5 °C and 9 °C, while negative effects were found in temperatures 3°C or colder, or 11 °C or warmer (Figure 4.30).

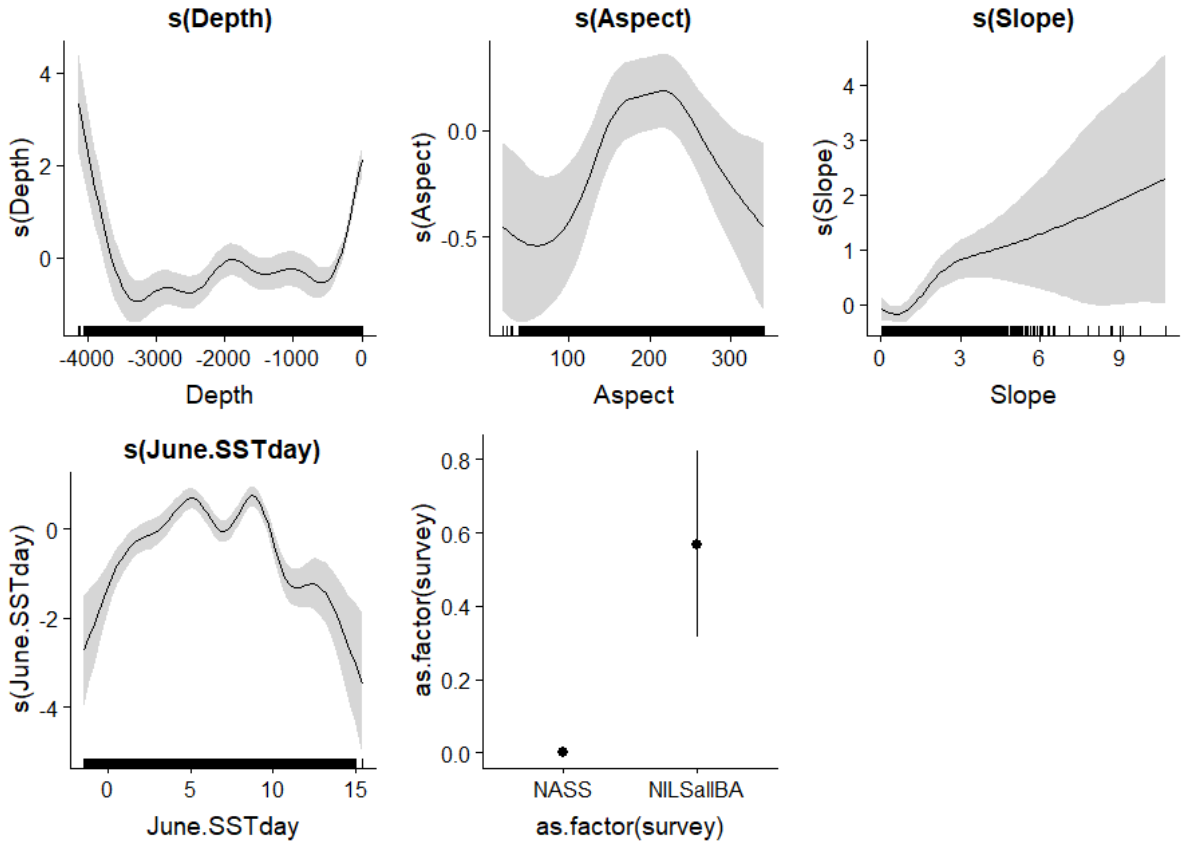

Figure 4.30. Relative density of minke whales as a smooth function of depth, June SST, aspect, and slope for 1987-1989. Zero on the vertical axes corresponds to no effect of the covariate on the relative density of minke whales. Shaded areas represent 95% confidence intervals. The scales on each vertical axis vary among plots. Data points are represented as rug plots on the horizontal axes.

Predictions of minke whale density for average values across 1987-1989 are show in Figure 4.31. The model predicts well the high observed occurrence of minke whales around Iceland, the Faroe Islands, in the North Sea, around Jan Mayen, in the Norwegian Sea, off south-west Svalbard and in the southern Barents Sea. High predicted density also occurred along the Reykjanes Ridge and in the southern North Sea, where there were no observations. The CV of the predictions shows high precision for the whole area (Figure 4.32).

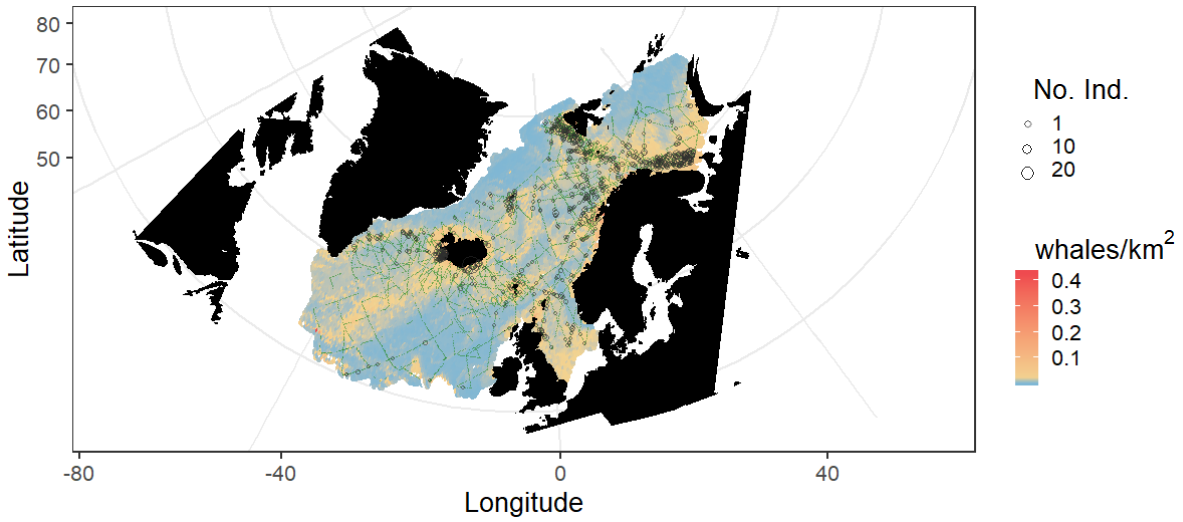

Figure 4.31. Predicted density of minke whales for the best-fitting model for 1987-1989, which included depth, slope, aspect and June SST. The map shows minke whale observations as grey circles, the size of which indicates the number of individuals (No. Ind.), the small green dots represent the effort.

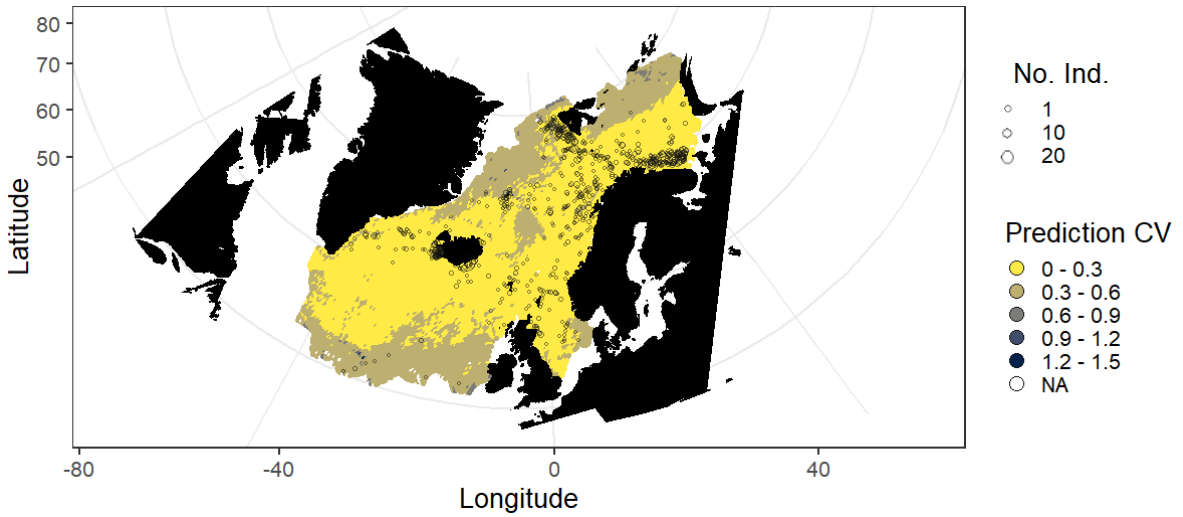

Figure 4.32. Coefficient of variation of the average predicted density of the best-fitting minke whale model for 1987-1989. Yellow areas show the highest precision (higher resolution than other species). Minke whale observations are indicated as grey circles and scaled to the number of individuals (No. Ind.).

4.3.3.5 Distribution and habitat use models: 1998-2015

The negative binomial was determined to be the best error distribution for minke whale spatial model between 1998-2015 (Appendix 4-V). A summary of all the fitted single variables models is in Appendix 4-W.

The best covariates for each variable family that were included for consideration in the full model were: depth, aspect, slope, August bT, June SST, June salinity, June SSH, July mixed layer

depth, June chlorophyll *a*, and August primary productivity. The terms removed by penalization were June chlorophyll *a,* June salinity, and aspect. In the remaining full model, after double penalization, collinearity and concurvity were found between bT/depth and bT/ssh (Appendix 4-C and Appendix 4-X) (see methods section 2.2.2.4.1).

The covariates selected in the best model thus included: depth, slope, June SST, June SSH, July mixed layer depth, and August primary productivity. The model fitted the data fairly (Figure 4.33). The best model had a deviance explained of 13.8% (Table 4.9).

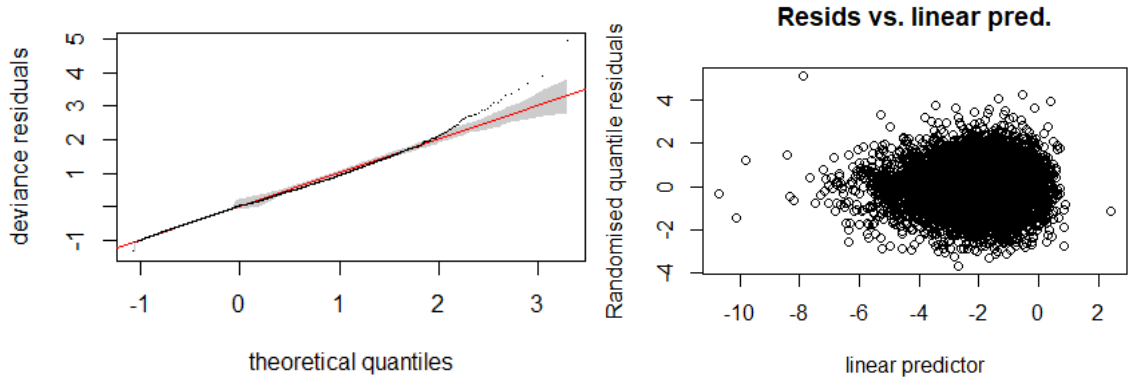

Figure 4.33. GAM diagnostics for the minke whale 1998-2015 best model. In the Q-Q plot (left) the shaded area represents 95% confidence interval, the circles represent the data, the line is the expected data distribution if the model fits the data perfectly. The residual versus linear predictor (right) does not show any patterns or presence of heteroscedasticity.

Table 4.9. Summary of the fitted models for minke whales 1998-2015 using a forward full model, double penalization and concurvity penalization. The best error structure for all models was the negative binomial distribution. All the models included the standard covariate survey

Model:	Deviance	Deviance explained (%)	AIC	REML	n
Best model (concurvity)	2776.59	13.78	7417.75	3727.47	7452
Penalized full model	2760.48	16.58	7340.07	3692.85	
Full model	2760.48	16.58	7340.07	3692.85	
Concurvity Model	2768.91	12.16	7461.99	3747.40	

The smooth functions show a predicted positive effect on minke whale density of depths greater than approximately 3500 m or shallower than 300 m. Water depths between 1500-400 m had a negative effect on minke whale density. Slopes with angles greater than 2.5-5˚ had a positive effect. June SST had a positive effect for temperatures between 1-6°C, while negative effects

were found in warmer temperatures above 6°C. June SSH had a negative effect at heights of -0.9 m or below, and a positive effect at heights between -0.8 to -0.5 m. Mixed layer depth did not show a clear signal. August primary productivity showed a positive effect at concentrations around 1200 mg C m^{-2} day^{-1} (Figure 4.34).

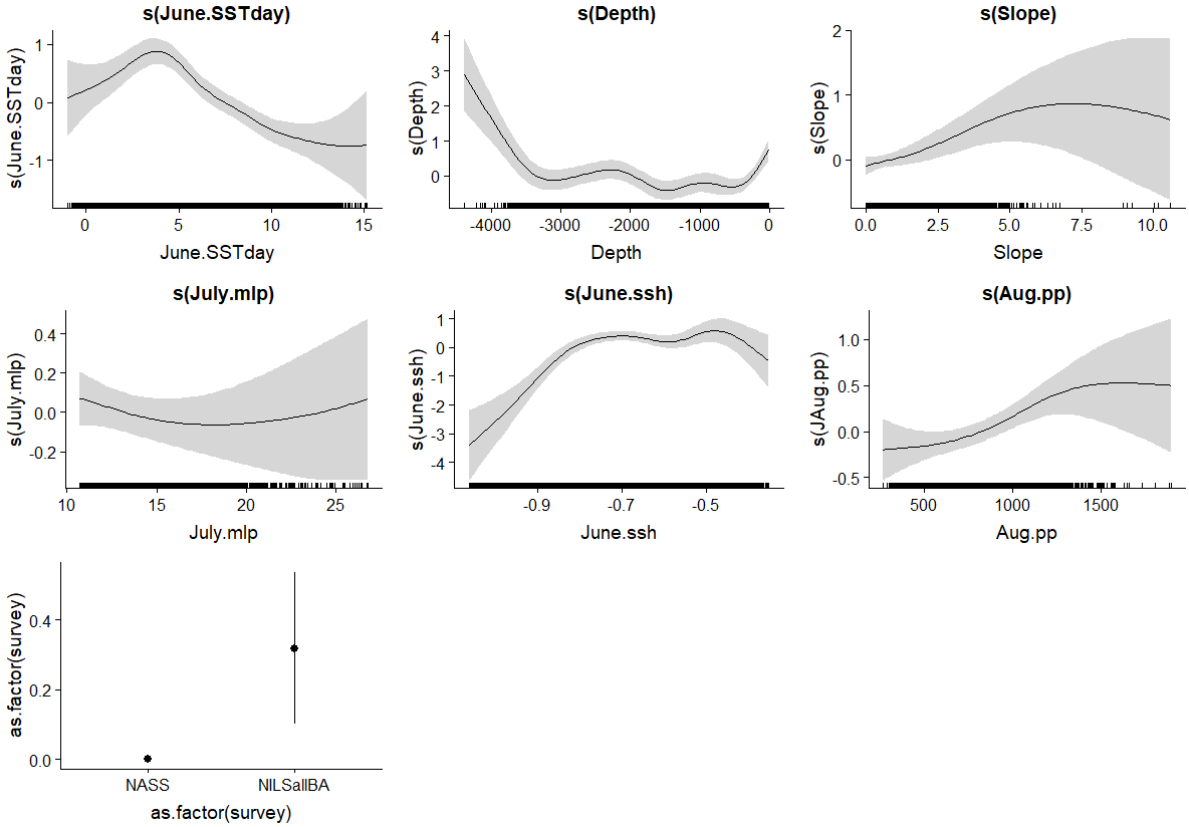

Figure 4.34. Relative density of minke whales as a smooth function of June SST, June SSH, depth, slope, August primary productivity, and July mixed layer depth for 1998-2015. Zero on the vertical axes corresponds to no effect of the covariate on the relative density of minke whales. Shaded areas represent 95% confidence intervals. The scales on each vertical axis vary among plots. Data points are represented as rug plots on the horizontal axes.

Predictions of minke whale density from 1998-2015 are shown in Figure 4.35. The model predicted well the high observed occurrence of minke whales around Iceland, in the North Sea, around the Iceland-Scotland Ridge, around Jan Mayen, along the Mohn Ridge, in the Norwegian Sea, off south-west Svalbard and in the Barents Sea. The CV of the predictions shows high precision for the whole area including the area edges (Figure 4.36).

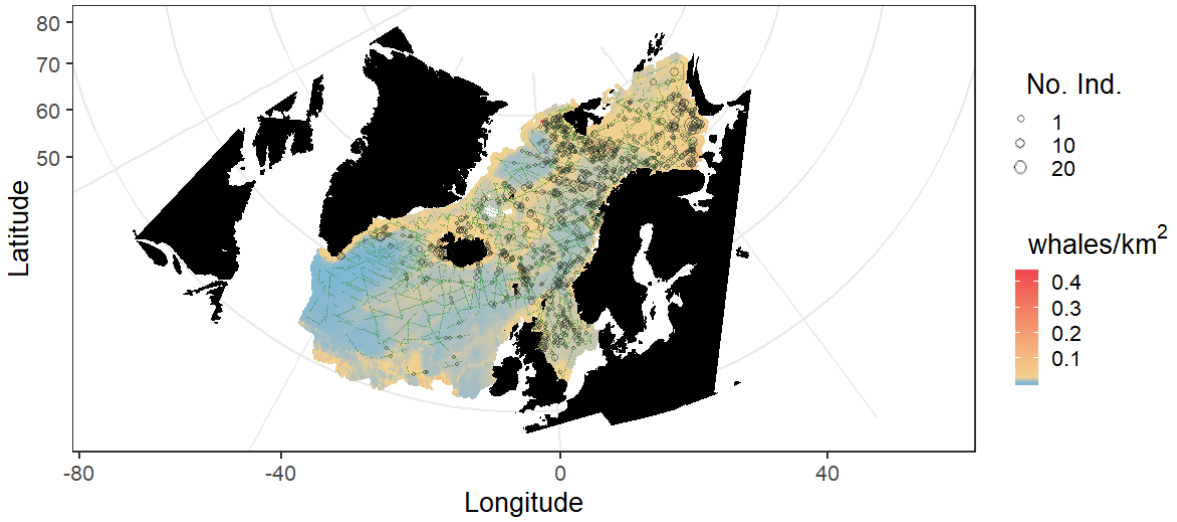

Figure 4.35. Predicted density of minke whales for the best-fitting model for 1998-2015, which included depth, slope, June SST, June SSH, July mixed layer depth, and August primary productivity. The map shows minke whale observations as grey circles, the size of which indicates the number of individuals (No. Ind.), the small green dots represent the effort.

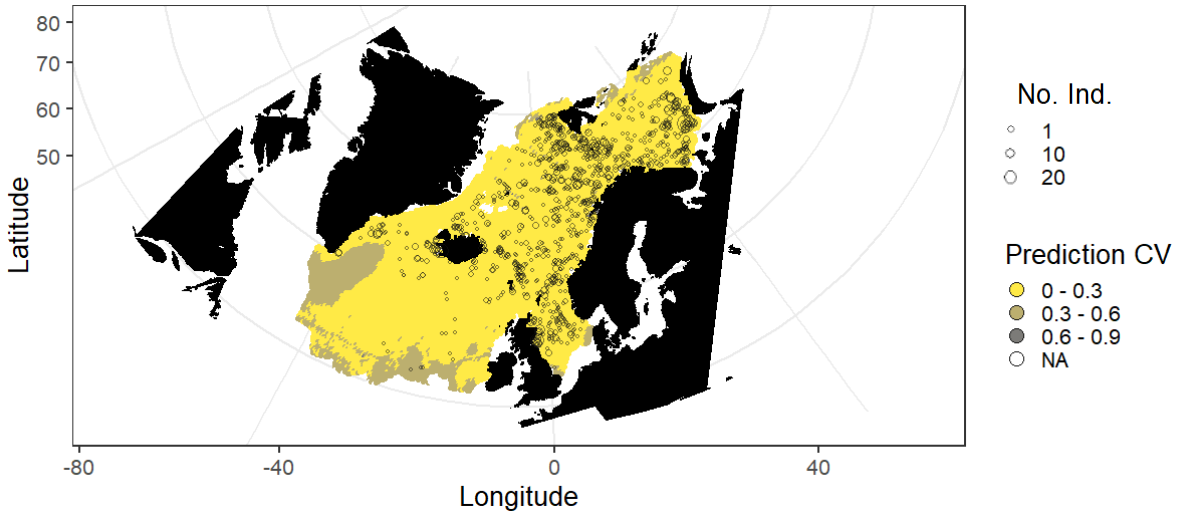

Figure 4.36. Coefficient of variation of the average predicted density of the best-fitting minke whale model for 1998-2015. Yellow areas show the highest precision (higher resolution than other species). Minke whale observations are indicated as grey circles and scaled to the number of individuals (No. Ind.).

4.4 Discussion

4.4.1 Fin whales

Relationships between fin whale density and oceanographic features

Fin whale distribution has previously been globally associated with the continental slope and deep waters (Aguilar and García-Vernet, 2018; Víkingsson et al., 2015, 2009). The relationships

with depth found in this study for both periods (1987-1989 and 1998-2015) show overall a similar pattern of positive effects on fin whale density in deep waters and negative effects in shallower waters. In the more recent period, positive effects were found at depths up to about 500 m compared with approximately 800 m in 1987-1989. Although the relationship between fin whale occurrence and slope has been widely described in the literature (Klinck et al., 2012; Vacquié-Garcia et al., 2017; Víkingsson et al., 2009), here it was only retained in the best model in the earlier period. The differences seen in 1998-2013 of shallower depths and weakened relationship with slope may be related to an increase in distribution into new areas, for example the presence of fin whales in recent surveys in the Barents Sea. In Norway, unlike around Iceland, fin whale occurrence has recently been related to depth and slope but also to shallow waters (Nøttestad et al., 2015; Vacquié-Garcia et al., 2017).

Relationships between fin whale distribution and sea surface water temperatures have already been found in the central and north-eastern North Atlantic (Nøttestad et al., 2015; Víkingsson et al., 2015, 2009). In this study, the best models found a summer relationship: July in 1987-1989 and August in 1998-2015. The effect on fin whale density in both periods was positive for cooler SST (between 4-9 °C and 6-12 °C, respectively) and negative for warmer SST (between 10-12 °C and 12-17 °C, respectively). These results support those found by Víkingsson et al., (2015) in the East Greenland/Iceland area, where the highest probability of encounter was at SST of 5-11 °C and an increase in abundance of fin whales in the East Greenland/Iceland area has been linked to an increase in SST (Figure 4.1). In the Norwegian Sea, however, changes in fin whale occurrence seems to be correlated with low water temperatures (Nøttestad et al., 2015). In this study, the temperatures at which positive and negative effects on fin whale density occur have increased. It is striking that the negative effect in 1987-1989 is at temperatures (10-12 °C) that are within the range of the positive effect in 1998-2015 (12-17 °C). The wider context for this is that ocean warming has been reported across the whole study area (Carr et al., 2017; Moore et al., 2019; Nøttestad et al., 2015; Vacquié-Garcia et al., 2017; Víkingsson et al., 2015). This may explain the expansion in fin whale distribution, where some fin whales occur in the same areas as previously but now also occur more commonly further north, such as in the Barents Sea and west/north of Spitsbergen (Ressler et al., 2015; Vacquié-Garcia et al., 2017). The underlying reason for the link between fin whale distribution/abundance and water temperature is believed to be through an indirect link with their prey (Nøttestad et al., 2015; Ressler et al., 2015; Víkingsson et al., 2015, 2009).

Additional covariates retained in the 1998-2015 best model were August salinity, August SSH and April primary productivity. The signals of salinity in the model are not very clear but overall, there is a negative effect on fin whale density in the less salty waters. This could be indicative of whales being less associated with Artic waters than the saltier waters of the North Atlantic or in areas where both water types occur (fronts) (Moore et al., 2019; Ressler et al., 2015; Skern-Mauritzen et al., 2011; Víkingsson et al., 2015). Although SSH measurements are not very accurate in terms of units and are hence not comparable to those reported by Víkingsson et al., (2015), the general signal is a positive effect on fin whale density when SSH is more negative. This matches the high density of fin whales around the Irminger Sea, an area with the strongest negative SSH anomaly (Hátún et al., 2009). But due to the poor quality of the SSH values predicted by the Copernicus model and the lack of SSH values in 1987-1989 is not possible to discuss further, for example, the recent increase in SSH in the Irminger Sea (Häkkinen et al., 2013; Hátún et al., 2009; Våge et al., 2009). Regarding the spring signal in primary productivity, fin whales in the study area have a preference for prey lower in the food web (krill) (Aguilar and García-Vernet, 2018; Nøttestad et al., 2014; Ressler et al., 2015; Sigurjónsson and Víkingsson, 1997; Víkingsson, 1997) and thus any relationship with primary productivity would be expected to have little lag. However, in this area, Friedland et al. (2016) and Waniek and Holliday (2006) have described both spring and summer phytoplankton blooms with variation in occurrence by year and area but in general in May (spring) and July (summer). Friedland et al. (2016) also found links with the duration of the bloom and copepods presence, where long lasting blooms may result from reduce grazing. The best model here shows a positive effect on whale density when primary productivity is either very low or very high. This relationship may result from spatial and temporal variability in productivity but may simply reflect the complexities in how primary productivity links to different trophic levels.

Changes in fin whale distribution

Predictions from the models in the two periods (Figure 4.9, Figure 4.10, Figure 4.13 and Figure 4.14) show that fin whale distribution in the overall area has expanded and that densities appear to be higher in the recent period. Such an expansion in distribution has been already described

in Icelandic and Norwegian waters; around Iceland/East Greenland whales are more broadly distributed in deeper waters while around Norway they are more commonly recorded in higher latitudes (Ressler et al., 2015; Skern-Mauritzen et al., 2011; Vacquié-Garcia et al., 2017; Víkingsson et al., 2015). Here this expansion was found over the whole study area and over a 30-year period including, as mentioned above, into the Barents Sea and west of Svalbard.

There seem to be two main drivers of the expansion in distribution: increasing densities and warming oceans. Fin whales were heavily exploited by whaling until the 1980s but abundance estimates and population models show that they have recovered in the North Atlantic (NAMMCO, 2019d, 2019a; Øien, 2009; Pike et al., 2020a, 2019b; Reilly et al., 2008b). Increases in densities do not seem to be linked with movement from southern areas, where estimates of abundance in 2007 and 2016 are very similar (Hammond et al., 2017, 2009). The increases in fin whale density in the study area is reflected in the model predictions here. Discussion above regarding the relationships between fin whale densities and SST concludes that warming waters are making available new areas for fin whales but also that whales are remaining in areas where they traditionally have been seen and where the oceanography is changing. For example, in the Iceland/East Greenland area, waters are warming and the ecosystem is changing but fin whale numbers are increasing (Astthorsson et al., 2012; Silva et al., 2014; Víkingsson et al., 2015).

Water temperature is not expected directly to influence fin whales but to have an indirect link through their prey. The main prey in the area is krill but fin whales globally are known to be generalists (Aguilar and García-Vernet, 2018). Krill has decreased in some areas, which has been also linked with oceanographic changes including in water temperature. In Icelandic and Norwegian waters, it seems that in the earlier years fin whales had a high preference for krill, but in the changing environment there may be a switch towards fish if krill is not available (Nøttestad et al., 2014; Melle et al., 2004 In: Øien, 2009; Ressler et al., 2015; Víkingsson et al., 2015). In the study area, fin whales seem to prefer krill and calanoids if available; an extreme case is at the Barents Sea where whales have been observed to compete with capelin to forage krill by arriving first to krill areas (Ressler et al., 2015). Lack of data impedes understanding prey switching in the area (Víkingsson et al., 2015). In any case, it is challenging to understand the mechanisms linking fin whale densities and prey in order to explain their distribution and changes over time. The results here show changes over the whole study area over the last 30 years and SST seems to be an important driver but the links between fin whales, their prey and oceanography are still poorly known.

4.4.2 Humpback whales

Relationships between humpback whale density and oceanographic features

Humpback whales have been traditionally associated with coastal and shallow waters in their feeding and breeding grounds, but they also occur in deeper waters including during migration (Clapham, 2018; Jefferson et al., 1993). In the early (1987-1989) and recent (1998-2015) models developed here, the positive relationship found with depth seems to follow the same pattern previously described, with positive effects on humpback whale density in shallower waters, in this case 1000 m depth or less (Figure 4.23). This relationship seems weaker in the early model (Figure 4.19), but this may be due to the higher number of sightings in the Norwegian Sea in earlier years compared to the recent period (Figure 4.20 and Figure 4.24). The effect of aspect on humpback whale density is not commonly mention in literature; here the early and recent models showed a positive effect in waters facing west/southwest (Figure 4.19 and Figure 4.23). Humpback whale is the only species in this study that presented a consistent relationship with aspect over the study period. Angles facing west/southwest could be linked to areas with the presence of warmer Atlantic water versus waters of polar origin (Figure 1.2). Higher humpback whale densities occur in these areas and this relationship has been maintained through the 30 years of this study. Depth and aspect are unlikely to be direct drivers of humpback whale distribution but are more likely indirectly linked with their prey as described below for the other covariates studied.

Regarding the relationship between humpback whale density and SST, indirect links with prey are again expected, especially for this study that focuses on summer distribution in high latitude productive areas. Because humpback whales have a more coastal distribution (Clapham, 2018; Jefferson et al., 1993) the relationship with SST is expected to be tighter than for other species with more offshore distributions such as fin whales (Aguilar and García-Vernet, 2018). Although positive effects on humpback whale density have been found at different temperature ranges depending on the area (e.g. Calambokidis et al., 2004; Dalla Rosa et al., 2012), in the study area (Iceland-Faroes) positive effects on distribution were limited to a maximum temperature of 8 ˚C (Neyman, 2018; Paxton et al., 2009). Although the lagged month selected in both the early (1987-1989) and recent (1998-2015) models was different, May and June, respectively, the temperature ranges of the positive effects were very similar; 0-7 ˚C in the early model (Figure 4.19) and below 8 ˚C in the recent model (Figure 4.23). These ranges are similar to those found

in other modelling exercises that included only Icelandic-Faroes data (Neyman, 2018; Paxton et al., 2009). These conserved temperature relationships are perhaps surprising because humpback whales are suggested to be very adaptable (Clapham, 2018; Moore et al., 2019; Reilly et al., 2008a), and this adaptability has been suggested as one of the reasons for the recovery from whaling (Reilly et al., 2008a). These relationships found in summer suggest that for the whole study area, humpback whales and SST (hence indirectly their prey) have a tight relationship which has not changed over the 30 years studied however, there have been some changes in the oceanography and prey species in the area (e.g. Alheit et al., 2014; Astthorsson et al., 2012; Nøttestad et al., 2015; Silva et al., 2014; Sundby et al., 2016; Valdimarsson et al., 2012; Víkingsson et al., 2015).

Other covariates selected in the best model for recent years were August SSH, August salinity, July mlp, April chlorophyll *a*, and August primary productivity. Almost all the covariates selected have relationships with summer months except for April chlorophyll *a*. Normally, only one biological covariate was retained/kept in the best model because of colinearity/concurvity but August primary productivity was retained because it did not show these features. One hypothesis supporting the inclusion of both covariates in the best model is the occurrence of multiple blooms of primary productivity in the study area. While there are seasonal blooms such as spring or summer blooms (e.g. Waniek and Holliday, 2006), there could also be multi-seasonal blooms (Friedland et al., 2016). Thus, the density of whales could relate both to the seasonal blooms and the multi-seasonal blooms, which are linked with humpback whale prey. However, we do not know if the different bloom types are related to different prey types. Although fish seem to be an important part of the diet in the area (Magnúsdóttir et al., 2014; NAMMCO, 2019a; Nøttestad et al., 2014; Pike et al., 2019b; Ryan et al., 2015), krill is also consumed (Christensen et al., 1992; Ressler et al., 2015; Víkingsson et al., 2015). Hence, the retention of both variables in the best model could suggest humpback whales are broadly generalist.

Changes in humpback whale distribution

The abundance of humpback whales has increased in the study area from the 1980s to the present, although the increase started even earlier in some areas (NAMMCO, 2019a; Øien, 2009; Pike et al., 2009a; Sigurjónsson and Gunnlaugsson, 1990), possibly due to recovery from whaling pressure (Reilly et al., 2008a). A similar pattern of higher densities in the recent model compared to the early model was found (Figure 4.20 and Figure 4.24) as to estimates of abundance (Øien,

2009; Pike et al., 2019b). There have been also changes in distribution and seasonality of humpback whales over the whole study area; whales are now frequently seen further north than before (Skern-Mauritzen et al., 2011; Vacquié-Garcia et al., 2017; Víkingsson et al., 2015), closer to East Greenland (Hansen et al., 2018), and present in winter (Magnúsdóttir et al., 2014; Rikardsen, 2020). The model predictions also show these changes in distribution when comparing the early and the recent models (Figure 4.20 and Figure 4.24); precision is best where there are observations but weaker around the edges (Figure 4.21 and Figure 4.25). The main changes in distribution predicted here support other studies. Around Iceland in the earlier years higher densities were predicted towards the south but higher densities of whale are now more to the north and north-east of Iceland (Víkingsson et al., 2015). Although with low precision, high densities are now predicted in East Greenland (West Iceland). Hansen et al. (2018) have also estimated higher abundance of humpback whales in that area recently. Sightings and predicted density of humpback whales now occur in the Barents Sea, showing that animals are occurring more frequently in northern latitudes due to changes in the ice coverage (Skern-Mauritzen et al., 2011).

Overall, the models appear to have captured a common pattern in humpback whale abundance/density and distribution in the central and north-eastern North Atlantic during the study period. Considering only relief related variables and SST over the 30-year period, the general relationships between humpback whale density and these covariates did not change but because waters have generally warmed (e.g. Alexander et al., 2014; Carr et al., 2017; Havforskningsinstituttet, 2020) new areas which were previously unavailable have become available (Skern-Mauritzen et al., 2011; Vacquié-Garcia et al., 2017). As the recent models indicate, whales are now found further north than before, presumably because prey are now available in these areas.

4.4.3 Minke whales

Relationships between minke whale density and oceanographic features

In the central and north-eastern North Atlantic minke whales are mainly distributed in coastal waters but area also found in offshore waters (e.g. Pampoulie et al., 2013; Pike et al., 2009a; Skern-Mauritzen et al., 2011; Storrie et al., 2018; Vacquié-Garcia et al., 2017; Víkingsson et al., 2014). Both the early (1987-1989) and recent (1998-2015) models predict higher minke whale

density of shallow waters ≤300 m and deep waters greater than 3500 m (Figure 4.30 and Figure 4.34). The relationships between minke whale density and depth have not changed much over time. As it has been repeatedly mentioned, the links between bathymetry and minke whales in the summer (essential for the net energy gain of the whales) are expected to be an indirect linked with the whales' prey. For example, changes at the ecosystem level in the Icelandic continental shelf (Astthorsson et al., 2012; Pálsson et al., 2012; Valdimarsson et al., 2012) are consistent with changes in minke whale prey composition (Víkingsson et al., 2015). These examples show that even though the relation with depth is broadly kept (see below in distribution), there has been oceanographical changes in the area and minke whales seem to have change part of their diet.

Minke whale occurrence in the study area has been related to a broad range of temperatures (Anderwald et al., 2012; Storrie et al., 2018). Here, June SST was selected in both early and recent models but the positive effects on minke whale density were found at SSTs 5-9°C in the early model and 1-6 °C in the recent model, while the overall temperature ranged 0-15°C for both models. Negative effects on density occurred when SST were ≤3 °C or ≥11 °C in the early model and SST warmer than 6 °C in the recent model (Figure 4.30 and Figure 4.34). That minke whales are associated with cooler waters now than previously but that in general the area seems to be warming (e.g. Astthorsson et al., 2012; Havforskningsinstituttet, 2020; Moore et al., 2019; Valdimarsson et al., 2012) and the species is believed to be expanding its range given the new available habitat (e.g. Hansen et al., 2018; Storrie et al., 2018) appears contradictory. Recent predictions show higher densities at the 'cold' edges of the area than in the earlier model, and precision was not lower than when compared with the early model (Figure 4.32 and Figure 4.36). One hypothesis is that these new areas are close to polar currents and ice edges where melting glaciers and Artic sea ice are present, so the SST is lower than previously used areas (in the 1980s). Other studies have also found minke whales in these 'cold' edge areas off East Greenland and Northwest Svalbard (Hansen et al., 2018; Storrie et al., 2018). There are no recent sightings in the modelled dataset but there are high predicted densities and low CVs in these areas, suggesting that the models are nevertheless capturing the difference between periods and warming of the ocean is not the driving the change in distribution.

Other covariates retained in the best recent model were June SSH, July mlp, and August primary productivity, all summer relationships (Figure 4.30 and Figure 4.34). Among the baleen whales studied, minke whales seem to have the most diverse diet in the area, from krill to gadoid fish (Haug et al., 2002; Nøttestad et al., 2015; Pampoulie et al., 2013; Sigurjónsson et al., 2000; Sigurjónsson and Víkingsson, 1997; Skern-Mauritzen et al., 2011). It might therefore be expected that some of the relationships between minke whales and the dynamic covariates would be more lagged than those of other baleen whales that mainly prey on krill. The relationships between minke whales and the dynamic variables do occur earlier in the summer than the other two species studied, but all still showed summer relationships (Figure 4.12, Figure 4.23 and Figure 4.34).

SSH and mixed layer depth (mlp) are indicative of water masses and may thus indicate prey aggregations (e.g. Hansen et al., 2010; Leterme and Pingree, 2008; Víkingsson et al., 2015). The clearest signal in the effect of SSH on minke whale density was the negative effect in the most depressed waters of -0.9 m or more (Figure 4.34). Such values are usually associated with cyclonic circulation (Leterme and Pingree, 2008) and in the study area the Irminger Sea presents the strongest negative SSH where minke whales are not very commonly seen or present (Víkingsson et al., 2015, 2014). The broad range of effects of SSH in minke whale density could be due to diverse conditions. Minke whales are found in the summer including the Norwegian Sea where anticyclonic eddies are known to be form, and the polar front along the northern Barents Sea, among others (e.g. Nøttestad et al., 2015; Skern-Mauritzen et al., 2011). Mixed layer depth did not show a clear signal. Primary productivity in August had positive effects on minke whale density at concentrations around 1200 mg C m^{-2} day^{-1}, these are high concentrations of primary productivity and it makes sense that summer productivity had a positive effect on minke whale occurrence in the area. It is expected that baleen whales do not have much lag in the dynamic covariates selected in the best model, as they usually prey upon krill or fish species that directly prey on krill (e.g. Magnúsdóttir et al., 2014; Nøttestad et al., 2015; Pampoulie et al., 2013; Skern-Mauritzen et al., 2011; Víkingsson et al., 2015). Overall, despite minke whales having a more diverse diet, summer production and accumulation appear to have a stronger effect than the seasonal progression. If prey availability and composition is changing as it has been suggested in the whole study area including Icelandic waters (Moore et al., 2019; Víkingsson et al., 2015), and feeding in the summer time is essential, it is expected that minke whales are becoming less selective in their habitat selection as it was observed in the model smooths.

Changes in minke whale distribution

There have been changes in densities in some areas, for example a decrease in Southeast Iceland (Figure 4.31 and Figure 4.35), the overall abundances and trends estimated by the different countries in the studied area seem to not have change. Although there is a decrease of minke whale abundance in Icelandic coastal waters (Figure 4.2) (NAMMCO, 2019a), there seem to be an increase in the 'CM' management area that corresponds to North Iceland/Jan Mayen (NAMMCO, 2018; Pike et al., 2019b) and possibly in East Greenland (Hansen et al., 2018). It is unknown if minke whales "missing" in South Iceland are now distributed in North Iceland/Jan Mayen and East Greenland, but the overall densities for the whole area suggest that this may be the case. Minke whale distribution has changed over time; in general animals have a broader distribution in the study area, but less in South Iceland. One link with the distribution could be given by some changes in the relationship of minke whales with depth. In the recent models there is a less restricted negative effects (in recent 400-1500 m vs in early model 400-3500 m) (Figure 4.34) that match the wider spread distribution more recently found (Figure 4.35). This wider distribution matches the increased densities in the northern part of the Iceland/Jan Mayen area which has been seen and suggested in the most recent surveys (NAMMCO, 2018; Víkingsson et al., 2015). Also striking is the broader distribution area especially in the Barents Sea, and at the other 'colder' edges of the study area around East Greenland (Figure 4.31 and Figure 4.35). The increases in abundance and occurrence in new areas are likely linked indirectly with prey availability and composition (Hansen et al., 2018; Moore et al., 2019; NAMMCO, 2018; Ressler et al., 2015; Skern-Mauritzen et al., 2011; Storrie et al., 2018; Víkingsson et al., 2015).

4.5 Comparison among species

The relation between density and depth was different between the species, but there were also areas of overlap among them. In general, fin whales were positively related with deep waters, minke whales with deep waters >3500 m but also with shallow waters ≤300 m, and humpback whales weakly with shallow waters (Figure 4.8, Figure 4.12, Figure 4.19, Figure 4.23, Figure 4.30 and Figure 4.34). Relationships with depth did not substantially change over time for any of the species between the early and recent periods. There was an overall tendency for high SST to have negative effects on density; this effect started at 6 to 12 °C depending on the species. There were also negative effects on density at the coldest temperatures close to 0 °C. However, there were differences between species in their relationships with temperature. In fin whales, the

relationship with SST changed over time; the strongest effect remained in waters at the colder end of the range of SST but at a warmer temperature in the recent period. Density was predicted to be higher in the Irminger Sea, where water warming has been described (e.g. Víkingsson et al., 2015). In contrast, the change in the relationship between minke whales and SST was for colder waters to have a more positive effect in the recent period, with a stronger effect in Norwegian waters. For humpback whales, the relationship with SST did not change over time.

Generally, all the dynamic environmental variables considered showed summer relationships, confirming the hypothesis that the lag between density and these variables is shorter for species that feed lower in the trophic web. However, there were some spring signals for chlorophyll *a* and primary productivity which could be related to different bloom types (Friedland et al., 2016; Waniek and Holliday, 2006) and the type of prey the animals were feeding on (e.g. Christensen et al., 1992; Heide-Jørgensen and Laidre, 2007; Nøttestad et al., 2015; Pampoulie et al., 2013; Ressler et al., 2015; Sigurjónsson and Víkingsson, 1997; Skern-Mauritzen et al., 2011; Víkingsson, 1997; Víkingsson et al., 2015, 2014; Windsland et al., 2007).

There were some areas of overlap in predicted distribution among the species, as expected given the similarity in some of the relationships between density and the environmental covariates. In general, in the recent period, all species showed higher density in more northerly areas including in the Barents Sea and north of Iceland; however, an exception is the predicted increase in density of fin whales in the Irminger Sea (Figure 4.9, Figure 4.13, Figure 4.20, Figure 4.24, Figure 4.31 and Figure 4.35). Predictions of high density in some northerly areas were not underpinned by observations but other studies in those areas have described the presence of the whales there (e.g. Hansen et al., 2018; Storrie et al., 2018). These extra surveys plus the relatively high precision of the predicted density (Figure 4.10, Figure 4.14, Figure 4.21, Figure 4.25, Figure 4.32 and Figure 4.36) support our findings suggesting changes in baleen whale distribution toward these northerly areas, especially for minke and humpback whales. Minke whale density seems to have changed in some areas, such as a decrease south of Iceland and an increase to the north (NAMMCO, 2019a, 2018; Pike et al., 2019b) (Figure 4.31 and Figure 4.35).

Overall, baleen whales have shown changes in distribution and density over time, which may be linked to oceanographical changes in the area that are indirectly linked to the whales' prey. The relationships between whale density and the environmental covariates have species-specific differences but there are general similarities that may be due to the ecology of the species, such as foraging and life history (e.g. Aguilar and García-Vernet, 2018; Clapham, 2018; Moore et al.,

2019; Perrin et al., 2018; Víkingsson et al., 2015). These are expected for species that have similar feeding strategies and are described as opportunistic feeders, although with different 'preferred' prey (e.g. Christensen et al., 1992; Heide-Jørgensen and Laidre, 2007; Nøttestad et al., 2015; Pampoulie et al., 2013; Ressler et al., 2015; Sigurjónsson and Víkingsson, 1997; Skern-Mauritzen et al., 2011; Víkingsson, 1997; Víkingsson et al., 2015, 2014; Windsland et al., 2007).

4.6 Appendix

4.6.1 All species

4.6.1.1 Distance sampling

Appendix 4-A. HR= hazard-rate, HN= Half-normal. p = average probability of detection, No. obs= number of observations, SE= standard error, Goodness of fit= Cramer-von Mises

Species	Truncation	Key function	Covariates	No. obs	*p*	SE	Goodness of fit (p-value)	AIC	Survey & Period
Fin whale	3800	HR	~ vessel ID	2073	0.482	0.014	0.280	33269.768	NASS 1987-2015
		HN	~ vessel ID		0.520	0.008	9.89E-05	33303.702	
		HR	**~ vessel ID + beaufort(3)**		**0.014**	**0.014**	**0.273**	**33261.796**	
		HN	~ vessel ID + beaufort(3)		0.008	0.008	0.0002	33290.531	
Humpback whale	3300	**HR**	**~1**	**731**	**0.535**	**0.027**	**0.452**	**11606.976**	NASS 1987-2015
		HN	~1		0.563	0.016	0.059	11611.091	
		HR	~ beaufort(3)		0.507	0.028	0.615	11606.486	
		HN	~ beaufort(3)		0.563	0.016	0.054	11616.087	
Minke whale	1500	HR	~ vessel ID	898	0.238	0.015	0.476	12276.862	NASS 1987-2015
		HN	~ vessel ID		0.410	0.008	0.002	12436.415	
		HR	**~ vessel ID + beaufort(3)**		**0.238**	**0.015**	**0.404**	**12262.426**	
		HN	~ vessel ID + beaufort(3)		0.402	0.008	0.001	12413.436	
Fin whale	2500	HR	~1	147	0.572	0.041	0.985	2236.282	NILS 1987-1989
		HN	**~1**		**0.508**	**0.033**	**0.931**	**2234.892**	
Fin whale	3200	HR	~ beaufort(3)	1106	0.414	0.015	0.817	17104.79	NILS 1995-2013
		HN	~ beaufort(3)		0.450	0.009	0.001	17129.267	
		HR	**~ vessel ID + beaufort(3)**		**0.410**	**0.015**	**0.845**	**17101.976**	
		HN	~ vessel ID + beaufort(3)		0.449	0.009	0.001	17128.596	
Humpback whale	2500	HR	~1	39	0.427	0.082	0.983	589.337	NILS 1987-1989
		HN	~1		0.462	0.050	0.814	588.804	
Humpback whale	3500	HR	~ beaufort	695	0.441	0.017	0.829	10846.422	NILS 1995-2013
		HN	~ beaufort		0.438	0.011	0.061	10866.501	
		HR	~ vessel ID		**0.441**	**0.017**	**0.887**	**10839.302**	

		HN	~ vessel ID		0.433	0.011	0.090	10857.355	
Minke whale	1000	HR	~1	999	0.493	0.021	0.224	13363.467	NILS 1987-1989
		HN	~1		0.523	0.012	0.001	13374.503	
		HR	**~ vessel ID**		**0.489**	**0.020**	**0.249**	**13341.283**	
		HN	~ vessel ID		0.516	0.012	0.516	13353.412	
Minke whale	1500	HR	~ beaufort	3551	0.444	0.007	0.170	49036.684	NILS 1995-2013
		HN	~ beaufort		0.407	0.005	0.183	49053.992	
		HR	**~ beaufort + vessel ID**		**0.442**	**0.007**	**0.202**	**49017.155**	
		HN	~ beaufort + vessel ID		0.406	0.005	0.145	49043.52	

4.6.1.2 Modelling

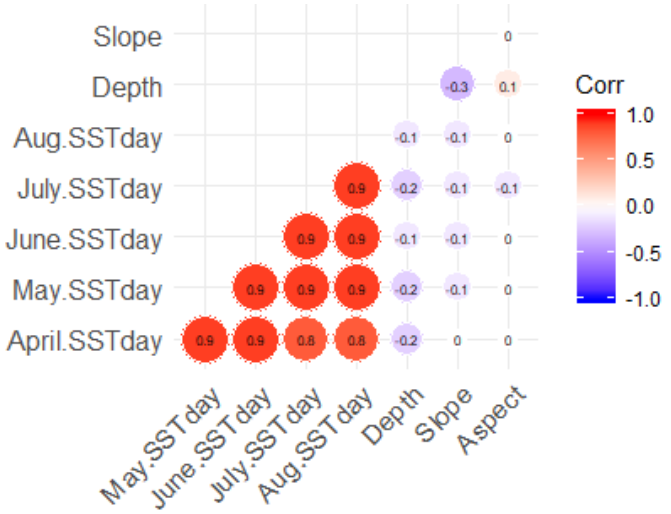

Appendix 4-B. Correlation matrix for fin, humpback, and minke whales 1987-1989 models.

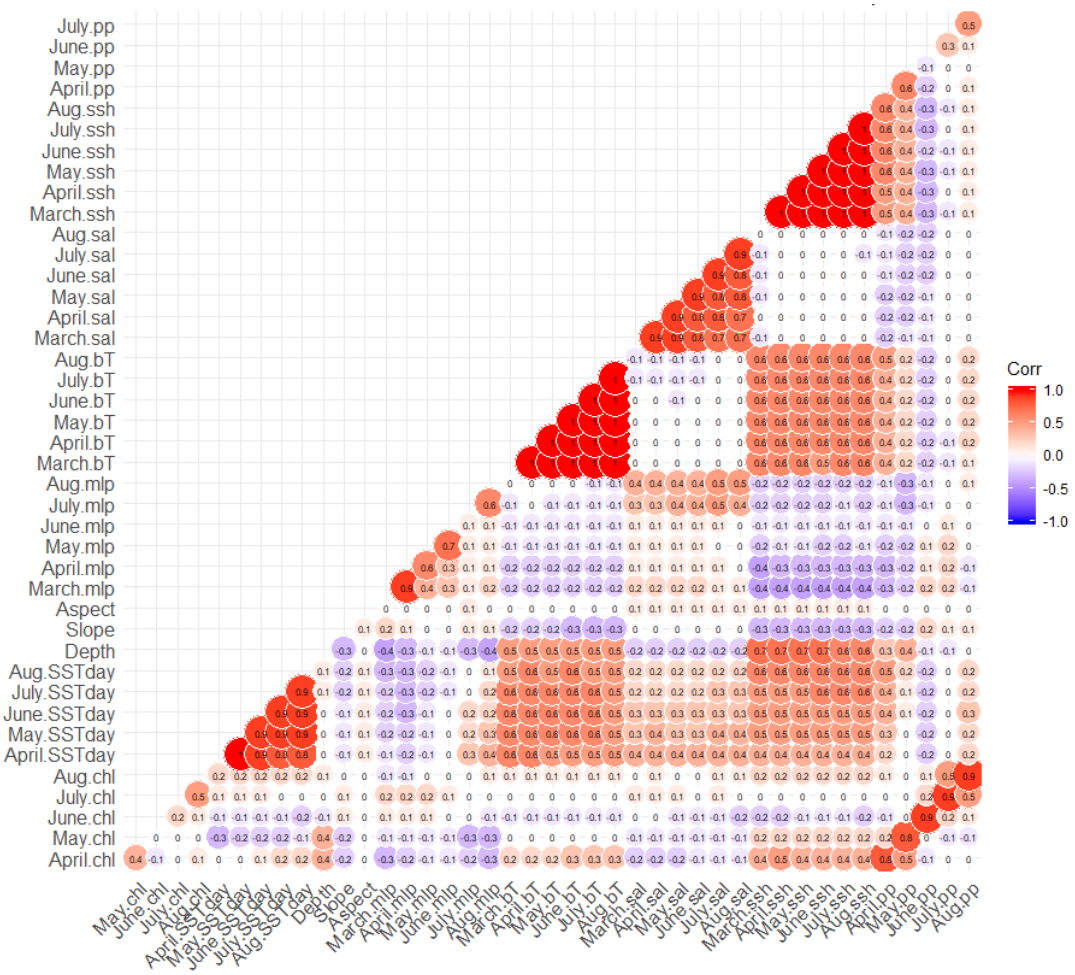

Appendix 4-C. Correlation matrix for fin, humpback, and minke whales 1998-2015 models.

4.6.2 Fin whales

4.6.2.1 Distance sampling

Appendix 4-D. ESW, effective strip width for the NASS 1987-2015 fin whales at all covariate/level combination. Levels of the covariate vessel relate to the abbreviation of the vessel's name. Covariate Beaufort has three levels: high (H), medium (M) and low (L).

Vessel (ID)	Beaufort	ESW (m)	Vessel (ID)	Beaufort	ESW (m)
A	H	1971.29	I	H	2410.65
A	L	2428.09	I	L	2879.16
A	M	2120.78	I	M	2569.27
B	H	1388.26	J	H	1778.22
B	L	1766.86	J	L	2216.13
B	M	1508.34	J	M	1919.86
F	H	1586.94	K	H	1859.91
F	L	1999.05	K	L	2306.73
F	M	1718.88	K	M	2005.13
G	H	2121.68	S	H	1605.26
G	L	2587.72	S	L	2020.12
G	M	2275.78	S	M	1738.21
H	H	1283.88	V	H	758.89
H	L	1642.37	V	L	993.26
H	M	1397.07	V	M	831.51

Appendix 4-E. ESW, effective strip width for the NILS 1995-2013 fin whales at the available covariate/level combination. The covariate vessel ID relates to the vessel's grouping explained in Chapter 2. Covariate Beaufort has three levels: high (H), medium (M) and low (L).

Vessel (ID)	Beaufort	ESW (m)
2	H	1386.21
2	L	1358.77
2	M	1078.20
3	H	1714.35
3	L	1683.03
3	M	1355.15
4	H	1425.44
4	L	1397.47
4	M	1110.68

4.6.2.2 Modelling

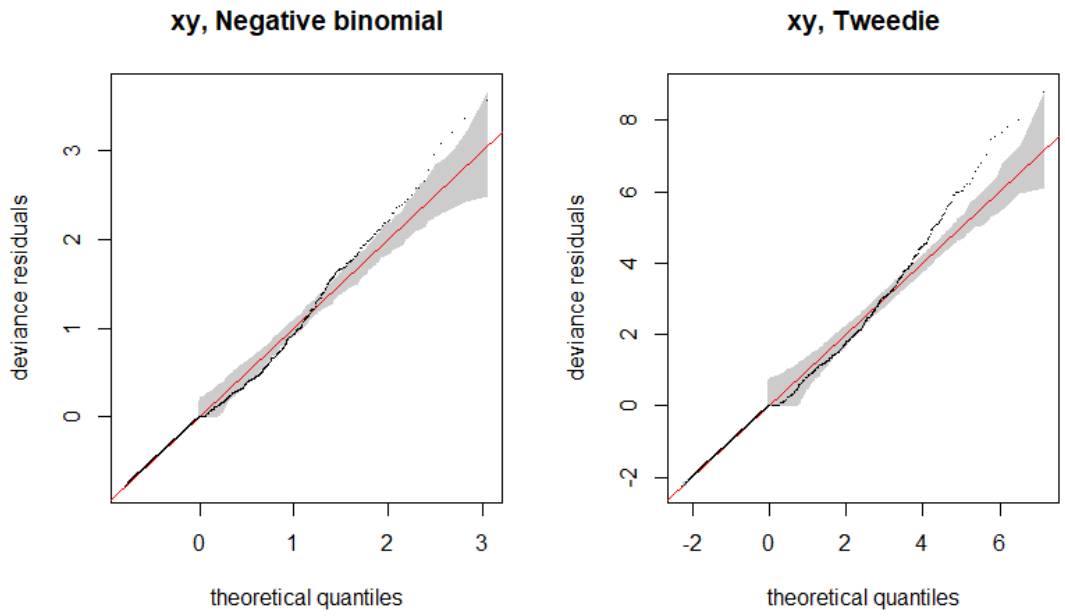

Appendix 4-F. Q-Q plots for error distribution selection for fin whale 1987-1989 models. Spatial models (xy) for negative binomial and tweedie distributions. The shaded area represents 95 % confidence interval, the circles represent the data, the line is the expected data distribution if the data fits precisely the model.

Appendix 4-G. Single model variables fitted models for fin whales 1987-1989 using double penalization. The best error structure for all models was the negative binomial distribution.

Model	Deviance	Deviance explained (%)	AIC	REML	n
Depth	1104.60	20.34	4003.28	2013.28	6697
May.SSTday	1109.10	11.73	4117.67	2069.21	
July.SSTday	1124.33	11.28	4121.52	2071.08	
June.SSTday	1103.33	9.86	4140.28	2078.97	
Aug.SSTday	1103.03	8.74	4151.62	2081.45	
Slope	1100.98	8.14	4156.93	2083.13	
April.SSTday	1105.92	6.93	4173.70	2094.39	
Aspect	1088.42	2.89	4210.88	2104.79	

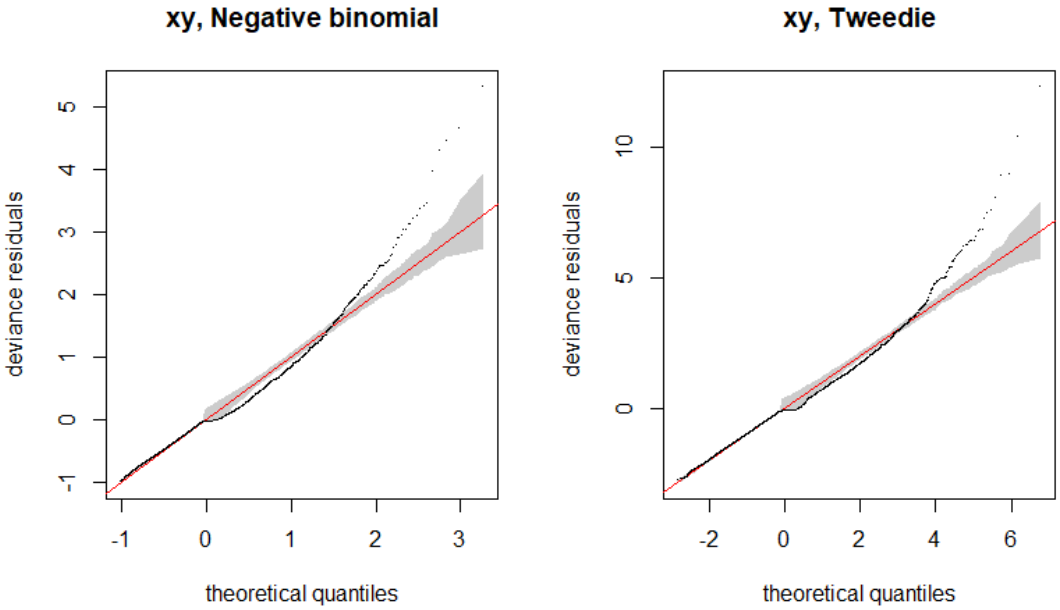

Appendix 4-H. Q-Q plots for error distribution selection for fin whale 1998-2015 models. Spatial models (xy) for negative binomial and tweedie distributions. The shaded area represents 95 % confidence interval, the circles represent the data, the line is the expected data distribution if the data fits precisely the model.

Appendix 4-I. Single model variables fitted models for fin whales 1998-2015 using double penalization. The best error structure for all models was the negative binomial distribution. The best covariate by each variable family is in bold letters.

Model: Survey +	Deviance	Deviance explained (%)	AIC	REML	n
July.bT	2030.68	20.13	6729.14	3372.60	7361
June.bT	2030.72	20.14	6729.39	3372.69	
Aug.bT	2024.18	20.09	6729.93	3373.09	
Aug.SSTday	2007.62	20.12	6732.86	3375.81	
Aug.ssh	2035.78	19.98	6736.59	3378.36	
May.bT	2036.14	19.75	6739.83	3377.97	
May.SSTday	2028.18	19.81	6742.00	3380.81	
July.SSTday	1996.77	19.55	6746.15	3380.55	
June.ssh	2027.65	19.52	6748.02	3383.44	
July.ssh	2023.45	19.42	6750.31	3383.44	
June.SSTday	1999.53	18.96	6762.35	3390.85	
April.bT	2033.77	18.75	6763.89	3388.94	
Depth	2037.02	18.90	6765.48	3394.12	
May.ssh	2029.27	18.78	6766.84	3393.23	
April.ssh	2035.41	18.27	6778.72	3397.81	
April.SSTday	2048.01	17.64	6794.35	3405.22	
April.pp	2053.25	17.30	6803.30	3408.72	
Slope	2010.26	16.88	6813.66	3416.84	
Aug.sal	2057.73	16.73	6816.91	3420.44	
April.chl	2053.98	16.18	6830.99	3425.99	
June.pp	2039.87	16.15	6832.71	3427.00	
April.sal	2052.87	15.26	6850.02	3433.22	
July.sal	2043.08	15.35	6850.26	3436.14	

Aug.pp	2040.38	14.98	6852.39	3429.76	
April.mlp	2038.64	15.04	6855.11	3433.07	
May.pp	2046.21	14.73	6857.22	3430.63	
May.sal	2046.92	14.92	6859.29	3437.49	
Aug.chl	2042.27	14.84	6859.70	3436.01	
July.pp	2024.67	14.92	6860.00	3437.47	
June.sal	2043.80	14.90	6860.89	3440.81	
May.chl	2039.63	14.63	6864.67	3436.84	
June.mlp	2020.59	13.98	6873.92	3441.96	
June.chl	2033.71	14.02	6877.91	3443.12	
May.mlp	2031.59	13.32	6890.79	3448.55	
July.mlp	2031.84	13.18	6891.46	3446.69	
Aug.mlp	2041.80	13.39	6891.80	3449.44	
July.chl	2028.40	13.34	6893.54	3450.75	
Aspect	2034.23	12.25	6907.74	3454.29	

Appendix 4-J. Concurvity values for fin whales 1998-2015 variables in remaining full model after double penalization. Key pairs evaluated are highlighted within coloured squares.

$`worst`

	para	s(Aug.SSTday)	s(Aug.ssh)	s(Aspect)	s(July.bT)	s(Depth)	s(April.pp)	s(April.chl)	s(Aug.sal)
para	1.000000e+00	7.303847e-28	2.297264e-28	7.876014e-32	1.385255e-28	3.228737e-27	8.519614e-28	1.273271e-27	3.079595e-28
s(Aug.SSTday)	5.782470e-28	1.000000e+00	4.968258e-01	2.667823e-02	4.162021e-01	1.960443e-01	3.081053e-01	2.411917e-01	2.213516e-01
s(Aug.ssh)	1.131681e-28	4.968258e-01	1.000000e+00	5.691339e-02	7.047259e-01	5.379606e-01	4.209481e-01	3.755870e-01	1.536271e-01
s(Aspect)	5.579415e-32	2.667823e-02	5.691339e-02	1.000000e+00	4.438432e-02	4.613535e-02	1.902103e-02	1.452810e-02	1.253567e-02
s(July.bT)	2.211615e-28	4.162021e-01	7.047259e-01	4.438432e-02	1.000000e+00	6.298698e-01	2.908233e-01	2.540409e-01	9.320278e-02
s(Depth)	4.083100e-27	1.960443e-01	5.379606e-01	4.613535e-02	6.298698e-01	1.000000e+00	2.998316e-01	3.405314e-01	1.247481e-01
s(April.pp)	7.662302e-28	3.081053e-01	4.209481e-01	1.902103e-02	2.908233e-01	2.998316e-01	1.000000e+00	9.153296e-01	8.630795e-02
s(April.chl)	1.291586e-27	2.411917e-01	3.755870e-01	1.452810e-02	2.540409e-01	3.405314e-01	9.153296e-01	1.000000e+00	1.031072e-01
s(Aug.sal)	3.661416e-28	2.213516e-01	1.536271e-01	1.253567e-02	9.320278e-02	1.247481e-01	8.630795e-02	1.031072e-01	1.000000e+00

$observed

	para	s(Aug.SSTday)	s(Aug.ssh)	s(Aspect)	s(July.bT)	s(Depth)	s(April.pp)	s(April.chl)	s(Aug.sal)
para	1.000000e+00	1.486623e-29	2.532511e-30	7.034133e-33	4.594437e-31	2.168427e-30	3.743191e-31	7.602510e-31	7.104246e-31
s(Aug.SSTday)	5.782470e-28	1.000000e+00	1.446689e-01	2.062672e-02	1.323325e-01	1.260180e-01	2.578672e-01	1.983806e-01	2.060727e-01
s(Aug.ssh)	1.131681e-28	3.971683e-01	1.000000e+00	1.181240e-02	2.811647e-01	4.394596e-01	3.713297e-01	3.501319e-01	1.178518e-01
s(Aspect)	5.579415e-32	5.386687e-03	2.935552e-02	1.000000e+00	5.005833e-03	1.054015e-02	3.738605e-03	3.216577e-03	6.314244e-03
s(July.bT)	2.211615e-28	3.101122e-01	6.825547e-02	2.312063e-02	1.000000e+00	4.821357e-01	2.676561e-01	2.412551e-01	7.462025e-02
s(Depth)	4.083100e-27	8.595780e-02	1.615719e-01	7.927451e-03	1.918736e-01	1.000000e+00	2.851119e-01	3.050546e-01	6.505594e-02
s(April.pp)	7.662302e-28	2.682372e-01	9.071492e-02	1.017618e-02	3.733807e-02	2.794962e-01	1.000000e+00	8.343367e-01	3.059115e-02
s(April.chl)	1.291586e-27	1.958970e-01	6.631091e-02	7.376435e-03	3.809552e-02	3.132091e-01	8.541788e-01	1.000000e+00	4.431590e-02
s(Aug.sal)	3.661416e-28	8.795877e-02	1.064976e-01	1.077496e-02	1.687313e-02	1.152467e-01	7.116419e-02	7.036778e-02	1.000000e+00

$estimate

	para	s(Aug.SSTday)	s(Aug.ssh)	s(Aspect)	s(July.bT)	s(Depth)	s(April.pp)	s(April.chl)	s(Aug.sal)
para	1.000000e+00	5.175421e-31	3.167305e-31	6.219906e-33	6.584834e-31	9.107996e-31	8.868309e-30	2.870267e-30	1.574089e-30
s(Aug.SSTday)	5.782470e-28	1.000000e+00	3.423210e-01	7.054267e-03	2.867292e-01	7.390609e-02	1.486505e-01	2.963174e-02	1.211438e-01
s(Aug.ssh)	1.131681e-28	3.545910e-01	1.000000e+00	1.025663e-02	5.039231e-01	3.607348e-01	2.226380e-01	7.499263e-02	6.777299e-02
s(Aspect)	5.579415e-32	4.878931e-03	1.548589e-02	1.000000e+00	1.287086e-02	1.010739e-02	3.403787e-03	1.482425e-03	6.452371e-03
s(July.bT)	2.211615e-28	2.893204e-01	4.489701e-01	9.420558e-03	1.000000e+00	5.380632e-01	1.463569e-01	6.987667e-02	4.044904e-02
s(Depth)	4.083100e-27	7.525581e-02	4.157378e-01	6.554564e-03	3.038748e-01	1.000000e+00	1.785641e-01	8.949932e-02	2.982285e-02
s(April.pp)	7.662302e-28	1.918448e-01	2.902842e-01	4.710489e-03	1.863514e-01	1.515361e-01	1.000000e+00	3.870536e-01	1.903222e-02
s(April.chl)	1.291586e-27	1.281610e-01	2.693049e-01	3.595482e-03	1.266444e-01	1.715847e-01	4.472119e-01	1.000000e+00	2.331682e-02
s(Aug.sal)	3.661416e-28	1.107043e-01	7.913702e-02	3.037207e-03	2.706066e-02	6.982670e-02	2.312842e-02	3.123674e-02	1.000000e+00

4.6.3 Humpback whales

4.6.3.1 Distance sampling

Appendix 4-K. ESW, effective strip width for the NILS 1995-2013 humpback whales at all levels of the covariate vessel. Vessel name is given as an abbreviation of the vessel's grouping base of vessel size (see methods).

Vessel (ID)	ESW (m)
2	1599.16
3	1858.51
4	1275.36

4.6.3.2 Modelling

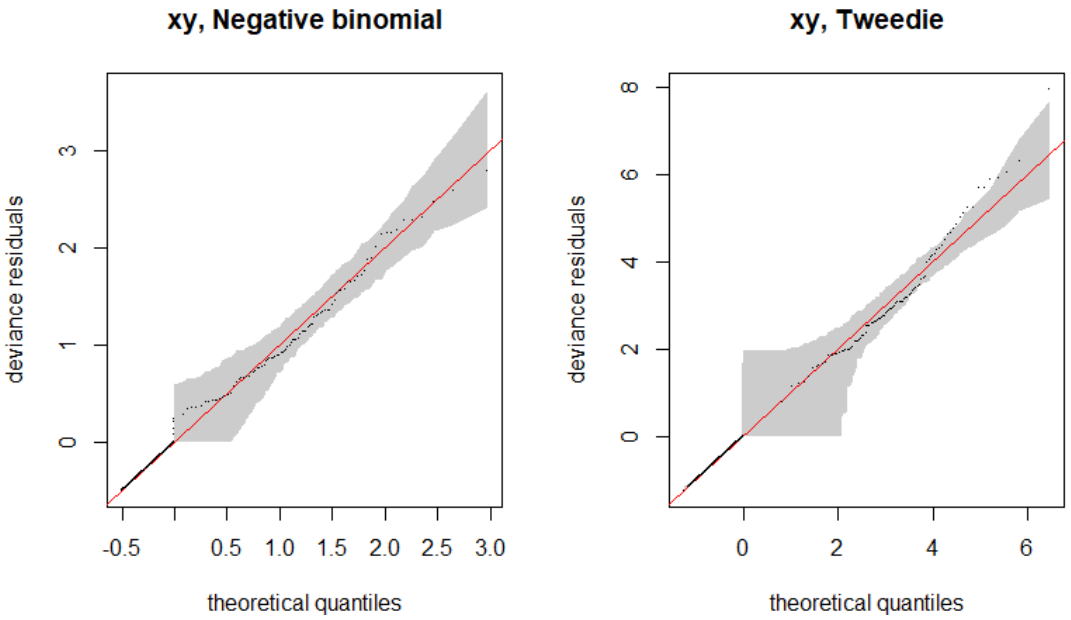

Appendix 4-L. Q-Q plots for error distribution selection for humpback whale 1987-1989 models. Spatial models (xy) for negative binomial and tweedie distributions. The shaded area represents 95 % confidence interval, the circles represent the data, the line is the expected data distribution if the data fits precisely the model.

Appendix 4-M. Single model variables fitted models for humpback whales 1987-1989 using double penalization. The best error structure for all models was the negative binomial distribution.

Model	Deviance	Deviance explained (%)	AIC	REML	n
May.SSTday	312.11	22.29	1173.44	594.87	6697
June.SSTday	317.37	14.91	1194.38	597.48	
April.SSTday	315.10	14.02	1199.06	599.99	
July.SSTday	323.12	13.58	1201.22	600.94	
Aug.SSTday	312.93	9.18	1215.11	607.15	
Aspect	299.99	4.86	1228.49	612.47	
Depth	302.60	2.31	1233.24	614.60	
Slope	301.62	2.23	1233.20	614.63	

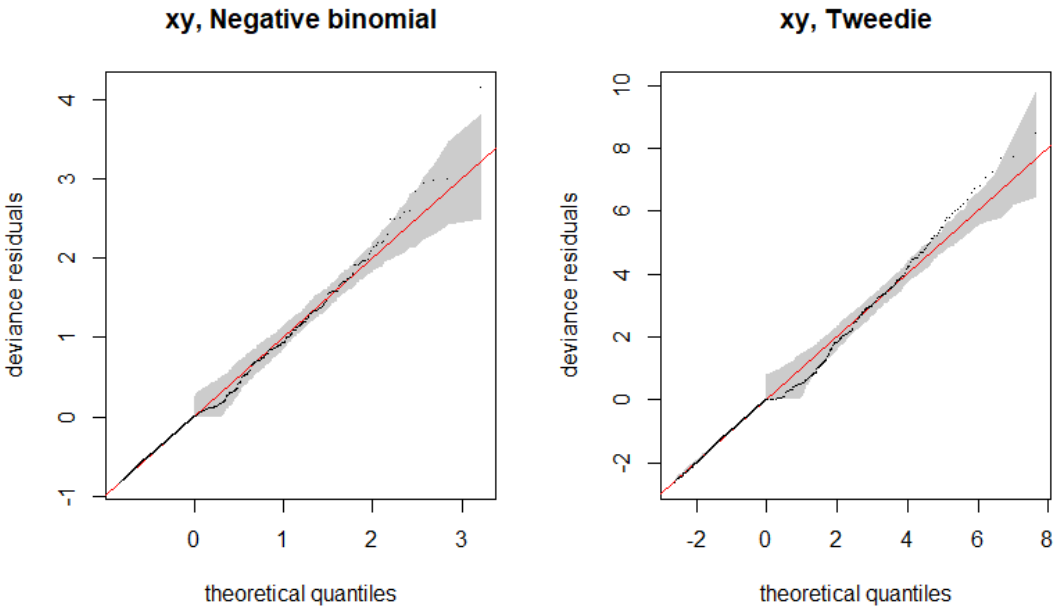

Appendix 4-N. Q-Q plots for error distribution selection for humpback whale 1998-2015 models. Spatial models (xy) for negative binomial and tweedie distributions. The shaded area represents 95 % confidence interval, the circles represent the data, the line is the expected data distribution if the data fits precisely the model.

Appendix 4-O. Single model variables fitted models for humpback whales 1998-2015 using double penalization. The best error structure for all models was the negative binomial distribution. The best covariate by each variable family is in bold letters.

Model: Survey +	Deviance	Deviance explained (%)	AIC	REML	n
June.SSTday	683.41	30.94	2643.99	1327.39	7361
July.SSTday	673.74	28.68	2665.45	1338.31	
July.bT	655.39	26.98	2679.08	1348.50	
Aug.SSTday	670.13	27.08	2679.26	1344.13	
June.bT	652.57	26.87	2680.93	1349.47	
April.bT	668.46	26.54	2686.41	1353.85	
May.bT	654.18	25.68	2692.06	1354.92	
Aug.bT	644.95	25.37	2693.27	1355.38	
Aug.ssh	653.31	23.63	2707.60	1358.71	
July.ssh	653.83	23.71	2709.53	1360.13	
Aug.sal	686.68	23.77	2711.07	1364.49	
May.sal	675.85	22.70	2714.49	1359.74	
May.SSTday	659.11	21.94	2719.74	1361.54	
June.ssh	650.63	22.16	2721.72	1364.86	
May.ssh	649.91	21.89	2724.40	1366.74	
July.mlp	686.04	21.17	2728.20	1367.14	
July.sal	667.51	21.12	2729.77	1368.14	
June.sal	667.27	20.63	2733.40	1370.57	
April.ssh	648.02	20.56	2734.90	1372.78	
Depth	664.78	19.65	2738.09	1370.89	
April.SSTday	655.73	20.13	2738.54	1373.56	
Aug.mlp	683.24	18.61	2749.66	1377.71	
April.sal	660.35	17.40	2758.86	1383.57	

June.mlp	655.98	10.33	2803.93	1403.39	
May.mlp	661.48	11.06	2804.94	1407.74	
April.mlp	643.78	7.84	2819.73	1410.15	
Aug.pp	639.76	9.36	2822.86	1417.44	
April.pp	634.86	8.59	2826.72	1419.88	
April.chl	633.17	7.69	2833.07	1423.46	
Slope	639.54	7.24	2835.49	1422.97	
Aug.chl	638.51	6.75	2835.75	1420.90	
May.chl	633.57	4.90	2842.59	1420.64	
June.pp	638.78	4.57	2846.20	1422.94	
June.chl	634.66	5.18	2846.83	1426.35	
July.chl	630.01	4.31	2852.28	1428.50	
May.pp	630.00	2.63	2856.06	1426.77	
Aspect	631.22	1.80	2857.91	1427.95	
July.pp	631.22	1.80	2857.92	1427.95	

Appendix 4-P. Concurvity values for humpback whales 1998-2015 variables in remaining full model after double penalization. Key pairs evaluated are highlighted within coloured squares.

$`worst`

	para	s(Depth)	s(Aspect)	s(April.chl)	s(June.SSTday)	s(July.mlp)	s(July.bT)	s(Aug.sal)	s(Aug.ssh)	s(Aug.pp)
para	1.000000e+00	3.228737e-27	7.876014e-32	1.273271e-27	3.604740e-29	6.192704e-24	1.385255e-28	3.079595e-28	2.297264e-28	5.170501e-29
s(Depth)	2.931616e-27	1.000000e+00	4.613535e-02	3.405314e-01	2.378928e-01	1.626304e-01	6.298698e-01	1.247481e-01	5.379606e-01	3.712960e-02
s(Aspect)	2.203560e-31	4.613535e-02	1.000000e+00	1.452810e-02	2.300414e-02	1.452347e-02	4.438432e-02	1.253567e-02	5.691339e-02	1.236760e-02
s(April.chl)	1.310112e-27	3.405314e-01	1.452810e-02	1.000000e+00	2.045644e-01	1.170074e-01	2.540409e-01	1.031072e-01	3.755870e-01	2.094512e-02
s(June.SSTday)	1.560201e-29	2.378928e-01	2.300414e-02	2.045644e-01	1.000000e+00	2.148209e-01	4.258043e-01	2.395991e-01	4.579449e-01	1.498720e-01
s(July.mlp)	6.211434e-24	1.626304e-01	1.452347e-02	1.170074e-01	2.148209e-01	1.000000e+00	1.406607e-01	4.315340e-01	1.024268e-01	2.489852e-02
s(July.bT)	1.443421e-28	6.298698e-01	4.438432e-02	2.540409e-01	4.258043e-01	1.406607e-01	1.000000e+00	9.320278e-02	7.047259e-01	3.097741e-01
s(Aug.sal)	3.600336e-28	1.247481e-01	1.253567e-02	1.031072e-01	2.395991e-01	4.315340e-01	9.320278e-02	1.000000e+00	1.536271e-01	3.430170e-02
s(Aug.ssh)	7.412767e-28	5.379606e-01	5.691339e-02	3.755870e-01	4.579449e-01	1.024268e-01	7.047259e-01	1.536271e-01	1.000000e+00	6.761170e-02
s(Aug.pp)	4.648681e-29	3.712960e-02	1.236760e-02	2.094512e-02	1.498720e-01	2.489852e-02	3.097741e-01	3.430170e-02	6.761170e-02	1.000000e+00

$observed

	para	s(Depth)	s(Aspect)	s(April.chl)	s(June.SSTday)	s(July.mlp)	s(July.bT)	s(Aug.sal)	s(Aug.ssh)	s(Aug.pp)
para	1.000000e+00	4.680845e-32	7.528148e-35	7.025024e-31	3.636588e-32	6.098381e-28	2.105538e-31	1.369061e-28	1.775069e-30	8.421417e-31
s(Depth)	2.931616e-27	1.000000e+00	1.691636e-02	2.883254e-01	3.607202e-02	1.228804e-01	2.437092e-01	5.149089e-02	9.096811e-02	1.973363e-02
s(Aspect)	2.203560e-31	1.454769e-02	1.000000e+00	3.541541e-03	5.937639e-03	8.148364e-03	3.605564e-03	3.724241e-03	1.239132e-02	9.711484e-03
s(April.chl)	1.310112e-27	1.315721e-01	5.025974e-03	1.000000e+00	8.042357e-02	8.765269e-02	6.721236e-02	4.172010e-02	1.492257e-02	4.733955e-03
s(June.SSTday)	1.560201e-29	3.215170e-02	1.527729e-02	1.821114e-01	1.000000e+00	1.845773e-01	2.113725e-01	6.121732e-02	4.696537e-02	4.427179e-02
s(July.mlp)	6.211434e-24	8.083618e-02	6.551790e-03	1.041655e-01	1.024305e-01	1.000000e+00	1.655221e-02	7.866122e-02	1.771188e-02	4.378348e-03
s(July.bT)	1.443421e-28	5.636531e-01	1.837545e-02	2.429809e-01	3.990612e-01	1.208974e-01	1.000000e+00	2.966479e-02	1.530146e-01	3.464766e-02
s(Aug.sal)	3.600336e-28	6.098424e-02	3.238405e-03	6.897322e-02	1.885289e-01	3.585642e-01	1.690660e-02	1.000000e+00	5.890780e-02	1.629264e-02
s(Aug.ssh)	7.412767e-28	3.525357e-01	2.817472e-02	3.489970e-01	3.317839e-01	7.762814e-02	4.953173e-01	5.201498e-02	1.000000e+00	1.702229e-02
s(Aug.pp)	4.648681e-29	1.948551e-02	8.958643e-03	7.898777e-03	9.100083e-02	1.124617e-02	1.053541e-01	1.755198e-02	3.808419e-02	1.000000e+00

$estimate

	para	s(Depth)	s(Aspect)	s(April.chl)	s(June.SSTday)	s(July.mlp)	s(July.bT)	s(Aug.sal)	s(Aug.ssh)	s(Aug.pp)
para	1.000000e+00	9.107996e-31	6.219906e-33	2.870267e-30	9.347483e-32	4.481448e-26	6.584834e-31	1.574089e-30	3.167305e-31	6.721428e-31
s(Depth)	2.931616e-27	1.000000e+00	6.554564e-03	8.949932e-02	5.824028e-02	9.789903e-02	3.038748e-01	2.982285e-02	4.157378e-01	1.889103e-02
s(Aspect)	2.203560e-31	1.010739e-02	1.000000e+00	1.482425e-03	5.854593e-03	5.583316e-03	1.287086e-02	6.452371e-03	1.548589e-02	3.866488e-03
s(April.chl)	1.310112e-27	1.715847e-01	3.595482e-03	1.000000e+00	8.367564e-02	5.771412e-02	1.266444e-01	2.331682e-02	2.693049e-01	4.668827e-03
s(June.SSTday)	1.560201e-29	4.246769e-02	5.777279e-03	3.987480e-02	1.000000e+00	9.046526e-02	2.932853e-01	9.330384e-02	2.905219e-01	9.328012e-02
s(July.mlp)	6.211434e-24	9.694799e-02	3.725170e-03	3.213742e-02	1.043697e-01	1.000000e+00	2.064758e-02	2.173361e-01	4.166376e-02	7.148796e-03
s(July.bT)	1.443421e-28	5.380632e-01	9.420558e-03	6.987667e-02	3.512336e-01	5.000346e-02	1.000000e+00	4.044904e-02	4.489701e-01	7.788836e-02
s(Aug.sal)	3.600336e-28	6.982670e-02	3.037207e-03	3.123674e-02	1.698875e-01	1.489982e-01	2.706066e-02	1.000000e+00	7.913702e-02	2.518806e-02
s(Aug.ssh)	7.412767e-28	3.607348e-01	1.025663e-02	7.499263e-02	3.021472e-01	4.901205e-02	5.039231e-01	6.777299e-02	1.000000e+00	4.341871e-02
s(Aug.pp)	4.648681e-29	2.160887e-02	3.389524e-03	1.111928e-02	8.243995e-02	1.687089e-02	8.479940e-02	1.152677e-02	2.223631e-02	1.000000e+00

4.6.4 Minke whales

4.6.4.1 Distance sampling

Appendix 4-Q. ESW, effective strip width for the NASS 1987-2015 minke whales at all covariate/level combination. Levels of the covariate vessel relate to the abbreviation of the vessel's name. Covariate Beaufort has three levels: high (H), medium (M) and low (L).

Vessel (ID)	Beaufort	ESW (m)		Vessel (ID)	Beaufort	ESW (m)
A	H	584.36		**I**	H	147.90
A	L	946.81		**I**	L	279.55
A	M	646.17		**I**	M	167.37
B	H	366.97		**J**	H	268.83
B	L	643.25		**J**	L	487.33

B	M	410.59		**J**	M	302.30
F	H	283.55		**K**	H	190.76
F	L	511.43		**K**	L	355.18
F	M	318.61		**K**	M	215.38
G	H	302.89		**S**	H	201.24
G	L	542.74		**S**	L	373.34
G	M	340.01		**S**	M	227.09
H	H	331.34		**V**	H	310.51
H	L	587.96		**V**	L	554.94
H	M	371.40		**V**	M	348.42

Appendix 4-R. ESW, effective strip width for the NILS 1987-1989 minke whales at all levels of the covariate vessel. Vessel name is given as an abbreviation of the vessel's grouping base of vessel size (see methods).

Vessel (ID)	ESW (m)
1	441.74
2	411.84
3	628.66

Appendix 4-S. ESW, effective strip width for the NILS 1995-2013 minke whales at all covariate/level combination. Levels of the covariate vessel name is given as an abbreviation of the vessel's grouping base of vessel size (see methods). Covariate Beaufort has six levels from 0-5.

Vessel (ID)	Beaufort	ESW (m)		Vessel (ID)	Beaufort	ESW (m)
2	0	879.39		**3**	3	683.75
2	1	833.03		**3**	4	503.17
2	2	710.57		**3**	5	443.61
2	3	616.72		**4**	0	768.21
2	4	452.10		**4**	1	725.89
2	5	398.22		**4**	2	615.82
3	0	964.51		**4**	3	532.79
3	1	915.88		**4**	4	389.03
3	2	785.35		**4**	5	342.35

4.6.4.2 Modelling

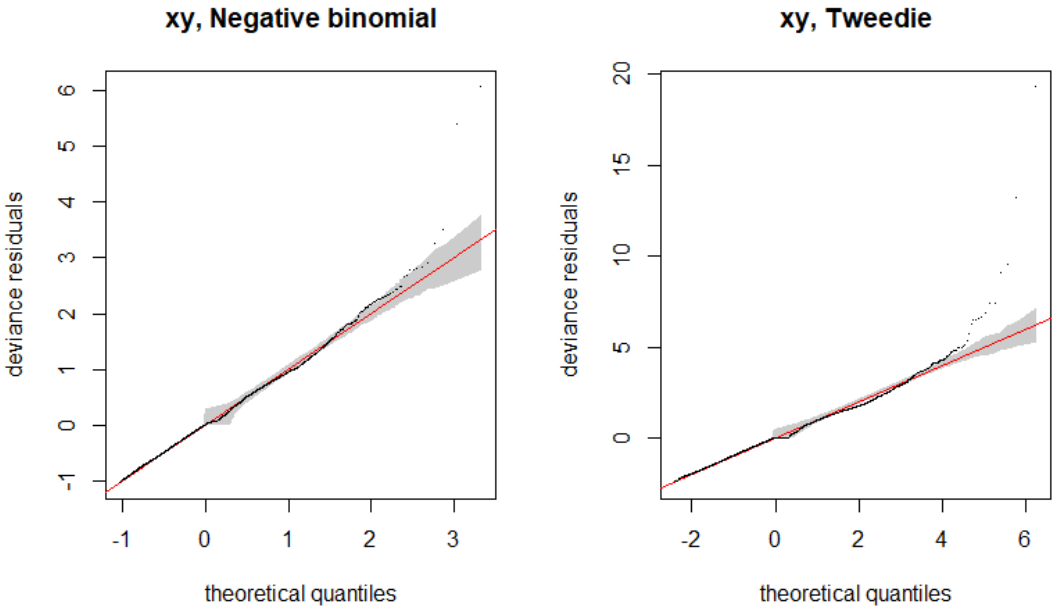

Appendix 4-T. Q-Q plots for error distribution selection for minke whale 1987-1989 models. Spatial models (xy) for negative binomial and tweedie distributions. The shaded area represents 95 % confidence interval, the circles represent the data, the line is the expected data distribution if the data fits precisely the model.

Appendix 4-U. Single model variables fitted models for minke whales 1987-1989 using double penalization. The best error structure for all models was the negative binomial distribution.

Model	Deviance	Deviance explained (%)	AIC	REML	n
Depth	1869.03	10.68	5783.77	2902.92	6695
Aug.SSTday	1901.55	7.38	5850.82	2935.97	
April.SSTday	1896.15	7.44	5851.19	2936.88	
June.SSTday	1872.05	7.07	5857.70	2942.41	
May.SSTday	1895.02	6.84	5863.78	2943.95	
July.SSTday	1891.82	6.20	5874.50	2945.36	
Slope	1867.63	3.72	5920.47	2966.36	
Aspect	1870.65	2.62	5941.76	2975.04	

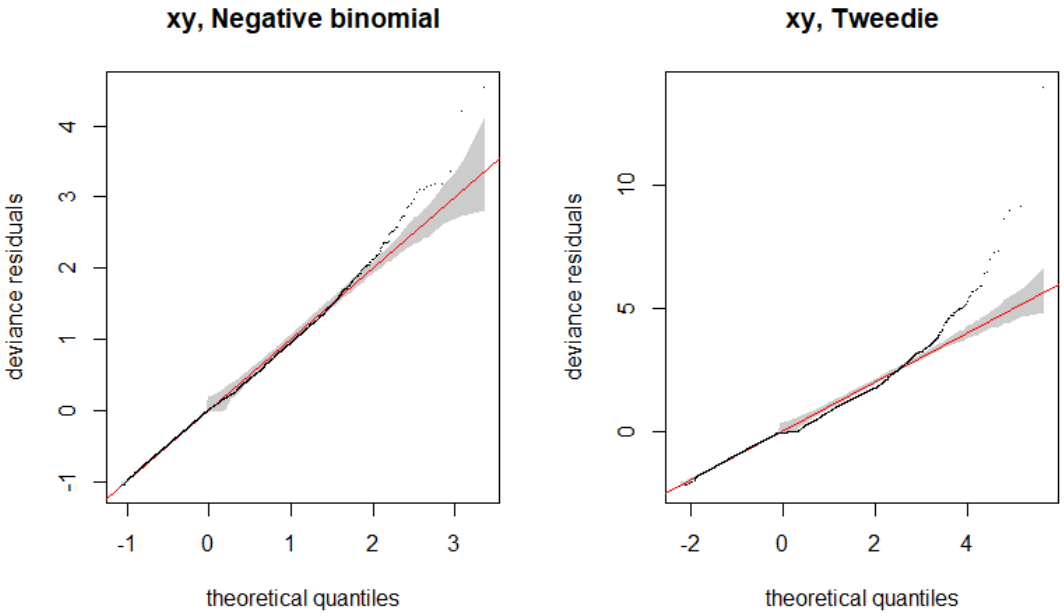

Appendix 4-V. Q-Q plots for error distribution selection for minke whale 1998-2015 models. Spatial models (xy) for negative binomial and tweedie distributions. The shaded area represents 95 % confidence interval, the circles represent the data, the line is the expected data distribution if the data fits precisely the model.

Appendix 4-W. Single model variables fitted models for minke whales 1998-2015 using double penalization. The best error structure for all models was the negative binomial distribution. The best covariate by each variable family is in bold letters.

Model: Survey +	Deviance	Deviance explained (%)	AIC	REML	n
June.SSTday	2793.17	6.15	7614.40	3816.40	7452
Aug.bT	2785.31	6.20	7614.92	3821.90	
June.ssh	2761.26	5.96	7619.23	3818.17	
May.ssh	2767.91	5.85	7622.18	3819.53	
July.ssh	2764.50	5.91	7622.36	3822.70	
Aug.ssh	2765.90	5.83	7625.40	3824.23	
April.bT	2781.47	5.34	7638.77	3832.39	
May.bT	2784.94	5.27	7639.74	3830.64	
July.bT	2783.51	5.24	7641.28	3832.49	
Depth	2785.78	4.96	7648.34	3832.56	
April.SSTday	2775.87	4.66	7650.22	3827.93	
June.bT	2785.33	4.82	7652.05	3835.54	
April.ssh	2763.70	4.72	7653.02	3832.70	
May.SSTday	2785.94	4.56	7654.91	3830.83	
July.SSTday	2782.72	4.25	7662.76	3834.05	
July.mlp	2786.02	4.11	7670.26	3839.67	
Aug.SSTday	2784.50	3.79	7673.55	3838.70	
June.chl	2794.37	4.11	7674.53	3848.42	
April.mlp	2784.69	3.91	7677.30	3844.63	
Aug.mlp	2783.62	3.74	7677.56	3841.39	
June.sal	2784.00	3.74	7680.30	3845.50	
Aug.pp	2778.77	3.70	7680.70	3843.53	
May.sal	2785.62	3.49	7687.11	3847.66	

April.sal	2787.96	3.47	7687.94	3847.73	
Aug.sal	2780.26	3.33	7689.93	3847.98	
July.pp	2792.68	3.19	7690.72	3847.24	
July.sal	2784.59	3.23	7693.23	3849.62	
April.chl	2798.13	3.04	7696.30	3850.55	
Slope	2793.79	3.07	7697.97	3852.33	
Aug.chl	2781.45	2.89	7698.55	3850.85	
May.chl	2786.74	3.02	7698.71	3852.32	
June.mlp	2779.92	3.01	7699.56	3853.63	
May.mlp	2788.80	2.91	7702.28	3854.44	
May.pp	2788.31	2.82	7705.96	3856.51	
July.chl	2789.49	2.62	7706.32	3854.46	
June.pp	2793.40	2.73	7708.16	3857.41	
April.pp	2792.63	2.28	7715.21	3858.57	
Aspect	2790.32	2.06	7717.72	3859.73	

Appendix 4-X. Concurvity values for minke whales 1998-2015 variables in remaining full model after double penalization. Key pairs evaluated are highlighted within coloured squares.

$worst

	para	s(June.SSTday)	s(June.ssh)	s(Aspect)	s(Aug.bT)	s(Depth)	s(Slope)	s(Aug.pp)	s(July.mlp)
para	1.000000e+00	1.299036e-28	4.649972e-29	1.828000e-31	1.845870e-27	2.629568e-27	3.218604e-26	3.911366e-29	4.094320e-23
s(June.SSTday)	8.437890e-29	1.000000e+00	5.331000e-01	2.348880e-02	4.160336e-01	2.419760e-01	1.053339e-01	1.487398e-01	2.148536e-01
s(June.ssh)	3.961365e-29	5.331000e-01	1.000000e+00	5.187670e-02	7.194378e-01	4.981386e-01	2.941876e-01	9.605823e-02	1.019773e-01
s(Aspect)	5.103146e-31	2.348880e-02	5.187670e-02	1.000000e+00	4.533801e-02	4.629320e-02	2.084461e-02	1.205168e-02	1.477542e-02
s(Aug.bT)	1.780750e-27	4.160336e-01	7.194378e-01	4.533801e-02	1.000000e+00	6.241616e-01	2.254112e-01	2.986539e-01	1.308549e-01
s(Depth)	2.547784e-27	2.419760e-01	4.981386e-01	4.629320e-02	6.241616e-01	1.000000e+00	5.058886e-01	3.629545e-02	1.612880e-01
s(Slope)	3.494576e-26	1.053339e-01	2.941876e-01	2.084461e-02	2.254112e-01	5.058886e-01	1.000000e+00	3.003630e-02	5.388067e-02
s(Aug.pp)	2.639829e-29	1.487398e-01	9.605823e-02	1.205168e-02	2.986539e-01	3.629545e-02	3.003630e-02	1.000000e+00	2.447869e-02
s(July.mlp)	4.094573e-23	2.148536e-01	1.019773e-01	1.477542e-02	1.308549e-01	1.612880e-01	5.388067e-02	2.447869e-02	1.000000e+00

$observed

	para	s(June.SSTday)	s(June.ssh)	s(Aspect)	s(Aug.bT)	s(Depth)	s(Slope)	s(Aug.pp)	s(July.mlp)
para	1.000000e+00	2.591617e-32	1.994315e-33	6.287808e-33	4.560623e-30	8.830386e-29	1.684196e-29	2.752459e-32	3.269793e-28
s(June.SSTday)	8.437890e-29	1.000000e+00	8.500672e-02	1.978733e-02	5.676851e-02	1.396337e-01	3.099261e-02	1.225985e-01	1.930221e-01
s(June.ssh)	3.961365e-29	3.196985e-01	1.000000e+00	2.054905e-02	1.163166e-01	4.298565e-01	1.409251e-01	3.610039e-02	7.725894e-02
s(Aspect)	5.103146e-31	7.063240e-03	3.045459e-02	1.000000e+00	1.766228e-02	5.277987e-03	9.781575e-03	3.103203e-03	8.468502e-03
s(Aug.bT)	1.780750e-27	3.348881e-01	1.820956e-01	2.084763e-02	1.000000e+00	5.130893e-01	7.379121e-02	8.036944e-02	1.039901e-01
s(Depth)	2.547784e-27	4.012327e-02	2.630791e-01	8.694603e-03	7.709430e-02	1.000000e+00	1.581470e-01	1.807862e-02	1.429205e-01
s(Slope)	3.494576e-26	2.249890e-02	6.572171e-02	2.766726e-03	3.455617e-02	4.216527e-01	1.000000e+00	1.623588e-02	3.552375e-02
s(Aug.pp)	2.639829e-29	6.318140e-02	3.224211e-02	7.116187e-03	8.241698e-02	3.490340e-02	8.021664e-03	1.000000e+00	1.535115e-02
s(July.mlp)	4.094573e-23	6.324304e-02	4.396936e-02	1.428467e-02	1.550212e-02	1.341701e-01	2.068397e-02	6.477241e-03	1.000000e+00

$estimate

	para	s(June.SSTday)	s(June.ssh)	s(Aspect)	s(Aug.bT)	s(Depth)	s(Slope)	s(Aug.pp)	s(July.mlp)
para	1.000000e+00	3.940544e-31	2.254742e-31	5.490627e-33	1.351630e-29	3.438851e-31	1.434310e-28	8.877096e-32	3.221772e-25
s(June.SSTday)	8.437890e-29	1.000000e+00	3.261048e-01	5.766671e-03	2.735452e-01	4.300195e-02	2.994491e-02	9.346655e-02	8.942962e-02
s(June.ssh)	3.961365e-29	3.281171e-01	1.000000e+00	8.885787e-03	5.004203e-01	3.738552e-01	6.927402e-02	4.113098e-02	4.858401e-02
s(Aspect)	5.103146e-31	5.791959e-03	1.353957e-02	1.000000e+00	1.231948e-02	1.010047e-02	4.750911e-03	3.549946e-03	3.626476e-03
s(Aug.bT)	1.780750e-27	3.380029e-01	4.627205e-01	9.668538e-03	1.000000e+00	5.376995e-01	4.207121e-02	8.460836e-02	4.832103e-02
s(Depth)	2.547784e-27	6.008741e-02	4.046328e-01	6.600615e-03	3.106629e-01	1.000000e+00	1.294803e-01	1.886016e-02	9.631378e-02
s(Slope)	3.494576e-26	2.328010e-02	1.775521e-01	4.076617e-03	9.797681e-02	2.104858e-01	1.000000e+00	1.253436e-02	3.250573e-02
s(Aug.pp)	2.639829e-29	8.112468e-02	2.228050e-02	3.351158e-03	8.980589e-02	2.093917e-02	6.670749e-03	1.000000e+00	1.654297e-02
s(July.mlp)	4.094573e-23	1.030642e-01	4.777329e-02	3.731857e-03	1.883789e-02	9.677980e-02	1.384755e-02	6.933063e-03	1.000000e+00

5 DISTRIBUTION AND HABITAT USE OF TWO DELPHINIDAE SPECIES IN THE CENTRAL AND NORTH-EASTERN NORTH ATLANTIC

5.1 Introduction

Killer whales and white-beaked dolphins are two Delphinidae species that inhabit the central and north-eastern North Atlantic throughout the year (e.g. Kovacs et al., 2009; Kuningas et al., 2014; Samarra et al., 2017; Similä et al., 1996; Tavares et al., 2017). In Icelandic, Faroese and Norwegian waters, both species are commonly found in coastal and offshore waters (e.g. Forney and Wade, 2007; Galatius and Kinze, 2016; Kovacs et al., 2009; Øien, 1988; Pike et al., 2009a; Similä et al., 1996) but were never a direct harvesting target rather opportunistic (Bloch and Lockyer, 1988; IWC, 2020; Kiszka and Braulik, 2018; Bloch and Allison, 2005 In: NAMMCO, 2020; Øien, 1988; Reeves et al., 2017). During the summer, prey availability may play an important role in determining the distribution of both these highly mobile species. In contrast to baleen whales, social interaction for killer whales and white-beaked dolphins may also be important (e.g. Hansen and Heide-Jørgensen, 2013; Jourdain et al., 2019; Kovacs et al., 2009; Samarra and Foote, 2015; Tavares et al., 2017).

Both species are opportunistic predators feeding high in the food web, with diverse diets that include cephalopods, fish and (for killer whales) marine mammals, but fish are likely to be the main prey for both, especially gadoid fish for white-beaked dolphins (e.g. Bloch and Lockyer, 1988; Canning et al., 2008; Christensen, 1988; Dong et al., 1996; Fall and Skern-Mauritzen, 2014; Jansen et al., 2010; Jonsgard and Lyshoel, 1970 In: NAMMCO, 1993; Øien, 1988; Samarra and Miller, 2015; Sigurjónsson and Víkingsson, 1997). Distribution changes have been seen in both species, which have been linked to changes in prey distribution, oceanographical changes (likely water warming) and/or interaction with other species (e.g. Canning et al., 2008; IJsseldijk et al., 2018; Øien, 1988; Katona et al., 1993; Kenney et al., 1996 In: Waring et al., 2006). This chapter investigates the oceanic drivers of distribution of these two species over 30 years. The distribution of both species in the area is poorly known, especially offshore; this information will provide a better understanding of how the species use the area at a broad scale and in comparison to each other.

5.1.1 State of knowledge about killer whales

The killer whale (*Orcinus orca*) is the largest species of the family Delphinidae, the most cosmopolitan of all cetaceans and after humans the second most widely distributed mammal. It is the only extant member of the genus *Orcinus* and currently only one species of *O. orca* is recognized (Committee on Taxonomy, 2018), but there are unresolved taxonomic issues. There are distinct populations described with differences in morphology, ecology, and genetics. For example, it is unclear whether killer whale ecotypes should be classified as different species, subspecies or still only one species. Males are larger than females: adult maximum body length has been reported as 9.0 m and 7.9 m, respectively. Male life expectancy has been estimated at about 30 years and maximum age is approximately 50-60 years. Female life expectancy has been estimated at around 50 years (from 6 months of age) and maximum age is believed typically to be about 80-90 years but the oldest known female in the wild was estimated to be 105 years old (Ford, 2018; NAMMCO, 2020).

The broad distribution of killer whales means they are found in a wide diversity of habitats at different water depths in offshore to coastal areas, where in the latter they can enter shallow bays, estuaries, river mouths, and fjords (Forney and Wade, 2007). They are also found at water temperatures ranging from tropical to high latitude areas including up to the ice edge; densities in high latitudes are 1-2 orders of magnitude greater than in other areas (Forney and Wade, 2007; Storrie et al., 2018). Prey is a determinant factor in killer whale distribution (e.g. Foote et al., 2010; Øien, 1988; Similä et al., 1996). See below for more detailed information about the relationship between killer whales and their prey.

Killer whales have been recorded in Norwegian waters along the coast and offshore, in the Barents Sea, and infrequently around Svalbard, including in fjords or along the ice edge (e.g. Figure 5.1) (e.g. NAMMCO, 2019a; Øien, 1988; Similä et al., 1996; Storrie et al., 2018). In Icelandic waters, killer whales are also found around the island and in deep waters of the Central North Atlantic (e.g. Figure 5.1) (Bloch and Lockyer, 1988; Øien, 1988; Samarra et al., 2018; Samarra and Foote, 2015). Similarly around the Faroe Islands whales have been sighted along the coast but large offshore aggregations have also been recorded (Figure 5.2) (Bloch and Lockyer, 1988). Sightings of killer whales in the northwest North Sea have led to the suggestion that there is a continuous distribution from the Faroes to the north of Scotland Figure 5.1 (e.g. Beck et al., 2014; Bloch and Lockyer, 1988; Foote et al., 2011, 2010; Luque et al., 2006; Robinson et al., 2017; Samarra and Foote, 2015). Killer whales have been also recorded/caught off East Greenland, as shown in Figure 5.1, where they have also been seen close to the coast near inhabited areas in the past (Heide-Jørgensen, 1988 In: Jourdain et al., 2019) and more recently also recorded/caught in the summer in Southeast Greenland (Foote et al., 2013; Lennert and Richard, 2017; NAMMCO, 1993).

Killer whales are found in the central and north-eastern North Atlantic throughout all seasons, but seasonal movements are poorly understood. In Svalbard, killer whales are summer season visitors only (Storrie et al., 2018). Along the Norwegian coast, killer whales are seen commonly during October to March, where the timing is area dependent and directly linked with the main prey, herring, but Lofoten is the only place where whales have been reported year-around (Øien, 1988; Similä et al., 1996). During the summer, offshore areas in the Norwegian Sea appear to be important habitat for the whales as suggested by local surveys (NAMMCO, 2019a, Øien, 1993 In: 1993; Similä et al., 1996). Killer whales also sporadically occur in the Barents Sea during summer as suggested by historical catch data and more recent studies (Kovacs et al., 2009; Øien, 1988). Around the Faroe Islands they have been recorded in summer in coastal and offshore waters (Bloch and Lockyer, 1988). Around Iceland, they are also present year-round and in the summer they can be found in coastal and offshore waters (e.g. Foote et al., 2007; Øien, 1988; Tavares et al., 2017). The continuous distribution from the Faroes to northern UK waters peaks during the summer; furthermore there is evidence of regular seasonal movements of a few individuals between Iceland (winter) and Scotland (summer) (Foote et al., 2010; Samarra and Foote, 2015). In East Greenland, summer occurrence has been indicated by historical catches (Figure 5.2) (Øien, 1988) and current catches (Lennert and Richard, 2017), but killer whale sightings during large scale surveys are scarce (Hansen et al., 2018).

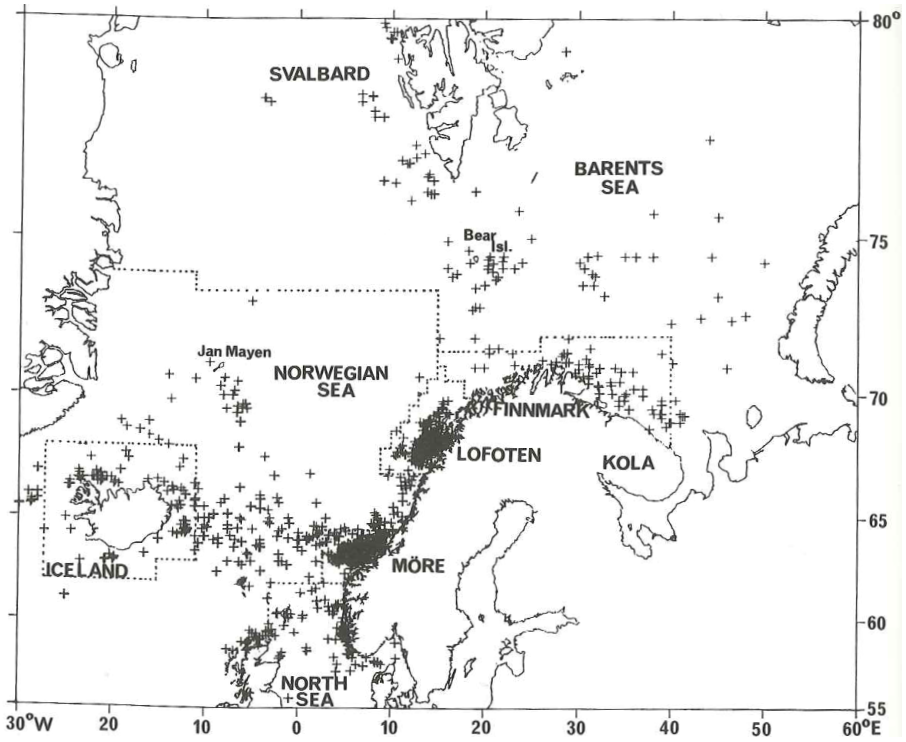

Figure 5.1. Catch positions for killer whales taken in the Northeast Atlantic by Norwegian small-type whalers 1938-1981. Each position may include more than one whale caught (Øien, 1988).

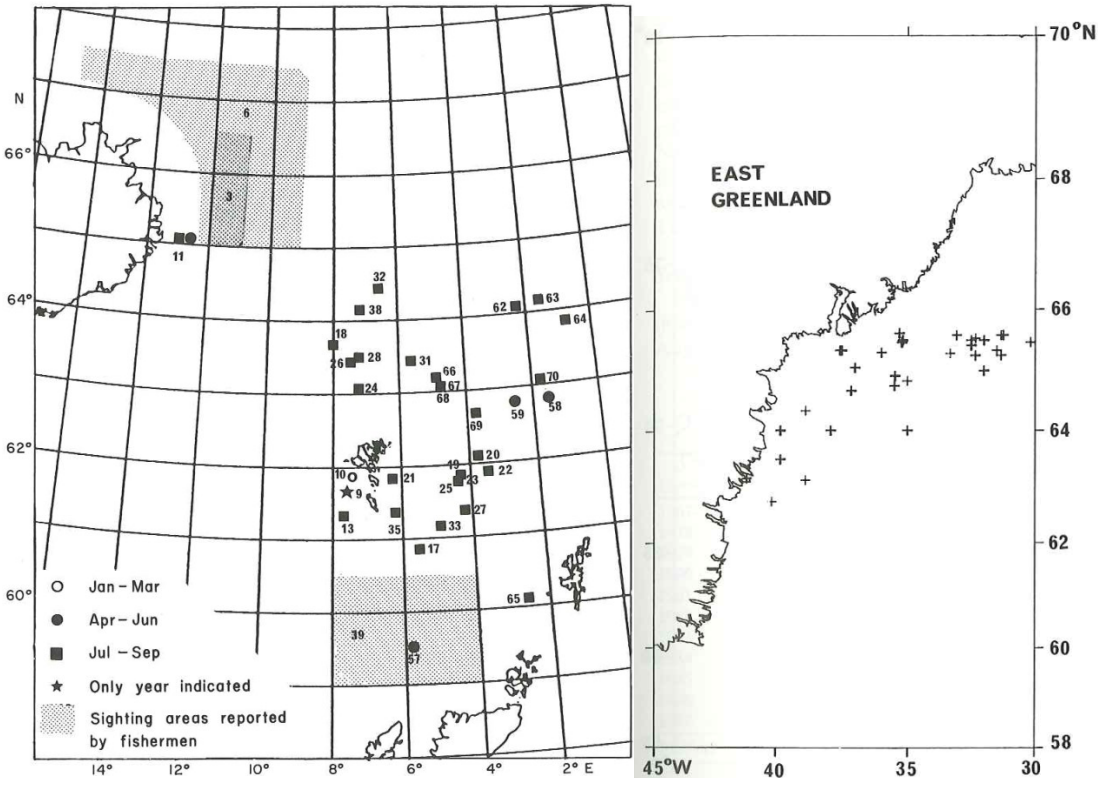

Figure 5.2. Left: Offshore sightings of killer whales from 1981-1984, 1986 and 1987 by quarter-years. Observations numbered are detailed in Bloch and Lockyer (1988). Right: Catch positions for 101 killer whales taken by Norwegian whalers off East Greenland, west of 30 ˚W. Each plotted position may include more than one whale caught (Øien, 1988).

Prey distribution is a determinant in killer whale dispersal (Foote et al., 2010), and these prey-whale links are more apparent than for the other cetacean species in the central and north-eastern North Atlantic. In this region, killer whales consume a wide diversity of prey from squid, fish, birds to marine mammals (e.g. Bloch and Lockyer, 1988; Foote et al., 2013; NAMMCO, 1993; Øien, 1988; Similä et al., 1996). In Norwegian coastal waters the main prey for killer whales is the Norwegian spring-spawning (NSS) herring, but other types of prey have been recorded such as, lumpfish (*Cyclopterus lumpus*), squid, cod, little auk (*Alle alle*), eider duck (*Somateria mollissima*), northern fulmar (*Fulmarus glacialis*), mackerel, and harbour seal (*Phoca vitulina*) (e.g. Jourdain et al., 2020; NAMMCO, 1993; Similä et al., 1996). There has been some indication that at least some of the killer whale pods follow the main migration of the NSS herring throughout the year, for example in the 1990s, staring in the wintering grounds in northern Norway (Lofoten area) to the spring-spawning grounds around Møre to the feeding grounds offshore in the Norwegian Sea (Øien, 1988; Similä et al., 1996). In more recent years, mackerel also seems an important prey for killer whales not only in the Norwegian Sea but also in the North Sea. Mackerel abundance has increased and distributed more to the north-west (e.g. Astthorsson et al., 2012); this matches with information from summer fish stock assessment surveys in the Norwegian Sea showing that killer whales have increased and were associated with mackerel even when herring was available (Nøttestad et al., 2015). Other prey recorded in Norwegian waters include northern bottlenose whales in Svalbard and seals in Møre (NAMMCO, 1993). In Icelandic waters, a key prey is Icelandic summer-spawning (ISS) herring (Samarra et al., 2018), which is also followed on migration by the whales (Sigurjónsson et al., 1988 In: Tavares et al., 2017). Other prey species that have been reported from observations are halibut (*Hippoglossus hippoglosus*), possibily bottlenose dolphins (*Tursiops truncatus*), and long-finned pilot whales (NAMMCO, 1993) and historically, squid and seals have been recovered from killer whales stomachs (Jonsgard and Lyshoel, 1970 In: NAMMCO, 1993).

In Faroese waters the main prey of killer whales is also fish such as mackerel, herring, halibut, and Greenland halibut (*Reinhardtius hippoglossoides*), but also there are reports of diverse prey such as eider ducks, kittiwakes (*Rissa tridactyla*), guillemots (*Uria aalge*), puffins (*Fratercula arctica*), grey seals (*Halichoerus grypus*), and harbour porpoises. Killer whale attacks have been also recorded on pilot whales and a fin whale (Bloch and Lockyer, 1988; NAMMCO, 1993). In Greenlandic waters, marine mammals dominate the diet; killer whales consume almost all species of whales and seals but fish and squid have also been found. Prey reports have included porpoises, belugas (*Delpinapterus leucas*), bowhead whales (*Balaena mysticetus*), humpback whales, walruses (*Odobenus rosmarus*), and of particular impotance narwhals (*Monodon monoceros*) (Eschricht, 1863; Heide-Jørgensen, 1988 In:

NAMMCO, 1993). The over-riding conclusion is that although killer whales may have a main prey in a particular area, they are highly opportunistic.

It is evident that killer whales in the North Atlantic have a dynamic relationship with their prey. It has been suggested historically and more recently that in the central and north-eastern North Atlantic killer whales migrate as herring migrate (e.g. Bloch and Lockyer, 1988; Christensen, 1988; Jonsgard and Lyshoel, 1970 In: NAMMCO, 1993; Øien, 1988; Samarra and Miller, 2015). Around the end of the 1960s, the NSS herring migrated between the Norwegian Sea between Iceland and Jan Mayen (feeding areas) to the coast of Norway (spawning areas). Subadult herring dispersed along the coast of northern Norway and the Barents Sea. In the 1970s, herring had collapsed and its migration to the Norwegian Sea had stopped, instead herring remained close to the Norwegian coast until maturity and spawning (Dragesund and Ulltang, 1978; Dragesund et al., 1980 In: Øien, 1988). This change in herring migration has been linked with changes in killer whale distribution; since the 1970s, whale abundance increased in coastal areas and the whaling peak also shifted from spring to late autumn and winter (Christensen, 1988; Øien, 1988).

Before the collapse in the 1970s, the migration of the NSS herring to the Norwegian Sea overlapped the distribution of the Icelandic spring and summer spawning herring stocks (Jakobsson and Østvedt, 1999). This area of herring stock overlap was also an area of Icelandic and Norwegian killer whale overlap as suggested by photoidentification studies (Jonsgard and Lyshoel, 1970 In: Jourdain et al., 2019; Øien, 1988). Since the collapse and change in distribution in NSS herring, the herring stocks have not overlapped and neither, apparently, have killer whales from Iceland and Norway (no matches of photo-identified whales) (Foote et al., 2010). In recent years NSS herring have returned to Iceland, to the east in 2004 and to the north in 2012. Comparison of current photo-identification catalogues is needed to evaluate if killer whales from Iceland and Norway are overlapping again (Jourdain et al., 2019).

The foraging ecology of killer whales is very diverse, in terms of their prey and their behaviour and preferences. Foraging ecology and genetics have been used to understand the connectivity among killer whales in the North Atlantic, but results are inconclusive, suggesting some level of similarity between the Norwegian, Icelandic (Faroese) groups but also some differences. Genetically Foote et al. (2011) suggested three populations, a) individuals from Norway, Iceland, and Scotland that are associated with North Atlantic herring, b) whales from Iceland, Ireland, Scotland, and North Sea that are associated with North Atlantic mackerel, and c) Canary Islands and Gibraltar associated with Atlantic bluefin tuna. However, some killer whales sampled in East Greenland were assigned to herring-eating population a but had marine mammal remains in their stomachs (Foote et al., 2013).

This is a clear example of the ecological complexity of killer whales in the area thus showing foraging diversity within the same population. Foote et al. (2009) suggested two types of whales: generalists and specialists. Generalists prey on mackerel and herring and isotopic signals also indicate some high trophic prey. Specialists show little variation in isotopic signal that indicates feeding at a high trophic level. However, Jourdain et al. (2020), found seasonal differences among isotopic signals, suggesting that whales may have some level of prey specialization but that preferences may also be seasonal.

Prey distribution in all seasons, including summer, is a determinant in killer whales distribution (Foote et al., 2010). Killer whales in the central and north-eastern North Atlantic are year-round residents with diverse ecological preferences, including dynamic foraging strategies (Kuningas et al., 2014; Samarra et al., 2017; Similä et al., 1996; Tavares et al., 2017). The modelled relationships are therefore likely to reflect environmental drivers related to finding prey. Killer whales are gregarious and social interactions may also influence distribution. Information on reproduction is limited; however, calves (new-born calves) are present all year-round.

Covariates included in the models have been chosen because they may have the power to explain foraging behaviour (see also general justification of the included covariates in section 2.2.2.1 and Table 2.3). Other studies have found relationships between killer whale density and dynamic relationships with its habitat (coastal to offshore, tropical to the Arctic) and prey species (see above). Covariates related to primary production are expected to have a lagged relationship with killer whale density because they typically feed high in the trophic web. Covariates linked with prey aggregation such as SSH and mlp are expected to be related to prey accumulation and to have little to no lag. Salinity is related to water masses and in the study area may explain the influence of Arctic versus temperate water on killer whale distribution. Bottom water temperature relates to deep water horizontal gradients which are relevant if killer whales are feeding on some benthic fish species.

In the North Atlantic killer whales are increasingly common in northern latitudes and rare to uncommon towards the tropics; they very abundant in Norwegian waters, common in Icelandic waters, and infrequent in the North Sea and UK waters (Forney and Wade, 2007). Abundance estimates are available from line-transect surveys (summer surveys) and from long-term photo-identification studies in coastal areas (partly in winter). Norwegian waters have the most available estimates for the area. Questionnaire surveys covering all seasons in the 1980s gave estimates of 483-1507 in coastal areas (Christensen, 1988). Summer line-transect surveys in 1989 estimated around 7,000 whales (95% CI = 3,400–14,400) in Norwegian waters, northern North Sea and eastern Norwegian Sea northward to Bear Island (NAMMCO, 1993). Summer mosaic surveys estimated 18,213 animals (95% CI: 11,486-29,992) in 2002-2007, and 18,213 animals (95%

CI: 11,486-29,992) in 2008-2013. The most recent estimates from the last cycle are in Table 5.1 (NAMMCO, 2019a).

The number of killer whales in northern Norway preying on NSS herring during winter between 1986-2003 was estimated to be highest in 2003 with 731 individuals (95% CI = 505–1,059) (Kuningas et al., 2014). The most recent minimum count in the same area between 2007-2018 was higher (Jourdain and Karoliussen, 2018) (Table 5.1).

In Icelandic-Faroes waters, summer line-transect killer whale abundance estimates are highly variable, partly because of differences in the area surveyed. The early Icelandic-Faroese surveys sometimes extended to southern Norwegian waters. Abundance estimates were 8,260 (95% CI = 3,516–19,408) in 1987, 26,774 (95% CI = 8,341–85,943) in 1989 and 4,413 whales (95% CI = 575–33,990) in 1995. The most recent estimate available for the area is from 2001 (Table 5.1) (Foote et al., 2007). In Iceland, photo-identification studies take place in summer and winter (Samarra et al., 2017; Tavares et al., 2017). There are no abundance estimates in East Greenland because of the low detection rate during surveys; however, in the last decade killer whales have been more commonly caught around Tasiilaq (Lennert and Richard, 2017; NAMMCO, 2013).

Table 5.1. Most recent abundance estimates of killer whales in the central and north-eastern North Atlantic.

Method	Areas / Years	Estimate	95% Confidence interval	Reference
Photo-identification	Northern Norway 2007-2018	971	Minimum counts excluding calves	Jourdain and Karoliussen (2018)
	Iceland 2006-2015	432		Samarra et al., (2017)
Line-transect	Northeastern* 2014-2018	13,909	7,733 – 25,018	NAMMCO (2019a)
	Central ** 2001	15,891	6,637-33,964	Foote et al., (2007)

*North-eastern includes Norway **Central includes Iceland, Faroes and Jan Mayen.

Regarding conservation status, the killer whale has been listed by the International Union for Conservation of Nature (IUCN) as data deficient (DD) since 2008, which should be maintained until taxonomical units are described (Reeves et al., 2017). There are some small apparently discrete groups of killer whales in the North Atlantic. One, seen seasonally hunting bluefin tuna in the Strait of Gibraltar, has about 39 individuals and is declining (Esteban et al., 2016). Another is a small community of about 10 killer whales off Western Scotland, Ireland and Wales, which appears not to associate with other killer whale groups and no new individuals have been born in the last 20 years (Beck et al., 2014).

There are a number of anthropogenic pressures on killer whales. In the past, killer whales have been caught during commercial whaling operations, and, although it was not a target species and catches in general were of minor commercial value, this could potentially have impacted populations. Since 2008 off Tasiilaq, East Greenland, a sharp increase in subsistence whaling catches has been recorded and killer whale hunting now has become a regular activity (Foote et al., 2013; IWC, 2020; Lennert and Richard, 2017; Ugarte et al., 2013 In: NAMMCO, 2013). Currently in Greenland, killer whales are legally hunted and since 1996 reporting catches is obligatory, but there are no hunting regulations and conservation concerns have been raised (Jourdain et al., 2019; NAMMCO, 2013).

Of all anthropogenic pressures, killer whales as top predators may be most susceptible to chemical contaminants. Killer whales in the North Atlantic have some of the highest concentrations of PCBs and DDTs, which could be causing impairments in physiology, immune response, and reproduction (Jepson et al., 2016; Pedro et al., 2017).

Pressures from fisheries could include prey reduction from overfishing and direct interactions with fishing gear. The change in killer whale distribution following the collapse of NSS herring in the 1970s could be an example of the former (Øien, 1988). There are also examples of direct interaction with herring, mackerel, and halibut fisheries (e.g. Bloch and Lockyer, 1988; Lennert and Richard, 2017; Luque et al., 2006; Samarra et al., 2018), and there have been some reports of lethal entanglement (Jourdain et al., 2019).

Acoustic pollution from naval sonar has been shown to generate various responses by killer whales, including changes in diving behaviour related with feeding. Studies have found that disruption can be more severe if animals are feeding, resting, or taking care of offspring (functional behaviours) (Kuningas et al., 2013; Miller et al., 2012; Sivle et al., 2012). However, in the North Atlantic the noise levels and the effects of vessel noise to which killer whales are exposed have not yet been assessed (Jourdain et al., 2019).

Environmental changes such as rising ocean temperatures and/or loss of sea ice in some areas is making new prey resources available for killer whales (Higdon and Ferguson, 2009; Lennert and Richard, 2017). Changes in prey distribution have been recorded (e.g. Astthorsson et al., 2012; Øien, 1988). It has been suggested that killer whales are adaptable to these effects because of their diverse diet but population-level consequences are unclear (Ford et al., 2010; e.g. Samarra and Miller, 2015).

5.1.2 State of knowledge about white-beaked dolphins

The white-beaked dolphin (*Lagenorhynchus albirostris*) is relative abundant and endemic to the North Atlantic; it is the dolphin species with the most northerly distribution (Kinze, 2018; Kiszka and Braulik, 2018). It shares the North Atlantic with the Atlantic white-sided dolphins (*Lagenorhynchus acutus*), with which it could be misidentified (Jefferson et al., 1993), but white-beaked dolphins are typically found further north. There is no accurate information regarding life-span but it is estimated that white-beaked dolphins can live more than 30 years old (Galatius et al., 2013b).

In the central and north-eastern North Atlantic, white-beaked dolphins range in the south from Cape Cod in the west, to around northern Portugal in the east. The range is limited in the north by Davis Strait in the west, and Svalbard and Novaya Zemlya in the east. There are also a few records of dolphins in the Baltic Sea (Kinze, 2018; Kiszka and Braulik, 2018). They can be found in shallow and deep waters, but are more commonly seen on the continental shelf (e.g. ASCOBANS, 2013; Canning et al., 2008; Kovacs et al., 2009; MacLeod et al., 2007). In the Barents Sea in August-September 2003-2009, dolphin density was found to be highest at depths of 150-200 m, but also at 400 m (Fall and Skern-Mauritzen, 2014). In the Norwegian Sea during the summers of 2009, 2010, and 2012, they were found predominantly along the shelf break (Nøttestad et al., 2015). In summer surveys of Icelandic waters between 1986 and 2001, they were observed more commonly in the northeast, southeast and southwest blocks but were rarely seen in the offshore blocks (Pike et al., 2009a). Off southwest Greenland, deep water with steep slopes seemed to have a high positive influence on density; large groups were found in depths of 300-1000 m and small groups (1-4 individuals) were found in deeper waters (Hansen and Heide-Jørgensen, 2013).

Water temperature has been described as an important driver of white-beaked dolphin distribution in several areas in the North Atlantic. Generally dolphins have been associated with waters 5-15 °C and limited to waters < 18°C (ASCOBANS, 2013; Kinze, 2018). A thermal niche function fitted to publicly available data on white-beaked dolphin presence-absence suggested the dolphins' core habitat to be in water temperatures 0-12 °C, with thresholds for marginal and unsuitable temperatures at around 12 °C and 16 °C, respectively (Lambert, 2012 In: ASCOBANS, 2013). During summer in the Barents Sea, white-beaked dolphin density peaked in water temperatures (at 50 m depth) around 2 °C and < 8°C (two peaks) in 2003-2006, but dolphins were associated with colder water temperatures around 2°C during 2007-2009. This association at 2°C in the later years has been linked with the Polar Front, which, compared to the weaker relationship in the earlier years, suggests an increase use of frontal areas (Fall and Skern-Mauritzen, 2014). In North Iceland at Skjálfandi Bay, in May-September 2004-2012, white-beaked dolphins were observed at water temperatures of 2.1-12 °C (Vallejo, 2013). In summer (June-July) west of Scotland, MacLeod et al. (2007) used

classification and regression trees to suggest preferred habitat in water temperatures < 11.9 °C. In this region, an increase in water temperature has been linked with an increase in white-sided dolphin occurrence and a decrease in white-beaked dolphins (MacLeod et al., 2005). In U.K. waters as a whole, white-beaked dolphin distribution seems limited by similar temperatures, as inferred from seasonal differences and a decline in reported strandings since 1970 (Canning et al., 2008). A more recent study including the whole North Sea in 1991-2017, found a slight increase in white-beaked dolphin strandings in the northwest (IJsseldijk et al., 2018).

Some changes in the distribution of white-beaked dolphins have been documented; seasonal changes could be influenced by summer being the most likely time for calving and mating (e.g. Canning et al., 2008; Galatius et al., 2013b; Galatius and Kinze, 2016). During the summer in UK waters, especially in the Scotland white-beaked dolphin females may move close to the coast to give birth. This matches with white-beaked dolphin sightings and calves and females strandings in the area (Canning et al., 2008). In the Western Atlantic, along the coasts of Labrador and West Greenland, white-beaked dolphins appear to move north in summer and south in winter (Hansen and Heide-Jørgensen, 2013; Alling and Whitehead, 1987 In: Lien et al., 2001). In US waters, a shift in distribution from the continental shelf before 1970 to the continental slope in the 1970s has been linked with changes in some prey and white-sided dolphin distribution (Katona et al., 1993; Kenney et al., 1996 In: Waring et al., 2006). In Greenland, it has been suggested that a decline in abundance in West Greenland (see below) could be due to migration to East Greenland driven by climate and productivity changes (Hansen et al., 2018).

White-beaked dolphins are mainly piscivorous, with a diet reflecting local prey abundance, although gadoid fishes are a major part of the diet (e.g. Canning et al., 2008; Dong et al., 1996; Fall and Skern-Mauritzen, 2014; Jansen et al., 2010). In the southern Barents Sea (Atlantic waaters), mesoscale association was found between white-beaked dolphins and blue whiting (gadoid), while variable relatioships were found in the nothern Barents Sea (Polar Front) area where capelin and gadoids occur (Fall and Skern-Mauritzen, 2014). In Icelandic waters, fish comprised 95% of the diet and squid 5% (Sigurjónsson and Víkingsson, 1997); more recent studies identified that the most dominant prey were the gadoids: haddock, cod, and saithe (*Pollachius virens*) (Vikingsson and Olafsdottir, 2004 In: Rasmussen et al., 2013). In the southern North Sea, stomach content analysis of data from 1968 to 2005 identified 25 fish species. Whiting and cod were the main components of the diet but no changes in diet were found over time or by sex or size class (Jansen et al., 2010). In Scottish waters, whiting and haddock were identified as the main prey species and cephalopods were also consumed (Canning

et al., 2008). Off West Greenland, white-beaked dophins have been observed in large numbers overlapping areas where haddock, capelin, and sandeel are distributed, suggesting that these fish species main form the main diet (Hansen and Heide-Jørgensen, 2013).

Foraging is assumed to be a primary activity for endemic and year-round resident white-beaked dolphins in the central and north-eastern North Atlantic (Kinze, 2018; Kiszka and Braulik, 2018; Kovacs et al., 2009), especially in summer because of the availability of abundant prey during this season. The modelled relationships are therefore likely to reflect environmental drivers related to finding prey. However, like killer whales, white-beaked dolphins are gregarious and social interactions including mating occur in summer (e.g. Canning et al., 2008; Galatius et al., 2013b; Galatius and Kinze, 2016). The modelled relations could thus explain the influence of environmental variables on activities other than foraging; for example, the influence of water temperature during calving.

Covariates included in the models have been chosen because they may have the power to explain foraging behaviour (see also general justification of the included covariates in section 2.2.2.1 and Table 2.3). Other studies have found relationships between white-beaked dolphin density and depth, slope, fronts, SST and prey species (see above). Covariates related to primary production are expected to have a lagged relationship with white-beaked dolphin density because they feed high in the trophic web. Covariates linked with prey aggregation such as SSH and mlp are expected to be related to prey accumulation and to have little to no lag. Salinity is related to water masses and in the study area may explain the influence of Arctic versus temperate water on white-beaked dolphin distribution. Bottom water temperature relates to deep water horizontal gradients which are relevant for white-beaked dolphins that mainly feed on benthic fish species.

White-beaked dolphin abundance has been estimated from line-transect surveys, for which other species have been the main target. In estimates from early Norwegian surveys all small dolphins were grouped but white-beaked dolphins were the most commonly observed species. In Norwegian waters, including the southern Barents Sea, south and west of Svalbard, and north of 56°N in the North Sea, white-beaked dolphin abundance has been estimated as 132,000 (95% CI: 79,000-220,000) in 1988 and 91,000 (*CV* = 0.59) in 1995 (Øien, 1996 In: Galatius and Kinze, 2016). In the more recent Norwegian surveys, estimates have been made for white-sided and white-beaked dolphins combined. In the Barents Sea, Greenland Sea, Norwegian Sea, and northern North Sea, estimates are 218,640 (95% CI: 150,330–318,000) in 2002-2007, 163,688 (95% CI: 112,673-237,800) in 2008-2013, and 187,482 (95% CI: 112,434-312,624) in 2014-2018 (NAMMCO, 2019a). Abundance in Icelandic-Faroese waters from shipboard surveys in 2007 is given in Table 5.2. The aerial survey around Iceland estimated 46,683 white-beaked dolphins (95% CI: 22,409-97,251) in the same year, and 75,959 (95% CI: 26,366-218,834)

in 2009. The most recent is given in Table 5.2. In Icelandic waters from 1986 to 2016, there has been an overall annual abundance increase of 0.07 (CV =0.22), which could be due to changes in distribution within and outside the survey area (NAMMCO, 2019a). In West Greenland, estimated abundance in 2015 is lower than in 2007, while the estimate from East Greenland in 2015 is the first available for the area Table 5.2 (Hansen et al., 2018).

Table 5.2. Most recent abundance estimates of white-beaked during line-transect surveys.

Areas	Year	Estimate	95% Confidence interval	Reference
West Greenland	2015	15,261	7,048-33,046	Hansen et al., (2018)
East Greenland (coastal)	2015	11,889	4,710-30,008	Hansen et al., (2018)
Iceland/Faroe Islands (shipboard)	2007	91,277	32,351-257,537	NAMMCO, (2019a)
Iceland (aerial)	2016	59,966	24,907-144,377	NAMMCO, (2019a)

White-beaked dolphins have been listed by the International Union for Conservation of Nature (IUCN) as Least Concern (LC) since 1996 (Kiszka and Braulik, 2018).

Anthropogenic pressures on white-beaked dolphins could include small scale harvest, by-catch, acoustic pollution, contaminants and oceanographic changes due to climate change. White-beaked dolphins have been hunted, but they have never been the target of a commercial harvest. Currently, they are only opportunistically caught in Greenland and the Faroe Islands (IWC, 2020). White-beaked dolphins can be bycaught or entangled in fishing gear, but the extent of this mortality is unknown (Galatius and Kinze, 2016; Northridge, 1991). In Icelandic waters, 25% of 90 photo-identified individuals have scars or wounds that could be from entanglement in fishing gear (Bertulli et al., 2012). White-beaked dolphins caught in pelagic trawls and driftnets-gillnets have been reported in the eastern and western North Atlantic (e.g. Dong et al., 1996; Northridge, 1991). White-beaked dolphins have been recorded to respond to airgun emissions used in seismic surveys in UK waters (Stone et al., 2017; Stone and Tasker, 2006). Pollutants such as heavy metals and organic contaminants are found in white-beaked dolphins in high concentrations, these are similar or higher than the ones found in pilot whales or harbour porpoises (Galatius et al., 2013a; Muir et al., 1988; Siebert et al., 1999). The effects of the contaminant burden are unknown (Galatius and Kinze, 2016) but it may have a detrimental effect on the immune and reproductive systems, as believed to be the case in other species, such as killer whales (Jepson et al., 2016; Pedro et al., 2017). Negative effects on white-beaked dolphins have been suggested by climate change scenarios in the future, where the species may suffer

a reduction and fragmentation of its range in the Northeast Atlantic (Fernandez et al., 2013 In: ASCOBANS, 2013).

5.2 Methods

5.2.1 Estimation of effective strip width

Distance sampling methods are described in Chapter 2 (see section 2.2.1)

5.2.2 Modelling distribution and habitat use

Distribution and habitat modelling methods were applied as described in Chapter 2. The effort and sightings used for modelling the two Delphinidae species are shown in Figure 5.3. The number of sighted animals made during this effort is summarized in Table 2.1 and Table 2.2.

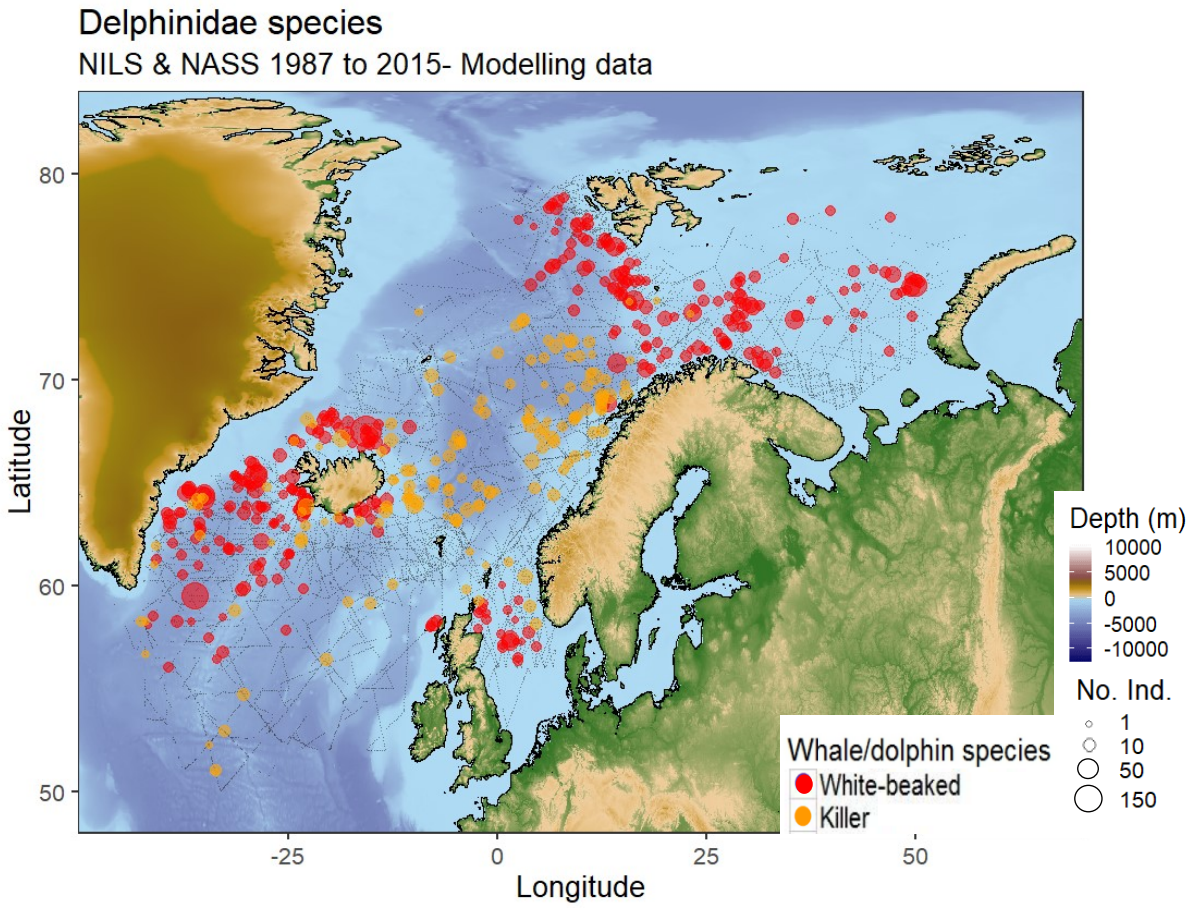

Figure 5.3. Summary of 1987 to 2015 NILS (Norway) & NASS (Iceland and Faroes) survey effort and sightings of killer whales and white-beaked dolphins used for modelling. Effort is depicted by segment mid-points as grey-dots. Sightings are shown as coloured dots, the size of which indicates the number of individuals (No. Ind.). The map was plotted using the geographic coordinate system WGS84 & overlaid over the bathymetry of the area (ETOPO2).

5.3 Results

5.3.1 Killer whales

5.3.1.1 Effective strip width – NASS (Iceland-Faroes) 1987-2015

The best detection function for the 1987-2015 killer whale NASS (Iceland and Faroese) data was a hazard rate model with a 2700 m truncation distance which included 127 sightings (Appendix 5-A). There were no covariates retained in the selected model. The fitted model is shown in Figure 5.4. The model fitted the data well as shown in the Q-Q plot Figure 5.4 and the goodness of fit test Cramer-von Mises test [unweighted] p = 0.939. The average probability of detection *p* was 0.262 (CV = 0.223). The estimated effective strip width was 888 m.

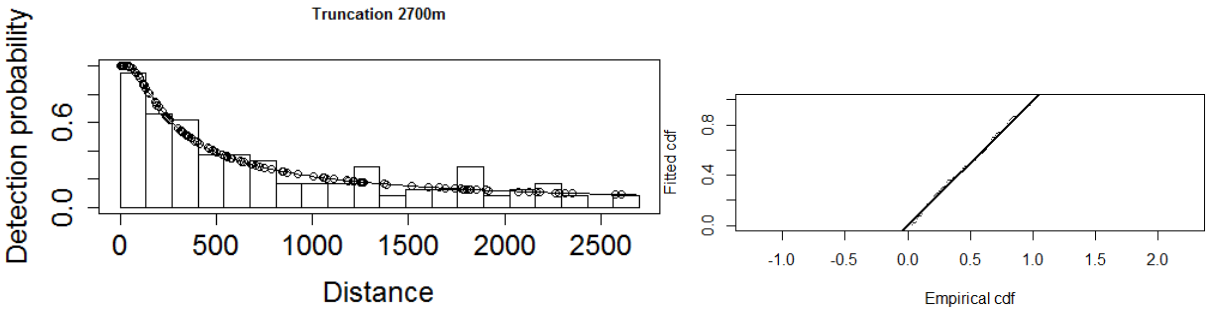

Figure 5.4. Detection probability (left) and Q-Q (right) plots for killer whale 1987-2015 NASS data. For detection probability, the open circles represent fitted values of the data, the line is the fitted model and the frequency histogram represents the observed data. In the Q-Q plot (right) the points are the fitted values while the solid line represents the expected data distribution.

5.3.1.2 Effective strip width – NILS (Norway) 1987-1989

The best detection function for the 1987-1989 killer whale NILS (Norwegian) data was a hazard rate model with no truncation distance, and it included a total of 31 sightings (Appendix 5-A). There were no covariates retained in the model. The model fitted the data well, as shown in the Q-Q plot Figure 5.5 and the goodness of fit test Cramer-von Mises test [unweighted] p = 0.992. The average probability of detection *p* was 0.341 (CV = 0.174). The estimated effective strip width was 873 m.

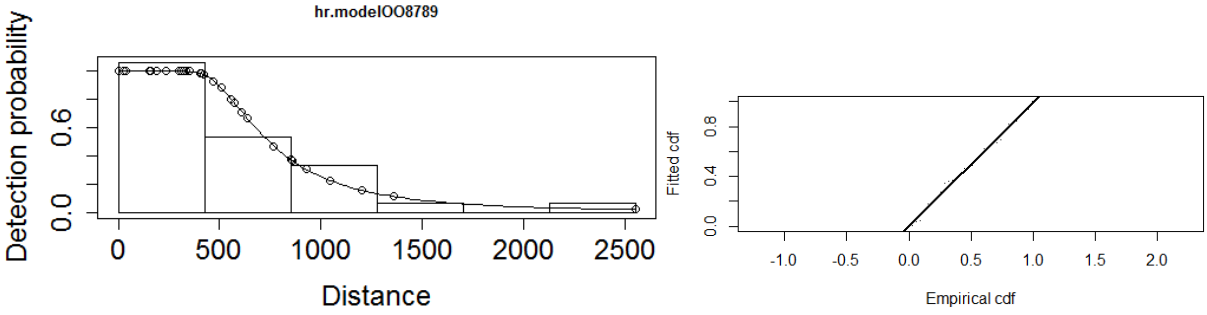

Figure 5.5. Detection probability (left) and Q-Q (right) plots for killer whale 1987-1989 NILS data. For detection probability, the open circles represent fitted values of the data, the line is the fitted model and the frequency histogram represents the

observed data. In the Q-Q plot (right) the points are the fitted values while the solid line represents the expected data distribution.

5.3.1.3 Effective strip width – NILS (Norway) 1995-2013

The best detection function for the 1995-2013 killer whale NILS (Norwegian) data was a hazard rate model with a 2000 m truncation distance which included a total of 353 sightings (Appendix 5-A). Beaufort (factor: three levels) was the only covariate retained in the selected model. As shown in the Q-Q plot Figure 5.6 and by the goodness of fit test Cramer-von Mises test [unweighted] p = 0.961, the model fitted the data well. The average probability of detection *p* was 0.32 (CV = 0.064). The estimated effective strip widths for the three covariate levels are given in Appendix 5-D.

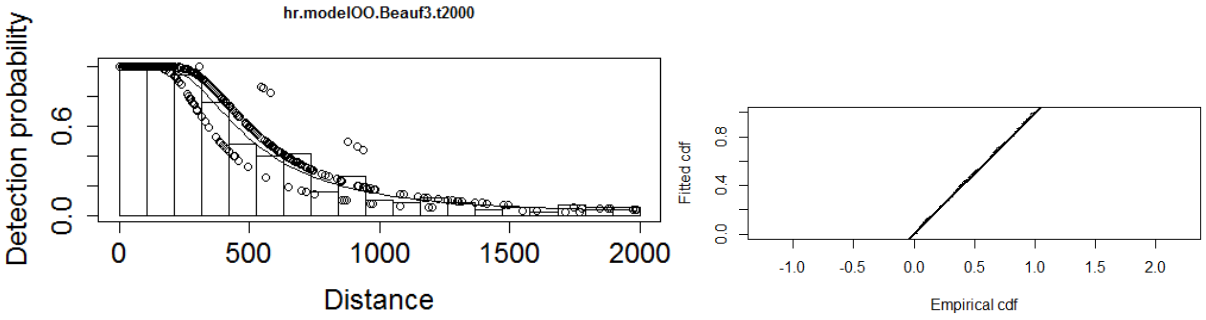

Figure 5.6. Detection probability (left) and Q-Q (right) plots for killer whale 1995-2013 NILS data. For detection probability, the open circles represent fitted values of the data, the line is the fitted model and the frequency histogram represents the observed data. In the Q-Q plot (right) the points are the fitted values while the solid line represents the expected data distribution.

5.3.1.4 Distribution and habitat use models: 1987-1989

The Tweedie was determined to be the best error distribution for the 1987-1989 spatial models for killer whales (Appendix 5-E). A summary of all the fitted single variable models is given in Appendix 5-F. The correlation evaluation between static variables and STT months is shown in Appendix 5-B, where none of the pairs had a Pearson's correlation coefficient greater than 0.7. As for other species, concurvity was not evaluated in the 1980s models (see methods section 2.2.2.4.1).

After fitting models to determine the best month for SST, the covariates selected in the best model included: depth, aspect, and May SST. The model fitted the data well as shown in Figure 5.7. Slope was penalized in the best model but also in all the other monthly SST models assessed. The best model had a deviance explained of 23.6% (Table 5.3). The AIC difference among all the SST models was no more than two AIC units.

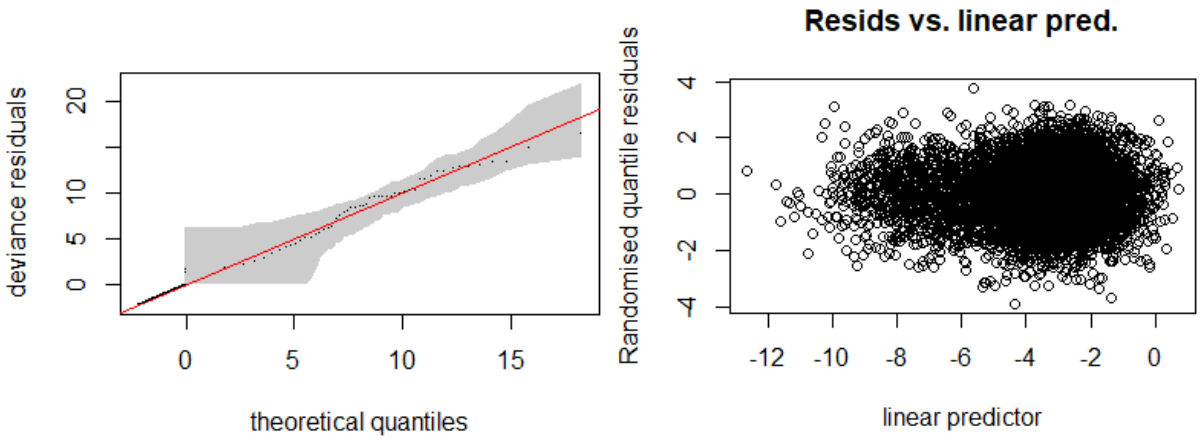

Figure 5.7. GAM diagnostics for the killer whale 1987-1989 best model. In the Q-Q plot (left) the shaded area represents 95% confidence interval, the circles represent the data, the line is the expected data distribution if the model fits the data perfectly. The residual versus linear predictor (right) does not show any patterns or presence of heteroscedasticity.

Table 5.3. Summary of killer whale 1987-1989 models at different SST months. The best error structure for all models was the Tweedie distribution. The model included the standard covariates survey and depth, and aspect plus the stated month for SST.

Model:	Deviance	Deviance explained (%)	AIC	REML	n
May	7275.85	23.63	6971.55	468.89	6695
April	8253.74	15.77	6971.69	472.78	
June	7656.74	20.46	6971.86	470.83	
July	8251.99	16.21	6972.68	472.99	
August	8413.31	15.18	6972.84	473.17	

The smooth functions show a predicted slight positive effect on killer whale density of depths around 1100 m, but overall the relationship with depth had high variability, showing no clear signal. Aspect had a positive effect towards north/northeast (0-120 °) and a negative effect to the southwest (190-230 °). May SST waters between 5-7 C˚ had a positive effect on killer whale density (Figure 5.8). All the other models with different SST months showed similar relationships with killer whale density, with positive effects between 6-10 C˚.

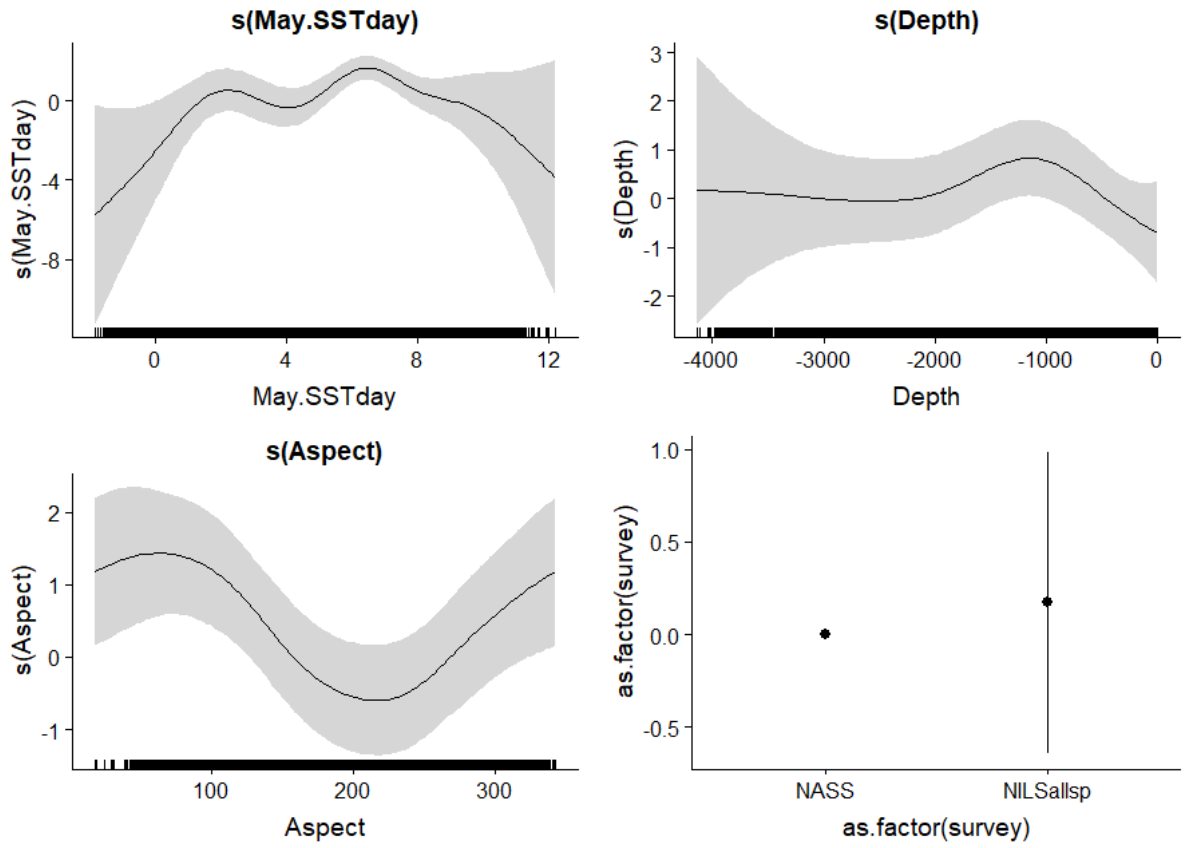

Figure 5.8. Relative density of killer whales as a smooth function of depth, aspect, and May SST for 1987-1989. Zero on the vertical axes corresponds to no effect of the covariate on the relative density of killer whales. Shaded areas represent 95% confidence intervals. The scales on each vertical axis vary among plots. Data points are represented as rug plots on the horizontal axes.

Predicted killer whale density 1987-1989 is show in Figure 5.9. Predicted density showed a good match to the observations off the coast of Norway in the Norwegian Sea, between the Faroes Islands and Iceland, around southeast Iceland and along the Reykjanes Ridge. The coefficient of variation (CV) of the predictions shows overall low precision in the predictions, except in the regions of highest predicted density (Figure 5.10).

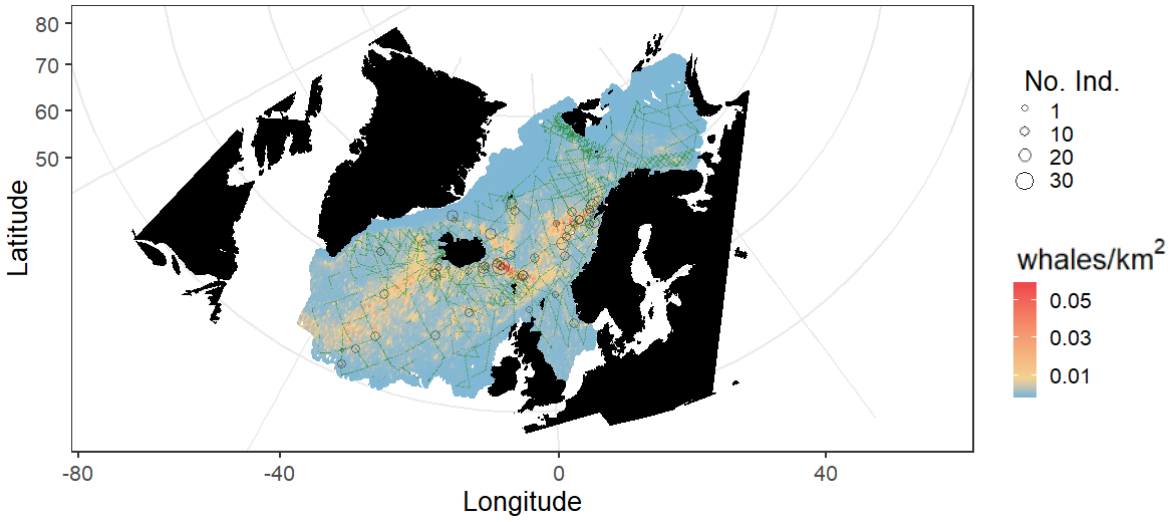

Figure 5.9. Predicted density of killer whales for the best-fitting model for 1987-1989, which included depth, aspect and May SST. The map shows killer whale observations as grey circles, the size of which indicates the number of individuals (No. Ind.), the small green dots represent the effort.

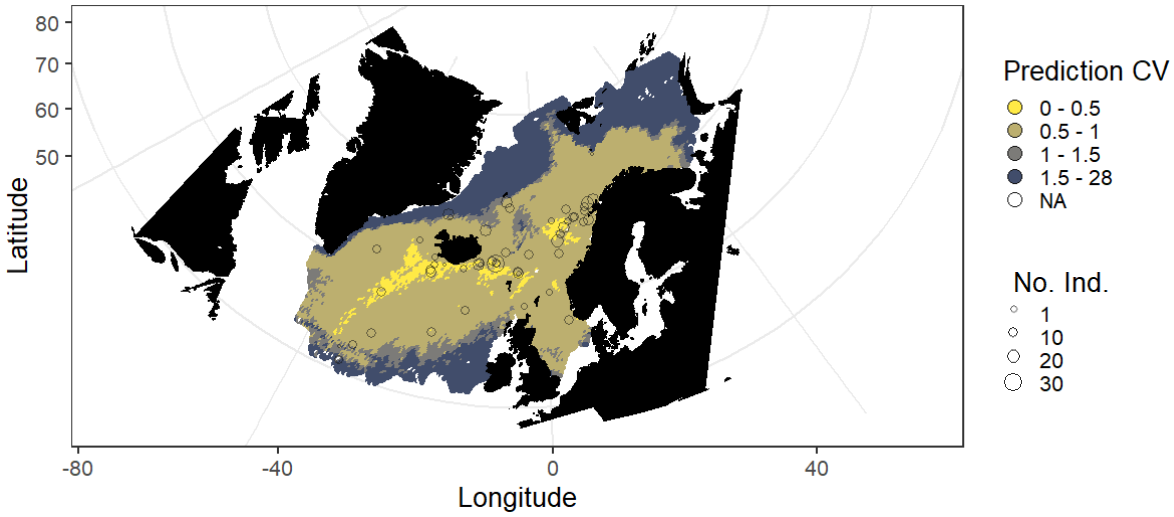

Figure 5.10. Coefficient of variation of the average predicted density of the best-fitting killer whale model for 1987-1989. Yellow areas show the highest precision. Killer whale observations are indicated as grey circles and scaled to the number of individuals (No. Ind.).

5.3.1.5 Distribution and habitat use models: 1998-2015

The negative binomial was determined to be the best error distribution for the killer whale spatial model for 1998-2015 (Appendix 5-G). A summary of all the fitted single variable models can be found in the Appendix 5-H. The best covariate for each variable family that were part of the candidate full model were: depth, aspect, slope, July bT, April SST, August salinity, April SSH, July mixed layer depth, May chlorophyll *a*, and May primary productivity. The terms that were removed by penalization were Aspect, August salinity, and May chlorophyll *a*. Further penalization due to collinearity and concurvity was needed, resulting in the removal of depth (Appendix 5-C and Appendix 5-I).

The covariates selected in the best model thus included: slope, July bT, April SST, April SSH, July mixed layer depth, and May primary productivity. The model fitted the data well Figure 5.11 and had a deviance explained of 30.14% (Table 5.4).

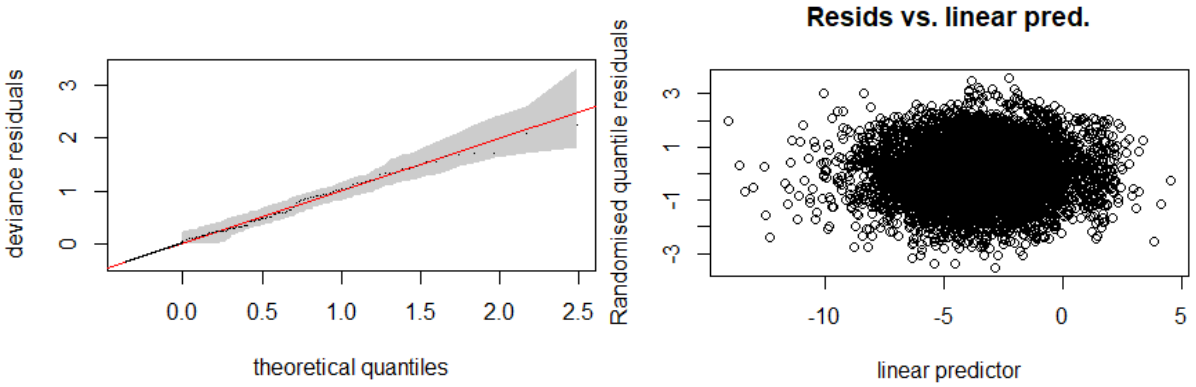

Figure 5.11.GAM diagnostics for the killer whale 1998-2015 best model. In the Q-Q plot (left) the shaded area represents 95% confidence interval, the circles represent the data, the line is the expected data distribution if the model fits the data perfectly. The residual versus linear predictor (right) does not show any patterns or presence of heteroscedasticity.

Table 5.4. Summary of the fitted models for killer whales 1998-2015 using a forward full model, double penalization and concurvity penalization. The best error structure for all models was the negative binomial distribution. All the models included the standard covariate survey.

Model: Survey +	Deviance	Deviance explained (%)	AIC	REML	n
Best model (concurvity)	263.70	33.69	1703.76	855.83	7452
Penalized full model	263.49	33.57	1704.74	855.65	
Full model	263.60	33.42	1703.15	855.48	

The best model only retained slope for the bathymetric variables, but it did not show a clear signal. April SST had a positive effect on killer whale density in waters between 3-7 C° and a negative effect either at colder or warmer temperatures. Bottom temperatures in July had a positive effect in waters of 274 K (0 C°) or colder and 281 K (8 C°) or warmer, and a negative effect in waters around 276 K (3 C°). Mixed layer depths in July and April SSH showed weak signals, higher densities were found at shallower mlp and less depressed SSH. May primary productivity had a positive effect in concentrations around 1000 C m^{-2} day^{-1} and a negative effect at lower and higher concentrations, especially above 1600 mg C m^{-2} day^{-1} (Figure 5.12).

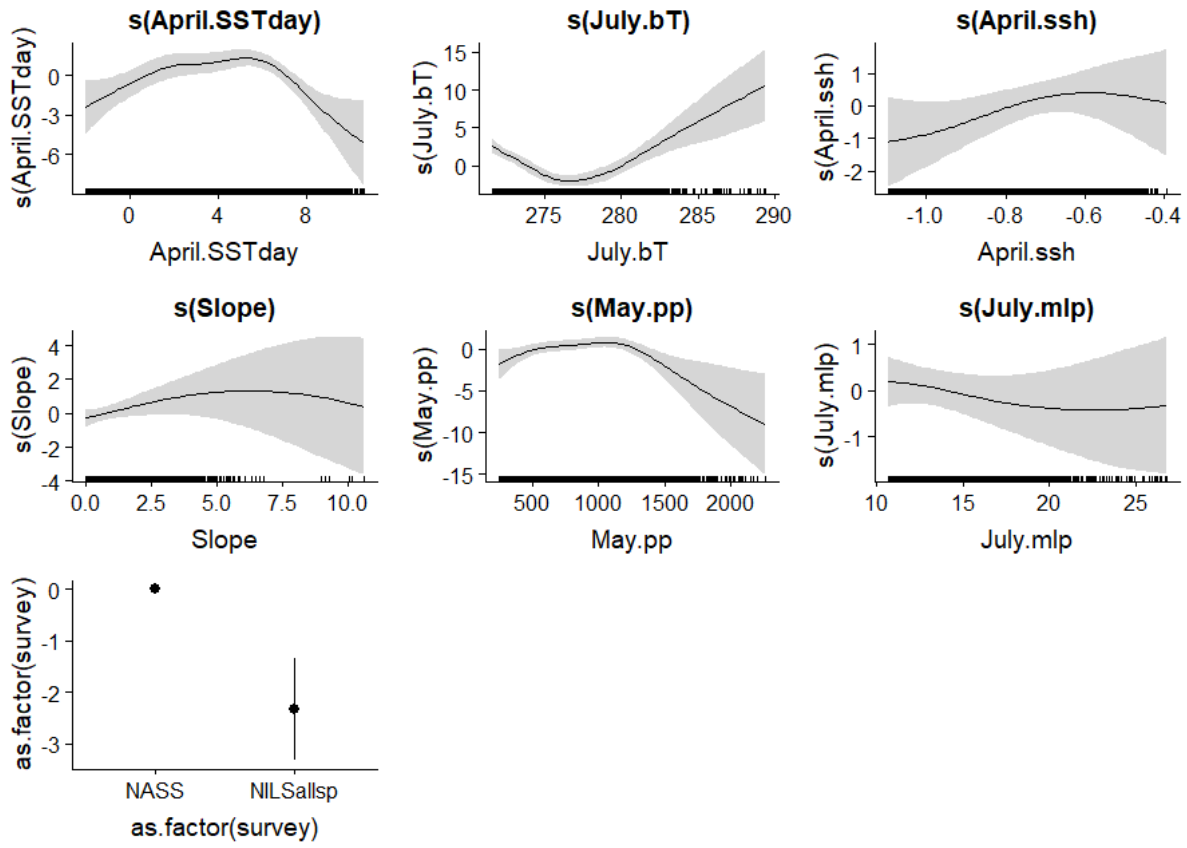

Figure 5.12. Relative density of killer whales as a smooth function of April SST, July bT, April SSH, slope, May primary productivity, and July mlp for 1998-2015. Zero on the vertical axes corresponds to no effect of the covariate on the relative density of killer whales. Shaded areas represent 95% confidence intervals. The scales on each vertical axis vary between plots. Data points are represented as rug plots on the horizontal axes.

Predicted killer whale density for the average values of the covariates across 1998-2015 is shown in Figure 5.13. The model reflected well the observations along the Norwegian coast, in the Norwegian Sea, to the north and northeast of Iceland and along the southern coast of Iceland. The CV of predicted density showed rather poor precision overall but generally better precision where the highest densities were predicted. There were high predictions with no observations around southwest Svalbard and at the southern edge of the study area in the North Sea. These may be edge effects resulting from the shape of the fitted relationship between density and bottom temperature (Figure 5.12). Around southwest Svalbard the precision was intermediate, while the very high-density values in the South of the North Sea have very low precision (Figure 5.14).

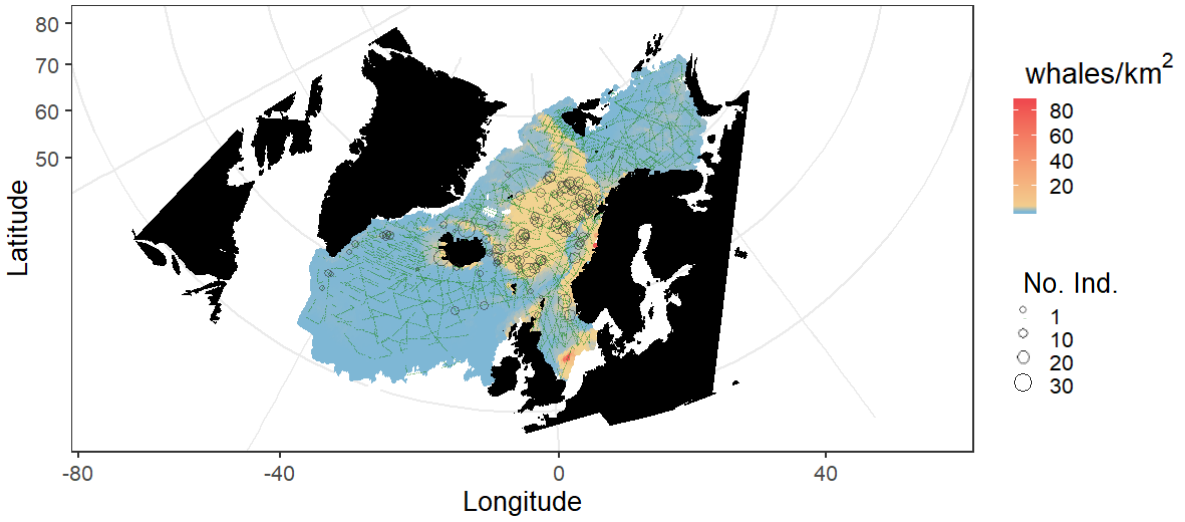

Figure 5.13. Predicted density of killer whales for the best-fitting model across 1998-2015 including April SST, July bT, April SSH, slope, May primary productivity, and July mlp. Killer whale observations are shown as grey circles, the size of which indicates the number of individuals (No. Ind.). Small green dots represent the effort.

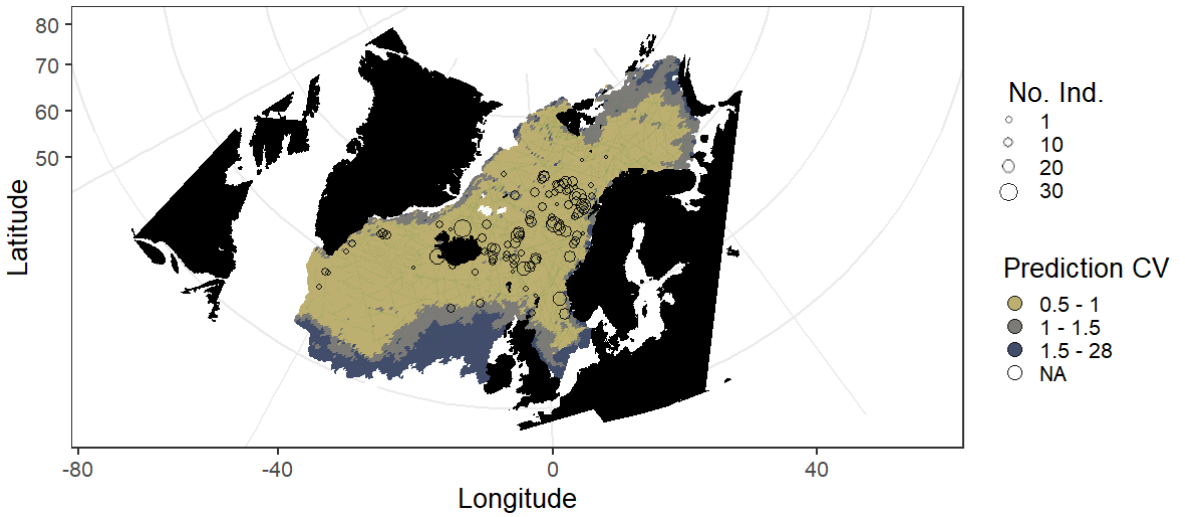

Figure 5.14. Coefficient of variation of the average predicted density of the best-fitting killer whale model for 1998-2015. Yellow areas show the highest precision. Killer whale observations are indicated as grey circles and scaled to the number of individuals (No. Ind.).

5.3.2 White-beaked dolphins

5.3.2.1 Effective strip width – NASS (Iceland-Faroes) 1987-2015

The best detection function for the 1987-2015 white-beaked dolphin NASS (Iceland and Faroese) data was a hazard rate model with a 1000 m truncation distance which included 308 sightings (Appendix 5-A). Vessel ID (ten levels) and Beaufort (two levels) were retained in the selected model. As shown in the detection probability, Q-Q plot Figure 5.15 and by the goodness of fit test Cramer-von Mises test [unweighted] p = 0.148, the model fitted the data well. The average probability of detection *p* was

0.089 (CV = 0.20). The estimated effective strip width for the combination of ten vessel ID covariate levels and two of Beaufort is given in Appendix 5-J.

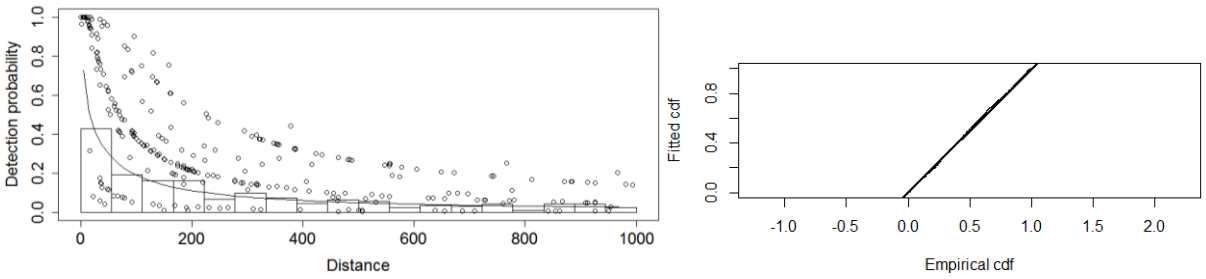

Figure 5.15. Detection probability (left) and Q-Q (right) plots for white-beaked dolphins 1987-2015 NASS data. For detection probability, the open circles represent fitted values of the data, the line is the fitted model and the frequency histogram represents the observed data. In the Q-Q plot (right) the points are the fitted values while the solid line represents the expected data distribution.

5.3.2.2 Effective strip width – NILS (Norway) 1987-1989

The best detection function for the 1987-1989 white-beaked dolphin NILS (Norwegian) data was a hazard rate model with a 800 m truncation distance which included a total of 22 sightings (Appendix 5-A). No covariates were retained in the selected model. As shown in the detection probability Q-Q plot Figure 5.16 and by the goodness of fit test Cramer-von Mises test [unweighted] p = 0.978, the model fitted the data well. The average probability of detection *p* was 0.223 (CV = 0.407). The estimated effective strip width was 178 m.

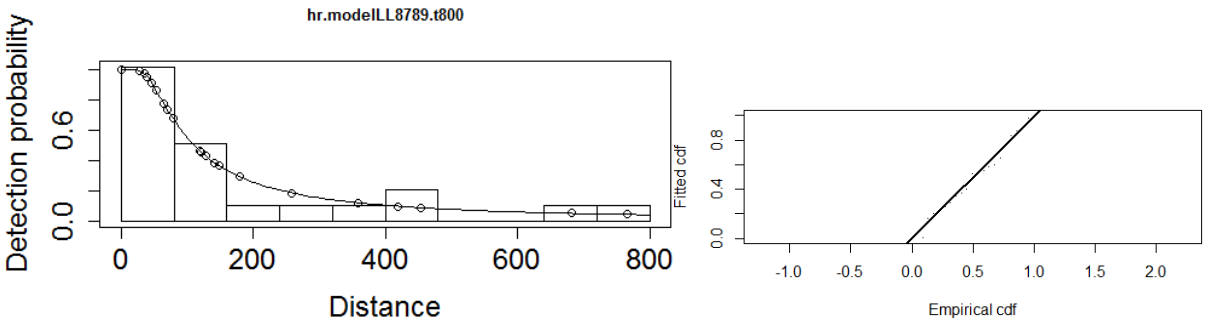

Figure 5.16. Detection probability (left) and Q-Q (right) plots for white-beaked dolphins 1987-1989 NILS data. For detection probability, the open circles represent fitted values of the data, the line is the fitted model and the frequency histogram represents the observed data. In the Q-Q plot (right) the points are the fitted values while the solid line represents the expected data distribution.

5.3.2.3 Effective strip width – NILS (Norway) 1995-2013

The best detection function for the 1995-2013 white-beaked dolphin NILS (Norwegian) data was a hazard rate model with a 1000 m truncation distance which included a total of 726 sightings (Appendix 5-A). Beaufort (three levels) was retained in the selected model. As shown in the detection probability

Q-Q plot Figure 5.17 and by the goodness of fit test Cramer-von Mises test [unweighted] p = 0.183, the model fitted the data well. The average probability of detection *p* was 0.317 (CV = 0.055). The estimated effective strip width for the three covariate levels is given in Appendix 5-K.

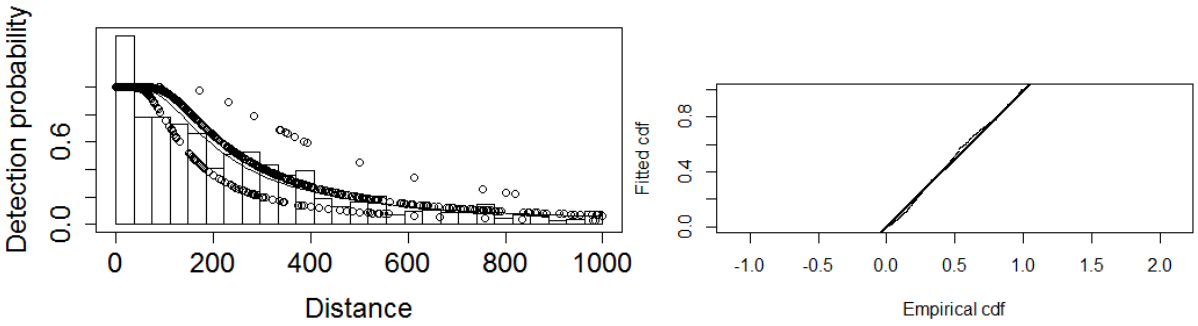

Figure 5.17. Detection probability (left) and Q-Q (right) plots for white-beaked dolphins 1995-2013 NILS data. For detection probability, the open circles represent fitted values of the data, the line is the fitted model and the frequency histogram represents the observed data. In the Q-Q plot (right) the points are the fitted values while the solid line represents the expected data distribution.

5.3.2.4 Distribution and habitat use models: 1987-1989

The negative binomial was determined to be the best error distribution for the 1987-1989 spatial models for white-beaked dolphins (Appendix 5-L). A summary of all the fitted single variable models is given in Appendix 5-M. The correlation evaluation between static variables and SST months is shown in Appendix 5-B, where none of the pairs had a Pearson's correlation greater than 0.7. As for other species, concurvity was not evaluated in the 1980s models (see methods section 2.2.2.4.1).

After fitting models to determine the best month for SST, the covariates selected in the best model included: depth, aspect, and April SST. The covariate slope was penalized and removed from the final model. The model fitted the data well as shown in Figure 5.18. The best model had a deviance explained of 41.4% (Table 5.5).

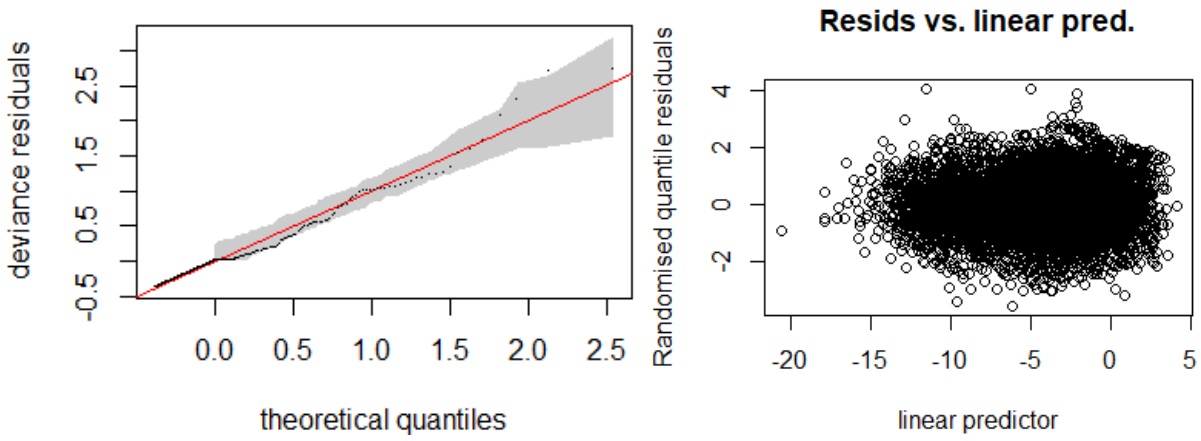

Figure 5.18. GAM diagnostics for the white-beaked dolphins 1987-1989 best model. In the Q-Q plot (left) the shaded area represents 95% confidence interval, the circles represent the data, the line is the expected data distribution if the model fits the data perfectly. The residual versus linear predictor (right) does not show any patterns or presence of heteroscedasticity.

Table 5.5. Summary of white-beaked dolphin 1987-1989 models at different SST months. The best error structure for all models was the negative binomial distribution. The model included the standard covariate survey and depth, slope, and aspect plus the stated month for SST. All the monthly models except April include slope.

Model:	Deviance	Deviance explained (%)	AIC	REML	n
April	276.73	41.40	1770.62	890.11	6695
May	272.31	42.29	1779.21	900.06	
July	276.47	36.50	1800.49	908.40	
June	274.16	36.93	1801.01	907.76	
August	280.83	17.15	1854.60	925.44	

The smooth functions show a predicted positive effect on white-beaked dolphin density of depths shallower than approximately 400 m; water deeper than 2900 m had a negative effect on density. Density was positively related to southerly aspects. April SST had a positive effect at temperatures between 2 °C and 6 °C (Figure 5.19).

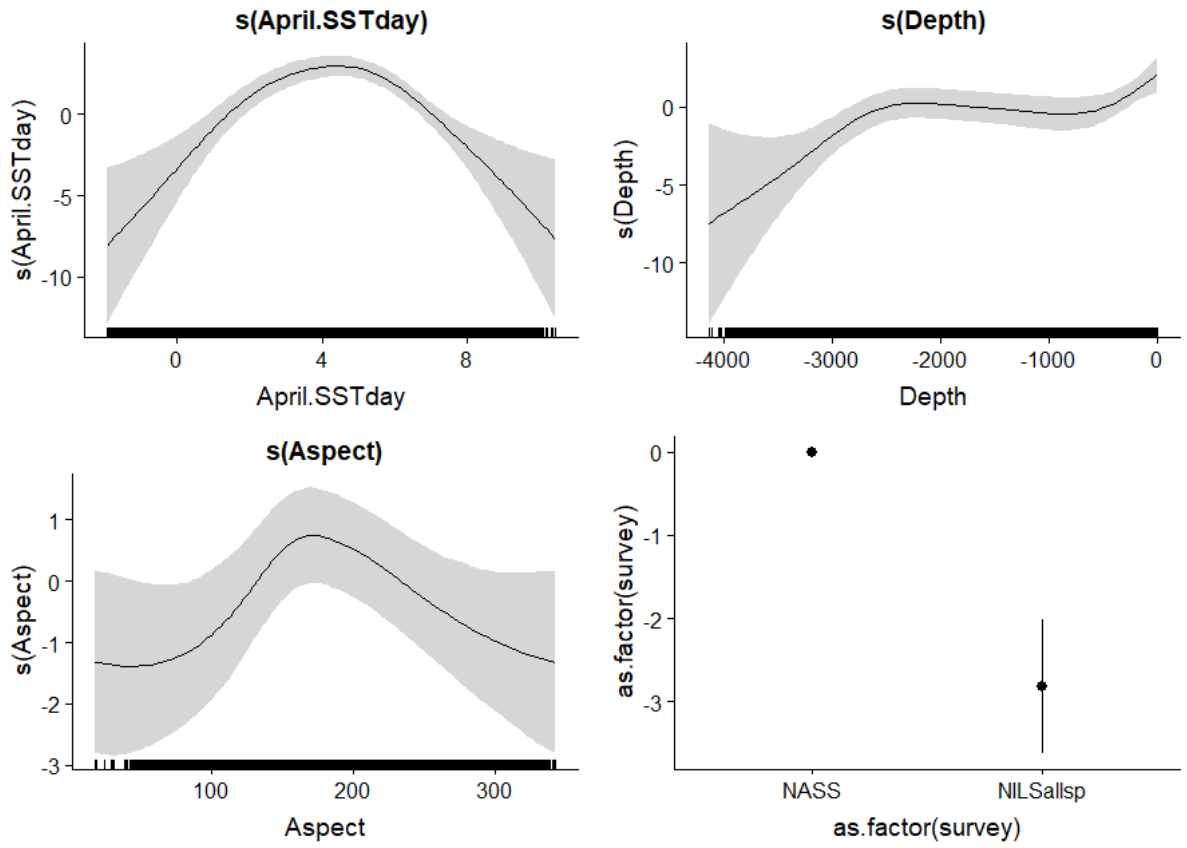

Figure 5.19. Relative density of white-beaked dolphins as a smooth function of depth, April SST, and aspect for 1987-1989. Zero on the vertical axes corresponds to no effect of the covariate on the relative density of white-beaked dolphins. Shaded areas represent 95% confidence intervals. The scales on each vertical axis vary among plots. Data points are represented as rug plots on the horizontal axes.

Predictions of white-beaked dolphin density for average values of covariates across 1987-1989 are show in Figure 5.20. The model reflected well the observations of white-beaked dolphin along the northern Norwegian coast (including the Barents Sea), around Iceland and the Reykjanes Ridge-Irminger Sea -Greenland southeast continental shelf area. High predicted density also occurred along the southern Norwegian coast and Danish waters in the North Sea, where there were few or no observations. The map of the CV of predicted density shows rather poor precision overall, with very poor precision around the edges of the area (Figure 5.21).

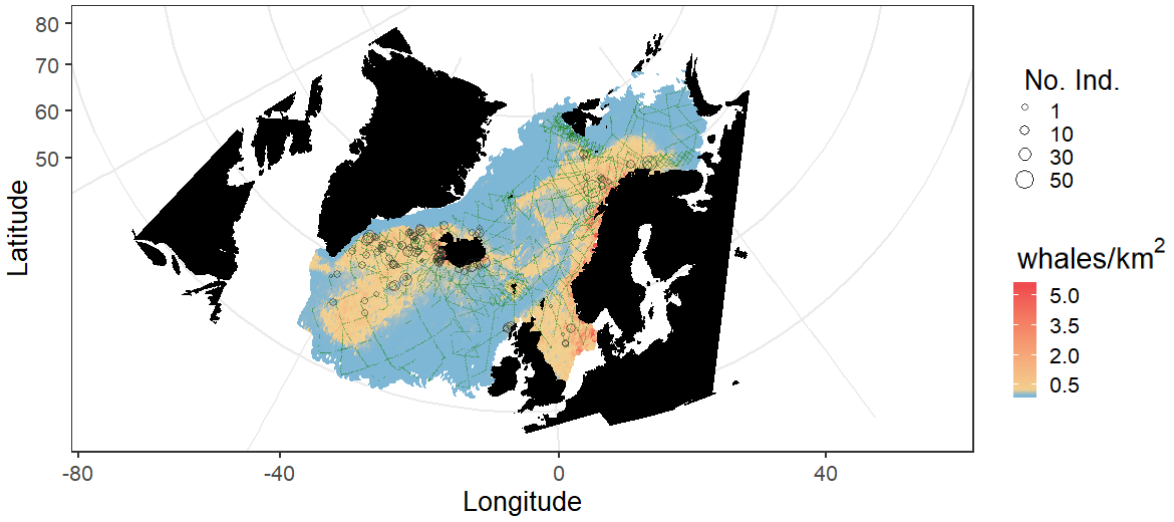

Figure 5.20. Predicted density of white-beaked dolphins for the best-fitting model for 1987-1989, which included depth, aspect and April SST. The map shows white-beaked dolphin observations as grey circles, the size of which indicates the number of individuals (No. Ind.), the small green dots represent the effort.

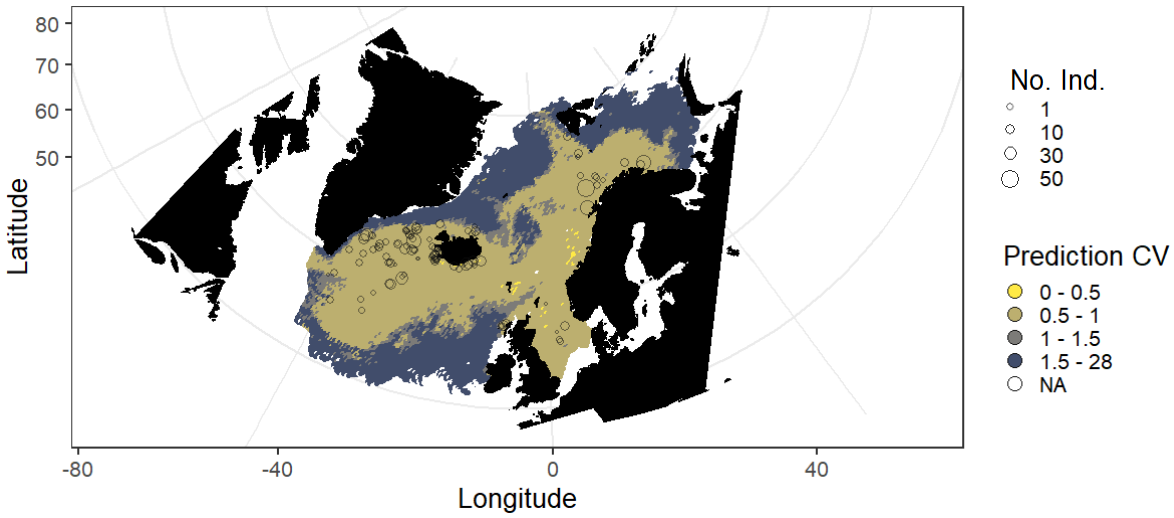

Figure 5.21. Coefficient of variation of the average predicted density of the best-fitting white-beaked dolphin model for 1987-1989. Yellow areas show the highest precision. White-beaked dolphins whale observations are indicated as grey circles and scaled to the number of individuals (No. Ind.).

5.3.2.5 Distribution and habitat use models: 1998-2015

The negative binomial was determined to be the best error distribution for the white-beaked dolphin spatial models for 1998-2015 (Appendix 5-N). A summary of all the fitted single variable models can be found in the Appendix 5-O. The best covariates for each variable family that were included for consideration in the full model were: depth, aspect, slope, April bT, August SST, May salinity, June SSH, April mixed layer depth, August chlorophyll *a*, and April primary productivity. The terms removed by penalization were slope, aspect, May salinity, August chlorophyll *a*, and April primary productivity. In the remaining full model, after double penalization, collinearity and concurvity were found between

bT/depth, consequently bT was retained (Appendix 5-C and Appendix 5-P) (see methods section 2.2.2.4.1).

The covariates selected in the best model thus included: April bT, August SST, June SSH, and April mixed layer depth. The model fitted the data well Figure 5.22. The best model had a deviance explained of 27.5 % (Table 5.6).

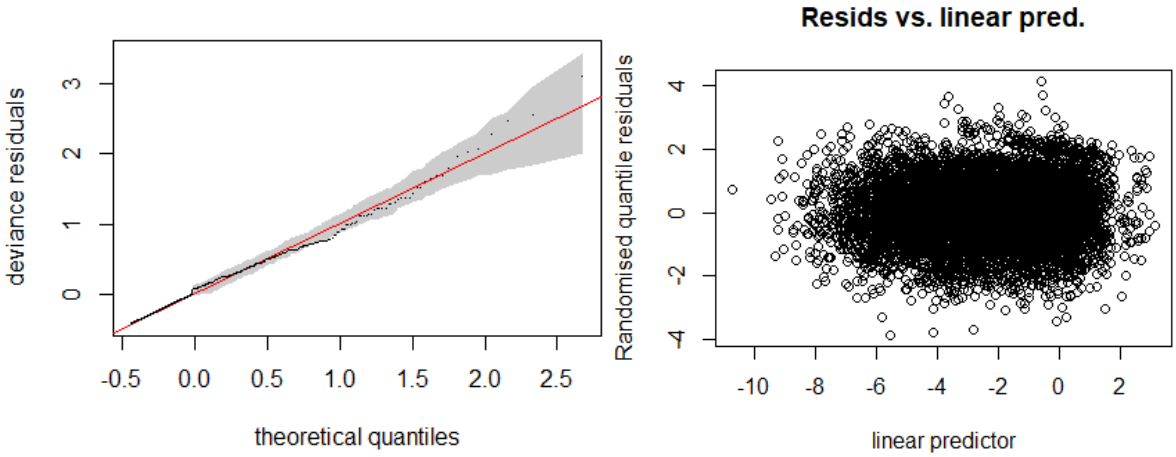

Figure 5.22. GAM diagnostics for the white-beaked dolphin 1998-2015 best model. In the Q-Q plot (left) the shaded area represents 95% confidence interval, the circles represent the data, the line is the expected data distribution if the model fits the data perfectly. The residual versus linear predictor (right) does not show any patterns or presence of heteroscedasticity.

Table 5.6. Summary of the fitted models for white-beaked dolphins 1998-2015 using a forward full model, double penalization and concurvity penalization. The best error structure for all models was the negative binomial distribution. All the models included the standard covariate survey.

Model:	Deviance	Deviance explained (%)	AIC	REML	n
Best model (concurvity)	546.30	27.50	3416.45	1719.89	7361
Penalized full model	546.80	27.09	3412.19	1712.70	
Full model	546.61	27.01	3413.53	1713.15	

The best model for white-beaked dolphins for 1998-2015 did not retain any bathymetric variables. The smooths showed that August SST had a positive effect on white-beaked dolphin density at temperatures between 5-10 °C, and negative in cooler and warmer waters. April bottom temperature had a rather strong positive effect at 276-279 K (3-6 °C), and a negative effect at waters around 273 K (0 °C) or colder. The effect of June SSH was negative above and positive below a depth of around -0.7 m. April mixed layer depth had a weak signal with shallow depths having a slight positive effect (Figure 5.23).

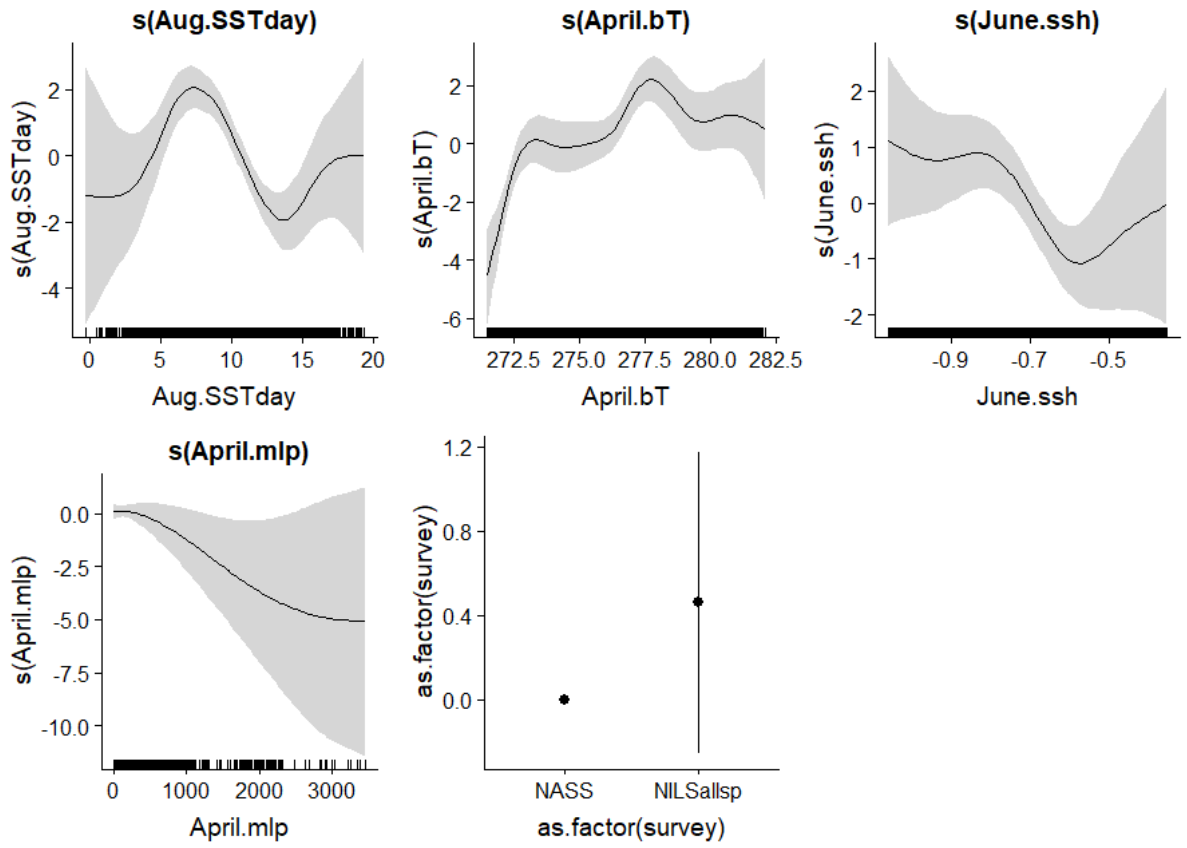

Figure 5.23. Relative density of white-beaked dolphins as a smooth function of August SST, April bT, June SSH, and April mixed layer depth for 1998-2015. Zero on the vertical axes corresponds to no effect of the covariate on the relative density of white-beaked dolphins. Shaded areas represent 95% confidence intervals. The scales on each vertical axis vary among plots. Data points are represented as rug plots on the horizontal axes.

Predictions of white-beaked dolphin density for 1998-2015 are shown in Figure 5.24. The model prediction reflected well the high number of observations in the Barents Sea, off southwest Svalbard, north of Iceland, in the Denmark Strait, and the Reykjanes Ridge - Irminger Sea -Greenland southeast continental shelf area. There were some sightings, but low predicted density in the North Sea. Conversely, there were no sightings but high predicted density around Jan Mayen and Mohns Ridge. The map of the CV of predicted density shows reasonable precision in areas where predicted density of white-beaked dolphins is high, except most of the Barents Sea, the North Sea and part of Denmark Strait. The lowest precision was around the extreme edges of the area (Figure 5.25).

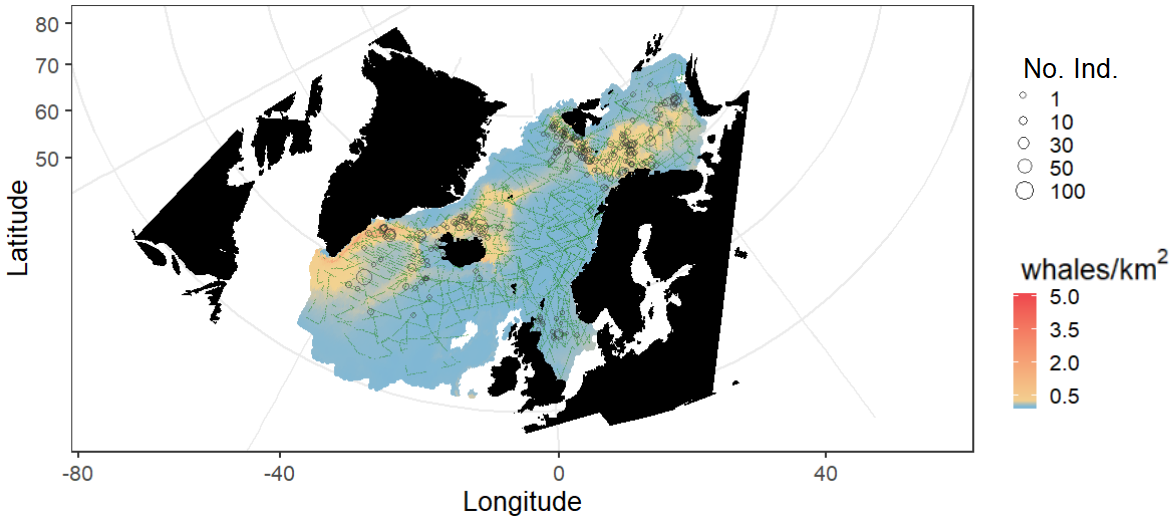

Figure 5.24. Predicted density of white-beaked dolphins for the best-fitting model for 1998-2015, which included April bT, August SST, June SSH, and April mixed layer depth. The map shows white-beaked dolphin observations as empty circles, the size of which indicates the number of individuals (No. Ind.), the small green dots represent the effort.

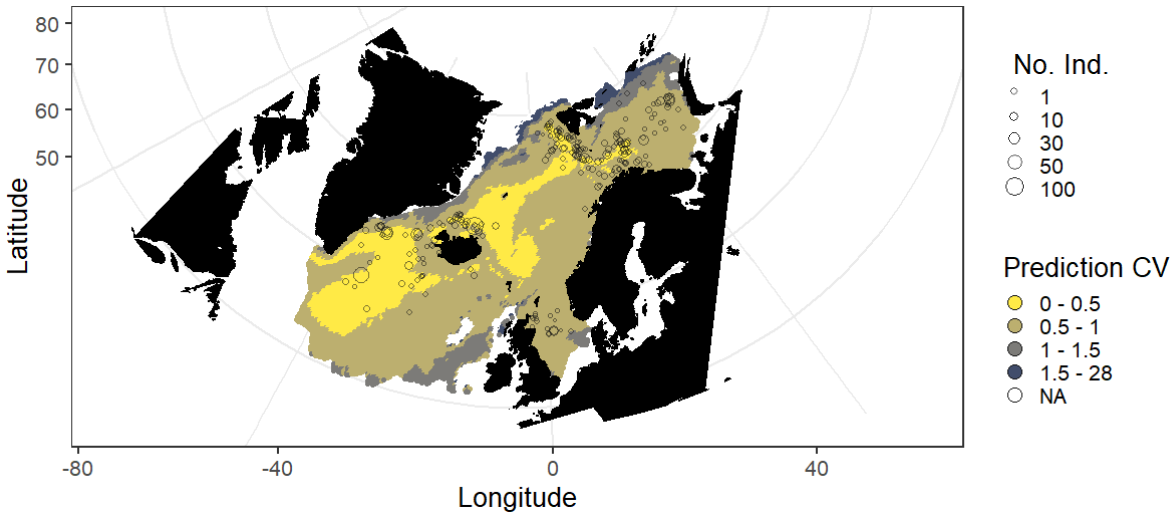

Figure 5.25. Coefficient of variation of the average predicted density of the best-fitting white-beaked dolphin model for 1998-2015. Yellow areas show the highest precision. White-beaked dolphin observations are indicated as grey circles and scaled to the number of individuals (No. Ind.).

5.4 Discussion

5.4.1 Killer whales

Killer whale distribution in the central and north-eastern North Atlantic is likely to be influenced to some extent by population structure. However, there is no clear definition between offshore and inshore killer whales in the Atlantic, nor are there different whales' types such as described in the North Pacific and the Antarctic (see section 5.1.1). There is evidence of foraging diversity in killer whales in the central and north-eastern North Atlantic (e.g. Foote et al., 2013, 2009). For example, in

the Norwegian Sea, killer whales isotopic signals had seasonal differences showing some prey specialization but also some changes in seasonal preference (Jourdain et al., 2020). Given the state of the knowledge of the species in the area indicating an absence of habitat divisions and given the dynamic relationship with their prey (see section 5.1.1), it is appropriate to analyse all killer whale data together.

Relationships between killer whale density and oceanographic features

The models predicting density of killer whales in 1987-1989 (early) and 1998-2015 (recent) did not show clear consistent relationships with oceanographic features. Of the bathymetric variables, the early model retained depth and aspect while the recent model only retained slope. Only aspect in the early model showed a clear signal (Figure 5.8 and Figure 5.12). These unclear signals related to bathymetry are consistent with the occurrence of killer whale over a broad range of depths (e.g. Bloch and Lockyer, 1988; Forney and Wade, 2007; Lennert and Richard, 2017; NAMMCO, 2019a; Øien, 1988; Samarra et al., 2018; Samarra and Foote, 2015; Similä et al., 1996; Storrie et al., 2018).

Killer whales also occur in a broad range of water temperatures. During the summer, they are found over the whole central and north-eastern North Atlantic including the Norwegian Sea, Icelandic-Faroes coast, East Greenland, and up to the ice edge in Svalbard and Barents Sea (e.g. Bloch and Lockyer, 1988; Foote et al., 2007; Kovacs et al., 2009; Lennert and Richard, 2017; NAMMCO, 2019a; Øien, 1988; Samarra and Foote, 2015; Storrie et al., 2018). In the best models, SST in spring months (May in the early model, April in the recent model) were retained, showing a positive effect at temperatures of 5-7°C and 3-7°C, respectively. Negative effects occurred at cold temperatures and, in the recent model, above 8°C (Figure 5.8 and Figure 5.12). The importance of spring SST must be treated cautiously because, in the early period all of the SST lagged months had some support from the data (Table 5.3), showing positive effects in the range 5-10°C. Overall, the temperature ranges suggested by the models are not as broad as might be expected given the broad distribution of killer whales in the area.

The predicted positive effects in the recent model were at slightly colder temperatures despite the warming of several areas in the central and north-eastern North Atlantic (e.g. Haug et al., 2017; Havforskningsinstituttet, 2020; Víkingsson and Heide-Jørgensen, 2015). This could be linked to changes in the distribution of the main prey (e.g. Astthorsson et al., 2012) but it could also indicate that killer whales are 'colonizing' new regions and consuming other types of prey that occur in polar regions (e.g. Higdon and Ferguson, 2009; Lennert and Richard, 2017). Although not always present in

all the early models, the negative effects at cold temperatures of 0°C or below match the ice-avoidance behaviour described in the western Atlantic (Matthews et al., 2011); ice-entrapment can be fatal for killer whales (Matthews et al., 2019). Overall, the prediction of killer whales within an unexpectedly narrow SST range may be a result of a combination of prey availability, including exploitation of new food resources, and avoidance of ice entrapments.

A number of studies have described tight relationships between the distribution of killer whales and their prey, including changing their distribution from offshore to coastal within a year to follow their prey (e.g. Øien, 1988; Samarra et al., 2018; Similä et al., 1996). Killer whales are apex predators, they have a varied diet from fish to marine mammals (e.g. Bloch and Lockyer, 1988; Samarra et al., 2018; Samarra and Miller, 2015; Similä et al., 1996), and it is possible that the additional variables retained in the best recent model might indirectly elucidate these predator-prey relationships. Besides relief and April SST, July bottom temperature, April SSH, July mlp, and May primary productivity were retained in the best recent model. The dynamic variables had lagged relationships with both spring and summer months (Figure 5.8 and Figure 5.12). These mixed seasonal signals could result from the diverse diet of killer whales. The longer lag between spring and summer could reflect that killer whales feed high in the tropic web. The shorter summer lag could indicate that the whales are also taking advantage of aggregation of resources within the season due to currents (small eddies), for example. But, using the covariates retained in the model it is not possible to suggest the exact mechanisms that are driving killer whales' distribution, which would be expected for species that feed on a wide variety of prey.

Changes in killer whale distribution

In general, in the central and north-eastern North Atlantic it seems that killer whale distribution (and abundance) is variable and that summer surveys likely sample several whale populations (Christensen, 1988; Foote et al., 2007; NAMMCO, 2019a, 1993). Although complete estimates of abundance and information on trend are not available, abundance does not seem to have changed as clearly as for other cetacean species that have been a direct target of whaling (e.g. Hansen et al., 2018; Øien and Bøthun, 2009; Pike et al., 2009a; Víkingsson et al., 2015). The variation in density in subareas and the lack of marked changes overall indicates that the distribution changes observed here are likely due to movements of the killer whales over the whole area. The early and recent models both predict high density in the Norwegian Sea, around the Faroe Islands, around Iceland, and southwest of Jan Mayen (Figure 5.9 and Figure 5.13). This indicates that these areas remain important for killer whales. One difference between the two periods is a slight south-to-north shift in distribution. In the early years,

the predicted density distribution reflected the observations south of Icelandic offshore waters along the Mid-Atlantic Ridge. In recent years, predicted density reflected observations in northern waters, including the wider distribution in the Norwegian Sea, southwest of Svalbard and in the Barents Sea. This greater occurrence in polar waters in recent years has also been described in waters off Greenland and Canada as previously discussed (e.g. Higdon and Ferguson, 2009; Lennert and Richard, 2017; Matthews et al., 2019, 2011). The Norwegian Sea seem of great importance in the recent model (Figure 5.13) and this may be linked with the increase in the NSS herring stock return to the previous feeding grounds (e.g. Dalpadado et al., 2000; Misund et al., 1997), as it was in the 1970s (Øien, 1988).

In summary, over the 30-year study period, there have been some changes in killer whale distribution from the south towards the north; however, there are also several areas that have maintained their importance over time. The high variability in the predicted density of killer whales in the area is likely linked to the highly mobile foraging of this species. This movement could relate to changes in prey distribution, including new resources that some of the whales in the area, at least, are taking advantage of (e.g. Lennert and Richard, 2017; NAMMCO, 1993; Samarra et al., 2018; Samarra and Miller, 2015; Similä et al., 1996). This high variability could also explain why no clear pattern in the model covariates was found, except for temperature, and the lack of clarity in the lagged relationships in some variables. The range in temperature seems important. There was some overlap between the early and recent periods; in the recent period a slight colder range could indicate that killer whales are now taking advantage of new available habitats/prey (e.g. Lennert and Richard, 2017; NAMMCO, 1993; Storrie et al., 2018).

5.4.2 White-beaked dolphins

Relationships between white-beaked dolphin density and oceanographic features

White-beaked dolphins are commonly found in shallow waters, but they can be common in deeper waters in some areas (e.g. ASCOBANS, 2013; Canning et al., 2008; Fall and Skern-Mauritzen, 2014; Hansen and Heide-Jørgensen, 2013; MacLeod et al., 2007). In the central and north-eastern North Atlantic most studies have described higher dolphin occurrence in shallower waters except off Greenland (e.g. ASCOBANS, 2013; Fall and Skern-Mauritzen, 2014; Hansen and Heide-Jørgensen, 2013; MacLeod et al., 2007). Here, the relationships found were similar, with a predicted higher probability to find dolphins in shallower waters in the early period (Figure 5.19). A similar relationship was found in the recent period, but depth was not retained in the model. Lien et al., (2001), stated

that the higher reported occurrence of white-beaked dolphins in coastal areas could be due to these areas being more likely to be surveyed and/or sightings to be reported. An important contribution of the work presented here is that the study area is broad, including coastal and offshore areas, and white-beaked dolphins have been found in coastal areas but also shallower areas away from the coast (Figure 5.20 and Figure 5.24).

The relationship between white-beaked dolphin distribution and sea surface water temperature has been described as one of the main drivers of their distribution (e.g. ASCOBANS, 2013; Fall and Skern-Mauritzen, 2014; MacLeod et al., 2007; Vallejo, 2013) in which species distribution range is limited by water temperature (Lambert, 2012 In: ASCOBANS, 2013). The months retained in the models presented here were April STT in the early period and August SST in the recent period (Appendix 5-O); that is, a different seasonal signal between the two periods. Generally, the main hypothesis is that species that feed higher in the tropic web (as do dolphins) may have a longer lagged relationship with variables that change as the season progresses, for example water temperature and chlorophyll *a* concentration. White-beaked dolphins inhabit and feed in the study area year–round (Kovacs et al., 2009; Magnusdottir, 2007 In: Rasmussen et al., 2013). Besides feeding, they mate and give birth during the summer (e.g. Canning et al., 2008; Galatius et al., 2013b; Galatius and Kinze, 2016). Therefore, the fitted relationships reflect not only factors influencing feeding but also mating and calving.

The effects on white-beaked dolphin density of temperatures in the early and recent models, although they come from different seasons, have in common positive effects in cold waters (Figure 5.19 and Figure 5.23). These ranges reflect the core habitat, preferred areas, or high density areas for white-beaked dolphins in the whole North Atlantic and also in smaller areas such as around Scotland, north of Iceland, or the Barents Sea (ASCOBANS, 2013; Fall and Skern-Mauritzen, 2014; MacLeod et al., 2007; Vallejo, 2013). Negative effects were found in very cold waters <1 °C or warmer waters >8 °C in the early model (spring signal) and 11-15 °C in the recent model (summer signal) (Figure 5.19 and Figure 5.23). Ice-related waters or waters warmer than 18 °C have been described as temperatures beyond the range limits for the white-beaked dolphins (e.g. Lambert, 2013 In: ASCOBANS, 2013). In summary, sea surface temperature has an effect on white-beaked dolphin distribution. The difference between the early and recent models in the temperature range having a positive effect may be a result of the different seasons retained in the two models.

Several covariates in addition to relief-related covariates and SST were retained in the best recent model: April bottom temperature, April mixed layer depth, and June SSH. The covariates selected have both spring and summer signals. April bottom temperature showed a positive effect at temperatures 3-6 °C and negative effect in very cold waters of 0 °C or less (Figure 5.23). This relationship suggests

the waters that influence their distribution along the water column (surface and bottom) are temperate. Fall and Skern-Mauritzen, (2014), found in the Barents Sea that white-beaked dolphins did not always occurred at the Polar Front and no prey associating were identified in that area. Mixed layer depth and SSH are related to the water column structure and possibly to prey aggregation. The effects of mixed layer depth are not clear. June SSH had a positive effect on dolphin density when it was more negative (Figure 5.23). This reflects the area of high white-beaked dolphin density around the Irminger Sea, an area with the strongest negative SSH anomaly (Hátún et al., 2009). More negative SSHs tend to be related to cyclonic (cold-core) rings and high Chlorophyll *a* (Leterme and Pingree, 2008), which could lead to prey accumulation due to high productivity. It would be expected that the dolphins would take advantage of prey accumulations as they formed, within the same season. A confounding factor in interpreting these results is that SSH has varied over time in the studied area (Broomé et al., 2019). Overall, these additional variables in the recent model suggest that in summer white-beaked dolphins occur in areas that are influenced by temperate waters with strong negative SSH.

Changes in white-beaked dolphin distribution

Changes in white-beaked dolphin distribution were predicted by the models, but the results are not very precise, especially in the early model (Figure 5.21 and Figure 5.25). In general, higher density is predicted in more northerly areas in recent years. The models predicted higher densities in the Barents Sea in recent years and lower density in the Norwegian Sea. White-beaked dolphins are believed to be year-round residents in the Barents Sea but their ecology in the area is poorly known (Fall and Skern-Mauritzen, 2014; Kovacs et al., 2009). It is also unknown if the lower densities of dolphins in the Norwegian Sea (Figure 5.24) are linked to increased temperatures there (Mork et al., 2019; Nøttestad et al., 2015). The recent model also predicts high density off SE Greenland; although this area is not in the north it is an area under the influence of polar and temperate waters (Figure 1.2). Despite the low coverage of the area by NASS, Greenland aerial surveys have also covered the area and found high density matching this prediction (Hansen et al., 2018). Overall, these results reflect the suggestion that a displacement in distribution to the north is linked to warming waters in the southern range of the species (e.g. Canning et al., 2008; IJsseldijk et al., 2018; MacLeod et al., 2005).

Comparing the covariates from the best early and recent models, as described above, there are no clear explanations for the differences. The early model retained relief covariates and spring SST, while the recent model did not keep any relief covariate but retained summer SST. Moreover, in the recent period, two different covariates were related to prey aggregation were retained, SSH and mlp, but the

lagged relationships again differed in season: summer and spring, respectively. These differences could be related to dolphins using different features, such as sometimes the Polar Front and sometimes not (Fall and Skern-Mauritzen, 2014). It is also possible that the mixed signals from the covariates between periods and within the recent period reflect relationships that may explaining types of behaviour other than foraging.

The results presented here are the first at this scale for white-beaked dolphins in the central and north-eastern North Atlantic. It was found that dolphins are distributed in general in coastal or shallower areas and, as suggested from smaller scale studies, that water temperature seems to have an important influence on distribution (e.g. Lambert, 2013 In: ASCOBANS, 2013; Fall and Skern-Mauritzen, 2014; Galatius and Kinze, 2016; MacLeod et al., 2007; Vallejo, 2013). Besides feeding, white-beaked dolphins also mate and give birth in the summer (e.g. Canning et al., 2008), hence the distribution during this season could also be influenced by these activities, that have not been included in the current models. White-beaked dolphins' social behaviour, high mobility, and opportunistic feeding may partly explain why the precision of predicted density was weak. Density did not seem to change over time, but the distribution did shift towards the north.

5.5 Comparison between species

There are some clear differences in the modelled relationships between density and environmental variables between the two delphinid species. Relationships with depth for killer whales were highly variable, but white-beaked dolphins showed a clear affinity to shallower waters (Figure 5.8, Figure 5.12, Figure 5.19 and Figure 5.23). There were no clear seasonal signals for SST for either species; this may be linked to the year-round presence of these species in the area (Foote et al., 2007; Kinze, 2018; Kiszka and Braulik, 2018; Øien, 1988; Similä et al., 1996; Tavares et al., 2017). The temperature ranges at which positive effects on density were predicted were similar: at around 3-7 °C in spring (5-7 °C in the early period and 3-7 °C in the later period) for killer whales and at 2-6 °C in spring and 5-10 °C in summer for white-beaked dolphins. Although the density of both species is negatively affected by warmer waters, the signal is especially strong in both periods for white-beaked dolphins (Figure 5.19 and Figure 5.23), which supports suggestions in other studies that the distribution of white-beaked dolphins is limited by a maximum temperature (Fall and Skern-Mauritzen, 2014; Kinze, 2018; MacLeod et al., 2007, 2005; Vallejo, 2013).

Despite the similarities in the relationships with the environmental covariates, there was little overlap in either period in the predicted distributions of killer whales and white-beaked dolphins, except in the north of the area (Figure 5.9, Figure 5.13, Figure 5.20 and Figure 5.24). Killer whales are distributed more in the Norwegian Sea, while white-beaked dolphins are distributed more off northern Iceland, in the Barents Sea and off southwest Svalbard. In the Norwegian Sea, warmer temperatures may have led to higher densities of killer and pilot whales (Nøttestad et al., 2015), and may have displaced white-beaked dolphins. Distribution changes could therefore not only be due to oceanography, but also potentially due to species competition - although all three species have diverse diets (e.g. Desportes and Mouritsen, 1993; Jansen et al., 2010; Nøttestad et al., 2015; Similä et al., 1996). Killer whales and white-beaked dolphins are piscivorous (Bloch and Lockyer, 1988; Canning et al., 2008; Dong et al., 1996; Fall and Skern-Mauritzen, 2014; Foote et al., 2013; Jansen et al., 2010; NAMMCO, 1993; Øien, 1988; Sigurjónsson and Víkingsson, 1997; Similä et al., 1996) but some killer whales in the area also prey on marine mammals (Bloch and Lockyer, 1988; Foote et al., 2013; NAMMCO, 1993), so it is possible that the separation in distribution could partly be a result of predator avoidance by white-beaked dolphins during the calving period in the summer (e.g. Canning et al., 2008).

5.6 Appendix

5.6.1 All species

5.6.1.1 Distance sampling

Appendix 5-A. HR= hazard-rate, HN= Half-normal. p = average probability of detection, No. obs= number of observations, SE= standard error, Goodness of fit= Cramer-von Mises.

Species	Truncation	Key function	Covariates	No. obs	*p*	SE	Goodness of fit (p-value)	AIC	Survey & Period
Killer whale	2700	**HR**	**~ 1**	**127**	**0.262**	**0.058**	**0.939**	**1938.344**	NASS 1987-2015
		HN	~ 1		0.514	0.032	0.005	1952.968	
		HR	~ vessel ID		0.134	0.086	0.612	1940.764	
		HN	~ vessel ID		0.452	0.048	0.015	1955.561	
		HR	~ beaufort(2)		0.245	0.057	0.962	1938.081	
		HN	~ beaufort(2)		0.514	0.033	0.005	1954.967	
White-beaked dolphin	1000	HR	~1	308	0.152	0.022	0.112	4012.912	NASS 1987-2015
		HN	~1		0.493	0.017	1.27E-05	4103.086	
		HR	~ vessel ID		0.091	0.018	0.113	4008.354	
		HN	~ vessel ID		0.463	0.022	4.42E-06	4100.71	
		HR	**~ vessel ID + beaufort(2)**		**0.089**	**0.018**	**0.148**	**4004.682**	
		HN	~ vessel ID + beaufort(2)		0.452	0.021	2.71E-06	4088.356	
Killer whale	No truncation	**HR**	**~1**	**147**	**0.341**	**0.059**	**0.992**	**454.507**	NILS 1987-1989
		HN	~1		0.368	0.031	0.636	457.133	
Killer whale	2000	HR	~1	353	0.324	0.021	0.995	5009.514	NILS 1995-2013
		HN	~1		0.386	0.011	4.0E-04	5044.915	
		HR	**~ beaufort(3)**		**0.320**	**0.020**	**0.961**	**5005.062**	
		HN	~ beaufort(3)		0.385	0.012	3.45E-04	5047.022	
White-beaked dolphin	800	**HR**	**~1**	**22**	**0.223**	**0.091**	**0.978**	**275.518**	NILS 1987-1989
		HN	~1		0.453	0.051	0.042	282.214	
White-beaked dolphin	1000	HR	~1	726	0.323	0.017	0.135	9443.444	NILS 1995-2013
		HN	~1		0.427	0.009	1.04E-06	9498.996	
		HR	**~ beaufort(3)**		**0.317**	**0.017**	**0.183**	**9434.65**	
		HN	~ beaufort(3)		0.422	0.009	7.98E-07	9491.051	

5.6.1.2 Modelling

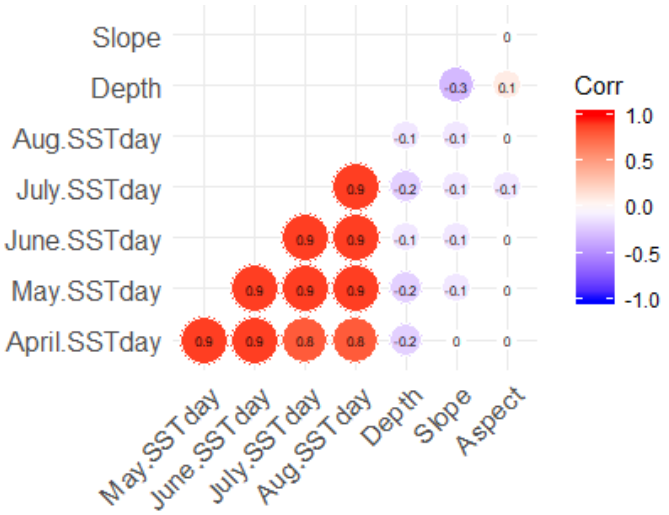

Appendix 5-B. Correlation matrix for killer whales and white-beaked dolphins 1987-1989 models.

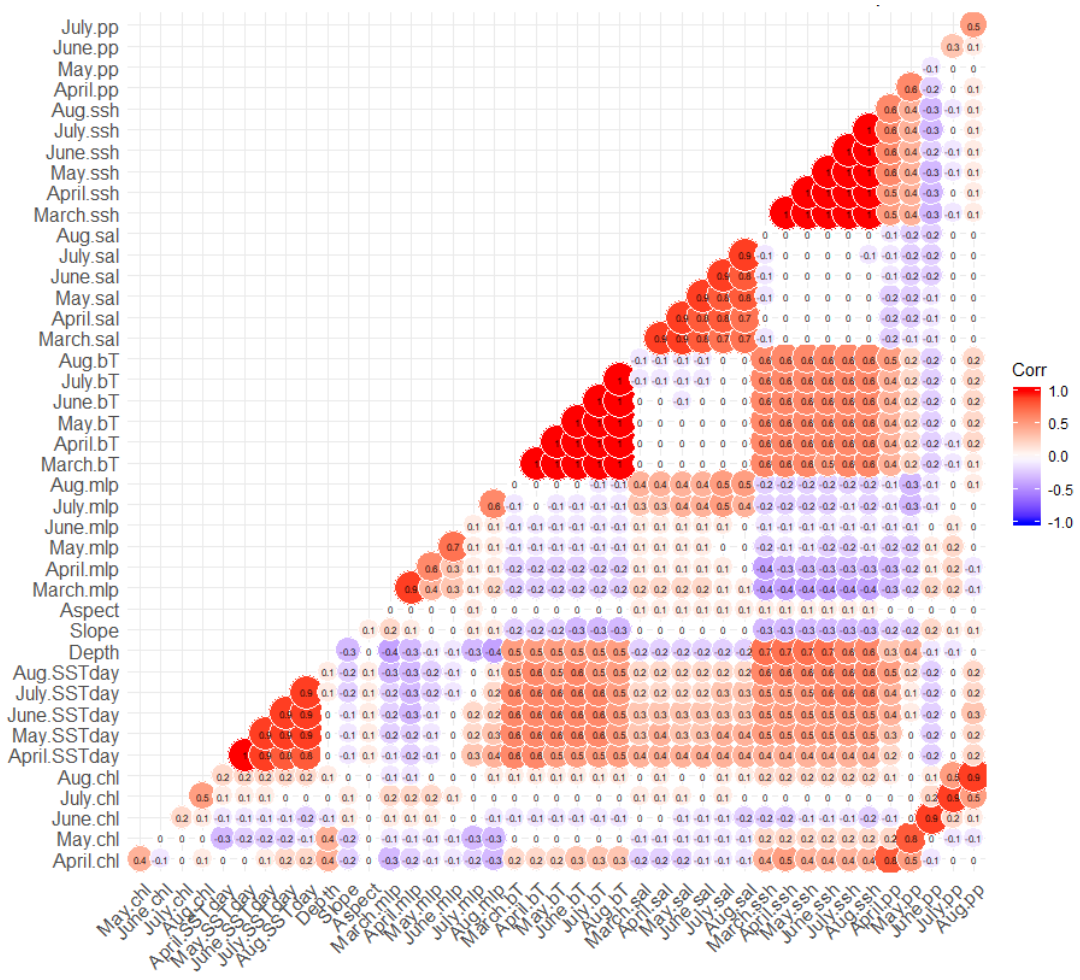

Appendix 5-C. Correlation matrix for killer whales and white-beaked dolphins 1998-2015 models.

5.6.2 Killer whales

5.6.2.1 Distance sampling

Appendix 5-D. ESW, effective strip width for the NILS 1995-2013 killer whales at all levels of the covariate Beaufort. Covariate Beaufort has three levels: high (H), medium (M) and low (L).

Beaufort	ESW (m)
H	493.17
M	696.18
L	1011.79

5.6.2.2 Modelling

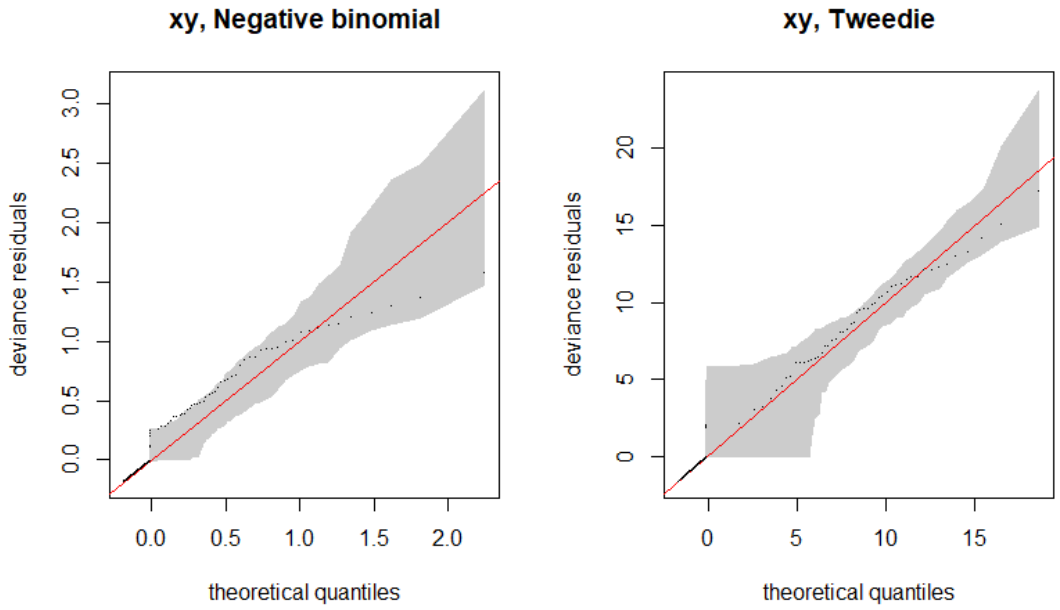

Appendix 5-E. Q-Q plots for error distribution selection for killer whale 1987-1989 models. Spatial models (xy) for negative binomial and tweedie distributions. The shaded area represents 95 % confidence interval, the circles represent the data, the line is the expected data distribution if the data fits precisely the model.

Appendix 5-F. Single model variables fitted models for killer whales 1987-1989 using double penalization. The best error structure for all models was the Tweedie distribution.

Model	Deviance	Deviance explained (%)	AIC	REML	n
Aspect	9301.18	8.70	6968.02	474.80	6695
May.SSTday	8821.15	14.59	6972.75	474.29	
June.SSTday	9335.39	10.50	6974.29	477.31	
Depth	10100.77	4.63	6974.56	480.23	
Slope	10854.68	1.18	6975.94	480.71	
April.SSTday	10486.50	3.55	6976.55	479.64	
July.SSTday	10483.14	3.85	6977.14	479.84	
Aug.SSTday	10701.62	2.73	6977.81	480.20	

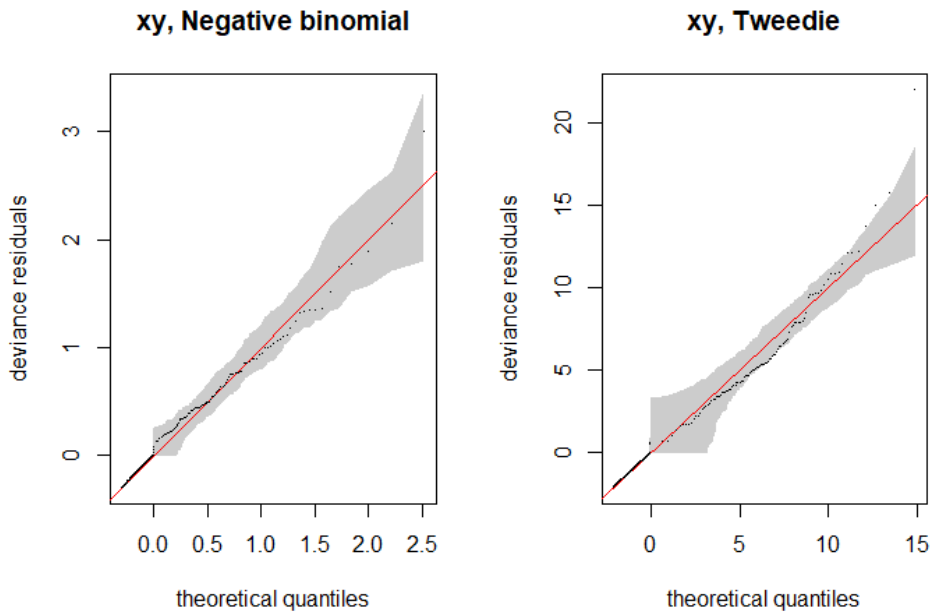

Appendix 5-G. Q-Q plots for error distribution selection for killer whale 1998-2015 models. Spatial models (xy) for negative binomial and tweedie distributions. The shaded area represents 95 % confidence interval, the circles represent the data, the line is the expected data distribution if the data fits precisely the model.

Appendix 5-H. Single model variables fitted models for killer whales 1998-2015 using double penalization. The best error structure for all models was the negative binomial distribution. The best covariate by each variable family is in bold letters.

Model: Survey +	Deviance	Deviance explained (%)	AIC	REML	n
July.bT	269.49	16.68	1734.90	868.00	7452
May.bT	270.61	16.32	1735.10	868.06	
June.bT	269.69	16.26	1735.62	868.38	
April.bT	271.21	15.88	1736.59	868.53	
Aug.bT	268.53	16.13	1737.10	869.04	
April.SSTday	263.98	7.21	1764.30	881.86	
July.SSTday	259.96	5.28	1768.95	883.50	
May.SSTday	261.39	4.29	1770.23	883.70	
May.chl	258.31	4.21	1770.81	884.23	
May.pp	258.71	4.12	1771.09	884.20	
July.mlp	258.02	4.76	1771.55	885.93	
April.mlp	259.45	2.20	1771.55	883.84	
Aug.SSTday	257.80	4.77	1772.02	885.65	
Aug.mlp	258.88	2.90	1772.51	884.41	
April.chl	258.71	2.92	1773.02	884.69	
June.SSTday	259.27	2.98	1773.17	884.67	
April.ssh	261.07	2.14	1774.42	884.91	
May.mlp	259.43	0.90	1774.70	885.04	
Aug.chl	259.91	0.00	1775.40	885.42	
Aug.sal	259.91	0.00	1775.40	885.42	

Slope	259.90	0.00	1775.40	885.42	
Aug.pp	259.91	0.00	1775.40	885.42	
June.chl	259.91	0.00	1775.40	885.42	
Aspect	259.91	0.00	1775.40	885.42	
June.mlp	259.91	0.00	1775.40	885.42	
July.chl	259.91	0.00	1775.40	885.42	
June.pp	259.91	0.00	1775.40	885.42	
July.ssh	259.90	0.00	1775.41	885.42	
June.ssh	259.91	0.00	1775.41	885.42	
Aug.ssh	259.90	0.00	1775.41	885.42	
April.pp	259.90	0.00	1775.42	885.42	
May.sal	259.87	0.03	1775.54	885.42	
May.ssh	260.94	1.45	1775.65	885.17	
April.sal	259.85	0.05	1775.69	885.42	
Depth	260.07	0.29	1775.76	885.39	
July.sal	259.77	0.13	1776.03	885.41	
June.sal	259.45	0.54	1776.07	885.28	
July.pp	259.40	0.51	1776.26	885.38	

Appendix 5-I. Concurvity values for killer whales 1998-2015 variables in remaining full model after double penalization. Key pairs evaluated are highlighted within coloured squares.

$`worst`

	para	s(April.SSTday)	s(April.ssh)	s(July.bT)	s(Depth)	s(Slope)	s(May.pp)	s(July.mlp)
para	1.000000e+00	1.199495e-27	1.557853e-28	2.988120e-28	3.130421e-28	6.661288e-27	1.640435e-28	2.076858e-23
s(April.SSTday)	1.052394e-27	1.000000e+00	2.605158e-01	4.109720e-01	1.940217e-01	5.148708e-02	9.218688e-02	2.297445e-01
s(April.ssh)	1.478267e-28	2.605158e-01	1.000000e+00	6.375473e-01	5.166689e-01	2.725346e-01	1.852009e-01	8.643253e-02
s(July.bT)	3.958198e-28	4.109720e-01	6.375473e-01	1.000000e+00	6.315241e-01	2.373447e-01	1.684938e-01	1.400147e-01
s(Depth)	3.397376e-28	1.940217e-01	5.166689e-01	6.315241e-01	1.000000e+00	5.059363e-01	2.625634e-01	1.611508e-01
s(Slope)	5.994451e-27	5.148708e-02	2.725346e-01	2.373447e-01	5.059363e-01	1.000000e+00	1.797596e-01	5.387785e-02
s(May.pp)	1.557101e-28	9.218688e-02	1.852009e-01	1.684938e-01	2.625634e-01	1.797596e-01	1.000000e+00	1.393678e-01
s(July.mlp)	2.077195e-23	2.297445e-01	8.643253e-02	1.400147e-01	1.611508e-01	5.387785e-02	1.393678e-01	1.000000e+00

$observed

	para	s(April.SSTday)	s(April.ssh)	s(July.bT)	s(Depth)	s(Slope)	s(May.pp)	s(July.mlp)
para	1.000000e+00	7.637947e-32	4.388746e-31	2.198776e-31	4.091621e-32	1.086580e-31	6.344234e-32	2.375909e-28
s(April.SSTday)	1.052394e-27	1.000000e+00	2.520178e-01	7.328770e-02	1.091090e-01	1.748025e-02	9.172614e-03	1.507190e-01
s(April.ssh)	1.478267e-28	6.798714e-02	1.000000e+00	1.192599e-01	4.535600e-01	1.742410e-01	1.711388e-02	7.207449e-02
s(July.bT)	3.958198e-28	8.826618e-02	3.497775e-01	1.000000e+00	5.966088e-01	9.848837e-02	8.781946e-02	8.418835e-02
s(Depth)	3.397376e-28	1.107953e-01	4.665443e-01	1.105160e-01	1.000000e+00	2.357995e-01	9.773102e-03	1.441636e-01
s(Slope)	5.994451e-27	6.758038e-03	2.166819e-01	2.255612e-02	2.016746e-01	1.000000e+00	1.308444e-02	4.746965e-02
s(May.pp)	1.557101e-28	4.063872e-02	1.426251e-01	5.098873e-02	1.614591e-01	7.082105e-02	1.000000e+00	1.232142e-01
s(July.mlp)	2.077195e-23	4.827990e-02	4.029809e-02	1.657786e-02	1.017034e-01	3.234533e-02	2.007624e-02	1.000000e+00

$estimate

	para	s(April.SSTday)	s(April.ssh)	s(July.bT)	s(Depth)	s(Slope)	s(May.pp)	s(July.mlp)
para	1.000000e+00	7.554368e-31	2.376212e-31	6.441610e-31	8.213734e-31	7.900360e-29	6.284517e-31	1.180958e-25
s(April.SSTday)	1.052394e-27	1.000000e+00	2.158366e-01	2.439788e-01	1.040568e-01	1.572984e-02	4.867514e-02	1.015267e-01
s(April.ssh)	1.478267e-28	1.686077e-01	1.000000e+00	4.417937e-01	4.088994e-01	6.382502e-02	1.322982e-01	3.869603e-02
s(July.bT)	3.958198e-28	3.352726e-01	4.563268e-01	1.000000e+00	5.397499e-01	4.272021e-02	1.301139e-01	4.976139e-02
s(Depth)	3.397376e-28	4.695083e-02	4.366994e-01	3.080433e-01	1.000000e+00	1.296487e-01	1.746332e-01	9.668035e-02
s(Slope)	5.994451e-27	2.764637e-02	1.921848e-01	9.820162e-02	2.101776e-01	1.000000e+00	1.201430e-01	3.262645e-02
s(May.pp)	1.557101e-28	2.158209e-02	1.455243e-01	7.239467e-02	1.478326e-01	3.051216e-02	1.000000e+00	8.408395e-02
s(July.mlp)	2.077195e-23	1.728658e-01	5.092313e-02	2.005846e-02	9.672219e-02	1.385201e-02	6.592532e-02	1.000000e+00

5.6.3 White-beaked dolphins

5.6.3.1 Distance sampling

Appendix 5-J. ESW, effective strip width for the NASS 1987-2015 white-beaked dolphins at all covariate/level combination. Levels of the covariate vessel relate to the abbreviation of the vessel's name. Covariate Beaufort has two levels: high (H), and low (L).

Vessel (ID)	Beaufort	ESW (m)	Vessel (ID)	Beaufort	ESW (m)
A	H	119.80	I	H	13.28
A	L	282.92	I	L	36.64
B	H	221.42	J	H	12.40
B	L	282.50	J	L	34.30
F	H	32.66	K	H	110.83
F	L	282.50	K	L	264.27
G	H	164.23	S	H	161.54
G	L	370.74	S	L	365.63
H	H	128.54	V	H	213.93
H	L	282.50	V	L	460.57

Appendix 5-K. ESW, effective strip width for the NILS 1995-2013 white-beaked dolphins at all levels of the covariate Beaufort. Covariate Beaufort has three levels: high (H), medium (M) and low (L).

Beaufort	ESW (m)
H	226.35
M	346.09
L	539.14

5.6.3.2 Modelling

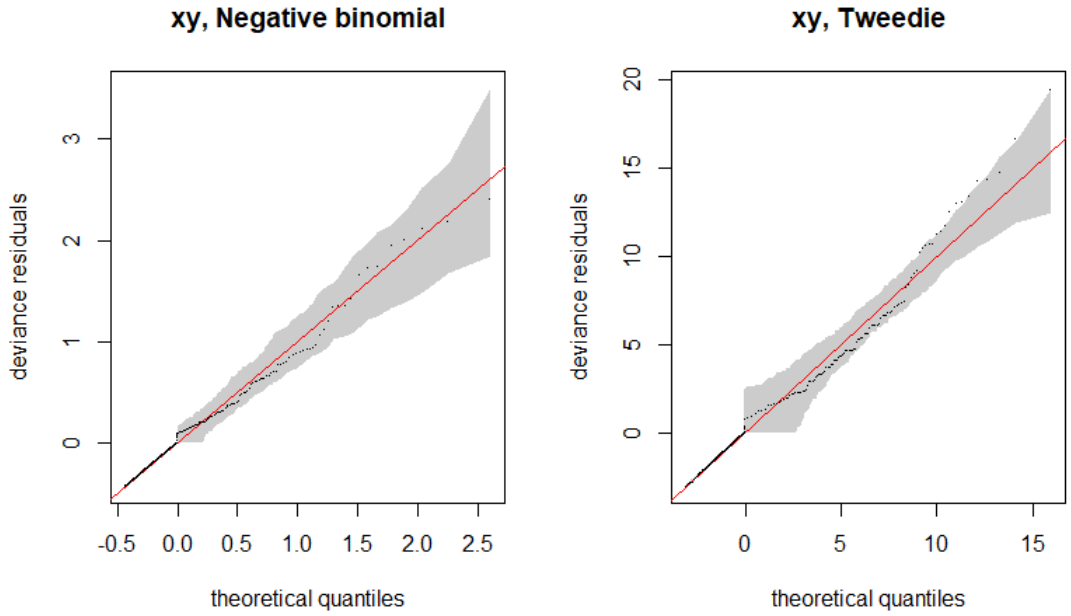

Appendix 5-L. Q-Q plots for error distribution selection for white-beaked dolphins 1987-1989 models. Spatial models (xy) for negative binomial and tweedie distributions. The shaded area represents 95 % confidence interval, the circles represent the data, the line is the expected data distribution if the data fits precisely the model.

Appendix 5-M. Single model variables fitted models for white-beaked dolphins 1987-1989 using double penalization. The best error structure for all models was the negative binomial distribution.

Model	Deviance	Deviance explained (%)	AIC	REML	n
April.SSTday	279.89	30.57	1801.40	901.39	6695
May.SSTday	278.61	30.34	1807.49	911.04	
July.SSTday	280.96	22.25	1835.28	920.18	
June.SSTday	281.41	18.17	1845.46	922.22	
Aug.SSTday	280.68	14.39	1856.01	926.40	
Aspect	281.50	13.95	1857.38	926.28	
Depth	281.76	12.00	1858.42	927.04	
Slope	281.76	12.00	1858.42	927.04	

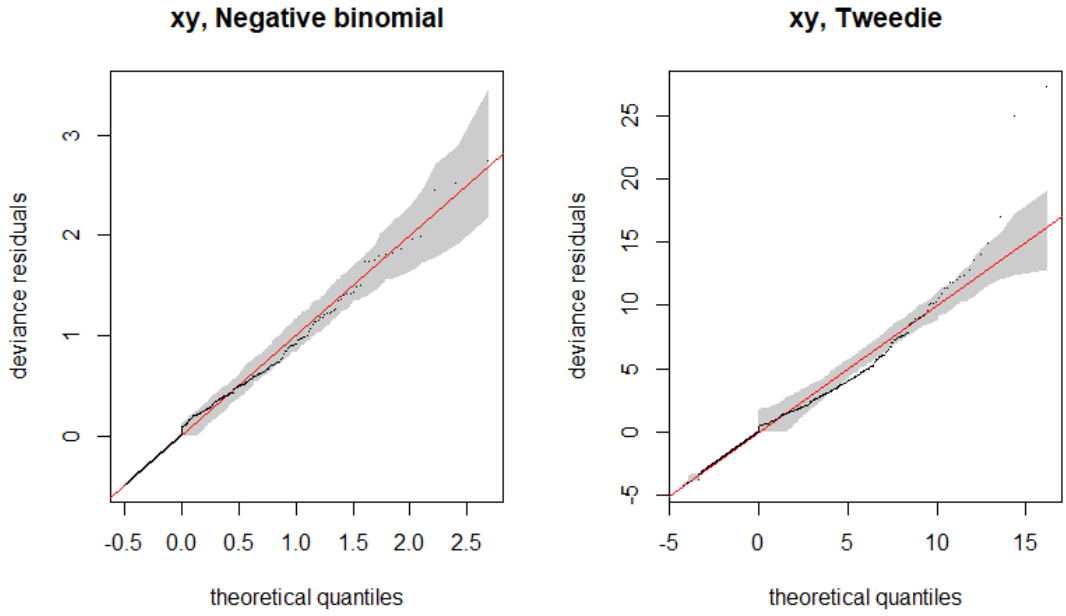

Appendix 5-N. Q-Q plots for error distribution selection for white-beaked dolphins 1998-2015 models. Spatial models (xy) for negative binomial and tweedie distributions. The shaded area represents 95 % confidence interval, the circles represent the data, the line is the expected data distribution if the data fits precisely the model.

Appendix 5-O. Single model variables fitted models for white-beaked dolphins 1998-2015 using double penalization. The best error structure for all models was the negative binomial distribution. The best covariate by each variable family is in bold letters.

Model: Survey +	Deviance	Deviance explained (%)	AIC	REML	n
Aug.SSTday	553.80	16.62	3462.97	1735.13	7361
July.SSTday	554.95	16.27	3463.96	1735.62	
May.SSTday	551.22	15.93	3469.41	1740.93	
April.SSTday	549.12	13.00	3481.31	1741.63	
June.SSTday	548.35	13.24	3484.37	1745.53	
May.sal	543.66	11.39	3496.27	1753.63	
April.bT	545.46	11.38	3498.62	1758.03	
June.sal	544.24	10.39	3502.11	1756.18	
Aug.sal	540.78	10.57	3503.26	1758.67	
May.bT	545.75	10.06	3505.10	1758.03	
July.sal	542.07	9.33	3510.08	1760.45	
Depth	544.93	8.74	3511.26	1758.66	
June.bT	544.54	8.67	3512.81	1760.92	
April.sal	540.72	8.20	3514.72	1760.55	
July.bT	543.91	8.39	3514.85	1762.13	
Aug.bT	543.52	8.27	3515.98	1763.11	
June.ssh	544.13	5.71	3523.15	1760.94	
Aug.ssh	544.22	5.52	3523.46	1761.00	
July.ssh	543.96	5.40	3524.63	1761.64	
May.ssh	543.63	5.20	3525.69	1762.17	
April.mlp	542.29	4.68	3528.89	1763.79	
April.ssh	543.02	4.37	3529.91	1763.94	
April.pp	543.37	3.30	3532.59	1765.14	

Aug.chl	542.31	3.61	3533.92	1765.92	
June.pp	542.60	3.15	3535.21	1766.15	
May.mlp	542.46	3.19	3535.38	1765.60	
July.pp	543.02	2.40	3535.68	1766.40	
May.pp	543.02	2.40	3535.68	1766.40	
April.chl	543.02	2.40	3535.68	1766.40	
July.mlp	543.02	2.40	3535.68	1766.40	
Aug.pp	543.02	2.40	3535.69	1766.40	
June.chl	543.02	2.40	3535.69	1766.40	
Aspect	543.02	2.40	3535.69	1766.40	
Slope	543.02	2.40	3535.70	1766.40	
Aug.mlp	542.74	2.63	3535.80	1766.29	
May.chl	542.88	2.50	3535.84	1766.38	
July.chl	542.67	2.64	3535.96	1766.30	
June.mlp	543.00	2.41	3536.29	1766.40	

Appendix 5-P. Concurvity values for white-beaked dolphins 1998-2015 variables in remaining full model after double penalization. Key pairs evaluated are highlighted within coloured squares.

	para	s(Aug.SSTday)	s(June.ssh)	s(April.bT)	s(Depth)	s(April.mlp)
para	1.000000e+00	7.303847e-28	1.261085e-28	1.232322e-27	3.228737e-27	2.377023e-26
s(Aug.SSTday)	5.782470e-28	1.000000e+00	5.778348e-01	4.037473e-01	1.960443e-01	2.009680e-01
s(June.ssh)	5.685761e-29	5.778348e-01	1.000000e+00	6.859468e-01	4.993913e-01	2.871483e-01
s(April.bT)	1.211953e-27	4.037473e-01	6.859468e-01	1.000000e+00	6.429678e-01	1.973963e-01
s(Depth)	3.907539e-27	1.960443e-01	4.993913e-01	6.429678e-01	1.000000e+00	2.348162e-01
s(April.mlp)	2.378016e-26	2.009680e-01	2.871483e-01	1.973963e-01	2.348162e-01	1.000000e+00

$observed

	para	s(Aug.SSTday)	s(June.ssh)	s(April.bT)	s(Depth)	s(April.mlp)
para	1.000000e+00	9.321493e-32	1.851520e-31	3.968890e-31	2.542910e-33	6.238593e-32
s(Aug.SSTday)	5.782470e-28	1.000000e+00	3.333080e-01	2.343076e-01	8.852593e-02	1.402909e-01
s(June.ssh)	5.685761e-29	2.583088e-01	1.000000e+00	2.482019e-01	4.387514e-01	1.204035e-01
s(April.bT)	1.211953e-27	1.988434e-01	3.893106e-01	1.000000e+00	6.140757e-01	7.904160e-02
s(Depth)	3.907539e-27	6.014960e-02	4.194193e-01	1.924041e-01	1.000000e+00	1.228372e-01
s(April.mlp)	2.378016e-26	7.146115e-02	1.079261e-01	5.706867e-02	1.379505e-01	1.000000e+00

$estimate

	para	s(Aug.SSTday)	s(June.ssh)	s(April.bT)	s(Depth)	s(April.mlp)
para	1.000000e+00	5.175421e-31	4.812233e-31	1.758264e-31	9.107996e-31	1.067272e-28
s(Aug.SSTday)	5.782470e-28	1.000000e+00	3.501417e-01	3.078600e-01	7.390609e-02	1.034218e-01
s(June.ssh)	5.685761e-29	3.873641e-01	1.000000e+00	4.994679e-01	3.759568e-01	1.063664e-01
s(April.bT)	1.211953e-27	2.977758e-01	4.303849e-01	1.000000e+00	5.518076e-01	6.387078e-02
s(Depth)	3.907539e-27	7.525581e-02	3.916696e-01	2.906255e-01	1.000000e+00	9.251802e-02
s(April.mlp)	2.378016e-26	1.347272e-01	1.598248e-01	7.200703e-02	1.313241e-01	1.000000e+00

6 GENERAL DISCUSSION

6.1 Summary of main results

The main goal of this thesis has been to improve the understanding of the environmental factors that influence summer distribution and habitat use of a range of cetacean species in the central and north-eastern North Atlantic over a period of three decades by modelling their relative abundance as a function of a series of static and dynamic variables. As well as increasing our understanding of these species, the study provides the opportunity to compare and contrast habitat use and changes in distribution among species within guilds and among guilds.

The three main guilds explored here are deep diving cetaceans, baleen whales and Delphinidae. The three main species of deep diving cetaceans found in study area are sperm, long-finned pilot, and northern bottlenose whales. These species use the area differently; pilot whales are year-round residents, sperm and northern bottlenose whales move in and out of the area with the highest densities for the three species being in the summer (e.g. Sigurjónsson and Víkingsson, 1997). All the deep diving species feed on squid, other cephalopods and less commonly fish (Bjørke, 2001; Bloch et al., 1996; Desportes and Mouritsen, 1993; Whitehead et al., 2003).

The three most commonly found baleen whales in the area are fin, humpback, and minke whales. These migratory species are only present in the summer to take advantage of the high seasonal productivity and characteristic prey aggregation. They have diverse diets that range from macro-zooplankton to various fish species and vary spatially and temporally with some evidence of prey preference; to feed baleen whales must find dense patches of prey (Moore et al., 2019; e.g. Nøttestad et al., 2015; Ressler et al., 2015; Sigurjónsson and Víkingsson, 1997; Skern-Mauritzen et al., 2011; Víkingsson et al., 2015).

Killer whales and white-beaked dolphins are Delphinidae species that inhabit the study area throughout the year (e.g. Kovacs et al., 2009; Kuningas et al., 2014; Samarra et al., 2017; Similä et al., 1996; Tavares et al., 2017). Both species are opportunistic predators feeding high in the food web, with diverse diets that include cephalopods, fish and (for killer whales) marine mammals, but fish are likely to be the main prey for both, especially gadoid fish for white-beaked

dolphins (e.g. Bloch and Lockyer, 1988; Canning et al., 2008; Christensen, 1988; Dong et al., 1996; Fall and Skern-Mauritzen, 2014; Jansen et al., 2010; Jonsgard and Lyshoel, 1970 In: NAMMCO, 1993; Øien, 1988; Samarra and Miller, 2015; Sigurjónsson and Víkingsson, 1997). These species contribute substantially to the summer prey consumption in the study area (e.g. Sigurjónsson and Víkingsson, 1997).

The summer distribution and habitat use of the three guilds, and the species within guilds, was evaluated in the central and north-eastern North Atlantic by dividing the study period in two periods, 1987-1989 and 1998-2015, based on observed environmental changes in the area and data availability. Models for all species were fitted using the same baseline variables, were based on a robust model selection framework and were used to predict distribution. The best models and selected variables differ among species and results from all eight species over the two periods can be compared to help understand the environmental drivers of their distribution. Overall, the common covariates that best explained the distributions of these species in both periods were relief and temperature related.

The relationships with depth were in general stable over time for the species. The predicted high-use areas for all species of deep divers were in deep waters, as expected. In the baleen whales, the relationships between density and depth differed among species. Fin whales were associated with deep waters, humpback whales were weakly associated with shallow waters. Minke whales overlapped to some extent with the other two species, being positively associated with deep waters >3500 m but also with shallow waters ≤300 m. For the delphinids, the relationship between killer whale density and depth was highly variable, but white-beaked dolphins showed a clear affinity to shallower waters.

In terms of seasonality, for the deep diving species, the selected dynamic temperature-related covariates were for spring for sperm and pilot whales, but for summer for northern bottlenose whales. In baleen whales generally, the dynamic environmental variables considered all showed summer relationships, supporting the hypothesis that the time lag between density and these environmental measures is shorter for species that feed lower in the trophic web. In the two delphinid species there were no clear seasonal signals for either species, which may be linked to the year-round presence of these species in the area.

In terms of predicted distribution, for the deep diving species, changes in distribution between the two periods appear more as a range expansion than a shift, with generally higher predicted densities in northern waters in recent years. For baleen whales, all species showed higher

density in more northerly areas including in the Barents Sea and north of Iceland; however, an exception is the predicted increase in density of fin whales in the Irminger Sea. There was little overlap in the distribution of the two delphinid species in either period; killer whales were distributed more in the Norwegian Sea, while white-beaked dolphins were distributed more off northern Iceland, in the Barents Sea and off southwest Svalbard.

At the regional level, some changes in cetacean diet are due to changes prey in availability and this is likely linked to changes in the environment (Nøttestad et al., 2015; Víkingsson et al., 2015). Oceanographic conditions have been changing in the central and north-east North Atlantic (e.g. Carr et al., 2017; Häkkinen et al., 2013; Hátún et al., 2009; Havforskningsinstituttet, 2020; Sundby et al., 2016). Physical changes during recent decades in the North Atlantic (including warmer temperatures) have been linked to biological changes, which have been detected in species such as krill, mackerel, herring, capelin, and blue whiting (Astthorsson et al., 2012; Canning et al., 2008; Hátún et al., 2009; Huse et al., 2015; IJsseldijk et al., 2018; Ressler et al., 2015; Silva et al., 2014; Skern-Mauritzen et al., 2011; Trenkel et al., 2014; Valdimarsson et al., 2012). These changes have thus affected the prey of some cetacean species but the extent to which cetaceans are responding is unknown (e.g. Moore et al., 2019; Nøttestad et al., 2015; Ressler et al., 2015; Silva et al., 2014; Skern-Mauritzen et al., 2011; Vacquié-Garcia et al., 2017; Víkingsson et al., 2015).

Such a comparison of the distribution and habitat use of multiple cetacean species over three decades has not previously been attempted for such an extensive area, 6.9 million km^2. This work provides a better understanding of the species ecology in the North Atlantic by identifying key factors that have influenced their summer distribution and habitat use in the last 30 years, while also providing clues about how environmental changes (including climate change) may affect cetacean populations in the future. This information could also inform assessments of human pressures on these species. For example, in consideration of overlap with areas of anthropogenic activities. Specifically, in the future, one area that will need to be carefully considered will be Arctic waters and the Barents Sea. All baleen whale species showed higher density in more northerly areas during the recent period, which is likely linked with climate change and new areas being available. An increase of anthropogenic activities is also expected. If impacts on species are poorly managed, the combination of this and the effects of climate change may push species to their limits.

6.2 Environmental drivers

Species are distributed within specific physiological tolerance limits, and changes in distribution have been suggested to follow these limits (Walther et al., 2002). Many cetacean species are highly mobile and range over large areas; however, variation in distribution patterns can be expected to be a response to environmental change (Forney, 2000). Relationships between species distribution and its drivers are complex. There can be direct and indirect links with the environmental drivers of distribution; elucidating them and the mechanisms can be difficult. Summer in the central and north-eastern North Atlantic is the season of peak occurrence of several cetacean species including fin, humpback, minke, sperm whale, and northern bottlenose whale. Pilot and killer whales, and white-beaked dolphins occur year-round (e.g. Øien, 1988; Sigurjónsson and Víkingsson, 1997). Feeding is the common primary activity for all these species in the central and north-eastern North Atlantic during the summer. Reproduction is also important for the odontocetes but limited information is available; there is a peak in calving for white-beaked dolphins in summer (Canning et al., 2008) and for pilot whales in spring and late summer (Martin and Rothery, 1993). Changes in the distribution patterns of these and other species of cetaceans are expected to be mediated by variation in the availability and distribution of their prey; in other words the result of food-web interactions linked strongly to prey-environment relationships (Hastie et al., 2004; Laran and Drouot-Dulau, 2007; Moore, 2008; Moore and Huntington, 2008).

Generally, the relationships between cetacean species distribution and static environmental variables are well known. Deep diving species mostly occur in deeper waters (Christensen et al., 1992; Gunnlaugsson et al., 2009; Hooker et al., 1999; MacLeod et al., 2007; Roberts et al., 2016; Rogan et al., 2017; Virgili et al., 2019; Whitehead, 2018; Whitehead and Hooker, 2012b, 2010). Some other species with broad distributions are found more often closer to the coast, such as minke and humpback whales (e.g. Clapham, 2018; Haug et al., 2002; Jefferson et al., 1993; Neyman, 2018; Paxton et al., 2009; Skern-Mauritzen et al., 2011; Storrie et al., 2018; Vacquié-Garcia et al., 2017). Most of the species distribution models developed in this study found relationships with depth (Table 6.1) similar to those described in the literature, as discussed in Chapters 3, 4, and 5. As expected, clear relationships between density and static variables were generally maintained temporally (i.e. in models of both periods) but there were three species where this was not the case; weak relationships were found in the three species that remain feeding in the area year-round: pilot whale, killer whale, and white-beaked dolphin (Table 6.1) (e.g. Jourdain et al., 2019; Øien, 1988; Samarra et al., 2017; Sigurjónsson and Víkingsson, 1997;

Similä et al., 1996; Tavares et al., 2017). This may cause their usage to be more flexible and prone to yearly variations, as has been described for pilot whales (Hátún et al., 2009).

Table 6.1. Summary of the best models by species in the two periods 87-89 (1987-1989) and 98-15 (1998-2015). Covariates retained in the best model were specified by: 'X' in static, and the specific month in dynamic covariates. Sp=Species codes are the following: PM- sperm, GM- pilot, HA- northern bottlenose, BP- fin, MN- humpback, BA- minke, OO- killer whale, and LL- white-beaked dolphins.

Guild	**Period**	**Sp**	**Covariates**									
			Depth	**Slope**	**Aspect**	**SST**	**bT**	**ssh**	**mlp**	**sal**	**chl*a***	**PP**
Deep Divers	87-89	PM	X	X	X	April						
		GM	X	X		May						
		HA	X		X	Aug						
	98-15	PM	X	X	X	April		Aug	July			July
		GM			X	April	April		July	July		
		HA	X		X	June		July	June	Aug	April	
Baleen Whales	87-89	BP	X	X	X	July						
		MN	X		X	May						
		BA	X	X	X	June/ May						
	98-15	BP	X			Aug		Aug		Aug		April
		MN	X		X	June		Aug	July	Aug	April	Aug
		BA	X	X		June		June	July			Aug
Delphini -dae	87-89	OO	X		X	May (all)						
		LL	X		X	April						
	98-15	OO		X		April	July	April	July			May
		LL				Aug/ July	April	June	April			

Regarding the dynamic environmental variables, SST is the most widely described variable affecting cetacean species distribution; SST is not only used to understand the drivers of distribution in feeding, but also in studies in other areas such as calving-mating grounds and migration routes (e.g. Bortolotto et al., 2017; Dalla Rosa et al., 2012; Gilles et al., 2016; Schleimer et al., 2019; Víkingsson et al., 2015). Available information on the relationships between the study species and SST in the area is patchy but here it was possible to evaluate patterns at a large scale between two time periods. SST was retained in all the best models for both periods for all the species, revealing it to be the most consistent driver of distribution of the eight cetacean species over 30 years of study (Table 6.1).

The oceanographic conditions of the study area have gone through some changes during the last decades (e.g. Carr et al., 2017; Häkkinen et al., 2013; Hátún et al., 2009; Havforskningsinstituttet, 2020; Sundby et al., 2016) (see introduction section 1.2). The consistent importance of depth and SST in the modelled relationships in both periods facilitate the comparison of any changes over time among species. If there are oceanographic changes, including water warming or cooling, one might expect animals to move to areas that retain the dynamic conditions in which they normally distribute or to display some level of static site-fidelity despite the changing conditions. Over time, modelled relationships with depth generally did not change, while those with SST did change for several of the species. The clearest changes were found for northern bottlenose, fin, and minke whales (Chapters 3 and 4). The sperm whale retained the same relationship with SST in both periods (Chapter 3), which is surprising given the described oceanographic changes in the Norwegian Sea, its area of highest occurrence (e.g. Moore et al., 2019; Nøttestad et al., 2015). Although not as clear as for sperm whales, the relationship between pilot whale density and SST had a similar pattern over time, in which density was positively affected by warmer waters (Chapter 3). Killer whale and white-beaked dolphin density were both negatively affected by warmer waters; however, this relationship was not strongly seasonal (Chapter 5), which may be linked to the year-round presence of these species in the area (Foote et al., 2007; Kinze, 2018; Kiszka and Braulik, 2018; Øien, 1988; Similä et al., 1996; Tavares et al., 2017). Pilot whales are also present year-round. Differences between pilot and killer whales could be due to the historical northern limits of the species; pilot whales are less common in northern latitudes (e.g. Bloch and Lockyer, 1988; Buckland et al., 1993; Christensen, 1988; Fall and Skern-Mauritzen, 2014; Foote et al., 2007; Hátún et al., 2009; Nøttestad et al., 2015; Øien, 1988; Storrie et al., 2018). Several of the studied species seem to be responding to the changing oceanographic conditions; the differences seen among species reflect the unique ecology of each species.

It is assumed that the observed changes in the cetacean species' relationships with SST are linked indirectly with prey availability. As discussed above (see introduction section 1.3), physical changes in the North Atlantic have been linked to changes in some of the cetaceans' prey species, including krill, mackerel, herring, capelin, and blue whiting (Astthorsson et al., 2012; Canning et al., 2008; Hátún et al., 2009; Huse et al., 2015; IJsseldijk et al., 2018; Ressler et al., 2015; Silva et al., 2014; Skern-Mauritzen et al., 2011; Trenkel et al., 2014; Valdimarsson et al., 2012). But how cetaceans respond to these changes remains unclear, for example whether they switch prey completely, partially or follow their prey. This study could not answer such

questions, but it has helped to understand the relationships between cetaceans and some environmental proxies for prey and whether these relationships change over time. In the future, more specific studies could be conducted, for example to investigate reasons for the difference between contrasting species that either showed no changes in relationships with SST and depth, such as sperm whales, or did show changes, such as fin or minke whales.

Comparisons of changes in the relationships between density and environmental variables and changes in predicted distribution between periods was undertaken using a simple early model (relief variables and SST) and a more complex recent model (relief variables, SST, and other dynamic variables). It is possible that the inclusion of additional candidate covariates in the recent model could have influenced the fitted relationships with relief variables and SST, thus affecting these comparisons. Houghton et al. (2020) investigated sei whale distribution using the same methodology as used here and additionally fitted simple models in the recent period to compare the results of models that included the same candidate covariates in both periods. They found that the relationships between sei whale density and depth were the same in the simple and more complex recent model, and that the relationships between sei whale density and SST were similar but not exactly the same. It would be useful to check that there are no major differences in the fitted relationships with depth and SST for the species investigated here.

Temporal changes in the relationships between cetacean density and environmental variables was limited to comparison of the results from the models for the two periods. These periods match ecosystem changes that have been described in the area and also match the latest change from a cold to a warm phase in the AMO (see sections 1.2 and 2.2.2.1). Combining several years in the recent period (1998-2013) means that aggregate or "average" effects were investigated; this may have concealed interesting inter-annual variability and even trends. Species that remain in the area year-round such as pilot and killer whales, and white-beaked dolphins do seem to show yearly variations (e.g. Øien, 1988; Sigurjónsson and Víkingsson, 1997). In future work, it would be informative to explore models fitted to shorter periods, if sufficient data are available. This may allow, for example, any responses of white-beaked dolphins to changes in the Polar Front at the Barents Sea to be investigated (Fall and Skern-Mauritzen, 2014).

6.3 Life-history strategies and resources -

Species fitness is optimized when survival and reproductive success are maximized, which is driven by how individual organisms acquire and allocate their resources (Stearns, 1989). Two

life history strategies that have evolved to achieve this are capital breeding and income breeding, which reflect this management of resources (allocation and storage) (Jonsson, 1997; Stearns, 1989). Capital breeders store the resources that later will be used in reproduction, including raising offspring. Income breeders depend on the continual availability of resources including during periods of reproduction and raising offspring (Alerstam et al., 2003; Jonsson, 1997; Stephens et al., 2009). In cetaceans, capital breeders are generally baleen whales, while toothed whales and dolphins are income breeders (e.g. Christiansen et al., 2014; Irvine et al., 2017; Oftedal, 1997). Both were studied here: capital breeders in Chapter 4, and income breeders in Chapters 3 and 5. Females have the highest energetic cost in reproduction (e.g. Christiansen et al., 2014; Houston et al., 2007; Irvine et al., 2017; Oftedal, 1997), so it is important to keep in mind when making broad comparison among species that sperm whales in the study area are mature males (Chapter 3).

Of all the species in this study, the capital breeders, fin, humpback, and minke whales, seemed to show the clearest change in distribution (Chapter 4). Although, as expected, there were species-specific differences, all have in common higher density in more northerly areas, including in the Barents Sea and north of Iceland, in the recent period. The one exception to this is the predicted increase in the density of fin whales in the Irminger Sea. The general pattern of an increase in the northern distribution around the Barents Sea in recent years for baleen whales has been suggested to be linked with ocean warming and loss of sea ice (e.g. Carr et al., 2017; Dalpadado et al., 2020; Havforskningsinstituttet, 2020), and increases in net primary production (Arrigo and van Dijken, 2015; Dalpadado et al., 2020) that may affect whales' prey. The stronger signal in changes in baleen whale distribution could possibly be a reflection of them moving to take advantage of newly available optimal areas because of their higher energetic demands.

In this thesis, the study species (deep diving cetaceans, baleen whales and Delphinidae) have been grouped into three guilds, components of a "community" that exploit the same kind of resources in a similar way (Simberloff and Dayan, 1991). Cetacean prey data could not be incorporated in the models, so proxies were used, and we assume that these proxies help to elucidate some of the large scale (general) relationships with the prey.

In the deep diving species, the best models included dynamic temperature-related covariates for sperm and pilot whales for spring, but for northern bottlenose whales they were for summer. The difference in the seasonal relationships for northern bottlenose whales may be related to the suggested north-south summer migration (Benjaminsen and Christensen, 1979; Bloch et al.,

1996; Miller et al., 2015; Reeves et al., 1993; Whitehead and Hooker, 2012a), and not only driven by prey availability. The relationship between density and spring SST for pilot and sperm whales could indicate support for the hypothesis that the lag between density and temperature variables (SST is the first indicator of seasonal progression) is longer (greater lag) for species that feed higher in the trophic web. Summer relationships were also found for the three deep diving species for the other dynamic variables, where some of these variables are linked to prey aggregation (Chapter 3).

In baleen whales generally, all the dynamic environmental variables showed summer relationships, supporting the hypothesis that the lag between density and these variables is shorter for species that feed lower in the trophic web (Chapter 4). In the Delphinidae, there were no clear seasonal signals for SST for either species. This could perhaps be a result of prey 'preferences', the relationships between prey and the proxies, and/or the year-round presence of these species in the area (Foote et al., 2007; Kinze, 2018; Kiszka and Braulik, 2018; Øien, 1988; Similä et al., 1996; Tavares et al., 2017) (Chapter 5).

Finally, the relationships between cetacean density and chlorophyll *a* and primary productivity had mixed seasonal signals that were difficult to interpret; there were some spring and some summer signals. These mixed signals could be related to the different bloom types that occur in the area (Friedland et al., 2016; Waniek and Holliday, 2006), the relationships between prey species and these blooms, and/or the type of prey the cetaceans were feeding on (e.g. Christensen et al., 1992; Heide-Jørgensen and Laidre, 2007; Nøttestad et al., 2015; Pampoulie et al., 2013; Ressler et al., 2015; Sigurjónsson and Víkingsson, 1997; Skern-Mauritzen et al., 2011; Víkingsson, 1997; Víkingsson et al., 2015, 2014; Windsland et al., 2007).

6.4 Distribution and niche partitioning

Guild members differ in their use of resources (Emlen, 1973 In: Whitehead et al., 2003); the way in which this is achieved is a fundamental question in ecology. Species could use the resources in different proportions, for example using more (wide niche breadths) or less (narrow niche breadths) resource types (Whitehead et al., 2003). In this study prey data have not been included in the models but, in the study area as a whole, within each guild there are regions of high, medium, and/or no overlap (patterns of space use) among species. This partially helps to understand the use of the area (and resources) spatially, that is, niche partitioning.

As discussed above (see Chapter 3: Figure 3.8, Figure 3.12, Figure 3.18, Figure 3.28, and Figure 3.32), in deep diving species the predicted high-use areas for all three species were, as expected, deep waters (Christensen et al., 1992; Gunnlaugsson et al., 2009; Hooker et al., 1999; MacLeod et al., 2007; Roberts et al., 2016; Rogan et al., 2017; Virgili et al., 2019; Whitehead, 2018; Whitehead and Hooker, 2012b, 2010), with some overlap among them in the central Norwegian Sea (e.g. Nøttestad et al., 2015), and the Central North Atlantic (e.g. Rogan et al., 2017), including the Irminger Sea (Abend and Smith, 1999; Gunnlaugsson et al., 2009; Whitehead and Hooker, 2012a). Looking more closely at each of the species in the Norwegian Sea, pilot whales tended to be closer to the coast, while sperm whales were in the central Norwegian Sea and northern bottlenose whales were more towards the Greenland-Norwegian Seas. Similar differentiation can be observed around the Faroe Islands, where all three species use the area but only with some overlap in distribution. These differences in distribution likely reflect species-specific differences in preferred prey and variation in these preferences according to the area (Benjaminsen and Christensen, 1979; Bjørke, 2001; Desportes and Mouritsen, 1993; Fernández et al., 2014; Martin and Clarke, 1986; Méndez-Fernandez et al., 2013; e.g. Nøttestad et al., 2015; Santos et al., 2014; Sigurjónsson and Víkingsson, 1997; Zachariassen, 1993).

Overlap in distribution among species of the same guild was also found in baleen whales. In general, the minke whale seems to act as a 'common player'; it has some overlap with humpback whales in waters closer to the coast and some overlap with fin whales in deeper waters. In the recent period (1998-2015), the distribution of fin and minke whales, especially, seems to have expanded through the area generating increased overlap among the species, including humpback whales (Chapter 4). This study could not use prey information, but it would be ecologically informative to know if these species are feeding on different prey species in the areas of overlap. We do not know if the broader distribution is a response only to observed oceanographic and prey changes (Astthorsson et al., 2012; Canning et al., 2008; Hátún et al., 2009; Huse et al., 2015; IJsseldijk et al., 2018; Ressler et al., 2015; Silva et al., 2014; Skern-Mauritzen et al., 2011; Trenkel et al., 2014; Valdimarsson et al., 2012) or if these environmental changes have generated areas of overlap and species are distributing more broadly as a response to avoid overlap.

There was little overlap in distribution between the two Delphinidae species. Both species are piscivorous, but their 'preferred' prey appear to be different. The key prey for killer whales are NSS herring, ISS herring, and mackerel, while for white-beaked dolphins they are gadoid fish

(Bloch and Lockyer, 1988; Canning et al., 2008; Dong et al., 1996; Fall and Skern-Mauritzen, 2014; Foote et al., 2013; Jansen et al., 2010; NAMMCO, 1993; Øien, 1988; Sigurjónsson and Víkingsson, 1997; Similä et al., 1996). Killer whales are apex predators with a very broad diet, including marine mammals. The difference in distribution between the two species could be a result of reducing competition for fish prey and/or because of predator avoidance by the white-beaked dolphins.

In summary, different distribution patterns were observed among all the cetacean species and guilds studied here but some degree of overlap was found even among species belonging to the same guild. No attempt to quantify the overlaps in distribution has been made here but this could be an informative exercise. In future research, the calculation of differences between species as suggested by Jones et al. (2015) could be used.

6.5 Conservation and management

Species distribution maps generated by habitat use models, such as those presented here for fin, humpback, minke, sperm, pilot, northern bottlenose, killer whales and white-beaked dolphins, can inform conservation assessments of the species and also management options to mitigate the impact of human activities.

The eight species investigated in this study have all been assessed by the IUCN, mostly quite recently. For the deep divers, the sperm whale, the pilot whale and the northern bottlenose whale are listed as Vulnerable, Least Concern, and Data Deficient, respectively (Minton et al., 2018; Taylor et al., 2019, 2008). In the baleen whales, the fin whale is listed as Vulnerable (the population in the central North Atlantic is considered to be in a healthy state), and the humpback and minke whale are listed as Least Concern (Cooke, 2018c, 2018b; IWC, 2019; Reilly et al., 2008a). The killer whale and white-beaked dolphin are listed as Data Deficient and Least Concern, respectively (Kiszka and Braulik, 2018; Reeves et al., 2017). The Vulnerable listings for fin whale and sperm whale globally are primarily a legacy of past industrial whaling; additional information on distribution and abundance will help in assessments of their future recovery. The two species with Data Deficient listings would clearly benefit from new information to allow assessments to be made.

Distribution maps can be used in conservation assessments to evaluate changes in distribution. In the IUCN process, distribution is one of the criteria used to inform assessment of species, in

which it is evaluated whether the extent of the species is declining or fluctuating in the area of occupancy or occurrence, or whether there is fragmentation (IUCN, 2016). Here, changes in distribution have been identified in most of the species and this information will be useful when they are next assessed by IUCN.

Distribution maps can also help in assessment of the impacts of anthropological pressures on species within ecosystems. The overlap of a species distribution with a specific anthropogenic pressure can be a first step towards understanding the direct impact on a species of that pressure. Deep diving cetaceans and killer whales are particularly vulnerable to ocean noise, including naval sonar (Hooker et al., 2019; Isojunno et al., 2018; Kuningas et al., 2013; Miller et al., 2015, 2012; Rendell and Gordon, 1999; Sivle et al., 2012; Tyack et al., 2006). Comparing species distribution maps with soundscape maps or, in a more targeted approach, with known/planned sources of noise such as pile driving to construct offshore wind farms (e.g. Gilles et al., 2009) could be beneficial in indicating the most important areas for focusing management action.

Species distribution maps such as those generated here could be used to inform the location of offshore marine protected areas (MPAs). There are many aspects to consider regarding the establishment of MPAs (e.g. Cañadas et al., 2005; Embling et al., 2010; Hooker et al., 1999) but a primary consideration is where an MPA should be located, for which a good understanding of species abundance and distribution is necessary. Relying on general species range maps for this is unlikely to be adequate and may be misleading (Williams et al., 2014). The distribution maps produced by this study allow the identification of high-density areas, which are so important in area-based conservation and management, should there be a future focus on the establishment of offshore MPAs in the North Atlantic.

In a multi-species context, the identification of core habitats of species allows evaluation of whether species diversity matches density. Williams et al. (2014) found species richness and density were inversely related. Species diversity “hotspots” may therefore contain lower densities of species indicating they may be sub-optimal areas. At a smaller scale, Jones et al., (2015) came to a similar conclusion when comparing harbour and grey seal distributions around Britain. Areas of high overlap between the species were not those with the highest densities for each species suggesting that areas for protection (MPAs) should not be restricted to areas of overlap (Jones et al., 2015). The distribution maps generated here are informative in a single species context but also in consideration of multi-species MPAs, which are more likely to be a

focus of MPAs for cetaceans – see, for example, the IUCN Marine Mammal Protected Areas Task Force Important Marine Mammal Areas initiative (https://www.marinemammalhabitat.org/immas/).

6.6 Future research

This multi-species project with a broad spatial-temporal scale has advanced our knowledge and understanding of the distribution and habitat use of cetaceans in the central and north-eastern North Atlantic but, inevitably, several important questions remain unanswered. Some of these are briefly outlined in the following paragraphs.

Predicting the impact of future environmental change:

In the North Atlantic and North Pacific, there has been rapid sea ice loss due to global warming (Laidre et al., 2015). In the north-eastern Atlantic this reduction has been reported in all seasons (Haug et al., 2017). The Barents Sea has the highest rate of sea ice loss of > 20 days/decade (Laidre et al., 2015), resulting in an overall increase in ocean heat content and to the northern Barents Sea seeming to become a well-mixed Atlantic system instead of the cold stratified Arctic (Lind et al., 2018). Such changes will set to continue and the consequences for the ecosystem, including marine mammals and their prey, are difficult to forecast. Using the models developed here to predict how cetacean distribution may change in the future as a result of environmental variability should help to understand possible scenarios of such change. Prior to using the models developed in this study to predict future impacts, the predictive power of the models will need to be checked. This can be done using cross-validation (e.g. Forney et al., 2012). If the predictive power of the models is adequate, future predictions of cetacean distribution can be made using covariate data from climate models that predict dynamic oceanographic variables into the future (e.g. Alexander et al., 2018). This could be done, for example, to predict future cetacean usage of the Barents Sea. Comparisons could be made between baleen whales that are already changing their distribution and other species like sperm whales that currently do not show much change. These predictions could inform conservation and the management of activities in potential new areas of conflict.

Studies targeted on specific areas:

This study has generated a broad-scale picture of environmental features that influence cetacean distribution in the central and north-eastern North Atlantic with a focus on comparing

multiple species over a large area. However, there were a number of environmental variables initially obtained for this project, such as on oceanographic fronts and phytoplankton size, which could not be used due to missing data, especially in waters around northern Norway. To explore more targeted ecological questions for specific species, such data could be incorporated in development of models for specific areas. For example, models of pilot whale distribution could be developed in the central North Atlantic because pilot whales are rare in northern Norway (Chapter 3). Other area-focussed studies could be undertaken incorporating prey in the models. Such data were not available over much of the central and north-eastern North Atlantic, but smaller-scale data sets are available for different prey types and some have shown changes over time (e.g. Jakobsson and Østvedt, 1999; Pálsson et al., 2012; Silva et al., 2014; Trenkel et al., 2014). In particular, data from fisheries collected around Iceland or the Norwegian Sea could be good candidates.

Extending the study to the wider North Atlantic:

Although this project has worked with extensive datasets covering a very large area (almost 7 million km^2), there are additional data available both within and outside the study area. Within the study area, although all the large-scale ship survey data were included, there are additional aerial survey data around the coast of Iceland (e.g. Pike et al., 2020b), and along the coast of East Greenland (Hansen et al., 2018). In addition, there are ship and aerial survey data in European Atlantic waters, including the North Sea (e.g. Gilles et al., 2016; Hammond et al., 2017, 2013) that were not included here but could be included in future research. These data would be treated as other levels in the 'survey' covariate. Acoustic data within the study area are scarce.

Outside the study area, large scale surveys have been conducted in European waters (SCANS and CODA) (e.g. Hammond et al., 2017), Ireland (ObSERVE) (Rogan et al., 2018), West Greenland (e.g. Hansen et al., 2018), Canada, and USA (e.g. Roberts et al., 2016). Currently there is a US navy project combining all these datasets to estimate abundance, but a future step is that all these datasets could also be used in the same analytical framework as in this project to investigate drivers of cetacean distribution for the whole North Atlantic.

Model-based abundance estimates:

Design-based abundance estimates have been published for the exploited species covered in this study and also for some other species, especially from the 2015 surveys (e.g. NAMMCO,

2019a; Pike et al., 2019b). Design-based methods provide abundance estimates for the defined survey blocks but not at a finer spatial scale. Investigating abundance at a finer scale can be done using model-based abundance estimation (e.g. Bortolotto et al., 2017; Cañadas and Hammond, 2008). Model-based abundance estimates could be generated from the models developed in this project but, as described above (see section 2.2.3), such estimates would be negatively biased because they would not be corrected for availability bias or perception bias. This bias would be severe for deep diving species, especially.

However, relative abundance could be estimated within the studied range in different years to explore changes over time. For example, minke whale (the species with the highest precision prediction) relative abundance could be estimated in the earlier and later years to explore if the broader distribution see in later years is a result of an increase in abundance, dispersal or both and maybe to understand better the decrease in abundance observed in south Iceland (Chapter 4). Another use of model-based abundance could be the estimation of pilot whale relative abundance (and changes over time) in an area around the Faroe Islands believed to support the population that is subjected to hunting (NAMMCO, 2018), which could allow a more focussed assessment of the sustainability of the hunt. Model-based abundance estimates could also be used to quantify the core areas for the different species and areas of overlap in the species distribution, in order to suggest areas for protection (MPAs) (Jones et al., 2015) (see section 6.5).

6.7 Concluding remarks

Spatial modelling can capture changes in species distribution through different temporal periods to help understand how species react to changes in their environment. Here it is shown that relationships between cetaceans and environmental variables can be stable or can change over time, and that this is species/variable specific.

Availability of environmental data was limited in the early years, and only bathymetric (depth, slope, and aspect) and SST were available to compare between periods. SST was always retained, and depth in most cases, in the best models for all species, even in the recent models where more covariates were available. This indicates that these two variables could be useful indirect proxies for the prey of cetacean species.

Relationships between cetacean density and depth were generally the same through both study periods. However, there were three species where this relationship was not maintained: pilot

whale, killer whale, and white-beaked dolphin. These species belong to different guilds, but a common feature is that their presence in the area is not seasonal and thus they feed all year long in the study area.

Relationships between cetacean density and dynamic oceanographic variables that are lagged in time could help to understand how cetacean-prey relationships develop seasonally. The hypothesis is that the lag between density and these variables is shorter for species that feed lower in the trophic web and *vice versa*. Baleen whales feed lower in the trophic web and showed summer relationships. In deep diving species, temperature-related covariates for sperm and pilot whales were lagged back to spring, but for northern bottlenose whales they were in the summer. In the two delphinid species there were no clear seasonal signals. There is therefore some support for this hypothesis for some species, but not all.

Changes in distribution between the two periods were found to vary among species and guilds. They can be generally summarized as an expansion to a broader distribution, with distribution in new areas close to the limits with Arctic waters, and increased usage of some areas, for example the Barents Sea for baleen whales.

7 REFERENCE LIST

Abend, A.G., Smith, T.D., 1999. Review of Distribution of the Long-finned Pilot Whale (Globicephala melas) in the North Atlantic and Mediterranean. NOAA Tech. Memo. NMFS-NE, 22.

Aguilar, À., Borrell, A., Reijnders, P.J.H., 2002. Geographical and temporal variation in levels of organochlorine contaminants in marine mammals. Mar. Environ. Res. 53, 425–452. https://doi.org/10.1016/S0141-1136(01)00128-3

Aguilar, À., García-Vernet, R., 2018. Fin Whale. Encycl. Mar. Mamm. 368–371. https://doi.org/10.1016/b978-0-12-804327-1.00128-x

Alerstam, T., Hedenström, A., Åkesson, S., 2003. Long-distance migration: Evolution and determinants. Oikos 103, 247–260. https://doi.org/10.1034/j.1600-0706.2003.12559.x

Alexander, M.A., Halimeda Kilbourne, K., Nye, J.A., 2014. Climate variability during warm and cold phases of the Atlantic Multidecadal Oscillation (AMO) 1871-2008. J. Mar. Syst. 133, 14–26. https://doi.org/10.1016/j.jmarsys.2013.07.017

Alexander, M.A., Scott, J.D., Friedland, K.D., Mills, K.E., Nye, J.A., Pershing, A.J., Thomas, A.C., 2018. Projected sea surface temperatures over the 21st century: Changes in the mean, variability and extremes for large marine ecosystem regions of Northern Oceans. Elem Sci Anth 6, 1–25. https://doi.org/10.1525/elementa.191

Alheit, J., Licandro, P., Coombs, S., Garcia, A., Giráldez, A., Santamaría, M.T.G., Slotte, A., Tsikliras, A.C., 2014. Reprint of “Atlantic Multidecadal Oscillation (AMO) modulates dynamics of small pelagic fishes and ecosystem regime shifts in the eastern North and Central Atlantic.” J. Mar. Syst. 133, 88–102. https://doi.org/10.1016/j.jmarsys.2014.02.005

Alves, F., Quérouil, S., Dinis, A., Nicolau, C., Ribeiro, C., Freitas, L., Kaufmann, M., Fortuna, C.,

2013. Population structure of short-finned pilot whales in the oceanic archipelago of Madeira based on photo-identification and genetic analyses: Implications for conservation. Aquat. Conserv. Mar. Freshw. Ecosyst. 23, 758–776. https://doi.org/10.1002/aqc.2332

Amodio, S., Aria, M., D'Ambrosio, A., 2014. On concurvity in nonlinear and nonparametric regression models. Statistica 74, 85–98. https://doi.org/10.6092/issn.1973-2201/4599

Anderwald, P., Evans, P.G.H., Dyer, R., Dale, A., Wright, P.J., Hoelzel, A.R., 2012. Spatial scale and environmental determinants in minke whale habitat use and foraging. Mar. Ecol. Prog. Ser. 450, 259–274. https://doi.org/10.3354/meps09573

Antunes, R., Kvadsheim, P.H., Lam, F.P.A., Tyack, P.L., Thomas, L., Wensveen, P.J., Miller, P.J.O., 2014. High thresholds for avoidance of sonar by free-ranging long-finned pilot whales (Globicephala melas). Mar. Pollut. Bull. 83, 165–180. https://doi.org/10.1016/j.marpolbul.2014.03.056

Arrigo, K.R., van Dijken, G.L., 2015. Continued increases in Arctic Ocean primary production. Prog. Oceanogr. 136, 60–70. https://doi.org/10.1016/j.pocean.2015.05.002

ASCOBANS, 2013. Proceedings of the ECS / ASCOBANS / WDC Workshop Towards a conservation strategy for white-beaked dolphins in the Northeast Atlantic. Warsaw, Poland.

Astthorsson, O.S., Valdimarsson, H., Gudmundsdottir, A., Óskarsson, G.J., 2012. Climate-related variations in the occurrence and distribution of mackerel (*Scomber scombrus*) in Icelandic waters. ICES J. Mar. Sci. 69, 1289–1297. https://doi.org/10.1093/icesjms/fss084

Auðunsson, G.A., Nielsen, N.H., Víkingsson, G.A., Daníel, S., 2013. Age estimation of common minke whales (*Balaenoptera acutorostrata*) in Icelandic waters by aspartic acid racemization (AAR), -AAR and earplug readings of Antarctic minke whales (*B . bonaerensis*) used as a reference. IWC Sci. Comm. SC/F13/SP1, 1–23.

Avila, I.C., Kaschner, K., Dormann, C.F., 2018. Current global risks to marine mammals: Taking stock of the threats. Biol. Conserv. 221, 44–58. https://doi.org/10.1016/j.biocon.2018.02.021

Bachiller, E., Skaret, G., Nøttestad, L., Slotte, A., 2016. Feeding ecology of Northeast Atlantic Mackerel, Norwegian spring-spawning herring and blue whiting in the Norwegian Sea. PLoS One 11, 25. https://doi.org/10.1371/journal.pone.0149238

Baumgartner, M.F., Mullin, K.D., May, L.N., Leming, T.D., 2001. Cetacean habitats in the northern Gulf of Mexico. Fish. Bull. 99, 219–239.

Bearzi, G., 2002. Interactions between cetacean and fisheries in the Mediterranean Sea, in: Notarbartolo di Sciara, G. (Ed.), Cetaceans of the Mediterranean and Black Seas: State of Knowledge and Conservation Strategies. A report to the ACCOBAMS Secretariat, Monaco, p. 20.

Bearzi, G., Agazzi, S., Gonzalvo, J., Costa, M., Bonizzoni, S., Politi, E., Piroddi, C., Reeves, R.R., 2008. Overfishing and the disappearance of short-beaked common dolphins from western Greece. Endanger. Species Res. 5, 1–12. https://doi.org/10.3354/esr00103

Beck, S., Foote, A.D., Kötter, S., Harries, O., Mandleberg, L., Stevick, P.T., Whooley, P., Durban, J.W., 2014. Using opportunistic photo-identifications to detect a population decline of killer whales (Orcinus orca) in British and Irish waters. J. Mar. Biol. Assoc. UK 94, 1327–1333. https://doi.org/10.1017/S0025315413001124

Benjaminsen, T., Christensen, I., 1979. The natural history of the bottlenose whale, *Hyperoodon ampullatus* (FORSTER), in: Winn, H.E., Olla, B.L. (Eds.), Behaviour of Marine Animals. Springer US, Boston, MA, pp. 143–164. https://doi.org/10.1007/978-1-4684-2985-5_5

Bersch, M., 2002. North Atlantic Oscillation–induced changes of the upper layer circulation in the northern North Atlantic Ocean. J. Geophys. Res. 107, 1–11. https://doi.org/10.1029/2001jc000901

Bertulli, C.G., Cecchetti, A., Van Bressem, M..-F., Van Waerebeek, K., 2012. Skin disorders in common minke whales and white-beaked dolphins off Iceland, a photographic assessment. J. Mar. Anim. Ecol. 5, 29–40.

Bettridge, S., Baker, C.S., Barlow, J., Clapham, P.J., Ford, M., Gouveia, D., Mattila, D.K., Pace, R.M., III, Rosel, P.E., Silber, G.K., Wade, P.R., 2015. Status review of the humpback whale (*Megaptera novaeangliae*) under the Endangered Species Act. NOAA-TM-NMFS-SWFSC-540 263.

Bjørke, H., 2001. Predators of the squid *Gonatus fabricii* (Lichtenstein) in the Norwegian Sea. Fish. Res. 52, 113–120. https://doi.org/10.1016/S0165-7836(01)00235-1

Bloch, D., Desportes, G., Zachariassen, M., Christensen, I., 1996. The northern bottlenose whale in the Faroe Islands, 1584-1993. J. Zool. 239, 123–140. https://doi.org/10.1111/j.1469-

7998.1996.tb05441.x

Bloch, D., Lockyer, C., 1988. Killer whales (*Orcinus orca*) in Faroese waters. Rit Fiskid. 11, 55–64.

Bloch, D., Lockyer, C., Zachariassen, M., 1993. Age and growth parameters of the long-finned pilot whale off the Faroe Islands. Rep. Int. Whal. Comm. 14, 163–207.

Bogstad, B., Gjøsæter, H., Haug, T., Lindstrøm, U., 2015. A review of the battle for food in the Barents Sea: cod vs. marine mammals. Front. Ecol. Evol. 3. https://doi.org/10.3389/fevo.2015.00029

Bortolotto, G.A., Danilewicz, D., Hammond, P.S., Thomas, L., Zerbini, A.N., 2017. Whale distribution in a breeding area: Spatial models of habitat use and abundance of western South Atlantic humpback whales. Mar. Ecol. Prog. Ser. 585, 213–227. https://doi.org/10.3354/meps12393

Broomé, S., Chafik, L., Nilsson, J., 2019. Mechanisms of the time-varying sea surface height and heat content trends in the eastern Nordic Seas. Ocean Sci. 25. https://doi.org/10.5194/os-2019-109

Buckland, S.T., Anderson, D.R., Burnham, K.P., Laake, J.L., Borchers, D.L., Thomas, L., 2001. Introduction to Distance Sampling : Estimating abundance of biological populations. Oxford University Press, New York.

Buckland, S.T., Bloch, D.R., Cattanach, K.L., Gunnlaugsson, T., Hoydall, K., Lens, S., Sigurjónsson, J., 1993. Distribution and abundance of long-finned pilot whales in the North Atlantic, estimated from NASS-87 and NASS-89 data. Reports Int. Whal. Comm. 14, 33–49.

Buckland, S.T., Turnock, B.J., 1992. A Robust Line Transect Method. Biometrics 48, 901–909. https://doi.org/10.2307/2532356

Calambokidis, J., Steiger, G.H., Ellifrit, D.K., Troutman, B.L., Bowlby, C.E., 2004. Distribution and abundance of humpback whales (*Megaptera novaeangliae*) and other marine mammals off the northern Washington coast. Fish. Bull. 102, 563–580.

Cañadas, A., Hammond, P.S., 2008. Abundance and habitat preferences of the short-beaked common dolphin Delphinus delphis in the southwestern Mediterranean: Implications for conservation. Endanger. Species Res. 4, 309–331. https://doi.org/10.3354/esr00073

Cañadas, A., Sagarminaga, R., De Stephanis, R., Urquiola, E., Hammond, P.S., 2005. Habitat

preference modelling as a conservation tool: Proposals for marine protected areas for cetaceans in southern Spanish waters. Aquat. Conserv. Mar. Freshw. Ecosyst. 15, 495–521. https://doi.org/10.1002/aqc.689

Canning, S.J., Santos, M.B., Reid, R.J., Evans, P.G.H., Sabin, R.C., Bailey, N., Pierce, G.J., 2008. Seasonal distribution of white-beaked dolphins (*Lagenorhynchus albirostris*) in UK waters with new information on diet and habitat use. J. Mar. Biol. Assoc. UK 88, 1159–1166. https://doi.org/10.1017/S0025315408000076

Carr, J.R., Bell, H., Killick, R., Holt, T., 2017. Exceptional retreat of Novaya Zemlya's marine-terminating outlet glaciers between 2000 and 2013. Cryosph. 11, 2149–2174. https://doi.org/10.5194/tc-11-2149-2017

Castellote, M., Clark, C.W., Lammers, M.O., 2012. Acoustic and behavioural changes by fin whales (*Balaenoptera physalus*) in response to shipping and airgun noise. Biol. Conserv. 147, 115–122. https://doi.org/10.1016/j.biocon.2011.12.021

Caurant, F., Amiard-Triquet, C., 1995. Cadmium contamination in Pilot Whales *Globicephala melas*: Source and potential hazard to the species. Mar. Pollut. Bull. 30, 207–210. https://doi.org/10.1016/0025-326X(94)00126-T

Caurant, F., Amiard-Triquet, C., Amiard, J.C., 1993. Factors influencing the accumulation of metals in pilot whales (*Globicephala melas*) off the Faroe Islands. Rep. int. Whal. Commn. 14, 369–390.

Cheung, W.W.L., Lam, V.W.Y., Sarmiento, J.L., Kearney, K., Watson, R., Pauly, D., 2009. Projecting global marine biodiversity impacts under climate change scenarios. Fish Fish. 10, 235–251. https://doi.org/10.1111/j.1467-2979.2008.00315.x

Christensen, I., 1988. Distribution, movements and abundance of killer whales (*Orcinus orca*) in Norwegian coastal waters, 1982-1987, based on questionnaire surveys. Rit Fiskid. 11, 79–88.

Christensen, I., Haug, T., Øien, N.I., 1992. Seasonal distribution, exploitation and present abundance of stocks of large baleen whales (Mysticeti) and sperm whales (physeter macrocephalus) in norwegian and adjacent waters. ICES J. Mar. Sci. 49, 341–355. https://doi.org/10.1093/icesjms/49.3.341

Christiansen, F., Víkingsson, G.A., Rasmussen, M.H., Lusseau, D., 2014. Female body condition

affects foetal growth in a capital breeding mysticete. Funct. Ecol. 28, 579–588. https://doi.org/10.1111/1365-2435.12200

Clapham, P.J., 2018. Humpback whale. Encycl. Mar. Mamm. 489–492. https://doi.org/10.1016/b978-0-12-804327-1.00154-0

Clarke, M.R., 1996. Cephalopods as prey. III. Cetaceans. Philos. Trans. R. Soc. B Biol. Sci. 351, 1053–1065. https://doi.org/10.1098/rstb.1996.0093

Committee on Taxonomy, 2018. List of Marine Mammal Species and Subspecies - Society for Marine Mammalogy [WWW Document]. URL https://www.marinemammalscience.org/species-information/list-marine-mammal-species-subspecies/#narrative (accessed 1.2.20).

Compton, R.C., 2004. Predicting key habitat and potential distribution of northern bottlenose whales (*Hyperoodon ampullatus*) in the Northwest Atlantic Ocean. University of Plymouth.

Cooke, J.G., 2018a. *Balaenoptera physalus*. IUCN Red List Threat. Species 2018 e.T2478A50349982. 26. https://doi.org/10.2305/IUCN.UK.2018-2.RLTS.T2478A50349982.en

Cooke, J.G., 2018b. *Megaptera novaeangliae*, Humpback whale. IUCN Red List Threat. Species 2018 e.T13006A50362794 26. https://doi.org/10.2305/IUCN.UK.2018-2.RLTS.T13006A50362794.en

Cooke, J.G., 2018c. *Balaenoptera acutorostrata*. IUCN Red List Threat. Species 2018 e.T2474A50348265 22. https://doi.org/https://dx.doi.org/10.2305/IUCN.UK.2018-2.RLTS.T2474A50348265.en.

Dalebout, M.L., Ruzzante, D.E., Whitehead, H., Øien, N.I., 2006. Nuclear and mitochondrial markers reveal distinctiveness of a small population of bottlenose whales (Hyperoodon ampullatus) in the western North Atlantic. Mol. Ecol. 15, 3115–3129. https://doi.org/10.1111/j.1365-294X.2006.03004.x

Dalla Rosa, L., Ford, J.K.B., Trites, A.W., 2012. Distribution and relative abundance of humpback whales in relation to environmental variables in coastal British Columbia and adjacent waters. Cont. Shelf Res. 36, 89–104. https://doi.org/10.1016/j.csr.2012.01.017

Dalpadado, P., Arrigo, K.R., van Dijken, G.L., Rune Skjoldal, H., Bagøien, E., Dolgov, A.,

Prokopchuk, I., Sperfeld, E., 2020. Climate effects on temporal and spatial dynamics of phytoplankton and zooplankton in the Barents Sea. Prog. Oceanogr. https://doi.org/10.1016/j.pocean.2020.102320

Dalpadado, P., Ellertsen, B., Melle, W., Dommasnes, A., 2000. Food and feeding conditions of Norwegian spring-spawning herring (*Clupea harengus*) through its feeding migrations. ICES J. Mar. Sci. 57, 843–857. https://doi.org/10.1006/jmsc.2000.0573

Dam, M., Bloch, D., 2000. Screening of mercury and persistent organochlorine pollutants in long-finned pilot whale (*Globicephala melas*) in the Faroe Islands. Mar. Pollut. Bull. 40, 1090–1099. https://doi.org/10.1016/S0025-326X(00)00060-6

Das, K., Debacker, V., Pillet, S., Bouquegneau, J.-M., 2003. Heavy metals in marine mammals, in: Vos, J.G., Bossart, G.D., Fournier, M., O'Shea, T. (Eds.), Toxicology of Marine Mammals. Taylor and Francis Publishers, Washington D.C, pp. 135–167. https://doi.org/10.1201/9780203165577.ch7

DeMaster, D.P., Fowler, C.W., Perry, S.L., Richlen, M.F., 2001. Predation and competition: the impact of fisheries on marine-mammal populations over the next one hundred years. J. Mammal. 82, 641–651. https://doi.org/10.1644/1545-1542(2001)082<0641:pactio>2.0.co;2

Desportes, G., Mouritsen, R., 1993. Preliminary results on the diet of long-finned pilot whales off the Faroe Islands. Reports Int. Whal. Comm. 14, 305–324.

Dong, J.H., Lien, J., Nelson, D., Curren, K., 1996. A contribution to the biology of the white-beaked dolphin, *Lagenorhynchus albirostris*, in waters off Newfoundland. Can. Field-Naturalist 110, 278–287.

Drinkwater, K.F., Belgrano, A., Borja, A., Conversi, A., Edwards, M., Greene, C.H., Ottersen, G., Pershing, A.J., Walker, H., 2003. The response of freshwater ecosystems to climate variability associated with the North Atlantic oscillation, in: Hurrell, J.W., Kushnir, Y., Ottersen, G., Visbeck, M. (Eds.), Geophysical Monograph Series. American Geophysical Union, Washington, D. C., pp. 211–234. https://doi.org/10.1029/134GM12

Embling, C.B., Gillibrand, P.A., Gordon, J., Shrimpton, J., Stevick, P.T., Hammond, P.S., 2010. Using habitat models to identify suitable sites for marine protected areas for harbour porpoises (*Phocoena phocoena*). Biol. Conserv. 143, 267–279.

https://doi.org/10.1016/j.biocon.2009.09.005

Esteban, R., Verborgh, P., Gauffier, P., Alarcón, D., Salazar-Sierra, J.M., Giménez, J., Foote, A.D., De Stephanis, R., 2016. Conservation status of killer whales, *Orcinus orca*, in the Strait of Gibraltar, Advances in Marine Biology. https://doi.org/10.1016/bs.amb.2016.07.001

Evans, P.G.H., 2009. Whales , porpoises and dolphins – Order Cetacea. Brugge, Belgium.

Fall, J., Skern-Mauritzen, M., 2014. White-beaked dolphin distribution and association with prey in the Barents Sea. Mar. Biol. Res. 10, 957–971. https://doi.org/10.1080/17451000.2013.872796

Faroe, I., 2019. Whales and whaling in the Faroe Islands: Catches 2000-2018 [WWW Document]. URL http://www.whaling.fo/en/regulated/450-years-of-%0Astatistics/catches/%0A

Fernández, R., Pierce, G.J., MacLeod, C.D., Brownlow, A., Reid, R.J., Rogan, E., Addink, M., Deaville, R., Jepson, P.D., Santos, M.B., 2014. Strandings of northern bottlenose whales, *Hyperoodon ampullatus*, in the north-east Atlantic: Seasonality and diet. J. Mar. Biol. Assoc. UK 94, 1109–1116. https://doi.org/10.1017/S002531541300180X

Fisheries and Oceans Canada, 2016. Recovery Strategy for the Northern Bottlenose Whale (*Hyperoodon ampullatus*), Scotian Shelf population, in Atlantic Canadian Waters [Final], Species at Risk Act Recovery Strategy Series. Fisheries and Oceans Canada, Ottawa.

Flatau, M.K., Talley, L., Niiler, P.P., 2003. The North Atlantic Oscillation, surface current velocities, and SST changes in the subpolar North Atlantic. J. Clim. 16, 2355–2369. https://doi.org/10.1175/2787.1

Foote, A.D., Newton, J., Ávila-Arcos, M.C., Kampmann, M.L., Samaniego, J.A., Post, K., Rosing-Asvid, A., Sinding, M.H.S., Gilbert, M.T.P., 2013. Tracking niche variation over millennial timescales in sympatric killer whale lineages. Proc. R. Soc. B Biol. Sci. 280, 9. https://doi.org/10.1098/rspb.2013.1481

Foote, A.D., Newton, J., Piertney, S.B., Willerslev, E., Gilbert, M.T.P., 2009. Ecological, morphological and genetic divergence of sympatric North Atlantic killer whale populations. Mol. Ecol. 18, 5207–5217. https://doi.org/10.1111/j.1365-294X.2009.04407.x

Foote, A.D., Similä, T., Víkingsson, G.A., Stevick, P.T., 2010. Movement, site fidelity and connectivity in a top marine predator, the killer whale. Evol. Ecol. 24, 803–814.

https://doi.org/10.1007/s10682-009-9337-x

Foote, A.D., Víkingsson, G.A., Øien, N.I., Bloch, D., Davies, C.G., Dunn, T.E., Harvey, P., Mandleberg, L., Whooley, P., Thompson, P.M., 2007. Distribution and abundance of killer whales in the North East Atlantic, Paper SC/59/SM5 presented to the IWC Scientific Committee.

Foote, A.D., Vilstrup, J.T., De Stephanis, R., Verborgh, P., Abel Nielsen, S.C., Deaville, R., Kleivane, L., Martińn, V., Miller, P.J.O., Øien, N.I., Pérez-Gil, M., Rasmussen, M., Reid, R.J., Robertson, K.M., Rogan, E., Similä, T., Tejedor, M.L., Vester, H., Víkingsson, G.A., Willerslev, E., Gilbert, M.T.P., Piertney, S.B., 2011. Genetic differentiation among North Atlantic killer whale populations. Mol. Ecol. 20, 629–641. https://doi.org/10.1111/j.1365-294X.2010.04957.x

Ford, J.K.B., 2018. Killer Whale. Encycl. Mar. Mamm. 531–537. https://doi.org/10.1016/b978-0-12-804327-1.00010-8

Ford, J.K.B., Ellis, G.M., Olesiuk, P.F., Balcomb, K.C., 2010. Linking killer whale survival and prey abundance: Food limitation in the oceans' apex predator? Biol. Lett. 6, 139–142. https://doi.org/10.1098/rsbl.2009.0468

Forney, K.A., 2000. Environmental models of cetacean abundance: reducing uncertainty in population trends. Conserv. Biol. 14, 1271–1286.

Forney, K.A., Ferguson, M.C., Becker, E.A., Fiedler, P.C., Redfern, J. V., Barlow, J., Vilchis, I.L., Ballance, L.T., 2012. Habitat-based spatial models of cetacean density in the eastern Pacific Ocean. Endanger. Species Res. 16, 113–133. https://doi.org/10.3354/esr00393

Forney, K.A., Wade, P.R., 2007. Worldwide distribution and abundance of killer whales, in: Estes, J., DeMaster, D.P., Brownell, R.L., Doak, D.F., Williams, T.M. (Eds.), Whales, Whaling, and Ocean Ecosystems. University of California Press, pp. 145–162. https://doi.org/10.1525/california/9780520248847.003.0012

Fransz, H.G., Colebrook, J.M., Gamble, J.C., Krause, M., 1991. The zooplankton of the north sea. Netherlands J. Sea Res. 28, 1–52. https://doi.org/10.1016/0077-7579(91)90003-J

Frederiksen, M., Furness, R.W., Wanless, S., 2007. Regional variation in the role of bottom-up and top-down processes in controlling sandeel abundance in the North Sea. Mar. Ecol. Prog. Ser. 337, 279–286. https://doi.org/10.3354/meps337279

Friedland, K.D., Record, N.R., Asch, R.G., Kristiansen, T., Saba, V.S., Drinkwater, K.F., Henson, S., Leaf, R.T., Morse, R.E., Johns, D.G., Large, S.I., Hjøllo, S.S., Nye, J.A., Alexander, M.A., Ji, R., 2016. Seasonal phytoplankton blooms in the North Atlantic linked to the overwintering strategies of copepods. Elem. Sci. Anthr. 1–19. https://doi.org/10.12952/journal.elementa.000099

Galatius, A., Bossi, R., Sonne, C., Rigét, F.F., Kinze, C.C., Lockyer, C., Teilmann, J., Dietz, R., 2013a. PFAS profiles in three North Sea top predators: metabolic differences among species? Environ. Sci. Pollut. Res. 20, 8013–8020. https://doi.org/10.1007/s11356-013-1633-x

Galatius, A., Jansen, O.E., Kinze, C.C., 2013b. Parameters of growth and reproduction of white-beaked dolphins (*Lagenorhynchus albirostris*) from the North Sea. Mar. Mammal Sci. 29, 348–355. https://doi.org/10.1111/j.1748-7692.2012.00568.x

Galatius, A., Kinze, C.C., 2016. *Lagenorhynchus albirostris* (Cetacea: Delphinidae). Mamm. Species 48, 35–47. https://doi.org/10.1093/mspecies/sew003

Gilles, A., Adler, S., Kaschner, K., Scheidat, M., Siebert, U., 2011. Modelling harbour porpoise seasonal density as a function of the German Bight environment: Implications for management. Endanger. Species Res. 14, 157–169. https://doi.org/10.3354/esr00344

Gilles, A., Scheidat, M., Siebert, U., 2009. Seasonal distribution of harbour porpoises and possible interference of offshore wind farms in the German North Sea. Mar. Ecol. Prog. Ser. 383, 295–307. https://doi.org/10.3354/meps08020

Gilles, A., Viquerat, S., Becker, E.A., Forney, K.A., Geelhoed, S.C.V., Haelters, J., Nabe-Nielsen, J., Scheidat, M., Siebert, U., Sveegaard, S., Van Beest, F.M., Van Bemmelen, R., Aarts, G., 2016. Seasonal habitat-based density models for a marine top predator, the harbor porpoise, in a dynamic environment. Ecosphere 7, 23. https://doi.org/10.1002/ecs2.1367

Gilles, G., Parent, L., 2017a. Quality information document for Global Ocean Reanalysis Products GLOBAL-REANALYSIS-PHY-001-025.

Gilles, G., Parent, L., 2017b. Product user manual for Global Ocean Reanalysis Products GLOBAL-REANALYSIS-PHY-001-025.

Gjøsæter, H., Bogstad, B., Tjelmeland, S., 2009. Ecosystem effects of the three capelin stock collapses in the Barents Sea. Mar. Biol. Res. 5, 40–53. https://doi.org/10.1080/17451000802454866

Gjøsæter, H., Hallfredsson, E.H., Mikkelsen, N., Bogstad, B., Pedersen, T., 2016. Predation on early life stages is decisive for year-class strength in the Barents Sea capelin (Mallotus villosus) stock. ICES J. Mar. Sci. J. du Cons. 73, 182–195. https://doi.org/10.1093/icesjms/fsv177

Glover, K.A., Kanda, N., Haug, T., Pastene, L.A., Øien, N.I., Goto, M., Seliussen, B.B., Skaug, H.J., 2010. Migration of Antarctic minke whales to the Arctic. PLoS One 5, 1–6. https://doi.org/10.1371/journal.pone.0015197

Glover, K.A., Kanda, N., Haug, T., Pastene, L.A., Øien, N.I., Seliussen, B.B., Sørvik, A.G.E., Skaug, H.J., 2013. Hybrids between common and Antarctic minke whales are fertile and can back-cross. BMC Genet. 14, 11. https://doi.org/10.1186/1471-2156-14-25

Gong, Z., Jain, A.D., Tran, D., Yi, D.H., Wu, F., Zorn, A., Ratilal, P., Makris, N.C., 2014. Ecosystem scale acoustic sensing reveals humpback whale behavior synchronous with herring spawning processes and re-evaluation finds no effect of sonar on humpback song occurrence in the Gulf of Maine in fall 2006. PLoS One 9, e104733. https://doi.org/10.1371/journal.pone.0104733

Greene, C., Pershing, A.J., 2004. North Atlantic right whales: the right whale at the wrong time? Front. Ecol. Environ. 2, 29–34.

Greene, C.H., Pershing, A.J., 2000. The response of Calanus finmarchicus populations to climate variability in the Northwest Atlantic: Basin-scale forcing associated with the North Atlantic Oscillation. ICES J. Mar. Sci. 57, 1536–1544. https://doi.org/10.1006/jmsc.2000.0966

Greenland, 2012. White Paper on Hunting of Large Whales in Greenland. Gov. Greenl. Minist. Fish. Hunt. Agric. 95.

Gulev, S.K., Latif, M., 2015. The origins of a climate oscillation. Nature 521, 428–430. https://doi.org/10.1038/521428a

Gunnlaugsson, T., Víkingsson, G.A., Pike, D.G., 2009. Combined line-transect and cue-count estimate of sperm whale abundance in the North Atlantic, from Icelandic NASS-2001 shipboard survey. NAMMCO Sci. Publ. 7, 73. https://doi.org/10.7557/3.2706

Häkkinen, S., Rhines, P.B., 2004. Decline of Subpolar North Atlantic Circulation during the 1990s. Science (80-.). 304, 555–559. https://doi.org/10.1126/science.1094917

Häkkinen, S., Rhines, P.B., Worthen, D.L., 2013. Northern North Atlantic sea surface height and ocean heat content variability. J. Geophys. Res. Ocean. 118, 3670–3678. https://doi.org/10.1002/jgrc.20268

Halpern, B.S., Frazier, M., Potapenko, J., Casey, K.S., Koenig, K., Longo, C., Lowndes, J.S., Rockwood, R.C., Selig, E.R., Selkoe, K.A., Walbridge, S., 2015. Spatial and temporal changes in cumulative human impacts on the world's ocean. Nat. Commun. 6, 1–7. https://doi.org/10.1038/ncomms8615

Halpern, B.S., Walbridge, S., Selkoe, K.A., Kappel, C. V., Micheli, F., D'Agrosa, C., Bruno, J.F., Casey, K.S., Ebert, C., Fox, H.E., Fujita, R., Heinemann, D., Lenihan, H.S., Madin, E.M.P., Perry, M.T., Selig, E.R., Spalding, M., Steneck, R., Watson, R., 2008. A Global Map of Human Impact on Marine Ecosystems. Science (80-.). 319, 948–952. https://doi.org/10.1126/science.1149345

Hamer, D.J., Childerhouse, S.J., Gales, N.J., 2012. Odontocete bycatch and depredation in longline fisheries: A review of available literature and of potential solutions. Mar. Mammal Sci. 28, 345–374. https://doi.org/10.1111/j.1748-7692.2011.00544.x

Hammond, P.S., Lacey, C., Gilles, A., Viquerat, S., Börjesson, P., Herr, H., Macleod, K., Ridoux, V., Santos, M.B., Scheidat, M., Teilmann, J., Vingada, J., Øien, N.I., 2017. Estimates of cetacean abundance in European Atlantic waters in summer 2016 from the SCANS-III aerial and shipboard surveys. Wageningen 40.

Hammond, P.S., Macleod, K., Berggren, P., Borchers, D.L., Burt, L., Cañadas, A., Desportes, G., Donovan, G.P., Gilles, A., Gillespie, D., Gordon, J., Hiby, L., Kuklik, I., Leaper, R., Lehnert, K., Leopold, M., Lovell, P., Øien, N.I., Paxton, C.G.M., Ridoux, V., Rogan, E., Samarra, F., Scheidat, M., Sequeira, M., Siebert, U., Skov, H., Swift, R., Tasker, M.L., Teilmann, J., Van Canneyt, O., Vázquez, J.A., 2013. Cetacean abundance and distribution in European Atlantic shelf waters to inform conservation and management. Biol. Conserv. 164, 107–122. https://doi.org/10.1016/j.biocon.2013.04.010

Hammond, P.S., Macleod, K., Gillespie, D., Swift, R., Winship, A., Burt, M.L., Cañadas, A., Vázquez, J.A., Ridoux, V., Certain, G., Van Canneyt, O., Lens, S., Santos, M.B., Rogan, E., Uriarte, A., Hernández, C., Castro, R., 2009. Cetacean Offshore Distribution and Abundance in the European Atlantic (CODA) 43.

Hansen, C., Kvaleberg, E., Samuelsen, A., 2010. Anticyclonic eddies in the Norwegian Sea; their generation, evolution and impact on primary production. Deep. Res. Part I Oceanogr. Res. Pap. 57, 1079–1091. https://doi.org/10.1016/j.dsr.2010.05.013

Hansen, R.G., Boye, T.K., Larsen, R.S., Nielsen, N.H., Tervo, O., Nielsen, R.D., Rasmussen, M.H., Sinding, M.H.S., Heide-Jørgensen, M.P., 2018. Abundance of whales in West and East Greenland in summer 2015. NAMMCO Sci. Publ. 11, 1–17. https://doi.org/doi.org/10.7557/3.4689

Hansen, R.G., Heide-Jørgensen, M.P., 2013. Spatial trends in abundance of long-finned pilot whales, white-beaked dolphins and harbour porpoises in West Greenland. Mar. Biol. 160, 2929–2941. https://doi.org/10.1007/s00227-013-2283-8

Harris, C.M., Sadykova, D., DeRuiter, S.L., Tyack, P.L., Miller, P.J.O., Kvadsheim, P.H., Lam, F.P.A., Thomas, L., 2015. Dose response severity functions for acoustic disturbance in cetaceans using recurrent event survival analysis. Ecosphere 6, 236. https://doi.org/10.1890/ES15-00242.1

Harwood, J., 2001. Marine mammals and their environment in the twenty-first century. J. Mammal. 82, 630–640. https://doi.org/http://www.jstor.org/stable/1383602

Hastie, G.D., Wilson, B., Wilson, L.J., Parsons, K.M., Thompson, P.M., 2004. Functional mechanisms underlying cetacean distribution patterns: Hotspots for bottlenose dolphins are linked to foraging. Mar. Biol. 144, 397–403. https://doi.org/10.1007/s00227-003-1195-4

Hátún, H., Payne, M.R., Beaugrand, G., Reid, P.C., Sandø, A.B., Drange, H., Hansen, B., Jacobsen, J.A., Bloch, D., 2009. Large bio-geographical shifts in the north-eastern Atlantic Ocean: From the subpolar gyre, via plankton, to blue whiting and pilot whales. Prog. Oceanogr. 80, 149–162. https://doi.org/10.1016/j.pocean.2009.03.001

Hátún, H., Sande, A.B., Drange, H., Hansen, B., Valdimarsson, H., 2005. Ocean science: Influence of the atlantic subpolar gyre on the thermohaline circulation. Science (80-.). 309, 1841–1844. https://doi.org/10.1126/science.1114777

Haug, T., Bogstad, B., Chierici, M., Gjøsæter, H., Hallfredsson, E.H., Høines, Å.S., Hoel, A.H., Ingvaldsen, R.B., Jørgensen, L.L., Knutsen, T., Loeng, H., Naustvoll, L.J., Røttingen, I., Sunnanå, K., 2017. Future harvest of living resources in the Arctic Ocean north of the Nordic

and Barents Seas: a review of possibilities and constraints. Fish. Res. 188, 38–57. https://doi.org/10.1016/j.fishres.2016.12.002

Haug, T., Lindstrøm, U., Nilssen, K.T., 2002. Variations in minke whale (*Balaenoptera acutorostrata*) diet and body condition in response to ecosystem changes in the Barents Sea. Sarsia 87, 409–422. https://doi.org/10.1080/00364820210001557l5

Havforskningsinstituttet, 2020. Barentshavet har blitt kjøligere – det flytter iskantsonen lengre sør | Havforskningsinstituttet [WWW Document]. URL https://www.hi.no/hi/nyheter/2020/januar/barentshavet-har-blitt-kjoligere-det-flytter-iskantsonen-lengre-sor (accessed 2.3.20).

Heide-Jørgensen, M.P., Laidre, K.L., 2007. Autumn space-use patterns of humpback whales (*Megaptera novaeangliae*) in West Greenland. J. Cetacean Res. Manag. 9, 121–126.

Higdon, J.W., Ferguson, S.H., 2011. Reports of humpback and minke whales in the Hudson Bay region, eastern Canadian Arctic. Northeast. Nat. 18, 370–377. https://doi.org/10.1656/045.018.0309

Higdon, J.W., Ferguson, S.H., 2009. Loss of Arctic sea ice causing punctuated change in sightings of killer whales (*Orcinus orca*) over the past century. Ecol. Appl. 19, 1365–1375. https://doi.org/10.1890/07-1941.1

Hijmans, R.J., 2017. Raster: Geographic data analysis and modeling.

Hobbs, K.E., Muir, D.C.G., Born, E.W., Dietz, R., Haug, T., Metcalfe, T., Metcalfe, C., Øien, N.I., 2003. Levels and patterns of persistent organochlorines in minke whale (*Balaenoptera acutorostrata*) stocks from the North Atlantic and European Arctic. Environ. Pollut. 121, 239–252. https://doi.org/10.1016/S0269-7491(02)00218-X

Hooker, S.K., De Soto, N.A., Baird, R.W., Carroll, E.L., Claridge, D., Feyrer, L., Miller, P.J.O., Onoufriou, A., Schorr, G., Siegal, E., Whitehead, H., 2019. Future directions in research on beaked whales. Front. Mar. Sci. 6. https://doi.org/10.3389/fmars.2018.00514

Hooker, S.K., Iverson, S.J., Ostrom, P., Smith, S.C., 2001. Diet of northern bottlenose whales inferred from fatty-acid and stable-isotope analyses of biopsy samples. Can. J. Zool. 79, 1442–1454. https://doi.org/10.1139/z01-096

Hooker, S.K., Whitehead, H., Gowans, S., 1999. Marine Protected Area Design and the Spatial

and Temporal Distribution of Cetaceans in a Submarine Canyon (Diseño de Areas Marinas Protegidas y la Distribución Espacial y Temporal de Cetaceos en un Cañón Submarino). Conserv. Biol. 13, 592–602. https://doi.org/10.1046/j.1523-1739.1999.98099.x

Houghton, L., Ramirez-Martinez, N., Mikkelsen, B., Víkingsson, G., Gunnlaugsson, T., Øien, N.I., Hammond, P., 2020. Oceanic Drivers of Sei Whale Distribution in the North Atlantic. NAMMCO Sci. Publ. 11, 1–10. https://doi.org/10.7557/3.5211

Houston, A.I., Stephens, P.A., Boyd, I.L., Harding, K.C., McNamara, J.M., 2007. Capital or income breeding? A theoretical model of female reproductive strategies. Behav. Ecol. 18, 241–250. https://doi.org/10.1093/beheco/arl080

Hoydal, K., Lastein, L., 1993. Analysis of Faroese catches of pilot whales (1709-1992), in relation to environmental variations. Reports Int. Whal. Comm. 14, 89–106.

Hoyt, E., 2013. The best whale watching in Europe. Whale and Dolphin Conservation Society, Unterhaching, Germany.

Huse, G., MacKenzie, B.R., Trenkel, V., Doray, M., Nøttestad, L., Oskarsson, G., 2015. Spatially explicit estimates of stock sizes, structure and biomass of herring and blue whiting, and catch data of bluefin tuna. Earth Syst. Sci. Data 7, 35–46. https://doi.org/10.5194/essd-7-35-2015

ICES, 2019a. Norway special request for revised 2019 advice on mackerel (*Scomber scombrus*) in subareas 1 – 8 and 14 , and in Division 9 . a (the Northeast Atlantic and adjacent waters). Rep. ICES Advis. Committee, 2019 ICES Advic, 1–17. https://doi.org/10.17895/ices.advice.5252

ICES, 2019b. Working Group on Bycatch of Protected Species (WGBYC). ICES Sci. Reports 1, 163. https://doi.org/10.17895/ices.pub.5563

ICES, 2013. Report of the Working Group on Bycatch of Protected Species (WGBYC) 2015 ICES Headquarters , Copenhagen , Denmark International Council for the Exploration of the Sea. Copenhagen, Denmark, 4-8 February.

ICES, 2002. Report of the ICES Advisory Committee on Ecosystems. ICES Coop. Res. Rep. 129.

ICES, 1992. Report of the study group on pilot whales, ICES C.M. Montreal, 3-4 December 1991.

IJsseldijk, L.L., Brownlow, A., Davison, N.J., Deaville, R., Haelters, J., Keijl, G., Siebert, U.,

Doeschate, M.T.I. ten, 2018. Spatiotemporal trends in white-beaked dolphin strandings along the North Sea coast from 1991-2017. Lutra 61, 153–164.

Irvine, L.G., Thums, M., Hanson, C.E., McMahon, C.R., Hindell, M.A., 2017. Quantifying the energy stores of capital breeding humpback whales and income breeding sperm whales using historical whaling records. R. Soc. Open Sci. 4, 160290. https://doi.org/10.1098/rsos.160290

Isojunno, S., Aoki, K., Curé, C., Kvadsheim, P.H., Miller, P.J.O., 2018. Breathing patterns indicate cost of exercise during diving and response to experimental sound exposures in long-finned pilot whales. Front. Physiol. 9, 1–17. https://doi.org/10.3389/fphys.2018.01462

IUCN, 2016. Rules of Procedure for IUCN Red List Assessments 2017-2020. Version 3.0., The IUCN SSC Steering Committee in September 2016.

IWC, 2020. International Whaling Commission Total catches data base [WWW Document]. URL https://iwc.int/total-catches (accessed 1.4.20).

IWC, 2019. Status of whales [WWW Document]. URL https://iwc.int/status (accessed 12.13.19).

IWC, 2016. Report of the Scientific Committee. Annex D: Report of the Sub-Committee on the Revised Management Procedure. J. Cetacean Res. Manag. 17, 106–184.

IWC, 2012. Report of the Scientific Committee. J. Cetacean Res. Manag. 13 SUPPL., 1–405.

IWC, 2002. Annex H: Report of the Sub-Committee on the Comprehensive Assessment of North Atlantic Humpback Whales, Journal Cetacean Research Management.

IWC, 1990. Report to the Scientific Committee. Reports Int. Whal. Comm. 40, 39–80.

IWC, 1989. Thirty-Ninth Report of the International Whaling Commission. The International Whaling Commission, Cambridge.

IWC, 1984. Thirty-fourth Report of the International Whaling Commission. International Whaling Commission, Cambridge.

Jakobsson, J., Østvedt, O.J., 1999. A review of joint investigations on the distribution of herring in the Norwegian and Iceland Seas 1950-1970. Rit Fiskid. 16, 209–238.

Jansen, O.E., Leopold, M.F., Meesters, E.H.W.G., Smeenk, C., 2010. Are white-beaked dolphins *Lagenorhynchus albirostris* food specialists? Their diet in the southern North Sea. J. Mar.

Biol. Assoc. UK 90, 1501–1508. https://doi.org/10.1017/S0025315410001190

Jefferson, T.A., Leatherwood, S., Webber, M.A., 1993. FAO species identification guide marine mammals of the world. FAO, Rome. https://doi.org/92-5-103292-0

Jepson, P.D., Deaville, R., Barber, J.L., Aguilar, À., Borrell, A., Murphy, S., Barry, J., Brownlow, A., Barnett, J., Berrow, S.D., Cunningham, A.A., Davison, N.J., Ten Doeschate, M., Esteban, R., Ferreira, M., Foote, A.D., Genov, T., Giménez, J., Loveridge, J., Llavona, Á., Martin, V., Maxwell, D.L., Papachlimitzou, A., Penrose, R., Perkins, M.W., Smith, B., De Stephanis, R., Tregenza, N., Verborgh, P., Fernandez, A., Law, R.J., 2016. PCB pollution continues to impact populations of orcas and other dolphins in European waters. Sci. Rep. 6, 1–17. https://doi.org/10.1038/srep18573

Jones, E.L., McConnell, B.J., Smout, S., Hammond, P.S., Duck, C.D., Morris, C.D., Thompson, D., Russel, D.J.F., Vincent, C., Cronin, M., Sharples, R.J., Matthiopoulos, J., 2015. Patterns of space use in sympatric marine colonial predators reveal scales of spatial partitioning. Mar. Ecol. Prog. Ser. 534, 235–249. https://doi.org/10.3354/meps11370

Jonsson, K.I., 1997. Capital and income breeding as alternative tactics of resource use in reproduction. Oikos 78, 57–66.

Jourdain, E., Andvik, C., Karoliussen, R., Ruus, A., Vongraven, D., Borgå, K., 2020. Isotopic niche differs between seal and fish-eating killer whales (*Orcinus orca*) in northern Norway. Ecol. Evol. 4115–4127. https://doi.org/10.1002/ece3.6182

Jourdain, E., Karoliussen, R., 2018. Identification catalogue of Norwegian killer whales: 2007-2018. https://doi.org/10.6084/M9.FIGSHARE.4205226.V3

Jourdain, E., Ugarte, F., Víkingsson, G.A., Samarra, F.I.P., Ferguson, S.H., Lawson, J., Vongraven, D., Desportes, G., 2019. North Atlantic killer whale *Orcinus orca* populations: a review of current knowledge and threats to conservation. Mamm. Rev. 49, 384–400. https://doi.org/10.1111/mam.12168

Kalland, A., Sejersen, F., 2005. Marine mammals and northern cultures. Canadian Circumpolar Institute Press, Edmonton.

Kann, L.M., Wishner, K., 1995. Spatial and temporal patterns of zooplankton on baleen whale feeding grounds in the southern Gulf of Maine. J. Plankton Res. 17, 235–262.

Kaschner, K., Pauly, D., 2005. Mammals and fisheries: food, in: Salem, D.J., Rowan, A.N. (Eds.), The State of the Animals III. Humane Society Press, Washington, DC, pp. 95–117.

Kaschner, K., Quick, N.J., Jewell, R., Williams, R., Harris, C.M., 2012. Global coverage of cetacean line-transect surveys: status quo, data gaps and future challenges. PLoS One 7. https://doi.org/10.1371/journal.pone.0044075

Kassambra, A., 2018. ggcorrplot: Visualization of a correlation matrix using "ggplot2."

Kawamura, A., 1980. A review of food of balaenopterid whales. Sci. Reports, Whales Res. Institute, Tokyo 32, 155–197.

Kerr, R.A., 2000. A North Atlantic climate pacemaker for the centuries. Science (80-.). 288, 1984–1986. https://doi.org/10.1126/science.288.5473.1984

Kinze, C.C., 2018. White-beaked dolphin. Encycl. Mar. Mamm. 74, 1077–1079. https://doi.org/10.1016/b978-0-12-804327-1.00274-0

Kiszka, J., Braulik, G., 2018. Lagenorhynchus albirostris. IUCN Red List Threat. Species 2018 e.T11142A5. https://doi.org/10.2305/IUCN.UK.2018- 2.RLTS.T11142A50361346.en

Kleivane, L., Skaare, J.U., 1998. Organochlorine contaminants in northeast Atlantic minke whales (*Balaenoptera acutorostrata*). Environ. Pollut. 101, 231–239. https://doi.org/10.1016/S0269-7491(98)00043-8

Klinck, H., Nieukirk, S.L., Mellinger, D.K., Klinck, K., Matsumoto, H., Dziak, R.P., 2012. Seasonal presence of cetaceans and ambient noise levels in polar waters of the North Atlantic. J. Acoust. Soc. Am. 132, EL176–EL181. https://doi.org/10.1121/1.4740226

Kovacs, K.M., Haug, T., Lydersen, C., 2009. Marine mammals in the Barents Sea, in: Sakshaug, E., Johnsen, G., Kovacs, K.M. (Eds.), Ecosystem Barents Sea. Tapir Academic Press, Trondheim, Norway, pp. 453–496.

Kuningas, S., Kvadsheim, P.H., Lam, F.-P.A., Miller, P.J.O., 2013. Killer whale presence in relation to naval sonar activity and prey abundance in northern Norway. ICES J. Mar. Sci. 70, 1287–1293. https://doi.org/10.1093/icesjms/fst127

Kuningas, S., Similä, T., Hammond, P.S., 2014. Population size, survival and reproductive rates of northern Norwegian killer whales (Orcinus orca) in 1986-2003. J. Mar. Biol. Assoc. UK 94, 1277–1291. https://doi.org/10.1017/S0025315413000933

Laake, J., Borchers, D.L., Thomas, L., Miller, D.L., Bishop, J., 2017. mrds: Mark-Recapture Distance Sampling.

Laidre, K.L., Heagerty, P.J., Heide-Jørgensen, M.P., Witting, L., Simon, M., 2009. Sexual segregation of common minke whales (*Balaenoptera acutorostrata*) in Greenland, and the influence of sea temperature on the sex ratio of catches. ICES J. Mar. Sci. 66, 2253–2266. https://doi.org/10.1093/icesjms/fsp191

Laidre, K.L., Stern, H., Kovacs, K.M., Lowry, L., Moore, S.E., Regehr, E. V., Ferguson, S.H., Wiig, Ø., Boveng, P., Angliss, R.P., Born, E.W., Litovka, D., Quakenbush, L., Lydersen, C., Vongraven, D., Ugarte, F., 2015. Arctic marine mammal population status, sea ice habitat loss, and conservation recommendations for the 21st century. Conserv. Biol. 29, 724–737. https://doi.org/10.1111/cobi.12474

Laist, D.W., Knowlton, A.R., Mead, J.G., Collet, A.S., Podesta, M., 2001. Collisions between ships and whales. Mar. Mammal Sci. 17, 35–75. https://doi.org/10.1111/j.1748-7692.2001.tb00980.x

Laran, S., Drouot-Dulau, V., 2007. Seasonal variation of striped dolphins, fin- and sperm whales' abundance in the Ligurian Sea (Mediterranean Sea). J. Mar. Biol. Assoc. United Kingdom 87, 345–352. https://doi.org/10.1017/S0025315407054719

Laran, S., Gannier, A., 2008. Spatial and temporal prediction of fin whale distribution in the northwestern Mediterranean Sea. ICES J. Mar. Sci. 65, 1260–1269. https://doi.org/10.1093/icesjms/fsn086

Larsen, A.H., Sigurjónsson, J., Øien, N.I., Vikingsson, G.A., Palsoboll, P.J., 1996. Populations genetic analysis of nuclear and mitochondrial loci in skin biopsies collected from central and northeastern North Atlantic humpback whales (*Megaptera novaeangliae*): Population identity and migratory destinations. Proc. R. Soc. B Biol. Sci. 263, 1611–1618. https://doi.org/10.1098/rspb.1996.0236

Lennert, A.E., Richard, G., 2017. At the cutting edge of the future: Unravelling depredation, behaviour and movement of killer whales in the act of flexible management regimes in Arctic Greenland. Ocean Coast. Manag. 148, 272–281. https://doi.org/10.1016/j.ocecoaman.2017.08.016

Leterme, S.C., Pingree, R.D., 2008. The Gulf Stream, rings and North Atlantic eddy structures

from remote sensing (Altimeter and SeaWiFS). J. Mar. Syst. 69, 177–190. https://doi.org/10.1016/j.jmarsys.2005.11.022

Levitus, S., Antonov, J.I., Boyer, T.P., Baranova, O.K., Garcia, H.E., Locarnini, R.A., Mishonov, A. V., Reagan, J.R., Seidov, D., Yarosh, E.S., Zweng, M.M., 2012. World ocean heat content and thermosteric sea level change (0-2000m), 1955-2010. Geophys. Res. Lett. 39, 1–5. https://doi.org/10.1029/2012GL051106

Lien, J., Nelson, D., Dong, J.H., 2001. Status of the white-beaked dolphin, *Lagenorhynchus albirostris*, in Canada. Can. Field-Naturalist 115, 118–126.

Lima, M., Estay, S.A., 2013. Warming effects in the western Antarctic Peninsula ecosystem: The role of population dynamic models for explaining and predicting penguin trends. Popul. Ecol. 55, 557–565. https://doi.org/10.1007/s10144-013-0386-1

Lind, S., Ingvaldsen, R.B., Furevik, T., 2018. Arctic warming hotspot in the northern Barents Sea linked to declining sea-ice import. Nat. Clim. Chang. 8, 634–639. https://doi.org/10.1038/s41558-018-0205-y

Lindstrøm, U., Smout, S., Howell, D., Bogstad, B., 2009. Modelling multi-species interactions in the Barents Sea ecosystem with special emphasis on minke whales and their interactions with cod, herring and capelin. Deep. Res. Part II Top. Stud. Oceanogr. 56, 2068–2079. https://doi.org/10.1016/j.dsr2.2008.11.017

Luque, P.L., Davis, C.G., Reid, D.G., Wang, J., Pierce, G.J., 2006. Opportunistic sightings of killer whales from Scottish pelagic trawlers fishing for mackerel and herring off North Scotland (UK) between 2000 and 2006. Aquat. Living Resour. 19, 403–410. https://doi.org/10.1051/alr:2007009

Lynch-Stieglitz, J., Curry, W.B., Slowey, N., 1999. Weaker Gulf Stream in the Florida straits during the Last Glacial Maximum. Nature 402, 644–648. https://doi.org/10.1038/45204

MacLeod, C.D., 2009. Global climate change, range changes and potential implications for the conservation of marine cetaceans: A review and synthesis. Endanger. Species Res. 7, 125–136. https://doi.org/10.3354/esr00197

MacLeod, C.D., Bannon, S.M., Pierce, G.J., Schweder, C., Learmonth, J.A., Herman, J.S., Reid, R.J., 2005. Climate change and the cetacean community of north-west Scotland. Biol. Conserv. 124, 477–483. https://doi.org/10.1016/j.biocon.2005.02.004

MacLeod, C.D., Weir, C.R., Pierpoint, C., Harland, E.J., 2007. The habitat preferences of marine mammals west of Scotland (UK). J. Mar. Biol. Assoc. UK 87, 157–164. https://doi.org/10.1017/S0025315407055270

Magnúsdóttir, E.E., Lim, R., 2019. Subarctic singers: Humpback whale (*Megaptera novaeangliae*) song structure and progression from an Icelandic feeding ground during winter. PLoS One 14, 1–26. https://doi.org/10.1371/journal.pone.0210057

Magnúsdóttir, E.E., Rasmussen, M.H., Lammers, M.O., Svavarsson, J., 2014. Humpback whale songs during winter in subarctic waters. Polar Biol. 37, 427–433. https://doi.org/10.1007/s00300-014-1448-3

Malmberg, S.-A., Valdimarsson, H., 2003. Hydrographic conditions in Icelandic waters, 1990–1999. ICES Mar. Sci. Symp. 50–60.

Malmberg, S.-A., Valdimarsson, H., 1999. Satellite tracked surface drifters and " Great Salinity Anomalies " in the Subpolar Gyre and the Norwegian Sea. ICES J. Mar. Sci. L:15, 10.

Marine Research Institute, 2015. Þættir úr vistfræði sjávar 2014. Environmental conditions in Icelandic waters 2014. Reykjavík.

Martin, A.R., Clarke, M.R., 1986. The Diet of Sperm Whales (*Physeter Macrocephalus*) Captured Between Iceland and Greenland. J. Mar. Biol. Assoc. UK 66, 779–790. https://doi.org/10.1017/S0025315400048426

Martin, A.R., Rothery, P., 1993. Reproductive parameters of female long-finned pilot whales (*Globicephala melas*) around the Faroe Islands. Rep. int. Whal. Commn. 263–304.

Martin, S.W., Martin, C.R., Matsuyama, B.M., Henderson, E.E., 2015. Minke whales (*Balaenoptera acutorostrata*) respond to navy training. J. Acoust. Soc. Am. 137, 2533–2541. https://doi.org/10.1121/1.4919319

Matthews, C.J.D., Luque, S.P., Petersen, S.D., Andrews, R.D., Ferguson, S.H., 2011. Satellite tracking of a killer whale (*Orcinus orca*) in the eastern Canadian Arctic documents ice avoidance and rapid, long-distance movement into the North Atlantic. Polar Biol. 34, 1091–1096. https://doi.org/10.1007/s00300-010-0958-x

Matthews, C.J.D., Raverty, S.A., Noren, D.P., Arragutainaq, L., Ferguson, S.H., 2019. Ice entrapment mortality may slow expanding presence of Arctic killer whales. Polar Biol. 42,

639–644. https://doi.org/10.1007/s00300-018-02447-3

Mead, J.G., 1989. Bottlenose Whales – *Hyperoodon ampullatus* (Forster, 1770) and *Hyperoodon planifrons* (Fowler, 1882), in: Ridgway, S.H., Harrison, S.R. (Eds.), Handbook of Marine Mammals. Volume 4: River Dolphins and the Larger Toothed Whales. Academic Press, London, UK., pp. 321–348.

Méndez-Fernandez, P., Pierce, G.J., Bustamante, P., Chouvelon, T., Ferreira, M., González, A.F., López, A., Read, F.L., Santos, M.B., Spitz, J., Vingada, J. V., Caurant, F., 2013. Ecological niche segregation among five toothed whale species off the NW Iberian Peninsula using ecological tracers as multi-approach. Mar. Biol. 160, 2825–2840. https://doi.org/10.1007/s00227-013-2274-9

Miller, D.L., 2017. Distance: Distance sampling detection function and abundance estimation.

Miller, P.J.O., Kvadsheim, P.H., Lam, F.P.A., Tyack, P.L., Curé, C., DeRuiter, S.L., Kleivane, L., Sivle, L.D., van IJsselmuide, S.P., Visser, F., Wensveen, P.J., von Benda-Beckmann, A.M., Martín López, L.M., Narazaki, T., Hooker, S.K., 2015. First indications that northern bottlenose whales are sensitive to behavioural disturbance from anthropogenic noise. R. Soc. Open Sci. 2, 140484. https://doi.org/10.1098/rsos.140484

Miller, P.J.O., Kvadsheim, P.H., Lam, F.P.A., Wensveen, P.J., Antunes, R., Alves, A.C., Visser, F., Kleivane, L., Tyack, P.L., Sivle, L.D., 2012. The Severity of behavioral changes observed during experimental exposures of killer (*Orcinus orca*), long-finned Pilot (*Globicephala melas*), and sperm (*Physeter macrocephalus*) whales to naval sonar. Aquat. Mamm. 38, 362–401. https://doi.org/10.1578/AM.38.4.2012.362

Minton, G., Reeves, R.R., Braulik, G., 2018. *Globicephala melas* , Long-finned Pilot Whale. IUCN Red List Threat. Species e.T9250A50. https://doi.org/http://dx.doi.org/10.2305/IUCN.UK.2018- 2.RLTS.T9250A50356171.en

Misund, O.A., Vilhjálmsson, H., Jákupsstovu, S.H.Í., Røttingen, I., Belikov, S., Asthorsson, O., Blindheim, J., Jónsson, J., Krysov, A., Malmberg, S.A., Sveinbjørnsson, S., 1997. Distribution, migration and abundance of norwegian spring spawning herring in relation to the temperature and zooplankton biomass in the Norwegian Sea as recorded by coordinated surveys in spring and summer 1996. Sarsia 83, 117–127. https://doi.org/10.1080/00364827.1998.10413677

Mizroch, S.A., Rice, D.W., Zwiefelhofer, D., Waite, J., Perryman, W.L., 2009. Distribution and movements of fin whales in the North Pacific Ocean. Mamm. Rev. 39, 193–227. https://doi.org/10.1111/j.1365-2907.2009.00147.x

Moore, S.E., 2008. Marine mammals as ecosystem sentinels. J. Mammal. 89, 534–540. https://doi.org/10.1644/07-mamm-s-312r1.1

Moore, S.E., Haug, T., Víkingsson, G.A., Stenson, G.B., 2019. Baleen whale ecology in arctic and subarctic seas in an era of rapid habitat alteration. Prog. Oceanogr. 176, 15. https://doi.org/10.1016/j.pocean.2019.05.010

Moore, S.E., Huntington, H.P., 2008. Arctic marine mammals and climate change: impacts and resilience. Ecol. Appl. 18, S157–S165. https://doi.org/10.1890/06-0571.1

Moore, S.E., Stafford, K.M., Melling, H., Berchok, C., Wiig, O., Kovacs, K.M., Lydersen, C., Richter-Menge, J., 2012. Comparing marine mammal acoustic habitats in Atlantic and Pacific sectors of the High Arctic: year-long records from Fram Strait and the Chukchi Plateau. Polar Biol. 35, 475–480. https://doi.org/10.1007/s00300-011-1086-y

Mork, K.A., Skagseth, Ø., Søiland, H., 2019. Recent warming and freshening of the Norwegian Sea observed by Argo data. J. Clim. 32, 3695–3705. https://doi.org/10.1175/JCLI-D-18-0591.1

Mortensen, J., Valdimarsson, H., 1999. Thermohaline changes in the Irminger Sea. ICES C.M. 50, 1–11.

Muir, D.C.G., Wagemann, R., Grift, N.P., Norstrom, R.J., Simon, M., Lien, J., 1988. Organochlorine chemical and heavy metal contaminants in white-beaked dolphins (*Lagenorhynchus albirostris*) and pilot whales (*Globicephala melaena*) from the coast of Newfoundland, Canada. Arch. Environ. Contam. Toxicol. 17, 613–629. https://doi.org/10.1007/BF01055830

Murphy, S., Barber, J.L., Learmonth, J.A., Read, F.L., Deaville, R., Perkins, M.W., Brownlow, A., Davison, N., Penrose, R., Pierce, G.J., Law, R.J., Jepson, P.D., 2015. Reproductive failure in UK harbour porpoises phocoena phocoena: Legacy of pollutant exposure? PLoS One 10, 1–32. https://doi.org/10.1371/journal.pone.0131085

NAMMCO, 2020. Killer whale [WWW Document]. URL https://nammco.no/topics/killer-whale/#1475762140566-81d47f7a-a145 (accessed 2.21.20).

NAMMCO, 2019a. Scientific Committee Report of the Working Group on Abundance Estimates. North Atlantic Marine Mammal Commission, Tromsø, Norway.

NAMMCO, 2019b. Long-finned pilot whales [WWW Document]. URL https://nammco.no/topics/long-finned-pilot-whale/#1475844711542-eedf1c7b-5dde

NAMMCO, 2019c. Northern Bottlenose Whale [WWW Document]. URL https://nammco.no/topics/bottlenose_whale/#1478699758629-7da126c3-48a6

NAMMCO, 2019d. Fin Whale [WWW Document]. URL https://nammco.no/topics/fin-whale/#1478699758629-7da126c3-48a6 (accessed 11.15.19).

NAMMCO, 2019e. Humpback Whale [WWW Document]. URL https://nammco.no/topics/humpback-whale/#1475762140566-81d47f7a-a145 (accessed 10.22.19).

NAMMCO, 2019f. Common Minke Whale [WWW Document]. URL https://nammco.no/topics/common-minke-whale/ (accessed 1.13.20).

NAMMCO, 2018. Scientific Committee Report of the Working Group on Abundance Estimates. North Atlantic Marine Mammal Commission, Copenhagen, Denmark, 22-24 May.

NAMMCO, 2015. Annual Report 2014. North Atlantic Marine Mammal Commission, Tromsø, Norway.

NAMMCO, 2013. Annual Report 2013. North Atlantic Marine Mammal Commission, Reykjavik, Iceland.

NAMMCO, 2011. Annual Report 2011. North Atlantic Marine Mammal Commission, Tromso, Norway.

NAMMCO, 2000. Annual Report 1999. North Atlantic Marine Mammal Commission, Tromsø, Norway.

NAMMCO, 1998. Annual Report 1997, NAMMCO. North Atlantic Marine Mammal Commission, Tromsø, Norway. https://doi.org/10.1037/h0090484

NAMMCO, 1997. Scientific Committee Report of the Working Group on Abundance Estimates. North Atlantic Marine Mammal Commission, Reykjavik, 21-23 February 1997.

NAMMCO, 1993. Report of the Scientific Committee working group on Northern Bottlenose and

Killer Whales. North Atlantic Marine Mammal Commission, Reykjavik, Iceland.

Neyman, L.C., 2018. Cetacean habitat-use in the Central North Atlantic: a comparison between three baleen whales and three deep-diving odontocetes. University of St Andrews.

Northridge, S., Cargill, A., Coram, A., Mandleberg, L., Calderan, S., Reid, B., 2010. Entanglement of minke whales in Scottish waters; an investigation into occurrence, causes and mitigation., Sea Mammal Research Unit, Final Report to Scottish Government CR/2007/49. St Andrews.

Northridge, S.P., 1991. An updated world review of interactions between marine mammals and fisheries. Food and Agriculture Organization of the United Nations, Rome, Italy.

Nøttestad, L., Krafft, B.A., Anthonypillai, V., Bernasconi, M., Langård, L., Mørk, H.L., Fernö, A., 2015. Recent changes in distribution and relative abundance of cetaceans in the Norwegian Sea and their relationship with potential prey. Front. Ecol. Evol. 2. https://doi.org/10.3389/fevo.2014.00083

Nøttestad, L., Sivle, L.D., Krafft, B.A., Langård, L., Anthonypillai, V., Bernasconi, M., Langøy, H., Axelsen, B.E., 2014. Ecological aspects of fin whale and humpback whale distribution during summer in the Norwegian Sea. Mar. Ecol. 35, 221–232. https://doi.org/10.1111/maec.12075

Nøttestad, L., Utne, K.R., Óskarsson, G.J., Jónsson, S.Þ., Jacobsen, J.A., Tangen, Ø., Anthonypillai, V., Aanes, S., Vølstad, J.H., Bernasconi, M., Debes, H., Smith, L., Sveinbjörnsson, S., Holst, J.C., Jansen, T., Slotte, A., 2016. Quantifying changes in abundance, biomass, and spatial distribution of Northeast Atlantic mackerel (*Scomber scombrus*) in the Nordic seas from 2007 to 2014. ICES J. Mar. Sci. J. du Cons. 73, 359–373. https://doi.org/10.1093/icesjms/fsv218

O'Shea, T.J., Brownell, R.L., 1994. Organochlorine and metal contaminants in baleen whales: a review and evaluation of conservation implications. Sci. Total Environ. 154, 179–200. https://doi.org/10.1016/0048-9697(94)90087-6

OBPG, 2014. Moderate-resolution imaging spectroradiometer (MODIS) Aqua Photosynthetically Available Radiation Data: 2014 Reprocessing. NASA OB. DAAC. Greenbelt, MD NASA Goddard Sp. Flight Center, Ocean Ecol. Lab. Ocean Biol. Process. Gr. https://doi.org/10.5067/AQUA/MODIS/L3B/PAR/2014

Oftedal, O.T., 1997. Lactation in whales and dolphins: Evidence of divergence between baleen- and toothed-species. J. Mammary Gland Biol. Neoplasia 2, 205–230. https://doi.org/10.1023/A:1026328203526

Øien, N.I., 2009. Distribution and abundance of large whales in Norwegian and adjacent waters based on ship surveys 1995-2001. NAMMCO Sci. Publ. 7, 31–47. https://doi.org/10.7557/3.2704

Øien, N.I., 1988. The distribution of killer whales (*Orcinus orca*) in the North Atlantic based on Norwegian catches, 1938–1981, and incidental sightings, 1967–1987. Rit Fiskid. 11, 65–78.

Øien, N.I., Bøthun, G., 2009. Trends in local abundance of large whales in the Northeast Atlantic, based on Norwegian surveys 1987-2004. IWC SC/57/O11, 1–7.

Øien, N.I., Haug, T., 2018. Norway - Progress Report on Marine Mammals 2018. North Atlantic Marine Mammal Commission SC/27/NPR-N.

Olsen, E., Aanes, S., Mehl, S., Holst, J.C., Aglen, A., Gjøsæter, H., 2010. Cod, haddock, saithe, herring, and capelin in the Barents Sea and adjacent waters: A review of the biological value of the area. ICES J. Mar. Sci. 67, 87–101. https://doi.org/10.1093/icesjms/fsp229

Olsen, E., Holst, J.C., 2001. A note on common minke whale (*Balaenoptera acutorostrata*). J. Cetacean Res. Manag. 179–183.

Olson, P.A., 2018. Pilot Whales, in: Perrin, W.F., Würsig, B., Thewissen, J.G.M. (Eds.), Encyclopedia of Marine Mammals. Elsevier, San Diego, CA :, pp. 701–705. https://doi.org/10.1016/B978-0-12-804327-1.00194-1

Oswald, J.N., Norris, T.F., Yack, T.M., Ferguson, E.L., Kumar, A., Nissen, J., Bell, J., 2016. Patterns of occurrence and marine mammal acoustic behavior in relation to navy sonar activity off Jacksonville, Florida, in: The Effects of Noise on Aquatic Life II. pp. 791–799. https://doi.org/10.1007/978-1-4939-2981-8_97

Ottersen, G., Planque, B., Belgrano, A., Post, E., Reid, P.C., Stenseth, N.C., 2001. Ecological effects of the North Atlantic Oscillation. Oecologia 128, 1–14. https://doi.org/10.1007/s004420100655

Palsbøll, P.J., Allen, J., Bérubé, M., Clapham, P.J., Feddersen, T.P., Hammond, P.S., Hudson, R.R., Jørgensen, H., Katona, S., Larsen, A.H., Larsen, F., Lien, J., Mattila, D.K., Sigurjónsson, J.,

Sears, R., Smith, T.D., Sponer, R., Stevick, P.T., Øien, N.I., 1997. Genetic tagging of humpback whales. Nature 388, 767–769. https://doi.org/10.1038/42005

Pálsson, Ó.K., Gislason, A., Gufinnsson, H.G., Gunnarsson, B., Ólafsdóttir, S.R., Petursdottir, H., Sveinbjörnsson, S., Thorisson, K., Valdimarsson, H., 2012. Ecosystem structure in the Iceland Sea and recent changes to the capelin (*Mallotus villosus*) population. ICES J. Mar. Sci. 69, 1242–1254. https://doi.org/10.1093/icesjms/fss071

Pampoulie, C., Gunnlaugsson, T., Elvarsson, B.Þ., Petursdottir, H., Chosson, V., Auðunsson, G.A., Kjeld, M., Hauksson, E., Karlsson, K.Æ., Guðnason, K., Svansson, V., Benonisdottir, S., Ólafsdóttir, D., Víkingsson, G.A., 2013. Research program on common minke whale (*Balaenoptera acutorostrata*) in Icelandic waters. An overview of implementation and results, SC/F13/SP1 for the IWC Scientific Committee.

Pante, E., Simon-Bouhet, B., 2013. marmap: A Package for importing, plotting and analyzing bathymetric and topographic data in R. PLoS One 8, e73051. https://doi.org/10.1371/journal.pone.0073051

Paxton, C.G.M., Burt, M.L., Hedley, S.L., Víkingsson, G.A., Gunnlaugsson, T., Desportes, G., 2009. Density surface fitting to estimate the abundance of humpback whales based on the NASS-95 and NASS- 2001 aerial and shipboard surveys. NAMMCO Sci. Publ. 7, 143. https://doi.org/10.7557/3.2711

Pedro, S., Boba, C., Dietz, R., Sonne, C., Rosing-Asvid, A., Hansen, M., Provatas, A., McKinney, M.A., 2017. Blubber-depth distribution and bioaccumulation of PCBs and organochlorine pesticides in Arctic-invading killer whales. Sci. Total Environ. 601–602, 237–246. https://doi.org/10.1016/j.scitotenv.2017.05.193

Perrin, W.F., Mallette, S.D., Brownell, R.L., 2018. Minke Whales. Encycl. Mar. Mamm. 608–613. https://doi.org/10.1016/b978-0-12-804327-1.00175-8

Perry, A.L., Low, P.J., Ellis, J.R., Reynolds, J.D., 2005. Ecology: Climate change and distribution shifts in marine fishes. Science (80-.). 308, 1912–1915. https://doi.org/10.1126/science.1111322

Pike, D.G., 2009. Introduction, in: Lockyer, C., Pike, D. (Eds.), North Atlantic Sightings Surveys: Counting Whales in the North Atlantic, 1987-2001. pp. 7–18. https://doi.org/10.7557/3.7

Pike, D.G., Gunnlaugsson, T., Desportes, G., Mikkelsen, B., Vikingsson, G.A., Bloch, D., 2019a.

Estimates of the relative abundance of long-finned pilot whales (*Globicephala melas*) in the Northeast Atlantic from 1987 to 2015 indicate no long-term trends. NAMMCO Sci. Publ. 11. https://doi.org/10.7557/3.4643

Pike, D.G., Gunnlaugsson, T., Mikkelsen, B., Halldórsson, S.D., Víkingsson, G., 2019b. Estimates of the abundance of cetaceans in the central North Atlantic based on the NASS Icelandic and Faroese shipboard surveys conducted in 2015. NAMMCO Sci. Publ. 11, 1–19. https://doi.org/10.7557/3.4941

Pike, D.G., Gunnlaugsson, T., Mikkelsen, B., Halldórsson, S.D., Víkingsson, G., Acquarone, M., Desportes, G., 2020a. Estimates of the Abundance of Cetaceans in the Central North Atlantic from the T-NASS Icelandic and Faroese Ship Surveys Conducted in 2007. NAMMCO Sci. Publ. 11. https://doi.org/10.7557/3.5269

Pike, D.G., Gunnlaugsson, T., Sigurjonsson, J., Vikingsson, G., 2020b. Distribution and Abundance of Cetaceans in Icelandic Waters over 30 Years of Aerial Surveys. NAMMCO Sci. Publ. 11, 1–62. https://doi.org/10.7557/3.4805

Pike, D.G., Paxton, C.G.M., Gunnlaugsson, T., Víkingsson, G.A., 2009a. Trends in the distribution and abundance of cetaceans from aerial surveys in Icelandic coastal waters, 1986-2001. NAMMCO Sci. Publ. 7, 117. https://doi.org/10.7557/3.2710

Pike, D.G., Víkingsson, G.A., Gunnlaugsson, T., Øien, N.I., 2009b. A note on the distribution and abundance of blue whales (Balaenoptera musculus) in the Central and Northeast North Atlantic. NAMMCO Sci. Publ. 7, 19. https://doi.org/10.7557/3.2703

Pirotta, E., Matthiopoulos, J., MacKenzie, M., Scott-Hayward, L., Rendell, L., 2011. Modelling sperm whale habitat preference: A novel approach combining transect and follow data. Mar. Ecol. Prog. Ser. 436, 257–272. https://doi.org/10.3354/meps09236

QGIS Development Team, 2018. QGIS Geographic Information System. Open Source Geospatial Found. Proj.

R Core Team, 2018. R: A Language and Environment for Statistical Computing.

Rahmstorf, S., 2003. Thermohaline circulation: The current climate. Nature 421, 699–699. https://doi.org/10.1038/421699a

Ramp, C., Delarue, J., Palsbøll, P.J., Sears, R., Hammond, P.S., 2015. Adapting to a warmer ocean

- Seasonal shift of baleen whale movements over three decades. PLoS One 10, 1–15. https://doi.org/10.1371/journal.pone.0121374

Rasmussen, M.H., Akamatsu, T., Teilmann, J., Vikingsson, G.A., Miller, L.A., 2013. Biosonar, diving and movements of two tagged white-beaked dolphin in Icelandic waters. Deep. Res. Part II Top. Stud. Oceanogr. 88–89, 97–105. https://doi.org/10.1016/j.dsr2.2012.07.011

Read, A.J., Northridge, S.P., 2006. By-catches of marine mammals in US fisheries and a first attempt to estimate the magnitude of global marine mammal by-catch. Reports Int. Whal. Comm. 12.

Redfern, J. V, Ferguson, M.C., Becker, E.A., Hyrenbach, K.D., Good, C., Barlow, J., Kaschner, K., Baumgartner, M.F., Forney, K.A., Ballance, L.T., Fauchald, P., Halpin, P., Hamazaki, T., Pershing, A.J., Qian, S.S., Read, A.J., Reilly, S.B., Torres, L., Werner, F., 2006. Techniques for cetacean – habitat modeling. Mar. Ecol. Prog. Ser. 310, 271–295. https://doi.org/10.3354/meps310271

Reeves, R.R., McClellan, K., Werner, T.B., 2013. Marine mammal bycatch in gillnet and other entangling net fisheries, 1990 to 2011. Endanger. Species Res. 20, 71–97. https://doi.org/10.3354/esr00481

Reeves, R.R., Mitchell, E., Whitehead, H., 1993. Status of the northern bottlenose whale, *Hyperoodon ampullatus*. Can. Field-Naturalist 490–508.

Reeves, R.R., Pitman, R.L., Ford, J.K.B., 2017. Orcinus orca: Killer whale. IUCN Red List Threat. Species 2017 e.T15421A5, 22. https://doi.org/T15421A50368125

Reid, J.B., Evans, P., Northridge, S., 2003. Atlas of Cetacean distribution in north-west European waters. Jt. Nat. Conserv. Comm. 77.

Reilly, S.B., Bannister, J.L., Best, P.B., Brown, M., Brownell, J.R.L., Butterworth, D.S., Clapham, P.J., Cooke, J.G., Donovan, G.P., Urbán, J., Zerbini, A.N., 2008a. Humpback whale: Megaptera novaeangliae. IUCN Red List Threat. Species 2008 e.T13006A3, 21. https://doi.org/10.2305/IUCN.UK.2008.RLTS.T13006A3405371.en

Reilly, S.B., Bannister, J.L., Best, P.B., Brown, M., Brownell Jr., R.L., Butterworth, D.S., Clapham, P.J., Cooke, J., Donovan, G.P., Urbán, J., Zerbini, A.N., 2008b. *Balaenoptera physalus*. IUCN Red List Threat. Species 2013 e.T2478A44, 20. https://doi.org/10.2305/IUCN.UK.2013-1.RLTS.T2478A44210520.en

Rendell, L.E., Gordon, J.C.D., 1999. Vocal response of long-finned pilot whales (*Globicephala melas*) to military sonar in the Ligurian Sea. Mar. Mammal Sci. 15, 198–204. https://doi.org/10.1111/j.1748-7692.1999.tb00790.x

Ressler, P.H., Dalpadado, P., Macaulay, G.J., Handegard, N., Skern-Mauritzen, M., 2015. Acoustic surveys of euphausiids and models of baleen whale distribution in the Barents Sea. Mar. Ecol. Prog. Ser. 527, 13–29. https://doi.org/10.3354/meps11257

Rice, D.W., 1989. Sperm whale, in: Ridgway, S.H., Harrison, S.R. (Eds.), Handbook of Marine Mammals. Volume 4: River Dolphins and the Larger Toothed Whales. Academic Press, London, UK., pp. 177–234.

Rikardsen, A., 2020. Whaletrack | UiT [WWW Document]. URL https://en.uit.no/prosjekter/prosjekt?p_document_id=505966 (accessed 1.4.20).

Risch, D., Castellote, M., Clark, C.W., Davis, G.E., Dugan, P.J., Hodge, L.E.W., Kumar, A., Lucke, K., Mellinger, D.K., Nieukirk, S.L., Popescu, C.M., Ramp, C., Read, A.J., Rice, A.N., Silva, M.A., Siebert, U., Stafford, K.M., Verdaat, H., Van Parijs, S.M., 2014. Seasonal migrations of North Atlantic minke whales: Novel insights from large-scale passive acoustic monitoring networks. Mov. Ecol. 2. https://doi.org/10.1186/s40462-014-0024-3

Risch, D., Corkeron, P.J., Ellison, W.T., van Parijs, S.M., 2012. Changes in humpback whale song occurrence in response to an acoustic source 200 km away. PLoS One 7, 2–7. https://doi.org/10.1371/journal.pone.0029741

Roberts, J.J., Best, B.D., Mannocci, L., Fujioka, E., Halpin, P.N., Palka, D.L., Garrison, L.P., Mullin, K.D., Cole, T.V.N., Khan, C.B., McLellan, W.A., Pabst, D.A., Lockhart, G.G., 2016. Habitat-based cetacean density models for the U.S. Atlantic and Gulf of Mexico. Sci. Rep. 6, 1–12. https://doi.org/10.1038/srep22615

Roberts, S.M., 2019. The role of cyclical climate oscillations in species distribution shifts under climate change, in: Cisneros-Montemayor, A.M., Cheung, W.W.L., Ota, Y. (Eds.), Predicting Future Oceans: Sustainability of Ocean and Human Systems Amidst Global Environmental Change. Elsevier Inc., pp. 129–135. https://doi.org/10.1016/B978-0-12-817945-1.00011-3

Robinson, K.P., Bamford, C.C.G., Airey, A., Bean, T.S., Bird, C., Haskins, G.N., Sim, T.M.C., Evans, P.G.H., 2017. Killer whale (*Orcinus orca*) occurrence in the Moray Firth, Northeast Scotland: Incidental sightings, behavioural observations, and photo-identification. Aquat. Mamm.

43, 26–32. https://doi.org/10.1578/AM.43.1.2017.26

Rogan, E., Breen, P., Mackey, M., Cañadas, A., Scheidat, M., Geelhoed, S.C.V., Jessopp, M., 2018. Aerial Surveys of Cetaceans and Seabirds in Irish waters: Occurrence, distribution and abundance in 2015-2017. Dublin, Ireland.

Rogan, E., Cañadas, A., Macleod, K., Santos, M.B., Mikkelsen, B., Uriarte, A., Van Canneyt, O., Vázquez, J.A., Hammond, P.S., 2017. Distribution, abundance and habitat use of deep diving cetaceans in the North-East Atlantic. Deep. Res. Part II Top. Stud. Oceanogr. 141, 8–19. https://doi.org/10.1016/j.dsr2.2017.03.015

Ryan, C., Leaper, R., Evans, P.G.H., Dyke, K., Robinson, K.P., Haskins, G.N., Calderan, S., van Geel, N., Harries, O., Froud, K., Brownlow, A., Jack, A., 2016. Entanglement: an emerging threat to humpback whales in Scottish waters. Int. Whal. Comm. SC/66b/HIM, 13.

Ryan, C., McHugh, B., Boyle, B., McGovern, E., Bérubé, M., Lopez-Suárez, P., Elfes, C.T., Boyd, D.T., Ylitalo, G.M., Van Blaricom, G.R., Clapham, P.J., Robbins, J., Palsbøll, P.J., O'Connor, I., Berrow, S.D., 2013. Levels of persistent organic pollutants in eastern North Atlantic humpback whales. Endanger. Species Res. 22, 213–223. https://doi.org/10.3354/esr00545

Ryan, C., Whooley, P., Berrow, S.D., Barnes, C., Massett, N., Strietman, W.J., Broms, F., Stevick, P.T., Fernald, T.W., Schmidt, C., 2015. A longitudinal study of humpback whales in Irish waters. J. Mar. Biol. Assoc. United Kingdom 96, 877–883. https://doi.org/10.1017/S0025315414002033

Samarra, F.I.P., Bassoi, M., Béesau, J., Elíasdóttir, M., Gunnarsson, K., Mrusczok, M.T., Rasmussen, M.H., Rempel, J.N., Thorvaldsson, B., Víkingsson, G.A., 2018. Prey of killer whales (*Orcinus orca*) in Iceland. PLoS One 13, 1–20. https://doi.org/10.1371/journal.pone.0207287

Samarra, F.I.P., Foote, A.D., 2015. Seasonal movements of killer whales between Iceland and Scotland. Aquat. Biol. 24, 75–79. https://doi.org/10.3354/ab00637

Samarra, F.I.P., Miller, P.J.O., 2015. Prey-induced behavioural plasticity of herring-eating killer whales. Mar. Biol. 162, 809–821. https://doi.org/10.1007/s00227-015-2626-8

Samarra, F.I.P., Tavares, S.B., Miller, P.J.O., Víkingsson, G.A., 2017. Killer whales of Iceland 2006-2015. Marine and Freshwater Research Institute in Iceland.

Sanpera, C., González, M., Jover, L., 1996. Heavy metals in two populations of North Atlantic fin whales (*Balaenoptera physalus*). Environ. Pollut. 91, 299–307. https://doi.org/10.1016/0269-7491(95)00068-2

Santos, M.B., Monteiro, S.S., Vingada, J. V., Ferreira, M., López, A., Martínez Cedeira, J.A., Reid, R.J., Brownlow, A., Pierce, G.J., 2014. Patterns and trends in the diet of long-finned pilot whales (*Globicephala melas*) in the northeast Atlantic. Mar. Mammal Sci. 30, 1–19. https://doi.org/10.1111/mms.12015

Santos, M.B., Pierce, G.J., Boyle, P.R., Reid, R.J., Ross, H.M., Patterson, I.A.P., Kinze, C.C., Tougaard, S., Lick, R., Piatkowski, U., Hernández-García, V., 1999. Stomach contents of sperm whales *Physeter macrocephalus* stranded in the North Sea 1990-1996. Mar. Ecol. Prog. Ser. 183, 281–294. https://doi.org/10.3354/meps183281

Santos, M.B., Pierce, G.J., Smeenk, C., Addink, M.J., Kinze, C.C., Tougaard, S., Herman, J., 2001. Stomach contents of northern bottlenose whales *Hyperoodon ampullatus* stranded in the North Sea. J. Mar. Biol. Assoc. UK 81, 143–150. https://doi.org/10.1017/S0025315401003484

Sathyendranath, S., Groom, S., Grant, M., Brewin, R.J.W., Thompson, A., Chuprin, A., Horseman, A., Jackson, T., Martinez Vicente, V., Platt, T., Brockmann, C., Zühlke, M., Doerffer, R., Valente, A., Brotas, V., Krasemann, H., Müller, D., Dowell, M., Mélin, F., Swinton, J., Farman, A., Lavender, S., Moore, T.S., Regner, P., Roy, S., Steinmetz, F., Mazeran, C., Brando, V.E., Taberner, M., Antoine, D., Arnone, R., Balch, W.M., Barker, K., Barlow, R., Bélanger, S., Berthon, J., Besiktepe, S., Canuti, E., Chavez, F., Claustre, H., Crout, R., Frouin, R., García-Soto, C., Gibb, S.W., Gould, R., Hooker, S.K., Kahru, M., Klein, H., Kratzer, S., Loisel, H., McKee, D., Mitchell, B.G., Moisan, T., Feldman, G., Franz, B., Muller-Karger, F., O'Dowd, L., Ondrusek, M., Poulton, A.J., Repecaud, M., Smyth, T., Sosik, H.M., Twardowski, M., Voss, K., Werdell, J., Wernand, M., Zibordi, G., 2016. ESA Ocean Colour Climate Change Initiative (Ocean_Colour_cci). https://doi.org/10.5285/b0d6b9c5-14ba-499f-87c9-66416cd9a1dc

Scheidat, M., Castro, C., Gonzalez, J., Williams, R., 2004. Behavioural responses of humpback whales (*Megaptera novaeangliae*) to whalewatching boats near Isla de la Plata , Ecuador. J. Cetacean Res. Manag. 6, 1–6.

Schleimer, A., Ramp, C., Plourde, S., Lehoux, C., Sears, R., Hammond, P.S., 2019. Spatio-temporal patterns in fin whale *Balaenoptera physalus* habitat use in the northern Gulf of St.

Lawrence. Mar. Ecol. Prog. Ser. 623, 221–234. https://doi.org/10.3354/meps13020

Schweder, T., Skaug, H.J., Dimakos, X. k, Langaas, M., Øien, N.I., 1997. Abundance of Northeastern Atlantic Minke Whales, estimates for 1989 and 1995. Rep. Int. Whal. Comm. 47, 453–484.

Selmes, N., 2018. Email: low quality values NOAA 1995.

Servidio, A., Pérez-Gil, E., Pérez-Gil, M., Cañadas, A., Hammond, P.S., Martín, V., 2019. Site fidelity and movement patterns of short-finned pilot whales within the Canary Islands: Evidence for resident and transient populations. Aquat. Conserv. Mar. Freshw. Ecosyst. 29, 227–241. https://doi.org/10.1002/aqc.3135

Siebert, U., Joiris, C., Holsbeek, L., Benke, H., Failing, K., Frese, K., Petzinger, E., 1999. Potential relation between mercury concentrations and necropsy findings in cetaceans from German waters of the North and Baltic Seas. Mar. Pollut. Bull. 38, 285–295. https://doi.org/10.1016/S0025-326X(98)00147-7

Sigurjónsson, J., Galan, A., Víkingsson, G.A., 2000. A note on stomach contents of minke whales (Balaenoptera acutorostrata) in Icelandic waters. NAMMCO Sci. Publ. 2, 82–90. https://doi.org/10.7557/3.2973

Sigurjónsson, J., Gunnlaugsson, T., 1990. Recent trends in abundance of blue (*Balaenoptera musculus*) and humpback whales (*Megaptera novaeangliae*) off west and southwest Iceland witha note on occurrence of other cetacean species. Reports Int. Whal. Comm. 40, 537–551.

Sigurjónsson, J., Víkingsson, G.A., 1997. Seasonal abundance of and estimation of food consumption by cetaceans in Icelandic and adjacent waters. J. Northwest Atl. Fish. Sci. 22, 271–287. https://doi.org/10.2960/J.v22.a20

Sigurjónsson, J., Vikingsson, G.A., Lockyer, C., 1993. Two mass strandings of pilot whales (*Globicephala melas*) on the coast of Iceland. Reports Int. Whal. Comm. 14, 407–424.

Silva, T., Gislason, A., Licandro, P., Marteinsdóttir, G., Ferreira, A.S.A., Gudmundsson, K., Astthorsson, O.S., 2014. Long-term changes of euphausiids in shelf and oceanic habitats southwest, south and southeast of Iceland. J. Plankton Res. 36, 1262–1278. https://doi.org/10.1093/plankt/fbu050

Simberloff, D., Dayan, T., 1991. The guild concept and the structure of ecological communities. Annu. Rev. Ecol. Syst. 22, 115–43.

Similä, T., Holst, J.C., Christensen, I., 1996. Occurrence and diet of killer whales in northern Norway: Seasonal patterns relative to the distribution and abundance of Norwegian spring-spawning herring. Can. J. Fish. Aquat. Sci. 53, 769–779. https://doi.org/10.1139/f95-253

Simon, M., Stafford, K.M., Beedholm, K., Lee, C.M., Madsen, P.T., 2010. Singing behavior of fin whales in the Davis Strait with implications for mating, migration and foraging. J. Acoust. Soc. Am. 128, 3200–3210. https://doi.org/10.1121/1.3495946

Sivle, L.D., Kvadsheim, P.H., Fahlman, A., Lam, F.P.A., Tyack, P.L., Miller, P.J.O., 2012. Changes in dive behavior during naval sonar exposure in killer whales, long-finned pilot whales, and sperm whales. Front. Physiol. 3, 1–11. https://doi.org/10.3389/fphys.2012.00400

Skaug, H.J., Øien, N.I., Bøthun, G., Schweder, T., 2002. Abundance of northeastern Atlantic minke whales for the survey period 1996-2001. Sci. Comm. Int. Whal. Comm. 1–42.

Skaug, H.J., Øien, N.I., Schweder, T., Bøthun, G., 2004. Abundance of minke whales (Balaenoptera acutorostrata) in the Northeast Atlantic: variability in time and space. Can. J. Fish. Aquat. Sci. 61, 870–886. https://doi.org/10.1139/f04-020

Skern-Mauritzen, M., Johannesen, E., Bjørge, A., Øien, N.I., 2011. Baleen whale distributions and prey associations in the Barents Sea. Mar. Ecol. Prog. Ser. 426, 289–301. https://doi.org/10.3354/meps09027

Smith, T.D., Reeves, R.R., 2010. Historical catches of humpback whales, *Megaptera novaeangliae*, in the North Atlantic Ocean: Estimates of landings and removals. Mar. Fish. Rev. 72, 1–43.

Smout, S., Lindstrøm, U., 2007. Multispecies functional response of the minke whale *Balaenoptera acutorostrata* based on small-scale foraging studies. Mar. Ecol. Prog. Ser. 341, 277–291. https://doi.org/10.3354/meps341277

Solvang, H.K., Skaug, H.J., Øien, N.I., 2015. Abundance estimates of common minke whales in the Northeast Atlantic based on survey data collected over the period 2008-2013, International Whaling Commission SC/66a/RMP/8.

Stearns, S.C., 1989. Trade-Offs in Life-History Evolution. Funct. Ecol. 3, 259–268.

https://doi.org/10.2307/2389364

Stefánsson, G., Sigurjónsson, J., Víkingsson, G.A., 1997. On dynamic interactions between some fish resources and cetaceans off Iceland based on a simulation model. J. Northwest Atl. Fish. Sci. 22, 357–370. https://doi.org/10.2960/J.v22.a25

Steiner, L., Lamoni, L., Plata, M.A., Jensen, S.K., Lettevall, E., Gordon, J., 2012. A link between male sperm whales, *Physeter macrocephalus*, of the Azores and Norway. J. Mar. Biol. Assoc. United Kingdom 92, 1751–1756. https://doi.org/10.1017/S0025315412000793

Stenseth, N.C., Mysterud, A., Ottersen, G., Hurrell, J.W., Chan, K.-S., Lima, M., 2002. Ecological effects of climate fluctuations. Science (80-.). 297, 1292–1296. https://doi.org/10.1126/science.1071281

Stephens, P.A., Boyd, I.L., McNamara, J.M., Houston, A.I., 2009. Capital breeding and income breeding: their meaning, measurement, and worth. Ecology 90, 2057–2067. https://doi.org/10.1890/08-1369.1

Stevick, P.T., Allen, J., Clapham, P.J., Friday, N., Katona, S.K., Larsen, F., Lien, J., Mattila, D.K., Palsbøll, P.J., Sigurjónsson, J., Smith, T.D., Øien, N.I., Hammond, P.S., 2003. North Atlantic humpback whale abundance and rate of increase four decades after protection from whaling. Mar. Ecol. Prog. Ser. 258, 263–273. https://doi.org/10.3354/meps258263

Stevick, P.T., Allen, J., Clapham, P.J., Katona, S.K., Larsen, F., Lien, J., Mattila, D.K., Palsbøll, P.J., Sears, R., Sigurjónsson, J., Smith, T.D., Vikingsson, G.A., Øien, N.I., Hammond, P.S., 2006. Population spatial structuring on the feeding grounds in North Atlantic humpback whales (Megaptera novaeangliae). J. Zool. 270, 244–255. https://doi.org/10.1111/j.1469-7998.2006.00128.x

Stone, C.J., Hall, K., Mendes, S., Tasker, M.L., 2017. The effects of seismic operations in UK waters: Analysis of Marine Mammal Observer data. J. Cetacean Res. Manag. 16, 71–85.

Stone, C.J., Tasker, M.L., 2006. The effects of seismic airguns on cetaceans in UK waters. J. Cetacean Res. Manag. 8, 255.

Storrie, L., Lydersen, C., Andersen, M., Wynn, R.B., Kovacs, K.M., 2018. Determining the species assemblage and habitat use of cetaceans in the Svalbard Archipelago, based on observations from 2002 to 2014. Polar Res. 37. https://doi.org/10.1080/17518369.2018.1463065

Sundby, S., Drinkwater, K.F., Kjesbu, O.S., 2016. The North Atlantic spring-bloom system-where the changing climate meets the winter dark. Front. Mar. Sci. 3, 1–12. https://doi.org/10.3389/fmars.2016.00028

Sverdrup, K.A., Armbrust, E.V., 2009. An introduction to the world's oceans. McGraw-Hill Higher Education, New York :

Tavares, S.B., Samarra, F.I.P., Miller, P.J.O., 2017. A multilevel society of herring-eating killer whales indicates adaptation to prey characteristics. Behav. Ecol. 28, 500–514. https://doi.org/10.1093/beheco/arw179

Taylor, B.L., Baird, R.W., Barlow, J., Dawson, S.M., Ford, J.K.B., Mead, J.G., Notarbartolo di Sciara, G., Wade, P.R., Pitman, R.L., 2019. *Physeter macrocephalus* (amended version of 2008 assessment). IUCN Red List Threat. Species 2019 e.T41755A1. https://doi.org/http://dx.doi.org/10.2305/IUCN.UK.2008.RLTS.T41755A160983555.en

Taylor, B.L., Baird, R.W., Dawson, S.M., Ford, J., Mead, J.G., Sciara, N.G., Wade, P., Pitman, R.L., 2008. *Hyperoodon ampullatus* , North Atlantic Bottlenose Whale. IUCN Red List Threat. Species 2008 e.T10707A3208523. 8235.

Trenkel, V.M., Huse, G., MacKenzie, B.R., Alvarez, P., Arrizabalaga, H., Castonguay, M., Goñi, N., Grégoire, F., Hátún, H., Jansen, T., Jacobsen, J.A., Lehodey, P., Lutcavage, M., Mariani, P., Melvin, G.D., Neilson, J.D., Nøttestad, L., Óskarsson, G.J., Payne, M.R., Richardson, D.E., Senina, I., Speirs, D.C., 2014. Comparative ecology of widely distributed pelagic fish species in the North Atlantic: Implications for modelling climate and fisheries impacts. Prog. Oceanogr. 129, 219–243. https://doi.org/10.1016/j.pocean.2014.04.030

Tyack, P.L., 2008. Implications for marine mammals of large-scale changes in the marine acoustic environment. J. Mammal. 89, 549–558. https://doi.org/10.1644/07-mamm-s-307r.1

Tyack, P.L., Madsen, P.T., Soto, N.A., Johnson, M., Sturlese, A., 2006. Extreme diving of beaked whales. J. Exp. Biol. 209, 4238–4253. https://doi.org/10.1242/jeb.02505

Unger, B., Rebolledo, E.L.B., Deaville, R., Gröne, A., IJsseldijk, L.L., Leopold, M.F., Siebert, U., Spitz, J., Wohlsein, P., Herr, H., 2016. Large amounts of marine debris found in sperm whales stranded along the North Sea coast in early 2016. Mar. Pollut. Bull. 112, 134–141. https://doi.org/10.1016/j.marpolbul.2016.08.027

Vacquié-Garcia, J., Lydersen, C., Marques, T.A., Aars, J., Ahonen, H., Skern-Mauritzen, M., Øien,

N.I., Kovacs, K.M., 2017. Late summer distribution and abundance of ice-associated whales in the Norwegian High Arctic. Endanger. Species Res. 32, 59–70. https://doi.org/10.3354/esr00791

Våge, K., Pickart, R.S., Thierry, V., Reverdin, G., Lee, C.M., Petrie, B., Agnew, T.A., Wong, A., Ribergaard, M.H., 2009. Surprising return of deep convection to the subpolar North Atlantic Ocean in winter 2007-2008. Nat. Geosci. 2, 67–72. https://doi.org/10.1038/ngeo382

Valdimarsson, H., Astthorsson, O.S., Palsson, J., 2012. Hydrographic variability in Icelandic waters during recent decades and related changes in distribution of some fish species. ICES J. Mar. Sci. 69, 816–825. https://doi.org/10.1093/icesjms/fss027

Vallejo, A.C., 2013. Potential Effects of Global Climate Change on Cetaceans Distribution in a Small Scale Feeding grounds in Iceland, Skjálfandi Bay. University of Iceland.

Van Waerebeek, K., Baker, A.N., Félix, F., Gedamke, J., Iñiguez, M., Sanino, G.P., Secchi, E., Sutaria, D., Van Helden, A., Wang, Y., 2007. Vessel collisions with small cetaceans worldwide and with large whales in the Southern Hemisphere, an initial assessment. Lat. Am. J. Aquat. Mamm. 6, 43–69. https://doi.org/10.5597/lajam00109

Venables, W.N., Ripley, B.D., 2002. Modern applied statistics with S. https://doi.org/10.1007/978-0-387-21706-2

Verborgh, P., De Stephanis, R., Pérez, S., Jaget, Y., Barbraud, C., Guinet, C., 2009. Survival rate, abundance, and residency of long-finned pilot whales in the strait of Gibraltar. Mar. Mammal Sci. 25, 523–536. https://doi.org/10.1111/j.1748-7692.2008.00280.x

Víkingsson, G.A., 1997. Feeding of fin whales (*Balaenoptera physalus*) off Iceland - diurnal and seasonal variation and possible rates. J. Northwest Atl. Fish. Sci. 22, 77–89. https://doi.org/10.2960/J.v22.a7

Víkingsson, G.A., Elvarsson, B.T., Ólafsdóttir, D., Sigurjónsson, J., Chosson, V., Galan, A., 2014. Recent changes in the diet composition of common minke whales (*Balaenoptera acutorostrata*) in Icelandic waters. A consequence of climate change? Mar. Biol. Res. 10, 138–152. https://doi.org/10.1080/17451000.2013.793812

Víkingsson, G.A., Heide-Jørgensen, M.P., 2015. First indications of autumn migration routes and destination of common minke whales tracked by satellite in the North Atlantic during 2001-

2011. Mar. Mammal Sci. 31, 376–385. https://doi.org/10.1111/mms.12144

Víkingsson, G.A., Pike, D.G., Desportes, G., Øien, N.I., Gunnlaugsson, T., Bloch, D., 2009. Distribution and abundance of fin whales (Balaenoptera physalus) in the Northeast and Central Atlantic as inferred from the North Atlantic Sightings Surveys 1987-2001. NAMMCO Sci. Publ. 7, 49–72.

Víkingsson, G.A., Pike, D.G., Valdimarsson, H., Schleimer, A., Gunnlaugsson, T., Silva, T., Elvarsson, B.Þ., Mikkelsen, B., Øien, N.I., Desportes, G., Bogason, V., Hammond, P.S., 2015. Distribution, abundance, and feeding ecology of baleen whales in Icelandic waters: have recent environmental changes had an effect? Front. Ecol. Evol. 3, 1–18. https://doi.org/10.3389/fevo.2015.00006

Virgili, A., Authier, M., Boisseau, O., Cañadas, A., Claridge, D., Cole, T., Corkeron, P.J., Dorémus, G., David, L., Di-Méglio, N., Dunn, C., Dunn, T.E., García-Barón, I., Laran, S., Lauriano, G., Lewis, M., Louzao, M., Mannocci, L., Martínez-Cedeira, J., Palka, D., Panigada, S., Pettex, E., Roberts, J.J., Ruiz, L., Saavedra, C., Santos, M.B., Van Canneyt, O., Vázquez Bonales, J.A., Monestiez, P., Ridoux, V., 2019. Combining multiple visual surveys to model the habitat of deep-diving cetaceans at the basin scale: Large-scale modelling of deep-diving cetacean habitats. Glob. Ecol. Biogeogr. 28, 300–314. https://doi.org/10.1111/geb.12850

Walther, G., Post, E., Convey, P., Menzel, A., Parmesan, C., Beebee, T.J.C., Fromentin, J.-M., Hoegh-Guldberg, O., Bairlein, F., 2002. Ecological responses to recent climate change. Nature 416, 389–395. https://doi.org/10.1038/416389a

Waniek, J.J., Holliday, N.P., 2006. Large-scale physical controls on phytoplankton growth in the Irminger Sea, Part II: Model study of the physical and meteorological preconditioning. J. Mar. Syst. 59, 219–237. https://doi.org/10.1016/j.jmarsys.2005.10.005

Waring, G.T., Josephson, E., Fairfield, C.P., Maze-Foley, K., 2006. U. S. Atlantic and Gulf of Mexico Marine Mammal Stock Assessments - 2005.

Weilgart, L.S., 2007. The impacts of anthropogenic ocean noise on cetaceans and implications for management. Can. J. Zool. 85, 1091–1116. https://doi.org/10.1139/Z07-101

Weinrich, M., Corbelli, C., 2009. Does whale watching in Southern New England impact humpback whale (*Megaptera novaeangliae*) calf production or calf survival? Biol. Conserv. 142, 2931–2940. https://doi.org/10.1016/j.biocon.2009.07.018

Whitehead, H., 2018. Sperm Whale, in: Encyclopedia of Marine Mammals. Elsevier, pp. 919–925. https://doi.org/10.1016/B978-0-12-804327-1.00242-9

Whitehead, H., 2003. Sperm whales: social evolution in the ocean. University of Chicago Press.

Whitehead, H., Hooker, S.K., 2012a. Uncertain status of the northern bottlenose whale *Hyperoodon ampullatus*: Population fragmentation, legacy of whaling and current threats. Endanger. Species Res. 19, 47–61. https://doi.org/10.3354/esr00458

Whitehead, H., Hooker, S.K., 2012b. Uncertain status of the northern bottlenose whale Hyperoodon ampullatus: Population fragmentation, legacy of whaling and current threats. Endanger. Species Res. 19, 47–61. https://doi.org/10.3354/esr00458

Whitehead, H., Hooker, S.K., 2010. Status of northern bottlenose whales. NAMMCO SC/63/SM4 1–11.

Whitehead, H., MacLeod, C.D., Rodhouse, P., 2003. Differences in niche breadth among some teuthivorous mesopelagic marine mammals. Mar. Mammal Sci. 19, 400–406. https://doi.org/10.1111/j.1748-7692.2003.tb01118.x

Wickham, H., 2016. ggplot2: Elegant graphics for data analysis. https://doi.org/10.1007/978-3-319-24277-4

Williams, R., Grand, J., Hooker, S.K., Buckland, S.T., Reeves, R.R., Rojas-Bracho, L., Sandilands, D., Kaschner, K., 2014. Prioritizing global marine mammal habitats using density maps in place of range maps. Ecography (Cop.). 37, 212–220. https://doi.org/10.1111/j.1600-0587.2013.00479.x

Williams, R., Vikingsson, G.A., Gislason, A., Lockyer, C., New, L., Thomas, L., Hammond, P.S., 2013. Evidence for density-dependent changes in body condition and pregnancy rate of North Atlantic fin whales over four decades of varying environmental conditions. ICES J. Mar. Sci. 70, 1273–1280. https://doi.org/10.1093/icesjms/fst059

Windsland, K., Lindstrøm, U., Nilssen, K.T., Haug, T., 2007. Relative abundance and size composition of prey in the common minke whale diet in selected areas of the northeastern Atlantic during 2000-04. J Cetacean Res Manag. 9, 167–178.

Wood, S.N., 2017. Generalized additive models: an introduction with R, 2nd ed. CRC Press/Taylor & Francis Group, Boca Raton : https://doi.org/10.1201/9781315370279

Wood, S.N., 2011. Fast stable REML and ML estimation of semiparametric generalized linear models. J. R. Stat. Soc. Ser. B 73, 3–36. https://doi.org/10.1111/j.1467-9868.2010.00749.x

Wood, S.N., 2004. Stable and efficient multiple smoothing parameter estimation for generalized additive models. J. Am. Stat. Assoc. 99, 673–686. https://doi.org/10.1198/016214504000000980

Wood, S.N., 2003. Thin plate regression splines. J. R. Stat. Soc. 65, 95–114.

Wood, S.N., Pya, N., Säfken, B., 2016. Smoothing parameter and model selection for general smooth models. J. Am. Stat. Assoc. 111, 1548–1563. https://doi.org/10.1080/01621459.2016.1180986

Woodley, T.H., Gaskin, D.E., 1996. Environmental characteristics of North Atlantic right and fin whale habitat in the lower Bay of Fundy, Canada. Can. J. Zool. 74, 75–84. https://doi.org/10.1139/z96-010

Yong-Qi, G., Lei, Y., 2008. Subpolar Gyre Index and the North Atlantic Meridional Overturning Circulation in a Coupled Climate Model. Atmos. Ocean. Sci. Lett. 1, 29–32. https://doi.org/10.1080/16742834.2008.11446764

Zachariassen, P., 1993. Pilot whale catches in the Faroe Islands. Reports Int. Whal. Comm. 14, 69–88.

Zerbini, A.N., Clapham, P.J., Wade, P.R., 2010. Assessing plausible rates of population growth in humpback whales from life-history data. Mar. Biol. 157, 1225–1236. https://doi.org/10.1007/s00227-010-1403-y

Zhukova, N.G., Nesterova, V.N., Prokopchuk, I.P., Rudneva, G.B., 2009. Winter distribution of euphausiids (Euphausiacea) in the Barents Sea (2000-2005). Deep. Res. Part II Top. Stud. Oceanogr. 56, 1959–1967. https://doi.org/10.1016/j.dsr2.2008.11.007

8 GENERAL APPENDIX

8.1 Ethical agreement

UNIVERSITY OF ST ANDREWS ANIMAL ETHICS FORM

This form provides the University of St Andrews' Animal Welfare and Ethics Committee (AWEC) with relevant information concerning non-licensed projects carried out on animals by a University member. This form aims to provide guidance, protect the animals, minimise the occurrence of research that damages the reputation to individuals or the university, and to provide a formal ethical approval required for grant applications and research publications. Completion of this form is not required for human studies that are covered by applications to UTREC, or for projects involving invertebrates other than cephalopods. A completed form (& any attachments) should be submitted to your School's Ethics Committee, for non-licensed work involving nonhuman vertebrates or cephalopods (see note 1) for consideration.

This form is intended for work NOT covered by Home Office approval; it includes overseas, non-invasive experimental or observational work with animals.

Name of supervisor/Principal Investigator: Philip Hammond Date: 14 May 2016

1. Species & Number of animals to be used (see note 1):
The species sighted were: minke, sei, fin, blue, humpback, right, sperm, pilot, killer, beluga, northern bottlenose and Sowerby's beaked whale; white-sided, white-beaked, common, striped, Risso's and bottlenose dolphin; and harbour porpoise. Approximately 35,000 individual cetaceans were sighted of these species. The project will analyse a subset of these data (see project description).

2. School/Department of associated PI/module organizer: Biology

3. Estimated start date: 2015

4. Estimated duration of project (see note 2): 6 years

5i. Estimated duration of involvement for animals:
No animals were actively involved in the research. Each group of whales, dolphins or porpoise was sighted for a period of a few seconds to a few minutes.

5ii. How often and for how long will each living individual animal be involved in this study? See response to 5i.

6. Location of animals: Central and eastern North Atlantic Ocean.

Choose ONE of the following:

☒ **Research Project**
Title of project: Factors Influencing Decadal-Scale Changes in Cetacean Distribution and Habitat Use in the North Atlantic

Name of researcher(s):		STAFF	PG	UG
1. Philip Hammond	☒	☐	☐	
2. Nadya C. Ramirez Martinez	☐	☒	☐	
3. Lisa Neyman		☐	☒	☐
4.		☐	☐	☐
5.		☐	☐	☐

(Please include additional group members in a separate attachment.)

☐ **Teaching Project**
Module Title:

Module Number:

1

SECTION 1 --	YES	NO	N/A
7. Have all persons involved familiarised themselves with the applicable legislation governing scientific work with animals (see below)?	☒	☐	☐
8. Can you confirm the project could not be completed using existing video records?	☒	☐	☐
9. If it is necessary to capture animals in the wild, is this to be done in as painless and humane a manner as possible and according to any relevant legislation? (see note 4)	☐	☐	☒
10. Can you confirm that your work does not involve procedures or housing conditions that could cause pain, stress or discomfort to vertebrates? (see note 3)	☒	☐	☐
11. Can you confirm that the project does not introduce deleterious conditions to your animals (disease, parasites, surgery, genetic modification, application of hormones or pharmaceuticals)?	☒	☐	☐
12. Can you confirm that there is no foreseeable reputational risk to the University?	☒	☐	☐
13. Is this research funded by any external sponsor or agency?	☒	☐	

If YES please state funder	**The governments of Iceland, Faroe Islands and Norway funded the sightings surveys which generated the data. The Colombian government (Colciencias) funds PG student tuition.**

	YES	NO	N/A
14. Does this research entail collaboration with researchers from other institutions? and/or across other University Schools/Units?	☒	☐	☐

If YES please state names and institutions of collaborators	**Dr Gisli Vikingsson, Marine Research Institute, Iceland; Dr Bjarni Mikkelson, Museum of Natural History, Faroe Islands; Dr Nils Øien, Institute of Marine Research, Norway**

	YES	NO	N/A
15. Have you obtained permission to access the site of research?	☐	☐	☒

If YES please state agency/authority etc. & provide documentation. If NO please indicate why	**The project will use existing data that were collected from 1987 to 2017.**

SECTION 2 --	YES	NO	N/A
16. Can you confirm that the animals will not be transported?	☒	☐	☐
17. Are the animals kept under appropriate conditions during the study, but also during periods when not being studied (i.e. cages with biologically relevant features such as natural material, refuges, baths, appropriate social companions; no overcrowding)?	☐	☐	☒
18. If it is necessary to procure animals from outside sources have you, or the person responsible, ensured that your supplier is reputable?	☐	☐	☒
19. Can you confirm that the animals will not be killed subsequent to the study? (see note 5)	☒	☐	☐

SECTION 3 --	YES	NO	N/A
20. Have you taken precautions to minimise interference, risk or adverse consequences to the animals, or the ecosystems of which they are a part?	☐	☐	☒
21. If your project involves work with endangered species (e.g. CITES I, II or III), can you confirm that your project could not be done with a species not listed by CITES?	☒	☐	☐

22. What licences and permissions will you require to conduct this study?

None.

Provision of the data by the data owners (project collaborators) constitutes permission to use the data for this study.

23. Can you confirm that your project does not require motivating or conditioning the animal with aversive stimuli? (see note 6)	☒	☐	☐
24. Can you confirm either that food or water deprivation will not be involved, or that you have received confirmation from a vet, Home Office inspector, or equivalent authority that the effects of the deprivation are mild? (see note 7)	☒	☐	☐
25. Can you confirm that your project does not involve regulated procedures (e.g. injection or application of hormones/pharmaceuticals, removal of blood, psychological stress, dietary manipulations and environmental changes)? (see note 3)	☒	☐	☐

*A **NO** answer to one of questions 10, 11, 23-25 implies that your work may require a Home Office Project Licence. Contact Home Office Liaison Officer <holo@st-andrews.ac.uk> for further details)*

26. If ethical approval has already been obtained for research so similar to this proposed project that a new review process may not be required, please give details of the application and the date of approval.

Please provide supporting details and sign the form. There is an obligation on the lead researcher/ module organizer to draw attention to any issues with ethical implications not clearly covered by the above checklist.

Please provide in the box below an abstract of no more than 300 words highlighting all ethical considerations as well as a full description of the project including the following information:
1. Purpose of project and its academic rationale. 2. Brief description of methods and measurements. 3. Animals: species, number, age, gender. 4. A clear but concise statement of the ethical considerations raised by the project & how you intend to deal with them. 5. Outline the benefits of the project. If additional space is required include a separate attachment.

ABSTRACT (<300 words):
This project will analyse existing data from observational surveys conducted 1987-2017 to explore the environmental factors that influence the distribution and habitat use of a range of cetacean species in the central and northeast Atlantic over a period of three decades. There are no ethical considerations raised by the project. The project is fully compatible with the SMRU Ethics Policy, 15 January 2016.

FULL PROJECT DESCRIPTION:

1. The main purpose of this project is to improve understanding of the environmental factors that influence the distribution and habitat use of a range of cetacean species in the central and northeast Atlantic over a period of three decades by modelling their relative abundance as a function of a series of static and dynamic variables.

2. Data on cetaceans are available from two series of visual observation surveys conducted since 1987 over a large part of the central and eastern North Atlantic: the North Atlantic Sightings Surveys (NASS); and the Norwegian Independent Line transect Surveys (NILS). These line transect surveys were funded by the governments of Iceland, Faroes, Norway and Greenland to estimate abundance of various cetacean species. The surveys search along predetermined transects; data collection was in "passing mode" and therefore by design involved no approach to the animals.

3. The focal study species will be fin, humpback, minke, sperm, and pilot whales. Additional species may also be investigated, including the northern bottlenose whale, killer whale and delphinids as a group. Environmental variables will include static variables such as depth and slope, and dynamic variables such as sea surface

temperature (SST), sea surface height (SSH), presence of fronts, structure of the water column, chlorophyll-a, primary productivity, and potentially distribution of zooplankton and fish.

4. There are no ethical considerations raised by this work.

5. An exploration of factors influencing distribution and habitat use over such large temporal and spatial scales has not previously been done. Conducting this work should result in a better understanding of the species ecology in the North Atlantic and provide clues on how cetacean populations may be affected by continuing environmental changes induced by climate warming.

SECTION 4 -- DOCUMENTATION CHECKLIST

Ethical Application Form	YES ☒	NO ☐
External permissions	YES ☐	NO ☒
Other (please list):		

I (see note 11) **can confirm that I have answered all above questions to the best of my knowledge. I am familiar with the *ASAB Guidelines for the Treatment of Animals in Behavioural Research & Teaching (ANIMAL BEHAVIOUR, 2003, 65, 249-255).***

Signed:

Print Name **Philip Hammond** Date **14 May 2016**

STATEMENT OF ETHICAL APPROVAL

☐ This project has been judged to have no significant ethical issues and is now approved.

☐ This project may have significant ethical issues and has been referred to AWEC for advice.

Signed …… Print Name …… Date ……
(Chair, School Ethics Committee)

NOTES

1. It is recommended that individuals complete the form when they are confident the project will occur (e.g. once funded). Individuals are free to apply for ethical approval prior to grant submission if this is required by the funder.
2. For teaching projects, it is necessary to complete the form every FOUR years even if the teaching project and supervisor do not change. However, any change in project related to the species studied, methods deployed, locations of animals, or module organizer, still requires a non-licenced SEC Amendment form to be completed.
3. Guidance on Home Office regulated procedures can be found on their website http://www.homeoffice.gov.uk/science-research/animal-research/
4. Please provide a photocopy of any relevant licences (e.g. Scottish National Heritage licence).
5. If the project requires a Schedule 1 kill (S1K), for instance, for tissue provide details. Although a Home Office licence is not required to carry out this procedure, it is controlled within the University premises. The Home Office require the University to maintain a register of those competent and authorised to carry out S1Ks and appropriate training must be undertaken.
6. An aversive stimulus is any negative stimulus to which an organism will learn to make a response that avoids it.

7. Definitions of significant food and water deprivation can be found in the Home Office 'Codes of Practice' document, please check the Home Office website.
8. Note, even in cases where ethical approval is granted by the School ethics committee, this form will still be forwarded to AWEC and, in the unlikely case that AWEC members raise concerns over the project, the PI may be required to stop the project until such a time as the issues of concern can be resolved to AWEC's satisfaction.
9. Where the project is part of an undergraduate teaching module describe the kinds of projects involved (e.g. 'laboratory based observational studies of bird foraging'), ensuring that all species, methods and locations are given. If the module involves several projects involving vertebrates a single form may be completed by the module organizer briefly describing the full range of projects involved. However, each senior honours research project involving animals requires a separate form. Where the research does not fit into clear, distinct projects, describe the general nature of the work.
10. If the School's Ethics Committee's judge, the project has significant ethical implications the Ethics Committee should engage in further discussion with the PI/Module Organizer. If the concerns are not completely alleviated the project will be referred to AWEC for advice. In such cases it is intended that this form will provide all of the necessary information required for AWEC evaluation.
11. **If more than one researcher is involved the signature should be from the PI; for teaching project the signature should be from the Module Organizer. If a student project, the signature should be that of the supervisor.**

Relevant legislation:
UK Guidance on the regulated procedures ***http://www.homeoffice.gov.uk/science-research/animal-research/***
EU Council of Europe convention on the use of vertebrate animals in research: ***http://conventions.coe.int/Treaty/en/Treaties/Html/123.htm***
US Animal Welfare Act, amendments and regulations (e.g. 1985 Amendment to the Animal Welfare Act)
Canada Guide for the Care and Use of Experimental Animals (Canadian Council on Animal Care 1992)